The anterior cingulate cortex in flexible behaviour

Cole, Nicholas

Awarding institution:
King's College London

Department of Developmental Neurobiology

The anterior cingulate cortex in flexible behaviour

Nicholas Cole

First supervisor: Dr Matthew Grubb

Second supervisor: Dr Adil Khan

Word count: 45,532

CONTENTS

Abstract and abbreviations:

Abstract

The primate anterior cingulate cortex (ACC) has a distinct role in cognition, active in attentional tasks involving conflicting responses, top-down control, and prediction-error signalling. While its homology in rodents is debated, corresponding functions have been shown in tasks involving flexible behaviour. A specific role for the ACC was found when mice switched attention between visual stimuli based on an expectation violation, the failure of an expected stimulus to arrive. Two-photon calcium imaging revealed a subset of neurons in the ACC that responded specifically when this stimulus was expected but did not arrive, in a manner predictive of subsequent attentional shifts. Their activity was limited to the instance of expectation violation, and could not be found in other cortical regions. The identified circuit re-configured over days and could be disrupted through selective perturbation of the surrounding disinhibitory network. These results demonstrate a dedicated circuit in the ACC for signalling prediction errors in order to provoke attentional shifts during flexible behaviour.

Abbreviations

ACC: anterior cingulate cortex, **ChR2:** channelrhodopsin2, **CTB:** cholera toxin subunit B, **dACC:** dorsal ACC, **ΔF/F:** relative change in fluorescence intensity, **EEG:** electroencephalography, **ERN:** error-related negativity, **EVC:** expected value of control, **fMRI:** functional magnetic resonance imaging, **GABA:** γ-aminobutyric acid, **IL:** infralimbic cortex, **LC:** locus coeruleus, **mPFC:** medial prefrontal cortex, **NAc:** nucleus accumbens, **NMDA:** N-methyl-D-aspartate, **OCD:** obsessive-compulsive disorder, **OFC:** orbitofrontal cortex, **PCC:** posterior cingulate cortex, **PET:** positron emission tomography, **PFC:** prefrontal cortex, **PL:** prelimbic cortex, **PRO:** predicted-response-outcome, **PSTH:** peri-stimulus time histogram, **PV:** parvalbumin-positive, **RPE:** reward prediction error, **ROI:** region-of-interest, **rvACC:** rostro-ventral ACC, **SD:** standard deviation, **SEM:** standard error of the mean, **SOM:** somatostatin-positive, **V1:** primary visual cortex, **VIP:** vasoactive intestinal peptide-positive, **VTA:** ventral tegmental area

INTRODUCTION

Introduction

The focus of this thesis is the anterior cingulate cortex, a brain area implicated in a variety of emotional and cognitive processes, and its contribution to flexible behaviour in mice. In this introduction, I will briefly summarise how our understanding of the importance of this region to higher-order processes has developed over time as the research techniques available have advanced. Starting with lesion studies, I will explain how the separate associations with emotional and cognitive processes have led to a division of the ACC into rostro-ventral and dorsal components. I will then describe the current major theories of primate dorsal ACC function in cognitive tasks. With these established, I will attempt to position this ACC function within the broader framework of a multiple-demand system sustaining fluid cognition. Finally, I will outline the issues with finding a direct rodent homologue for the primate ACC, and summarise the identified cognitive functions of the rodent ACC that parallel those seen in primates.

1. The human anterior cingulate cortex

Renowned for his pioneering work in speech and language, the French physician Pierre Paul Broca (1824-1880) had a fascination with comparative neuroanatomy. After comparing the brains of 41 mammalian species, he described three significant differences he considered fundamental for the relative intellectual superiority of the primate brain (Broca, 1978). He observed in the primate brain a more developed frontal lobe, a reduced and rudimentary olfactory bulb, and an atrophy of the anterior portion of the cingulate gyrus. Broca believed this "frontal dominance" reflected an evolutionary shift to promote the "highest intellectual functions".

The concurrent atrophy of what he called the *great limbic lobe* ("le grand lobe limbique") was no coincidence. This band of brain tissue, bordering the corpus callosum – from *limbus*, meaning border – was considered part of the rhinencephalon, or 'smell brain'. Broca deemed olfaction a "bestial sense", the antithesis of the visual system whose value "to an animal is the value of its intelligence". The sense of smell required little intellectual involvement, he said, and derived from a brain structure that "ranks low in the cerebral hierarchy". Thus, to access this higher plane of cognitive function, intelligence must "gain supremacy over this bestial sense".

The cingulate cortex is the most dorsal part of this *great limbic lobe*, forming a cingulum, or collar, around the corpus callosum. The limbic system, incorporating Broca's *great limbic lobe* as well as deeper brain structures such as the hypothalamus, hippocampus, and thalamus, provides the

"mechanism of emotion" (Papez, 1937). This system is largely responsible for our "emotional life" (Boeree, 2008), receiving low order emotional processing of sensory inputs and promoting the formation of memories (Roxo et al., 2011). The cingulate cortex incorporates the cingulate gyrus and its continuation into the cingulate sulcus, and is divided into anterior (Broadmann's areas 24, 32, and 33) and posterior (areas 23 and 31) sub-compartments.

The posterior cingulate cortex (PCC) projects to both deep and superficial layers of the neocortex, including the parietal, temporal and frontal lobes. It also connects to subcortical nuclei such as the thalamus, pons, and basal ganglia, and receives inputs from the cortex and thalamus (Cohen, 2014). The anterior cingulate cortex (ACC) instead receives the majority of its inputs from the frontal and posterior parietal cortices, as well as from the PCC and thalamus. It has fewer projection targets than PCC, but is highly interconnected with the PCC and basal ganglia. Unlike the PCC, it also connects to limbic structures such as the amygdala. The regions can be distinguished by this connectivity, with the PCC interconnected with several cortical areas while the ACC predominantly receives frontal and parietal inputs and projects to the limbic system. This has provoked a characterisation of the PCC as 'evaluative', involved in monitoring one's own behaviour and sensory input, while the ACC is 'executive' (Vogt et al., 1992).

The ACC in emotion

It is this anterior portion of the cingulate that Broca observed atrophying as he advanced up his intellectual hierarchy of mammalian species. James Papez (1883-1958) developed Broca's concept of a limbic system to include midbrain structures with a role in emotional regulation. Though directly accessing the ACC in patients at the time was impossible, Papez was able to infer a potential function of the cingulate from patients suffering from tumours of the corpus callosum (Papez, 1937). He observed the common symptoms of a "loss of spontaneity in emotion, thought, and activity" across these patients. He attributed these symptoms to the tumours' encroachment into the ACC, and thus positioned the ACC as "the seat of dynamic vigilance by which the environmental experiences are endowed with an emotional consciousness". Just as the visual system receives inputs from the retina, he saw the cingulate gyrus as a "receptive organ" for emotion conveyed by signals from the hypothalamic region.

Further insight into the function of the ACC came from lesions performed in the name of therapy since the late 1940s (Devinsky et al., 1995). Bilateral cingulotomies were performed to reduce aggression in psychosis patients (Whitty et al., 1952), anxiety in patients with obsessive-compulsive disorder (OCD) or anxiety neurosis (Jimeno & Paniagua, 1969), and chronic pain across a variety of diseases (Wilson & Chang, 1974). Patients were observed to later seem tired, more apathetic, and slower in thoughts and actions, but showed no changes in memory (Tow & Whitty,

1953). In fact, no significant long-term changes were seen across a battery of cognitive and personality tests following cingulotomy, except for a reduction in anxiety (Long et al., 1978). Despite their relatively minor impact on long-term cognitive function, the modern cingulotomy has been largely relegated to a last-resort treatment for chronic, intractable pain. Bilateral ACC lesions can be achieved using MRI-guided laser-induced thermal therapy (Allam et al., 2022), and produce significant post-operative pain relief in over 60% of patients (Pouratian, 2016).

An interesting observation after these surgeries was that patients typically continued to report pain, but now expressed little interest in it (Cohen et al., 2001). This indifference manifested across a variety of emotional measures, with an overall reduction in emotional tension, distress, rumination, and anxiety. The authors speculated that the reason cingulotomies could be effective for treating OCD, pain, and addiction, but not for schizophrenia or bipolar disorder was because the former disorders involve a "ruminative" aspect of emotional processing. Both groups of diseases feature emotional processing, but only those alleviated by cingulotomies involved the patient internally evaluating their own experience of an emotion. They proposed that ACC represents an integration point of attention and emotion, serving its 'executive' characterisation (Vogt et al., 1992).

The ACC in pain

Evidence from human ACC recordings support this hypothesis. Different sub-regions of the ACC are responsive to pain and different emotions (Vogt, 2005), while increased regional cerebral blood flow in the medial prefrontal cortex (mPFC), including ACC, was associated with improved emotional suppression scores (Abler et al., 2008). Patients with psychopathy, characterised by a "severe disruption of moral behaviour due to interpersonal and emotional detachment" (Hare & Neumann, 2008), showed decreased ACC activity when performing dishonest actions for personal gain, compared to non-psychopathic participants (Abe et al., 2018). The ACC can also mediate fear behaviour in threat scenarios in humans and monkeys (Jhang et al., 2018). When presented with words evoking conflict, compared to words evoking other general-negative emotions, functional magnetic resonance imaging (fMRI) of Vietnam war veterans with and without post-traumatic stress disorder (PTSD) revealed significantly increased ACC activity only in the non-PTSD group (Shin et al., 2001). These studies suggest that the ACC has a specific role in emotional regulation.

Pain is intrinsically linked to emotion, being similarly evoked by negative events or memories. Of all the cortical sub-regions, ACC seems to be the most associated with the production of pain – even more than sensory cortices such as somatosensory. While many brain structures are activated during pain sensation, only ACC activity encoded the relative unpleasantness of the sensation (Tölle et al., 1999). This could be interpreted as the ACC again providing an integration point

between attention and emotion. The ACC might integrate the somatosensory features of pain, from the sensory cortex, with prefrontal circuits that compute the ruminative aspects, the importance and long-term implications of the pain – a feature of secondary pain affect (Price, 2000). Similarly, during threat perception the ACC might integrate inputs from the parietal areas with these prefrontal circuits to plan a response to an imminent bodily threat.

It seems that while Broca's defined role for the limbic system in olfaction was misguided, his overall conception of this system fulfilling a role in the "bestial" components of thought may have had substance. Emotion and pain can be thought of as irrational and unsophisticated, a feature of mammal behaviour present throughout this intellectual hierarchy. According to Broca, some "other brain" structures must be computing the higher-order functions required for cognition. Indeed, we see that lesions of the ACC are often insufficient to disrupt cognition. The ACC's function, however, is not limited solely to emotional regulation.

2. A cognitive-emotional structure

The ACC, unlike the PCC, was initially thought to be uninvolved in cognitive processing, as lesions would frequent disrupt affective processing and change personality characteristics while leaving cognition largely unimpaired (Cohen, 2014). However, more recent lesion and neuroimaging studies have revealed a role for the ACC in several executive functions.

The ACC in cognition

Patients who underwent cingulotomies to treat chronic, intractable pain often experienced long-term deficits to attention, with a particular impact on vigour, intention, and self-initiated behaviour (Cohen et al., 2001). During evaluations the patients would produce fewer spontaneous verbalisations, fewer responses when multiple responses were possible, and generated less effort overall during tasks (Cohen et al., 1999). Similar deficits were seen in patients who underwent the same surgery to treat depression (Janer & Pardo, 1991). Conversely, when the ACC is stimulated using implanted electrodes in patients with refractory epilepsy, the patients reported a subjective increase in their "will to persevere" (Parvizi et al., 2013). The patients suddenly started to anticipate an upcoming challenge, and felt a strong concurrent motivation to overcome it when it came. One patient described "this feeling like…I was driving into a storm" and a "positive thing like…push harder to try and get through this". It seems that the ACC has a clear role in providing motivation during challenges.

Bilateral ACC damage could also disrupt habituation, measured by the time taken for patients to stop orienting their heads to an auditory tone (Cohen et al., 1999). This effect was not

straightforward, with some patients habituating faster than controls but struggling to sustain their habituation, while others were slower from the start. This suggests a role in self-monitoring, like what was seen during emotional processing. Similarly, male patients instructed to inhibit their sexual arousal while observing erotic video clips showed activations in the ACC, but not in the other limbic areas customarily activated by these stimuli (Beauregard et al., 2001).

The ACC seems to contribute meaningfully to motivation and to self-monitoring, and to executive functions such as inhibitory control. However, the strongest support for its characterisation as 'executive', in contrast to the PCC (Vogt et al., 1992), comes from its role in attention. Unilateral visuospatial neglect is a disorder of attention in which a subject cannot perceive details from an area of sensory space, despite the primary sensory regions being intact (Bisiach & Luzzatti, 1978). Animal studies showed that unilateral lesions in the ACC of Rhesus monkeys can cause neglect of the contralateral space (Watson et al., 1973), while stimulation causes head and eye movements towards the contralateral space in cats (Jansen et al., 1955).

Observing unilateral neglect in humans was more difficult, as cingulotomies tended to be bilateral. Instead, the attention deficits caused by lesions to the ACC were more subtle. In humans, bilateral cingulotomies did not impair attention span or working memory but produced mild deficits in the Stroop task (Fig 1.01A), requiring focused and selective attention, and the adaptive-rate continuous performance task, requiring sustained attention (Cohen et al., 1999). Focused attention most closely resembles a classical definition of attention, describing the active engagement of cognitive resources in a directed manner to select the information required for the current task. Selective attention is the ability to orient attention to one source of information over another. Sustained attention describes how this performance may vary over time: an individual may be able to sustain focused attention in short bursts, but cannot sustain it over a longer-duration task (Cohen, 2014). These selective roles for the ACC in certain types of attention-demanding tasks have become a defining feature of ACC function.

Conflict monitoring tasks

The seminal study of the role of ACC in conflict monitoring was performed by Pardo and colleagues in 1990. They used positron emission tomography (PET) imaging to record metabolic changes across the brain while human participants performed the Stroop task (Fig 1.01A). In the classical Stroop task, participants are presented with words for colours that are themselves physically coloured. Participants must report the physical colour of the word. If the physical colour of the word matches the actual word the trial is congruent, as there is no conflict between the word's appearance and meaning. If the physical colour does not match the word the trial is incongruent, as the participant must ignore the meaning of the word to correctly identify its

colour. These incongruent trials require greater attentional control, as the participant must attend to certain features of the word and actively ignore others. Across the brain, the ACC was the area that showed the greatest difference in activity between congruent and incongruent trials (Pardo et al., 1990). This task is an example of focused and selective attention: it demands brief periods of attention when generating the response in order to identify the colour but suppress the appearance, but does not require sustained attention for long periods. When the stimuli are incongruent, focused attention is critical for correctly responding.

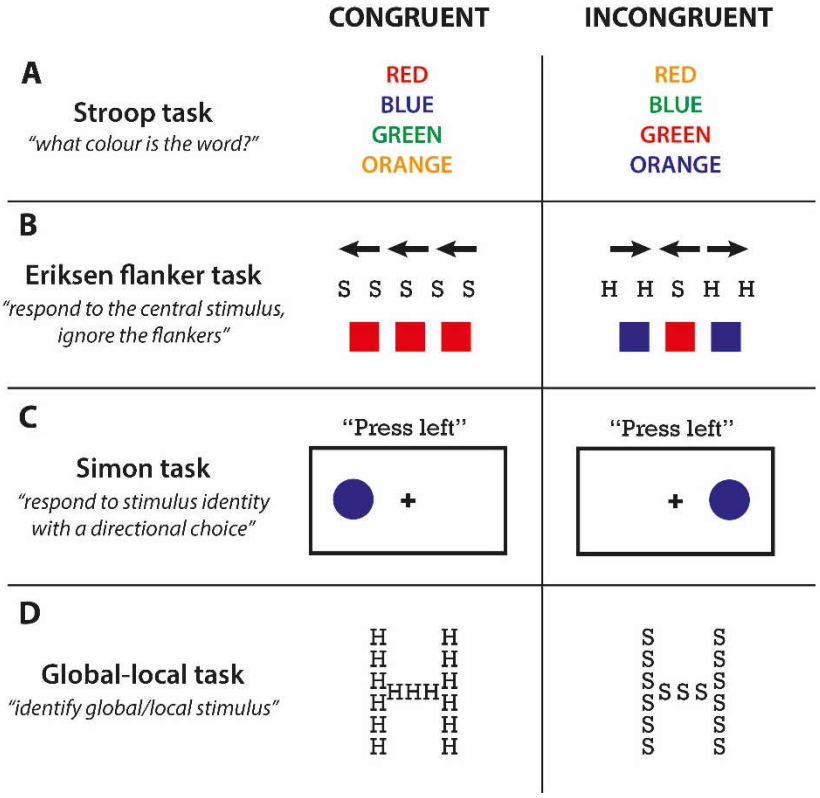

Figure 1.01. Conflict monitoring tasks. Schematic of the rules of common behavioural tasks designed to elicit response conflict. A: Stroop task – participants must report the colour of the presented word. B: Flanker task – participants must respond to central stimulus and ignore surrounding stimuli. Examples given here are directional (top), letter (middle), or colour (bottom) stimuli. C: Simon task – participants must respond to stimulus by making a directional choice e.g., pushing left/right button. They must ignore placement of stimulus and respond only to identity. D: Global-local task. Participants must respond to the global or local features of a task. Example here is Navon's task, in which participants must either report the global letter (H in both cases) or the local letter (H when congruent, S when incongruent).

Across a range of tasks, ACC activity was most consistently observed in these focused attention tasks that required the participant to choose between different possible responses (Botvinick et al., 2001). The ACC was particularly active in tasks which required the participant to override a prepotent response (Fig 1.01). In the flanker task, participants had to ignore distracting stimuli and respond only to the central stimulus. fMRI showed increased ACC activity during incongruent trials (Bunge et al., 2002), which scaled dependent on the number of preceding congruent trials (Durston, 2003). In the Simon task, where conflict arises from the position of the stimulus not conforming to the directional choice it denotes, ACC activation was observed with a time-course similar to in the Stroop task (Peterson et al., 2002). In Navon's global-local paradigm, in which participants must either respond to the local or global features of a letter comprised of smaller

letters, fMRI showed ACC activation when the global and local letters were in conflict (Weissman et al., 2003).

In these tasks, the responses required by the conflicting stimuli are typically symmetrical - a participant would respond with one of two directional responses, such as a button press or saccade. However, even when the stimuli require a go/no-go response respectively, their conflict recruits the ACC. A task in which participants responded to regular target visual stimuli with a button press and withheld their responses to the less frequent non-targets showed increased activity in the ACC during no-go trials, which again scaled with the number of preceding go trials (Durston et al., 2002). In fact, the type of response required did not seem to influence ACC involvement at all. Across a range of tasks including go/no-go, oddball (in which participants responded only to the rare stimulus), and two-alternative forced-choice (in which participants made one of two possible responses to each stimulus), fMRI showed ACC activity only during the low frequency trials (Braver, 2001). It seemed the ACC was active whenever the required response conflicts with the common response, regardless of what that response is.

Another feature of this ACC activity is that it correlates with the number of permissible responses. In word generation tasks, in which a participant must generate as many words as possible from a given stem, fMRI showed higher ACC activity when there was greater competition between acceptable responses (Barch et al., 2000). This activation was seen regardless of whether the participant was required to speak the word aloud or just think it (Palmer et al., 2001). When participants were told to respond to a given cue with any action within a modality (either a finger movement or speech), PET imaging showed increased ACC activity compared to when the action was precisely defined by the cue (Frith et al., 1991).

Error-signalling in conflict

There is, however, another view of this role of ACC that could explain its involvement across these tasks. For trials in which the conflict between the stimuli is high, or in which the number of possible responses could be overwhelming, the chance of an error would obviously be higher. Associations between the ACC and error-signalling are extensive, most regularly studied using electroencephalography (EEG). Upon error occurrences, an error-related negativity (ERN) was recorded whose distribution across the scalp electrodes indicated that the ACC was its source (Gehring et al., 2018). These could be seen both following an incorrect response itself and when subjects received feedback following an incorrect response. Similar error-related activity has been observed in the ACC using fMRI (Braver, 2001; Menon et al., 2001).

The association between the ACC and conflict monitoring cannot be fully explained by its role in signalling errors. In conflict-monitoring tasks, an ERN was seen in high-conflict trials, which are associated with a higher rate of error (Yeung et al., 2004). However, an ERN-like potential was still seen when participants did not make an error in these trials. An ERN with an ACC source could even be seen when a subject made an error, but was not aware of it (Miltner et al., 1997). In fMRI studies, different regions of the ACC were associated with activations during conflict and error. The caudal, dorsal region was active both during errors and high-conflict correct responses, while the rostral, ventral region was much more active during errors (Braver, 2001; Menon et al., 2001), although both were active to some degree in either (di Pellegrino et al., 2007). The sub-structure of the ACC may explain these inconsistencies in contributions during these conflict-monitoring tasks.

The structure of ACC

These aforementioned functions of the ACC can be generally divided into serving cognitive or emotional processes. Attentional neglect and conflict monitoring would be categorised as the first, while emotional regulation and pain would be the latter. This division holds true when looking at the structure of ACC. The ACC consists of two major sub-divisions, a dorsal (dACC) and rostro-ventral (rvACC) compartment with discrete patterns of connectivity. Meta-analyses of neuroimaging studies support an understanding of these areas as processing cognitive information (in the dACC) and emotional information (in the rvACC) separately (Bush et al., 2000, Fig 1.02).

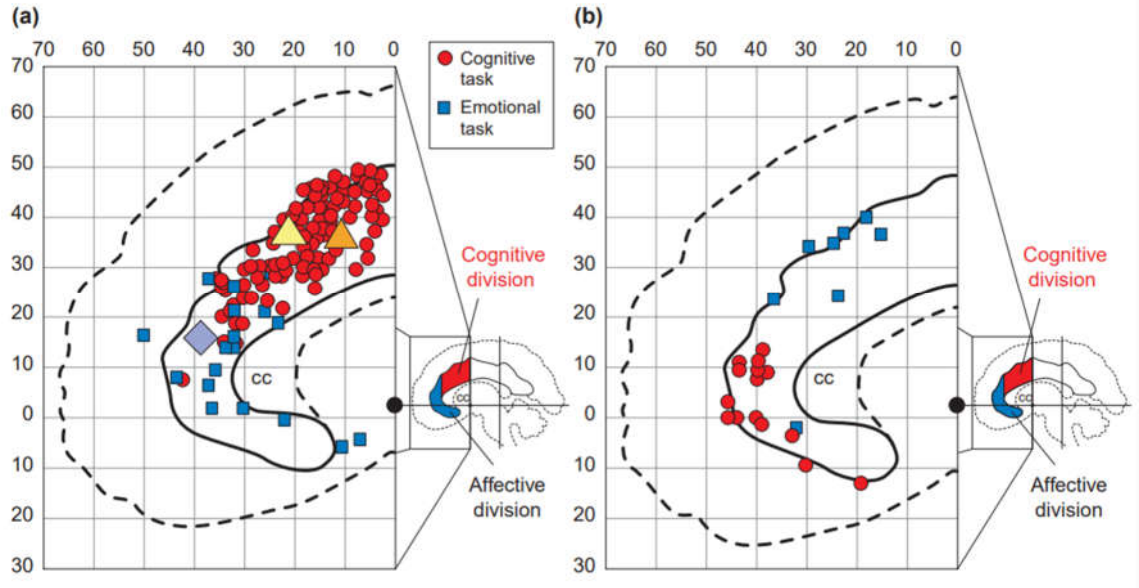

Figure 1.02. The function of ACC sub-divisions, from Bush et al. (2000). Meta-analysis of studies investigating regions of human ACC activated/deactivated during cognitive or emotional tasks. A: Regions that were activated by the task. B: Regions that were deactivated by the task. Special symbols denote tasks performed on the same group of subjects: the counting Stroop task (yellow, orange triangles) and emotional Stroop task (blue diamond). Co-ordinates are shown in 2D space. CC denotes corpus callosum.

The dACC connects more strongly with lateral PFC, as well as parietal cortex, premotor cortex, and supplementary motor areas to form an attentional network (Devinsky et al., 1995). It is believed to be responsible for the identified roles of ACC in motivation, response selection, and conflict monitoring. The rvACC instead connects more strongly with the amygdala and basal ganglia, and sends outputs to the autonomic, visceromotor, and endocrine systems. It is believed to be involved in regulating responses to painful or emotional stimuli. We can see from Fig 1.02 how two different types of Stroop task can activate a different sub-division in the same subjects. In the counting Stroop task, participants count the appearance of a certain word, and in conflict blocks the word will itself be a number to confuse their counting. The emotional Stroop task has no conflict dimension: instead the words to be counted will either have a neutral or emotionally-negative meaning. Activation in dACC was seen during the counting Stroop task (Bush et al., 1998), and activation in rvACC was seen during the emotional Stroop task (Whalen et al., 1998).

This bimodality may contribute to the error-signalling inconsistencies seen in ACC studies. Patients with rvACC lesions slowed less following errors and moved onto the next trial quicker in a conflict-monitoring task, compared to healthy patients (Carter et al., 2000). However, in a visual search task in which subjects could choose to abort trials to avoid errors, when unconfident, and receive extra rewards when highly confident, dACC was activated during these error-avoidance and high reward trials but was not activated on error trials (Magno et al., 2009). This suggests that dACC is involved when assessing one's own likeliness to commit an error, but not in error prediction or detection itself. An error could be considered to represent an unpleasant event, requiring uncomfortable introspection and self-assessment similar to an emotionally-negative event or memory. Greater activity in rvACC was when subjects made errors that lead to money loss, a negative event, compared to errors with no financial implication (Taylor, 2006). It could be that rvACC is involved in processing this emotional component of errors, rather than signalling the error itself. As errors are also more common in cognitively demanding high-conflict tasks, this could explain the attribution of error signalling to both sub-divisions of the ACC.

3. Cognitive roles for primate dorsal ACC

Adaption and persistence

Upon closer inspection it appears the ACC does not simply serve Broca's low-order, "bestial" functions, but instead describes his model of the two brains in a microcosm. The rostral-ventral compartment contributes to emotional responses while the dorsal compartment is involved in different facets of cognition, particularly conflict monitoring. However, to this point our focus has

been on studies of the ACC performed in humans. Studies in other primates, fellow constituents of this highest level of Broca's intellectual mammalian hierarchy, have yielded results that seem to contradict those from human studies.

During a saccade countermanding task, in which a subject must saccade in a given direction unless a stop signal is given, single-unit recordings from the dACC of two macaque monkeys found no conflict-responsive neurons (Ito et al., 2003). Instead, they found cells that responded to errors and rewards, particularly to unexpected rewards and the omission of an expected reward. Conflict was defined as trials in which the stop signal caused the monkey to successfully hold their fixation, despite the stop signal and initial cue being in conflict. In contrast, fMRI of humans performing the same task revealed increased activity in the dACC during these conflict trials (Curtis et al., 2005). If the conflict-monitoring theory does not hold with non-human primates, is this a genuine role of the ACC?

A potential explanation for this contradiction comes from the behavioural adaption and persistence model of ACC function (Kolling et al., 2016). In this model, the ACC encodes the value of alternative options to the one currently employed. During conflict monitoring, therefore, the ACC does not respond to the conflict itself, but the alternative response options implied by the conflict. This was demonstrated using single-unit recordings in the dACC of macaque monkeys performing a colour version of the Simon task, in which the colour of the stimulus denotes the required saccade direction (Nakamura et al., 2005). Conflict was introduced by either positioning the stimulus on the opposite side of the screen to the required saccade direction, or by changing the stimulus colour suddenly before the saccade to change the required response at the last minute. These recordings again revealed no neurons whose responses were enhanced during either conflict trial. Instead, the researchers found different sub-populations of neurons that became active when a specific response was required, even when the evidence for this was only partial (due to stimulus positioning or colour changes). This meant that during conflict trials, more activity was seen overall as over the course of the trial neurons coding for either response were active. In human studies, most evidence comes from non-invasive neuroimaging techniques such as fMRI and EEG are used which are incapable of distinguishing individual neuron firing. Thus, during the same task we could see what appears to be a conflict-related increase in dACC activity which in reality reflects the firing of two separate sub-populations of neurons coding the differing responses denoted by the conflicting stimuli.

The behavioural adaption and persistence view suggests that, rather than signalling conflict in stimuli or responses, the ACC signals the values of the presently available offers and outcomes. In particular, it signals the relative value of accepting a new offer and rejecting the current one –

adaption – or continuing to accept the current offer – persistence. This is frequently described in terms of foraging behaviour: an animal foraging for food in one location must weigh up the potential benefits of foraging in a new location, relative to the cost in terms of effort and potential food lost during the time they are travelling to the new location. An fMRI study in humans found dACC activity that encoded the value of searching the environment relative to the current option, as well as the cost of changing option (Kolling et al., 2012). However, in ecological foraging these choices would be made sequentially as the value of each option changes over time (Freidin & Kacelnik, 2011).

To model this, investigators used sequential decision-making tasks in which reward probabilities of each choice or response would change between trials and had to be estimated from recent response outcomes, similar to a depleting food source in foraging. Activity in the dACC was highest when subjects chose to reject their default option and choose a new one (Boorman et al., 2013). Single-unit recordings in macaque dACC found neurons that encoded the relative value of leaving one foraging patch for another (Hayden et al., 2011). The neurons fired during each sequential decision to stay at the current patch, and once the responses reached a threshold the monkey would choose to leave the patch. Optogenetic inactivation of the ACC in mice reduced this switching behaviour, with the mice electing to spend longer foraging at the current site (Vertechi et al., 2020).

These findings across species gave rise to the idea that the dACC functions by driving an animal away from their current behavioural state and towards an alternative. From this perspective, it is understandable that dACC was implicated in conflict monitoring, as many tasks would require a form of this behaviour. This adaption and persistence function relies on the dACC encoding choice value - the potential reward value of each alternative choice with its related effort cost subtracted. Across single-unit recordings throughout the PFC and ACC, the dACC showed the most significant encoding of choice value, with individual neurons responsive to the value of decisions across three dimensions: reward value, probability of success, and the time and effort required (Kennerley et al., 2009)These neurons were able to encode these three parameters, as well as reward prediction error, using a positively-valenced unified encoding scheme (Kennerley et al., 2011). Lesioning this area of monkey dACC did not impair performance after errors, but instead prevented them from being able to sustain performance in a reinforcement-guided task and to use their history of reward to balance persistence and adaption in a dynamic foraging task (Kennerley et al., 2006). Monkeys were also unable to refer back to their recent choice outcomes during rule-based decision making (Buckley et al., 2009).

These studies support this view of dACC encoding choice value in service of a larger role in promoting behavioural changes towards an alternative option. These choice value signals themselves are not unique to the ACC – they can also be found in the parietal cortex, striatum, amygdala, and dopaminergic system (Kolling et al., 2016). However, this role in signalling specifically the value of alternate options to drive adaption seems unique to the dACC, and can explain much of its earlier association with conflict monitoring. Despite this, there is another explanation for the engagement of dACC by conflict that challenges this adaption and persistence view of its function.

The expected value of control

A feature of focused attention is the application of top-down control from executive regions to lower-order regions, in order to better regulate the information permitted to working memory. Complex cognition relies on flexibly selecting only the information that is relevant to the current task. In visual attention, for example, long-range projections from the PFC can bias processing in the visual cortex in favour of attended-to visual features (Paneri & Gregoriou, 2017). During high-conflict trials, which require focused attention towards specific features of the stimuli and not others, a greater degree of top-down control is required to resolve the problem (Posner & DiGirolamo, 1998). However, top-down control is required in many tasks that do not feature conflict.

By manipulating conflict separately from the requirement of top-down control, it seemed dACC activation more closely tracked the application and cost of this control (Magno, 2006; McGuire & Botvinick, 2010). The expected value of control (EVC) theory postulates that the dACC is responsible for calculating the benefits (in terms of reward) and costs (in terms of cognitive effort) of top-down control in a given situation (Shenhav et al., 2016). This idea of cognitive control comes from the premise that all processes which contribute to behaviour exist on a spectrum between automatic and observed (Westbrook & Braver, 2015). Automatic behaviours are quick, low-effort, and inflexible, while observed behaviours require greater time and effort but can be flexible. These observed behaviours required cognitive effort, the subjective sensation of a task being demanding and effortful - though its neural basis is not well established (Kolling et al., 2012)(Rimpler, 2020). The objective of the dACC in this framework is to minimise cognitive effort expenditure while maximising potential gains, with the idea that this cognitive effort is taken from a finite supply.

The dACC therefore detects the need for cognitive control in the current task, compares this with learned costs and benefits from previous iterations, then dependent on the depletion of cognitive resources will execute the task or choose to avoid it. In cognitively-demanding tasks, dACC activity

scaled with the probability that the subject would choose to give up (Magno et al., 2006), or avoid the task in the next round (McGuire & Botvinick, 2010).

We can see how the EVC theory ties together earlier observations of ACC function. The effects on motivation, where ACC stimulation gave a subjective sense of a will to overcome, could be the mental manifestation of allocating cognitive control. The choice-value signals in dACC would also serve this purpose, as this value of control judgement would require encoding the learned benefits and costs of alternate strategies. It could explain why we see greater dACC involvement in conflict-monitoring and foraging tasks, as both demand control allocation to determine between competing alternatives.

The key difference between this theory and the adaption and persistence theory is that this theory states that dACC involvement is contingent only on the degree to which the current choice or behaviour demands control, rather than relating to a specific competition between persisting with or changing behaviour. These are understandably hard to untangle, overlapping considerably in many tasks. In a foraging scenario, if the value of staying and the value of leaving are the same, the two views would be inseparable: both would predict high levels of dACC engagement. However, when the value of leaving substantially outweighs the value of staying, they can be separated. The adaption and persistence model would predict that dACC engagement would be high, as it is signalling the value of this alternate option. The EVC model would predict low dACC engagement, as the optimal choice between the two is so obvious that the calculations of the value of control for either option needed are minimal.

Kolling and colleagues (2012) attempted this disambiguation by varying the probabilities of reward associated with the current and alternate options in a foraging-like task. They found that dACC activity correlated positively with the value of the alternate option and negatively with the value of the current option. Furthermore, they argued that because they did not see high dACC engagement when both reward values were equal, and therefore the choice should be at its most difficult, dACC was not involved in signalling choice difficulty. In a rebuttal, Shenhav and colleagues (2014) pointed out that choosing the alternative option in this task incurred a loss of points and a time delay, designed to model loss of reward and travel time in a real foraging task. This means that when both reward values are equal, the value of staying is still higher because it does not incur these punishments. They shifted this estimation of the difficulty peak to the right, closer to the highest alternative value, and found that now it predicted dACC activity even better than the reward value of the alternative option. Finally, they repeated the same experiment with more participants and found that this estimate of choice difficulty alone, without reward value, best predicted dACC activity (Shenhav et al., 2016).

From here comes the genuine conflict in dACC function, as both theories claim the others' is a side effect of its role in theirs. Recent and current cognitive load is encoded in the human dACC (Sheth et al., 2012), but so are different options during extended sequences of goal-directed behaviour (Holroyd & Yeung, 2012). The most important implication of either theory is where it places the dACC in human cognition. The adaption and persistence model portrays the dACC as a central integrator, assimilating choice-value inputs and triggering behavioural changes. The EVC model instead has the ACC as a kind of "fifth lobe", auxiliary to the rest of the frontal cortex in mediating the allocation of control to all other parts of the brain (Ebitz & Hayden, 2016). The unique diversity of the ACC's inputs and outputs make this at least possible, but these theories will ultimately be difficult to truly reconcile without developing a behavioural task that could truly isolate one from the other.

Prediction-error signalling

Both theories agree that the dACC is involved in monitoring the value of actions within a task, whether for evaluating control costs or alternate options. These rely on forming associations between an action and its outcome, whether negative or positive. Lesions to the monkey dACC impaired selection of actions associated with reward (Hadland et al., 2003), and performance in tasks that required learning which action was rewarded via reinforcement (Kennerley et al., 2006). When macaques had to pair either a presented stimulus or their own action with an outcome, dACC lesions impaired action-outcome pairing but not stimulus-outcome pairings (Rudebeck et al., 2008). In humans, action-outcome pairings were degraded by increasing the probability that the outcome will occur without performing the action. Activity in the dACC tracked these changes in action-outcome association strengths (Morris et al., 2022). The dACC was not responsive to motor actions themselves, instead responding to the valence of their outcomes (Weiss et al., 2018).

Clearly dACC is required to learn and maintain these associations between a given action and its outcome. However, dACC is particularly implicated when the associated outcome does not occur. Neurons in the monkey dACC encoded the degree to which a reward was anticipated (Amiez et al., 2005; Shidara & Richmond, 2002), and encoded prediction-errors when the reward was not received (Amiez et al., 2005; Ito et al., 2003; Matsumoto et al., 2007). Varying the number of predicted outcomes and the degree to which the outcome was unexpected revealed different regions of the dACC sensitive to each (Jahn et al., 2014). These effects were not limited to unexpected reward omissions. In a gambling task, ACC responds more strongly to losses when wins are more likely, but more strongly to wins when losses are more likely (Jessup et al., 2010). The feedback ERN seen following errors could also be seen following positive feedback, if the person was expecting the feedback to be negative (Oliveira et al., 2007). These suggest that dACC

is sensitive to violations of expectation, regardless of what the expectation is for. In fact, the frequently observed role of dACC in signalling errors may just reflect the optimistic expectations that a typical reinforcement task creates.

Can we conclude that dACC is simply involved in signalling surprise? In an fMRI study, humans responded to a target that appeared at an unexpected location. On some trials, the target's colour indicated that its location was informative for where future targets would appear. On others, the location was not predictive. Both trial types involved an unexpected event, reflected in the participants' slower reaction times. However, dACC activity was only seen when the target's location was meaningful for upcoming trials (O'Reilly et al., 2013). This suggests that the dACC does not respond to general surprise, and instead responds to surprising events only when they are useful for updating an internal model. In a Stroop task featuring occasional cues predicting whether the upcoming trial was congruent or incongruent, the highest dACC activation was seen during uncued incongruent trials (Carter et al., 2000), when the incongruence was unexpected.

This activation during the violation of expectations implies that dACC is comparing predictions about the outcomes of actions with their observed outcomes. Given its connectivity with both prefrontal areas and sensory cortices, the ACC could achieve this by integrating top-down predictions and bottom-up sensory errors. Predictive coding in sensory regions has been seen across a range of modalities. Cells in the primary visual cortex (V1) can respond to auditory tones that predict upcoming visual gratings even in the absence of visual input, in a manner predictive of the identity of the grating (Kok et al., 2014). This predictive coding has been speculated to underpin the formation of receptive fields (Jehee et al., 2006) and binocular rivalry (Hohwy et al., 2008) in visual development. The key is the integration of feedback connections from higher visual areas, conveying predictions, with feedforward connections conveying sensory input. This prediction-error signalling is widespread throughout the brain, with prediction-based modulation of responses to sensory input also seen in the retina (Srinivasan et al., 1982), lateral geniculate nucleus (Dan et al., 1996), motor areas (Deecke et al., 1969), auditory cortex (Rubin et al., 2016), and olfactory systems (Zelano et al., 2011).

What separates this lower-order predictive coding from the prediction-error signalling seen in the dACC is the relationship with attention. Predictive coding in V1 occurs constantly during vision (Attinger et al., 2017), and can even be seen in under anaesthesia (Muckli et al., 2005). The dACC, on the other hand, monitors the outcome of actions performed in service of a current task or goal, in order to update behaviour and improve performance.

Predicted-response-outcome

The predicted-response-outcome model (PRO) portrays the medial PFC, and dACC in particular, as primarily involved in predicting the probable outcomes of actions (Alexander & Brown, 2011). The model proposes that the dACC learns to predict future outcomes by following the principles of reinforcement learning, using prediction errors rather than reward to optimise action selection by inhibiting the actions that lead to negative outcomes and promoting those that lead to positive outcomes. The model incorporates several action-outcome predictions in parallel, each with their own respective probability. This is not just the probability of the outcome occurring, but of it occurring at that time – so an outcome occurring late will also trigger a prediction error. More probable outcomes will cause greater prediction activity, peaking at the expected time of the outcome. If the outcome does not match the prediction, a surprise signal proportionate to the probability of the outcome will feed back to influence future action-outcome predictions. These surprise terms do not reflect reward or punishment, but instead reflect positive or negative surprise: an unexpected occurrence or non-occurrence of an outcome respectively. The dACC will encode the number of different possible outcomes, with an activation that reflects the probability of each, and with each action-outcome probability re-assessed between events.

This model was able to simulate empirical findings using two tasks that frequently recruit ACC: the change-signal task and Eriksen flanker task. In the change signal task, a cue indicates the difficulty of the upcoming trial. A go signal is then presented - an arrow showing which button to press – after which a change signal – a larger arrow pointing in the other direction, instructing the participant to change their response – appeared in 33% of trials. In the difficult trials, the change signal appeared later, so participants had less time to respond. The PRO model would predict that ACC activity would be highest during the high-difficulty trials, as they are associated with the highest error likelihood and thus require the greatest outcome monitoring. fMRI confirmed that high-difficulty change trials and high-difficulty go trials engaged the dACC more than either low-difficulty trial (Brown & Braver, 2005). The flanker task was modified so that the central target and flankers both required a response, and conflict occurred when the two responses were incompatible. The PRO model here would predict similar activations in dACC when the responses were in conflict or could be executed simultaneously, as the dACC signals the number of predicted responses or outcomes rather than response conflict itself. Again, fMRI data corroborated this prediction (Brown, 2009).

The PRO model was also able to account for ERNs and potentials reflecting cognitive load from EEG studies, as well as psychometric observations in conflict-monitoring tasks such as the speed-accuracy trade-off (Schouten & Bekker, 1967). This describes how responses are made either slowly

but with high accuracy or quickly but with low accuracy. It is possible to reconcile parts of the PRO model with the EVC model, such as increased ACC activity during high error-likelihood, and the adaption and persistence model, like ACC activation proportionate to the number of possible action-outcomes. The three models are heavily interlinked: a task with a greater number of possible responses would require greater encoding of the possible responses, possible response-outcomes, and control value calculations.

PRO model in cognition

Finding prediction signals throughout the brain has led to a number of models that incorporate prediction-error signalling to give a unified account of processing across the cortex, such as the Free-Energy (Friston, 2010), Predictive Coding (Rao & Ballard, 1999), and Hierarchical Bayesian Inference (T. S. Lee & Mumford, 2003) principles. The PRO model is no different – Alexander and Brown (2019) propose that an intricate hierarchy of action-outcome prediction-error signalling loops could eventually yield a system capable of complex cognition.

There is a mechanism for such a hierarchy in frontal regions. The rostro-caudal axis of the PFC is thought to reflect an abstraction gradient, with the caudal regions associated with processing direct stimulus-response associations, and rostral regions associated with representing abstract information pertaining to goals and rules (Badre & D'Esposito, 2009). This is supported by the differences in connectivity and structure along this axis. Caudal areas are more differentiated and have greater interconnectivity, while rostral areas have more diverse projections, supporting a role near the bottom and top of a hierarchy respectively. A study using task switches of increasing abstraction, from stimulus-switch to response-switch to cognitive set-switch, found different domains in the PFC activated by each type, with activation becoming progressively more rostral as the switches became more abstract (C. Kim et al., 2011).

We have seen a similar rostro-caudal separation within ACC, although this gradient seems to run between emotion and cognition rather than through levels of cognitive abstraction. In the previous study (Kim et al., 2011), the least abstract response-switch condition also activated rostral areas of ACC, suggesting it too may lie upon this axis. Furthermore, abstract errors in the task activated more rostral areas of the ACC than concrete errors. Along the rostro-caudal axis of the ACC, a distinct topography of connectivity to different regions of the body is repeated in distinct clusters, with only minor differences in their motor responsiveness (Amiez & Petrides, 2014). This provides the potential framework for a hierarchical axis of repeating prediction-error loops, potentially one role within the greater hierarchy of the PFC. Through the motif of comparing the outcomes of events to their expected events, organised so that the events and predictions being

compared move up a hierarchy of complexity, prediction-error signalling across the ACC could be a contributory mechanism to the production of sophisticated cognitive behaviours.

4. The ACC in the multiple-demand system

Attentional episodes

Clearly the ACC is playing a small, not pivotal, role in cognition. This concept of hierarchical events, allowing for regimented processing loops to be co-ordinated to construct cognition, is not original to the PRO model. Cognition can be understood as divided into a series of organised attentional episodes, each with a sub-goal involving distinct actions, inputs, and potential outcomes arranged in a hierarchy towards the service of a larger overall goal (Duncan, 2013). The hierarchy here is key: if the sub-goals were not arranged in this structured manner, the overall problem would be unsolvable.

The multiple-demand system

Much of the brain's function is modular, dependent on specific specialised regions of the brain. This idea originated with Franz Joseph Gall (1758-1828) and was developed considerably by Broca's identification of the left inferior frontal lobe being highly specialised for language production (Broca, 1861). This localisation of function, though controversial at the time, is now thought to underlie many sensory and motor processes. However, it is not possible to attribute these attentional episodes to a single brain structure. Instead, they are attributed to the multiple-demand system, a collection of regions across the fronto-parietal cortices, including dACC, as well as subcortical structures like the basal ganglia and thalamus (Duncan, 2010a). These regions are active across neuroimaging studies employing a range of cognitive tasks, requiring different skills such as perception, language, and memory. Their activation scaled with the difficulty in task, determined from the participant's reaction times (Crittenden & Duncan, 2014).

The common activation of these regions across these cognitive tasks suggests that they may underpin fluid intelligence, driving processing in other brain regions to solve the problems posed by the particular task. One key role for the multiple-demand system is in decomposing these complex problems into this sub-goal hierarchy, which could explain the disorders of executive function seen following damage. At a network level, the system could sustain this procession through different sub-goals by having neurons with dynamic response profiles, able to code whatever information is the focus of the current attentional episode and quickly re-organise between episodes (Duncan, 2001). This has been shown in primates: when trained to categorise presented images as either "cats" or "dogs", around 20-40% of cells in the lateral PFC responded

selectively to one over the other (Roy et al., 2010). When new categorisation boundaries are applied on generated stimuli arranged along a gradient from 100% cat to 100% dog, these cells re-oriented their selectivity to reflect whatever categorisation boundary was in effect (Freedman et al., 2001). It seems that cells in the lateral PFC are capable of coding incoming information flexibly depending on what the current task demands. If dACC was contributing to these attentional episodes, it would need to show similar flexibility in its predictive coding to only represent predictions that are task-relevant.

The multiple-demand system attests that no single brain structure is responsible for fluid intelligence. Lesion studies of the ACC confirm that much of cognition is spared, with only select deficits in attentional tasks. But we can speculate about the ACC's contributions to complex behaviours based on what is known about its unique connectivity with cognitive and emotional regions, and about its function. Within these attentional episodes, prediction-error signalling in the dACC may facilitate monitoring of outcomes to judge the effectiveness of a given action towards achieving a sub-goal. Once a prediction error has been signalled, the dACC may drive behavioural changes away from the current strategy and towards a new approach. It may be involved in evaluating the required cognitive control when segmenting an abstract goal into hierarchical sub-goals, a process that may be impaired during goal neglect. The rvACC may also be contributing, evaluating incoming emotional and painful outcomes to provide feedback within an episode. As a part of the multiple-demand system the ACC may not be solely responsible for any one process, but through studies of lesions and activity during different cognitive tasks we can better characterise its contribution to fluid intelligence within the multiple-demand system.

5. Structure of the rodent ACC

Homology with the primate ACC

Thus far, nearly all of the studies mentioned have been in humans and other primates. The relative homology of the ACC across primate species, positioned around the superior and anterior border of the corpus callosum, led Broca to assume a negative correlation with intelligence. However, the homology between other mammalian species is still a subject of debate. We might assume from Broca's assertions that the rodent ACC, possessed by an order that prioritise their "bestial" smell over vision, would be far more elaborate and sophisticated than any primate ACC. However, many of the complex cognitive processes for which a role has been found for the primate ACC are much rarer in rodents. Establishing a homologue of the human ACC in rodents is important for these models to be useful for ACC research.

Medial prefrontal studies in rodents have typically targeted one of three anatomically-defined regions: the prelimbic cortex (PL), infralimbic cortex (IL), and ACC (Laubach et al., 2018). These areas are considered to be homologous to the primate mPFC, with the PL composing dorsomedial PFC and the IL composing ventromedial PFC. The ACC in this designation is divided into cingulate areas 1 (Cg1) and 2 (Cg2), rough equivalents of the primate dACC and rvACC respectively (Fig. 1.03, nonhomologous – *here dACC, and the anterior portion of PCC, are referred to as midcingulate cortex (MCC) and rvACC is referred to as ACC*). The sub-compartments of ACC are divided close to the horizontal axis, while in primates the division is closer to the coronal axis. This rodent ACC has strong inter-connectivity with PL and IL, and projects to sensorimotor and visual cortices (Sesack et al., 1989). Whether the lateral PFC has a rodent homologue is less clear (Preuss, 1995), but many regions in the mouse PFC are thought to be computationally, if not anatomically, homologous (Brown & Bowman, 2002).

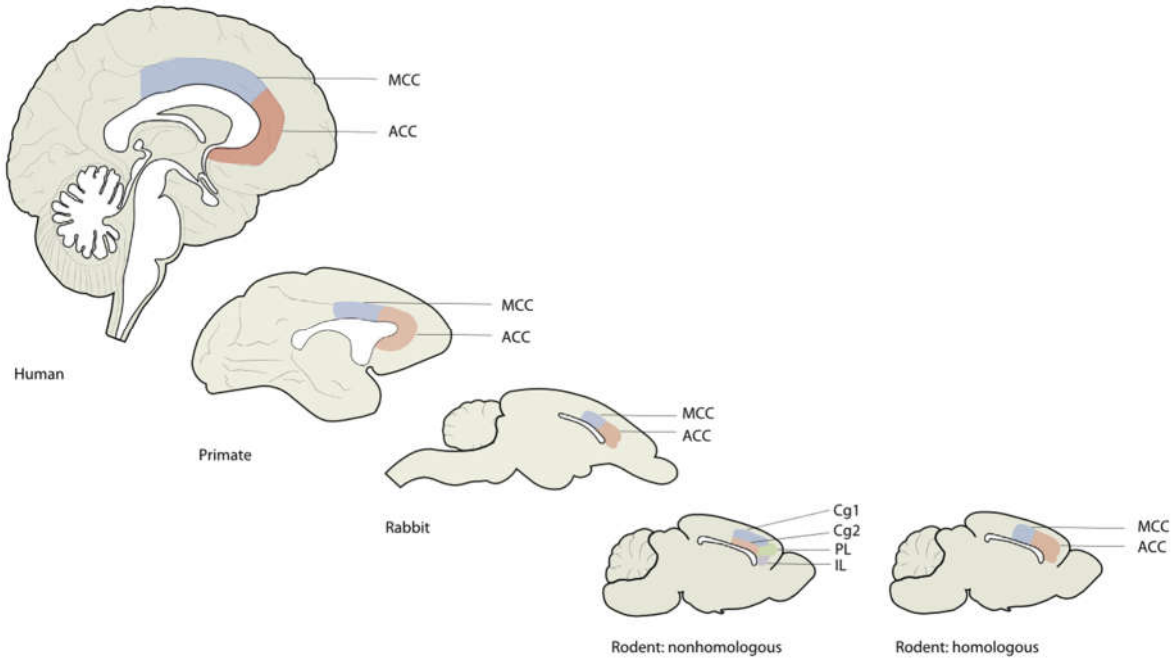

Figure 1.03. ACC homology across mammalian species, from van Heukelum et al., 2020. Regions designated as MCC (equivalent to dACC) and ACC (equivalent to rvACC) across humans, primates, rabbits, and rodents. Rodent: non-homologous reflects the structure of rodent PFC used across the majority of studies. Rodent: homologous reflects the structure recommended by the authors, with a greater equivalence to primate MCC and ACC in terms of connectivity and function.

However, in a recent review tracking the definitions used by a wide range of researchers purporting to study the rodent mPFC, Laubach and colleagues (2018) found a surprising lack of consistency in terminology. Comparisons of cytoarchitecture between the rodent and primate cingulate demonstrated that these medial frontal areas actually conform to the ACC in primates (Vogt et al., 2013), and many studies refer to these rodent areas as such. Despite this, when they asked researchers whether they considered PL part of the ACC in rodents, only a minority said yes.

The authors suggested that this discrepancy comes from the difference in the shape of the primate and rodent brain. As the rodent brain is flatter, the cingulate is less curved, causing a misattribution of the more rostral parts of rodent ACC to be separate structures.

If we instead consider the homology of the ACC in terms of connectivity and function, we arrive at a conception that stretches further rostro-ventrally across the rodent corpus callosum (Fig 1.03 – homologous). This new division between dACC and rvACC becomes more similar to that in primates, closer to the coronal axis. This separation better preserves the connectivity patterns with primate ACC, with rvACC connecting to the amygdala, basal ganglia, and autonomic brainstem nuclei, and dACC connecting to the parietal and premotor cortices (van Heukelum et al., 2020). Electrical stimulation of the rvACC in rodents produces effects consistent with those seen in macaques and humans: depressed autonomic activity causing reductions in blood pressure, heart rate, and breathing rate (Vogt et al., 2013). To corroborate this homology the rodent dACC would need to serve a comparable role in cognition. Testing this is limited by a rodent's capacity for performing complicated tasks, but there are many examples of successfully training rodents to model complex behaviours in a laboratory setting. From these we can see many of the features of the primate PFC that support attentional episodes are preserved in the rodent PFC.

Rodent models of fluid intelligence

In primate studies, adaptive coding was observed at the single-cell level as prefrontal neurons re-oriented their firing to the parameters of the current attentional episode. Probing the rodent PFC during the same behaviours is challenging, as a series of tasks with discrete stimuli, rules, and actions could easily overwhelm them. Durstewitz and colleagues (2010) overcame this by designing a task in which rats could press one of two levers. Initially, a light cue above one of the levers would tell the rat which to press to obtain a reward. After a given number of trials, the light cue stopped being informative, and instead only the choice of lever was important for triggering a reward. This way, they were able to force the rat to shift between two sets of rules, stimulus-led and response-led, without changing the stimuli or actions required. Implanting a 32-channel electrode into the rat's PFC allowed them to simultaneously record from many cells, including in the ACC. They found distinct patterns of network activity encoding each of the rules, which remained stable over time but transitioned abruptly following a rule change. This provided an example of how cognitive flexibility might be modelled in the rodent, using task-enforced rule changes while maintaining a manageable number of possible stimuli and responses. By using creativity in constructing the task, they demonstrated that the rodent PFC, like the categorising neurons of the primate PFC, is capable of fluidly coding the current task requirements.

This task simulated the changes in strategy that might occur between attentional episodes. But crucially in humans the episodes would be arranged in a sequential manner, with each sub-goal completed progressing the agent further towards completing a larger objective. To model this, rats were trained in a spatial decision-making task designed to reflect ecological food-searching (Lapish et al., 2008). In a delayed-win-shift radial arm-maze task, rats started with 4 of the available 8 arms open. Once they had explored all 4, they were locked into their final arm while all 8 arms were opened. Single-cell recordings from the ACC were performed as the rats moved through the maze, with any re-entries into a previously visited arm marked as an error. They found neuronal ensembles within the ACC with co-ordinated firing patterns that were distinct between the two phases of the task, seemingly tracking the different number of possible actions and outcomes in each. When the organisation of these ensembles' activity broke down, the rat made a greater number of errors. Like the previous study, it appears that these neurons are capable of fluidly encoding different stages of a task, but here the rules stay the same while the number of potential actions and outcomes change.

The rodent ACC seems to retain many of the properties of the primate PFC that are necessary for fluid intelligence - able to encode different rules, actions, and outcomes in a flexible manner depending on the current context. These tasks lack the abstraction of some of the primate tasks; training a mouse to categorise visual stimuli as "cat" or "dog" would likely prove challenging. In addition to participating in the multiple-demand system, the human ACC has specialised roles in behaviours involving adaption and persistence, EVC, and prediction-error signalling. By carefully choosing complementary tasks we can ask how well the rodent ACC conforms to these other theories of ACC function.

6. Function of the rodent ACC

Adaption and persistence in the rodent ACC

Behavioural adaption and persistence have been frequently modelled using a foraging-like task in humans (Kolling et al., 2012). Similar tasks, requiring decisions between persisting with the same response or choosing an alternate response in the hope of better rewards, are commonplace in rodent studies. Lesions of the rat ACC reduced competitive food foraging behaviour, while having no effect in other tasks probing exploratory behaviour such as the elevated plus-maze or open field test (F. Li et al., 2012). Optogenetic inhibition of the ACC in a hidden-states foraging task caused mice to spend longer at the current port (Vertechi et al., 2020), suggesting a role in encoding the decision to leave as in humans. However, while the rat ACC encoded decision

variables in a foraging task, the decision to leave was still made once the reward value of the current patch depleted to the value of the other patches during ACC inactivation (Kane et al., 2022). Here it seemed that the ACC was not essential for the decision to leave.

In a two-stage task rats made an initial decision between two nose poke ports. Depending on the first choice, one of another two ports became active. The second pair of ports could have a high, medium, or low reward value, which changed between blocks within a session. Which of the first pair of ports would activate each of the second pair also changed between blocks. This meant that the rats needed a co-ordinated strategy for which of the first ports to choose to access the highest reward in the second port, which they updated over time as the rules changed. Recordings from ACC showed abrupt changes in activity when a prior belief was abandoned, with a brief period of network instability as the rat begins to explore different strategies. As they formed a new strategy, stable representations of the new contingencies emerged (Karlsson et al., 2012). This suggests a role for the ACC not in directly encoding the decision to leave, but encoding the current strategy even across multiple stages. Encoding of task features is so flexible that ACC neurons can even show spatial mapping – like broadly-tuned place cells – when the task requires spatial decision-making (Euston & McNaughton, 2006). When a mouse planned an excursion to a specific feeder, the spatial position that could be decoded from their ACC activity resembled the target feeder rather than their current position (Mashhoori et al., 2018).

Behavioural strategy encoding

It seems that instead of encoding the specific decision to leave, the rodent ACC encodes the behavioural strategies themselves in an organised manner, with transitions between these activity patterns as the strategies change. This encoding appears to be necessary for the animal to coherently employ strategies. Rats competing against a computer had to choose between a left or right reward port, and only received a reward if their response differed from the computer competitor's response. They learned to use a counter-prediction strategy, essentially choosing the opposite of whichever port the computer would consider them to be biased towards from their past behaviour. When the competitor pattern changed to one that encouraged unpredictable responding, the rats needed to switch to using a stochastic approach with no developed strategy. When the experience-dependent counter-prediction strategy was abandoned in favour of random responding, the ACC was suppressed. Compellingly, they found that chemogenetic enhancement of inputs into the ACC from the locus coeruleus (LC), a brainstem nucleus thought to control arousal via noradrenaline secretion, triggered switching between these two modes of responding (Tervo et al., 2014). This suggests a role for the ACC in maintaining internal representations of strategies, with projections from the LC promoting strategy shifts.

How are these strategies encoded in the ACC? An advantage of rodent research is the greater variety of tools available to discriminate different sub-classes among the cells recorded. Using opto-tagging (expressing Channelrhodopsin2 selectively in one sub-class, then seeing which of the recorded cells respond when light is applied) allowed the main two sub-classes of interneuron in the rodent cortex, fast-spiking parvalbumin (PV) and slower-spiking somatostatin (SOM) positive interneurons, to be recorded with an implanted microdrive while mice performed a foraging task. SOM interneurons responded when mice approached a reward, while PV interneurons responded when mice left the reward and encoded the duration of the time they had stayed at that patch (Kvitsiani et al., 2013). It seems that by balancing inhibition through these two sub-classes, with PV cells typically targeting the soma to elicit fast, synchronised inhibition and SOM cells targeting the dendrites of pyramidal cells to elicit slower, output-selective inhibition (Kepecs & Fishell, 2014), ACC neurons can bookend the behavioural epoch of the mouse's decision to stay.

Rodent ACC circuits seem specialised for encoding strategies during decision-making, and able to fluidly transition as the required strategy changes. But are they actually required for any one part of decision-making? We have seen conflicting results in foraging tasks, with ACC lesions reducing competitive foraging (Li et al., 2012), increasing time spent choosing to stay (Vertechi et al., 2020), but not changing the threshold for the decision to leave in hidden-states tasks (Kane et al., 2022). The key here may be in the effort required to leave: when the options in a foraging task require competitive effort, ACC neurons exhibited heightened activity for the trajectory involving greater effort (Hillman & Bilkey, 2012). This pattern has been observed in humans - greater activity in the dACC during tasks a participant was more likely to abandon (Magno et al., 2006) or avoid in the future (McGuire & Botvinick, 2010). This suggests a similar role for the rodent ACC in estimating control costs.

EVC in the rodent ACC

The challenge in researching control value estimates in rodents is creating a task which drives them simultaneously appraise different costs – in terms of effort expended - and benefits – in terms of rewards earned - before choosing a response. Tasks offering mice a low effort, low reward option or high effort, high reward option found that ACC lesions biased them towards selecting the low effort option (Kashay et al., 2022; Rudebeck et al., 2006). This was not caused by a failure to compute the relative reward sizes, as when the effort required was equal they instead chose the high reward option (Kashay et al., 2022). This low-effort bias was reproduced when optogenetically inhibiting projections to the ACC from the nucleus accumbens (NAc) specifically, implicated in reward-driven motivation (Hauber & Sommer, 2009). Blocking excitatory synaptogenesis in the mutant mouse ACC caused them to exert less effort to gain the same amount of reward as

wildtype mice (Severino et al., 2021). While rats travel across an angled chamber, their ACC neurons encoded the different effort conditions with an overall bias for the easiest condition (a steep downhill gradient) and the largest reward (Porter et al., 2019). These studies point to a clear role for the rodent ACC in evaluating effort costs and reward sizes in decision-making, using input from the striatum.

Is this a true EVC function, or simply an overall loss of motivation following a disruption of ACC signalling? The EVC model is rooted in neuroeconomics, with the idea of a finite pool of cognitive effort that must be apportioned responsibly (Westbrook & Braver, 2015) – a difficult concept to simulate with rodents. One study used an economics approach, offering rats one of two flavoured soya milk rewards. Each rat had a preferred flavour, so the experimenters modified the number of nose pokes required to obtain each so that one flavour would have a higher cost, in terms of effort, than the other. They also simulated the idea of a budget by restricting each rat to a certain number of nose pokes per session before they no longer had an effect, which the rats would learn over repeated sessions. They found that when prices changed, rats would bias their preferences towards whichever reward was cheaper. When the total budget was not increased as well, this effect was more pronounced – except in rats with ACC lesions (Hu et al., 2021). It seems that rodents are capable of something approaching a genuine evaluation of how to apportion effort in finite conditions, and that their ACC is necessary for this process.

Prediction-error signalling in the rodent ACC

The primate dACC has a consistent role in encoding predicted outcomes of actions (Rudebeck et al., 2008), whether positive or negative. When these predictions were violated, dACC signalled a prediction error only if the violation proved meaningful to an internal model (O'Reilly et al., 2013). Similarly, research in rodents has attempted to manipulate the predictability of outcomes throughout a session. When reward size was smaller or larger than expected, activity in the rat ACC was increased (Bryden et al., 2011). But are these outcome predictions similarly being used by the animal to update their internal model of the task, in order to maximise reward?

In one such task, rats were presented with three nose poke ports. The central port had a 50% chance of giving a reward throughout the session, while the lateral ports had a 25% and 75% chance of being rewarded respectively and switched throughout the session. Electrophysiological recordings revealed ACC neurons whose firing reflected recent reward outcomes at a given port. Depending on the port and the recent history, these neurons would encode a prediction of reward or non-reward. When an unexpected outcome occurred, the neurons would shift to representing the actual outcome rather than the predicted, in order to form a new mapping for this port. During each nose poke, the firing states of ACC neurons correlated so strongly with their firing states

following the actual occurrence of the predicted outcome that the prediction could be decoded from these initial states (Hyman et al., 2017). The researchers also found a local field potential that resembled the feedback ERN seen in humans and monkeys, whose existence in rodents had been a subject of controversy. It seems that like in primates, the rodent ACC is heavily involved in encoding predicted outcomes of actions.

In the previous task, the action and the outcome are inseparable as the reward will immediately follow the nose poke. Another task attempted to separate these in time by incorporating a two-step task, in which the mouse had to initially choose between a top or bottom port. Based on this first choice, either a left or right port was illuminated, each with a probability of giving reward. Two facets of the task could change between blocks of trials: the reward probability of this second pair of ports, or the 'transition probabilities' linking the first choice to which of the second pair was illuminated. *In vivo* calcium imaging showed that the ACC encoded both probabilities as predictions, allowing the ACC to predict both future rewards and future states depending on the action chosen. It also responded when these predictions were violated following a block transition. Optogenetic ACC inhibition reduced their ability to integrate recent block transitions into their choice on each trial (Akam et al., 2021), which would rely on updating these predictions. This showed that like in the other foraging tasks, ACC activity seems to be necessary for sustaining coherent strategies via predictions based on recent action-outcomes.

In a similar task, a tone denoted whether the upcoming trial involved the left or right port. As each port had its own probability of reward, mice could choose to nose poke at the given port or in the central port to trigger a new trial, if they deemed the chance of reward at the given port too small. Reward probabilities changed over time, and the rats changed their preferred side accordingly. ACC ensembles encoded both the strategy to repeatedly choose the preferred side, and the strategy to sample the non-preferred side after probability shifts. Optogenetic perturbation of the ACC during the tone increased the probability they would choose the preferred option, but perturbation just after an anticipated reward was not received increased acceptance of the non-preferred option (Tervo et al., 2021). These studies have demonstrated that the rodent ACC encodes outcome predictions that change as probabilities shift, and are required for changes in strategy based on recent violations of these predictions.

Passive prediction-error signalling

There is evidence that these predictions may not be limited to the animal's own actions. In a chronic pain experiment, the rat ACC encodes predictions of pain which enhance avoidance behaviour via projections to the periaqueductal grey (Lee et al., 2022). When anaesthetised rats were presented with repeated ascending, descending, or statically-pitched auditory tone

sequences, electrophysiological recordings revealed responsiveness in the ACC to tones that were deviant – the wrong pitch relative to its neighbours – or oddball – missing entirely within the sequence. The ACC, in contrast to the auditory cortex, was less responsive to regular tones and more responsive to these prediction-error tones. These ACC prediction errors were slow, appearing around 120ms after the expected onset of the tone, but sustained for more than 600ms, enduring past the next tone in the sequence (Casado-Román et al., 2020). This suggests some kind of prediction-error tuning in the rodent ACC that exists beyond any requirement for subsequent behavioural adaptation, unlike in the primate PFC (O'Reilly et al., 2013).

It seems Broca's observation of the atrophy of the cingulate in primates has not caused a contrast of purpose: functionally, it seems that the dACC is relatively well-preserved from primates to rodents. The three major theories of dACC function in primates - adaption and persistence, EVC, and prediction-error signalling – concur with many studies of the rodent ACC's contributions to behaviour. In foraging-like studies, the ACC encodes decision variables and is required for the implementation of model-based strategies. When greater effort is required to earn a larger reward, ACC lesions bias rodents to the easier option. During hidden-states tasks, the ACC encodes action-outcome predictions and uses violations of these predictions to guide future actions.

However, there are some key differences with this prediction-error signalling. These predictions do not need to be action-oriented or even behaviourally-relevant, as it seems the rodent ACC can respond to general expectation violations even unconsciously. This is a key difference: if we are positioning the ACC within the multiple-demand system sustaining attentional episodes, it should only be encoding information that is behaviourally-relevant at that moment. If predictive coding in the ACC is not influenced by attention, it may simply be a passive encoder of expectations across different modalities without any grating dependent on what is behaviourally-relevant. One of the first observations linking the primate ACC to cognition came from attentional studies, finding unilateral neglect and impairments to focused and sustained attention following lesions. Does the rodent ACC have a similar role in facets of attention?

Selective attention

Conflict-monitoring tasks require two aspects of attention: focused attention to produce a response, but also selective attention to ignore the conflicting features of the stimulus. Selective attention is the ability to dedicate sensory processing resources in favour of behaviourally-relevant stimuli and away from behaviourally-irrelevant stimuli (Cohen, 2014). We see this in conflict-monitoring, when the participant ignores the meaning of the word or local features in order to report the colour of the word or global features. The process relies on top-down attentional signals from executive regions biasing sensory processing to enhance task-relevant signals and suppress

task-irrelevant signals (Posner & Driver, 1992). The ACC is one possible source: ACC inactivation in schizophrenia (Carter et al., 1997) and cingulotomies (Janer & Pardo, 1991) both cause impairments in selective attention.

Attentional modulation of processing

Selective attention is frequently modelled using attention-switching tasks. Often in these tasks certain stimuli or features of stimuli are behaviourally-relevant, while others are behaviourally-irrelevant, and the categorisation can shift within a session depending on the rule. In the Stroop task (Pardo et al., 1990), depending on the rule either the colour or the meaning of the word can be relevant or irrelevant. Recordings from the sensory areas implicated in processing the relevant and irrelevant stimuli or features can show how attention influences this local processing. Cells in the mouse visual cortex are more selective for visual stimuli when they are motivationally relevant, compared to the same stimuli when they are irrelevant (Poort et al., 2015). Similar results have been seen in somatosensory areas with tactile tasks (Burton et al., 1999), and in auditory cortex with acoustic stimuli (Atiani et al., 2014).

The multiple-demand system must filter the otherwise overwhelming volume of incoming bottom-up information to remove inputs irrelevant to the current sub-goal. Top-down control of sensory processing provides a mechanism for this, by which specific sensory inputs can be prioritised according to the needs of current episode. Lesions to the rodent ACC can impair visual selective attention (Kim et al., 2016), suggesting a role in mediating this top-down control. As the agent progresses through attentional episodes with different priorities, the targets of this top-down control would need to change accordingly, so the source of the top-down control would need to flexibly represent the current task. This can be modelled using attentional set-shifting tasks, in which both the identities of the relevant stimuli and the rules for separating them can change.

Attentional set-shifts

In a set-shifting task, the subject must learn an initial rule, then must learn to shift this rule as the task changes. These shifts can be intra-dimensional, requiring a new rule to be applied to the same stimuli, or extra-dimensional, requiring the same rule to be applied to different stimuli (Bissonette et al., 2013). Revisiting the Stroop task (Pardo et al., 1990), ACC engagement is most evident when comparing across an extra-dimensional shift, when participants must report the colour of either congruent or incongruent words. In this case, the rule remains the same – report the colour – but the possible stimuli are different between incongruent and congruent trials. An intra-dimensional shift can be enforced by requiring participants to switch from reporting the colour of the word to

the meaning of the word, thus shifting their attention from the word's appearance to the word's meaning.

In mice, lesions to the mPFC (including ACC) during an odour discrimination task impaired extra-dimensional set-shifts while lesions to the more lateral orbitofrontal cortex (OFC) impaired reversal learning, when mice had to reverse the rules they had associated with two odour cues (Bissonette et al., 2008). Within the mPFC, ACC was required for attention-switching between closely-related stimuli, such as two different odours, while the PL and IL were required for attention-switching between obviously contrasting stimuli, such as different modalities (Ng et al., 2007). This suggests a critical function for the ACC when switching attention between stimuli with overlapping features. This fits with many of the ascribed functions of ACC: in processing conflict, prediction errors, or for apportioning control during more difficult tasks.

While the mPFC signals the associations between stimuli, responses, and outcomes inherent in these rules (Boettiger, 2005), lesions do not prevent initial rule learning (Birrell & Brown, 2000; Bissonette et al., 2008). These rules instead seem to be stored in the hippocampus, with its projections to the mPFC conveying rule-related information (Navawongse & Eichenbaum, 2013). PL neurons seem to encode initial rule-learning, while IL neurons encode the relevant action required by the rule (Rich & Shapiro, 2009). During intra-dimensional set shifts, IL was required for choosing the required strategy and PL for sustaining it (Oualian & Gisquet-Verrier, 2010). ACC neurons instead seem to be critical for extra-dimensional shifts, particularly when the stimuli are perceptually similar (Bissonette et al., 2008).

However, exactly what the ACC is contributing to these extra-dimensional set-shifts is unclear. As with so many of its associated cognitive tasks, the contribution of the ACC could be explained by any of its attributed functions. In its classical role, it could be monitoring response conflict and thus be most engaged by these perceptually overlapping stimuli. It could be signalling the two possible responses associated with different features of this same stimulus, in order to override the default pre-shift response. Overlapping stimuli are difficult to discriminate, so the ACC may instead be estimating and apportioning control to this high-difficulty task to give the animal a needed sensation of motivation in order to apply careful selective attention. This could all also fit into the framework of the ACC as an action-outcome predictor, signalling prediction-errors when the previously-used response to the stimulus does not yield a reward, in order to trigger a change in response selection. This project aims to challenge these hypotheses by investigating this role of the ACC both at a neural and behavioural level.

7. Project aims

This project's behavioural paradigm models attention switching in flexible behaviour by using extra-dimensional set-shifts. Different blocks require selective attention either towards visual stimuli, or away from these same visual stimuli and towards odour stimuli. This allowed the examination of how processing of the same stimuli in the visual cortex differs when they are relevant or irrelevant (Poort et al., 2015). The use of 2-photon calcium imaging allowed these recorded cells to be classified as pyramidal or belonging to one of the three major interneuron sub-classes (Khan et al., 2018). V1 neurons were shown to increase their selectivity for the visual stimuli when they were relevant to the mouse. This attentional modulation can be attributed to some form of top-down control, as has been seen from mPFC (Delatour & Gisquet-Verrier, 2000), retrosplinial cortex (Makino & Komiyama, 2015), and the thalamus (Wimmer et al., 2015).

The ACC is a strong candidate for this role – we have seen its role specifically in extra-dimensional attention switches, as well as in tasks that require response selection, conflict resolution, and control allocation like this one. In the rodent brain it projects directly to V1, unlike PL and IL (Sesack et al., 1989), and these top-down projections can influence local processing (Zhang et al., 2008). However, it is just one of many possible candidates for a source of control. The aims of this project are:

- To use temporary bilateral lesions to determine what, if any, role the mouse ACC plays in an attention-switching task requiring extra-dimensional shifts between visual and olfactory stimuli.
- Once any role has been established, to use 2-photon calcium imaging to examine how the ACC encodes this task-critical information at a network level, including:
    - The appearance and projection targets of these task-relevant signals and their underlying circuits.
    - Establishing how stable this network encoding is over repeated recording sessions on subsequent days.
    - Examining whether interneuron-specific circuit perturbations at specific times can disrupt this encoding of task-critical information.

In line with this two-step approach, the results in this thesis are split into two sections: the first investigating which aspects of the behaviour rely on the ACC, and the second investigating how this role is represented at a neuronal level. Each has a separate discussion chapter discussing the implications and caveats of each set of findings, with a final discussion chapter summarising and contextualising all of the results.

MATERIALS AND METHODS

Materials and Methods

All experimental procedures were carried out in accordance with the institutional animal welfare guidelines and licensed by the UK Home Office.

1. Surgical Procedures

During all surgeries, anaesthesia was induced at 4% concentration and maintained at 1% using isoflurane, mixed with oxygen delivered at 1l/min. Following induction mice were fixed in place using stereotaxic ear bars and anaesthesia was delivered via a nose cone. Additional drugs were used to provide analgesia (Metacam 5mg/kg), anti-inflammatory effects (dexamethasone 3.8mg/kg), and to reduce mucus secretions (Atropine 0.08mg/kg). Eye-cream (Maxitrol) was applied to the eyes to prevent drying and body temperature was maintained at 37°C using a heating mat and rectal temperature probe (Harvard Apparatus).

Following anaesthesia induction, hair on the scalp was trimmed using an electric razor and removed using depilation cream. A circular area of scalp was removed above the ACC, and the underlying skull was cleaned.

Silencing experiments

For the muscimol infusion silencing experiments, 4 male wildtype C57Bl/6j mice (P42) were implanted with a 26 gauge bilateral guide cannula (Plastics1, Bilaney) in the ACC (-1.1mm DV, +0.7mm AP relative to bregma, ±0.5mm ML, bilaterally). Small holes were drilled for implantations using stereotaxic co-ordinates. During infusions, an internal cannula with a 0.1mm projection was inserted into the guide cannula to give an effective infusion depth of -1.2mm DV. Between infusions, a dummy cannula was inserted into the guide cannula and held in place with a dust cap to prevent debris entering the infusion channel.

For the ACC/PL optogenetic silencing experiments (Fig 2.01), 8 transgenic mice (P42-49, 4 males and 4 females) expressing Channelrhodopsin-2 in parvalbumin-expressing interneurons were used, obtained by crossing Gt(ROSA)26Sor$^{tm32(CAG-COP4*H134R/EYFP)Hze}$ and Pvalb$^{tm1(cre)Arbr}$ mice (The Jackson Laboratory, strains # 204109 and # 017320 respectively). Two small holes were drilled above the ACC and prelimbic cortex (PL) of each hemisphere. Dual-core cannulae with bilateral optical fibres (Thorlabs), each with a 200µm diameter, 0.39 numerical aperture, and cut to a length of < 3mm, were implanted in the ACC (+0.9mm AP relative to bregma, -1.2mm DV, +/-0.35mm ML) and PL (+2.6mm AP relative to bregma,-1.25mm DV, +/- 0.35mm ML), and the stainless steel ferrules were bonded to the skull using dental cement (C&B Superbond), along with a custom

machined head-plate. PL implants were inserted at a 25° angle (relative to vertical) through holes drilled 0.8mm anterior to PL. This allowed sufficient space above the skull between the two implants to later connect both to optic fibres.

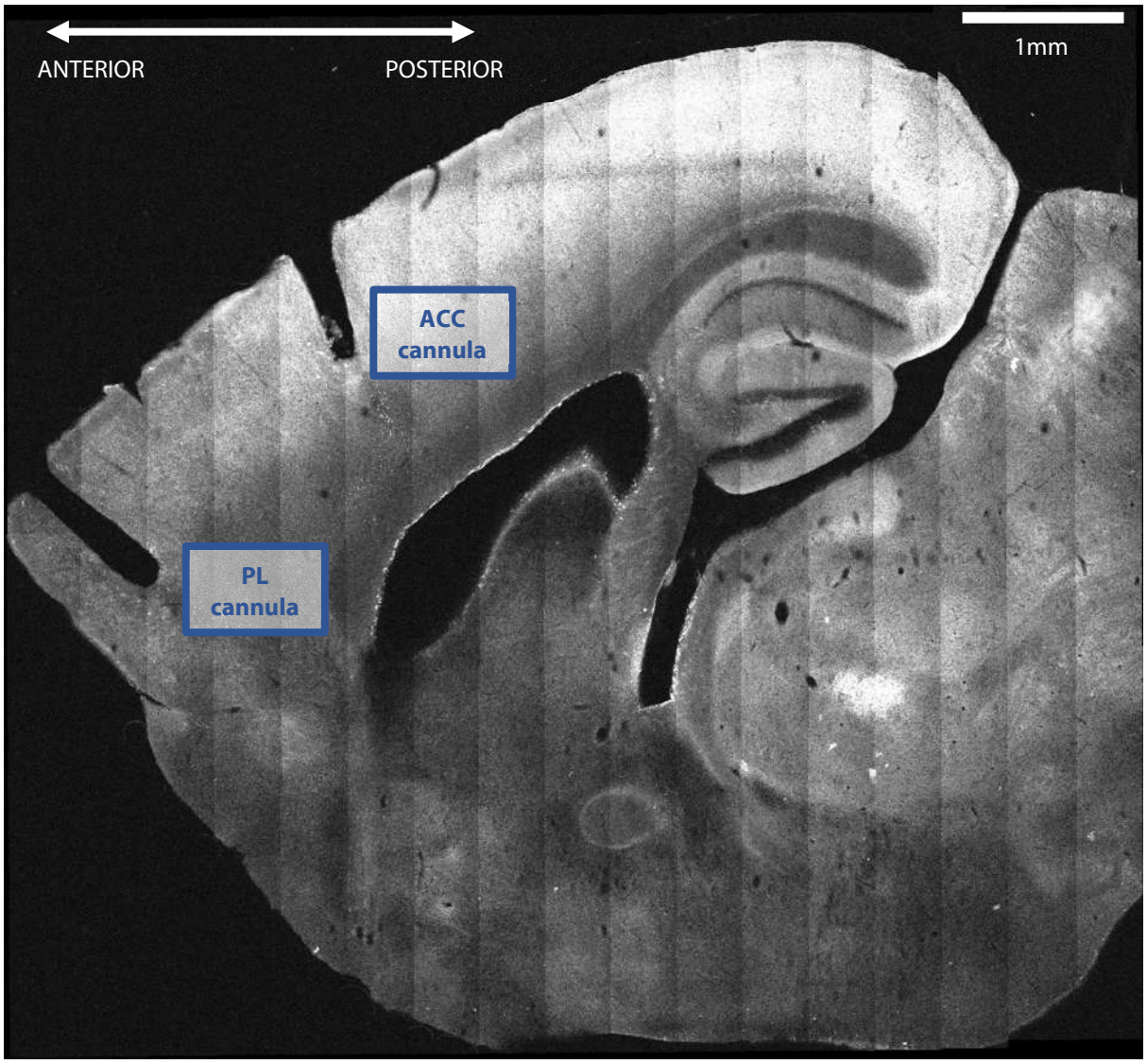

Figure 2.01. Optogenetic cannulae implants. Sagittal brain slice (0.4mm ML) from representative PV-Cre; Channelrhodopsin2 mouse showing locations of ACC and PL optogenetic cannulae implantations. Image taken by Marian Fernandez-Otero.

For ACC-only optogenetic silencing experiments (Fig. 3.19), 3 Pvalb$^{tm1(cre)Arbr}$ mice (1 male and 2 females) and 3 Gt(ROSA)26Sor$^{tm32(CAG-COP4*H134R/EYFP)Hze}$;Pvalb$^{tm1(cre)Arbr}$ crossed mice (2 males and 1 female) were implanted with cannulae above ACC only. Optogenetic cannulae were covered with plastic dust caps to prevent debris entering the internal fibres.

Injections of antibiotic (Betamax 120mg/kg) and analgesia (methadone hydrochloride 10mg/kg) were given at least 2 minutes before the withdrawal of anaesthesia. For at least 2 days following surgery post-operative pain relief was administered orally or subcutaneously (Meloxicam). After at least 5 days of recovery post-surgery, mice began habituation then behavioural training.

Imaging experiments

For the coronal microprism implantations, 10 C57BL/6-VIP$^{tm1(cre)zjh}$ mice (The Jackson Laboratory, strain # 010908, P42-49, 6 males and 4 females) were used. Small holes were drilled in the skull above injection sites, located using stereotaxic co-ordinates. Injections of a mixture of viruses expressing GCaMP7f (pGP-AAV9-syn-jGCaMP7f-WPRE, ~3x10^{-11}vg/ml Addgene) and Chrimson (pAAV5-syn-FLEX-rc[ChrimsonR-tdTomato], ~7.5x10^{-12} vg/ml Addgene) were made in the ACC (+0.9mm AP relative to bregma, -1.3 rising to -0.55mm DV, Fig 2.02) in layers II/III and layers V/VI of either the left or right hemisphere (+/- 0.25 and 0.55mm ML respectively), using glass pipettes and a pressure micro-injection system (Picospritzer III, Parker). The decision on hemisphere to use was made based on which had the sparsest blood vessel coverage, which was visible following skull cleaning. Up to 100nl of virus mixture was injected at each 250µm interval. An injection of Cholera Toxin Subunit B (recombinant, 1µg/µl) conjugated to Alexa Fluor 647 (ThermoFisher) was made in the dorsomedial striatum of the same hemisphere (+1.2mm AP relative to bregma, +/- 1.5mm ML, -2.5 rising to -2.0mm DV, 200nl per 250µm) to retrogradely label all cells projecting to this area of the striatum. 8 out of the 10 injected mice had sufficiently high-quality z-stacks taken from their imaging sites to visualise CTB-Alexa-647 and were used to identify striatal projecting ACC neurons.

A circular craniotomy (diameter = 3mm) was made above the ACC imaging site, with a centre on average 300µm posterior to ACC injections. This centre was moved to account for the position of the microprism relative to the centre of the coverslip, as the vertical face of the microprism was never perfectly positioned along the diameter of the coverslip. As this craniotomy always overlapped with the superior sagittal sinus, it was rare to complete drilling without any bleeding – this was controlled using a haemostatic sponge (Medispon) and saline. Once the drilling was complete, a constant flow of saline over the craniotomy site was maintained using a gravity-flow system and vacuum. The skull flap was removed and the microprism could be implanted. A 1.5mm x 1.5mm x 1.5mm right-angled microprism with a reflective hypotenuse (Tower Optical) fixed to a glass coverslip using ultraviolet light-cured glue (Norland, Thorlabs) was slowly lowered into the craniotomy, with the vertical face closest to the injection site. Suction applied through a glass filament, manoeuvred by a stereotaxic arm, allowed the microprism/coverslip to be held and gently lowered from the superior face of the coverslip. Once the glass coverslip had been moved into position, the saline flow was stopped and cyano-acrylic glue (Loctite) was used to secure the coverslip in place. Next, a custom machined aluminium head-plate was cemented onto the skull using dental cement (C&B Superbond).

For sagittal implantation surgeries (Fig 4.06), 3 wildtype C57Bl/6j mice, 2 C57BL/6-VIP$^{tm1(cre)zjh}$ mice, and 2 C57BL/6 Sst$^{tm2.1(cre)Zjh}$/J mice (The Jackson Laboratory strain #013044, P42-49, all female) were

used. Injection co-ordinates were the same but in the contralateral hemisphere to the implantation hemisphere. The microprism was implanted at a different orientation, with the vertical face of the microprism parallel to the midline of the brain. The two mice in Fig 4.32 came from these surgeries, with the VIP-Cre mouse injected with GCaMP7f diluted in ArchT (pAAV5-FLEX-ArchT-tdTomato, ~2.6x10^{-12}, Addgene). One further coronal implantation mouse was included in Fig 4.06, a male wildtype C57Bl/6J mouse P42.

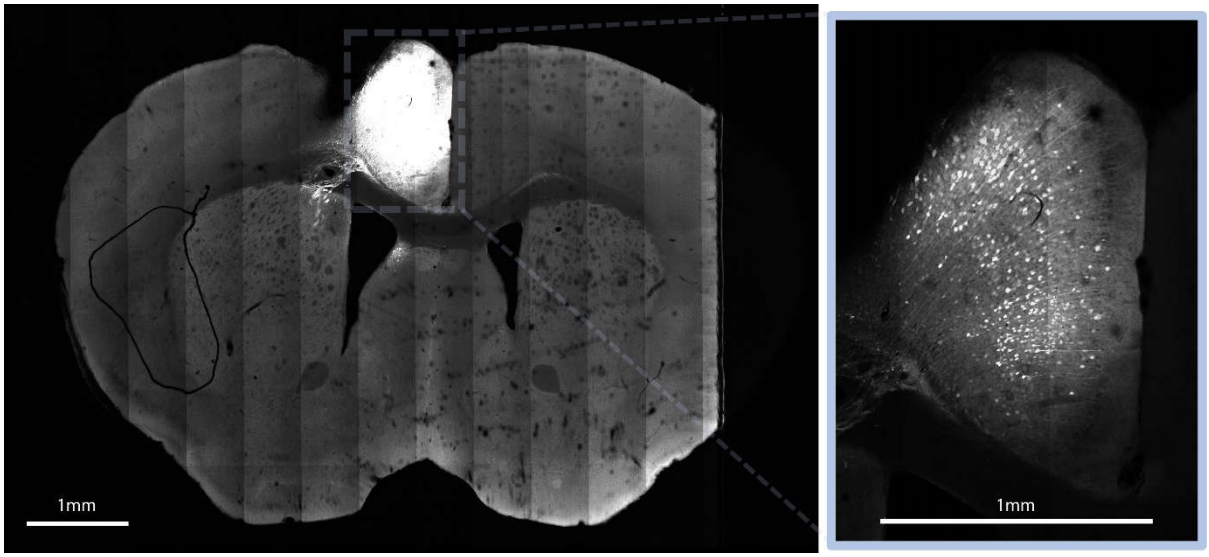

Figure 2.02. GCaMP7f expression for coronal microprism implants. Left, whole brain image of coronal microprism slice (~+1.2mm AP) from example coronal microprism mouse, to show location of GCaMP expression relative to the rest of the brain. Right, expanded image of injection site from same brain, to show expression of GCaMP among cells in the ACC. Image taken by Marian Fernandez-Otero.

For V1 imaging surgeries (Fig 4.10), 4 CaMK2a-tTA;tetO-GCaMP6s mice (The Jackson Laboratory, strain #024742 and #003010 respectively, P42-49) were used. No injection was needed, as mice expressed GCaMP6s endogenously in excitatory neurons. Following craniotomy, a 3mm coverslip was positioned over V1 (+0.6mm AP relative to lambda, +/- 2.7mm ML). Surgeries, imaging, and analyses of these mice were performed by Dylan Myers-Joseph.

Injections of antibiotic (Betamax 120mg/kg) and analgesia (methadone hydrochloride 10mg/kg) were given at least 2 minutes before the withdrawal of anaesthesia, and further analgesia was given daily for at least 2 days during recovery of the animal. Habituation to head-fixing then screening for viable imaging sites was performed 2.5 weeks following surgery. If an acceptable imaging site could be found, imaging and behavioural training started approximately three weeks after surgery.

2. Behavioural training

The behaviour apparatus and training were similar to previous studies (Poort et al., 2015, Khan et al., 2018). Mice were trained on the visual discrimination task for up to two weeks, until discrimination performance reached threshold, before training them on the switching task (see below). Mice had free access to water but were food restricted to maintain at least 85% of their free-feeding body weight (typically 85-90%, 2-3g of standard food pellets per animal per day). A reward delivery spout was positioned near the snout of the mouse, and licks to this spout were detected using a piezo disc sensor and custom electronics. The reward was a 10% solution of soya milk powder (SMA Wysoy) delivered by opening a pinch valve (NResearch) controlled through custom electronics. The mouse's running speed on the cylinder was measured using an incremental rotary encoder (Kübler). Two luminance-corrected monitors (luminance meter LS-100, Konica Minolta) positioned at 45° angles and 25cm distance from the mouse delivered visual stimuli.

Visual discrimination training

The mice were habituated to handling and gentle restraint over two to three days, before they were head-fixed and trained to run on a polystyrene cylinder (20cm diameter) for one to four days. This period was also used to find suitable imaging sites. After the habituation phase, mice performed one behaviour session in which the movement of the gratings was linked to the mouse's movement on the wheel to facilitate them associating their running with the gratings. Subsequently, mice were trained to self-initiate trials via sustained running on the wheel for at least 2.8s and an added random duration drawn from an exponential distribution with mean 0.4s. At this point one of two drifting sinusoidal visual gratings were randomly presented, drifting in the opposite direction to the direction of running, with a fixed spatial and temporal frequency of 0.1 cycles per degree and 2Hz respectively. The rewarded and unrewarded gratings were oriented +/- 20° relative to vertical, symmetrically on both screens. When the rewarded grating was displayed the mouse could trigger the delivery of a reward, a drop of soya milk, by licking the spout during the 'reward period', lasting from 1.5s after the appearance of the grating to its disappearance, maximum 1.53 s into the reward period. This was recorded as a 'hit'. If the mouse did not lick during this period, the trial was recorded as a 'miss', and a drop of soy milk was delivered shortly before the disappearance of the grating. When the unrewarded grating was presented, a single lick or more at any time until the stimulus disappearance was recorded as a 'false alarm', triggering a time-out period of 4s in which the unrewarded grating remained on screen, and any further licks restarted the time-out. During early training the probability of unrewarded trials was occasionally increased transiently up to 0.8 to discourage erroneous licking. All mice learned the visual

discrimination task in 5-10 days, with post-learning defined as three consecutive days of discrimination with a behavioural d-prime score of 2 or above. Behavioural d-prime was calculated as: $bd' = \Phi^{-1}(H) - \Phi^{-1}(F)$, where Φ^{-1} is the normal inverse cumulative distribution function, H is the rate of hit trials, and F is the rate of false alarm trials.

Odour discrimination training

Once mice had learned the visual discrimination task, they were trained in odour discrimination. After the same randomised period of sustained running, one of two odour stimuli were presented to the mouse via a polyethylene tubing positioned above the snout of the mouse. Odours were delivered through a custom-built flow dilution olfactometer calibrated with a mini PID (Aurora) at 10-20% saturated vapour concentration of two solutions, 10% soy milk (rewarded odour) and 10% soy milk with 0.1% p-Cymene mixture (unrewarded odour). This initial odour task structure was identical to the visual task, with the rewarded and unrewarded odours presented with a 50% probability of each.

Full attention-switching task training

Once animals were discriminating the odours accurately (typically after 30-40 trials), they were trained to switch between blocks of the olfactory and visual discrimination task. Mice typically learned to switch successfully in 1-3 days. In the olfactory blocks, 70% of odour stimuli were preceded with one of the two same visual gratings featured in the visual discrimination task (fixed duration of 1.8s, with an identical onset delay distribution as in the visual block). In this instance neither grating was rewarded or punished, and mice learned to ignore these irrelevant gratings while accurately discriminating the odours, which were presented after the irrelevant visual grating (delay between visual grating offset and odour onset 1.5s, plus an added random duration drawn from an exponential distribution with mean 0.2s in imaging sessions). In initial switching training sessions, a reward was delivered at the end of a rewarded grating in a visual block if the mouse had failed to lick, giving a clear indication that the grating was now relevant. By the end of training - so for all data in this project except for odour learning speeds (Fig 3.31) - this feature was removed, requiring mice to switch between blocks through noticing unexpected stimuli or outcomes alone. Block switches occurred automatically when a mouse had demonstrated a > 80% discrimination performance to the relevant stimuli (visual gratings in visual block, odours in odour block) over the last 30 trials of a block. Additionally in odour blocks mice were required to have successfully ignored all irrelevant visual gratings over the previous 10 trials. Blocks typically contained 30 to 40 non-transition trials. Mice were deemed to have learned the switching task when they could complete sessions at these parameters with at least 3 repeats of each block type.

Transition states

In order to compare the speed of switching between blocks, the selection of visual stimuli immediately after a block transition was made uniform. In the first trials of a visual block only the rewarded grating was shown, while in the first trials of an odour block the otherwise rewarded grating preceded every odour stimulus as the irrelevant grating. Odour stimuli selection itself was kept random. When a mouse responded correctly to these grating stimuli on three consecutive trials, by licking in the visual block and by withholding licks in the odour block, this transition period ended and the block continued with the normal 50% probabilities of visual grating identities. Transition states could therefore last a minimum of three trials, if the mouse responded correctly immediately, or indefinitely if the mouse could not produce three consecutive correct responses. If a mouse was unable to produce the correct response within 20 trials of the switch into a visual block, an automatic reward was added to the end of each visual grating that appeared regardless of licking. This encouraged the mouse to switch attention back to the visual gratings and allowed it to resume performing the task. These transition trials were not included in the calculation of task performance when determining whether to switch the block. Therefore, a minimum block length was 33 trials: 3 transition trials, and 30 trials of above threshold discrimination.

These transition states were used in all behaviour sessions except muscimol silencing experiments (Figs 3.09-3.12) and light-only controls (Fig 3.19), in which case either visual stimulus was presented from the start of the block with 50% probability.

Comparisons of task performance

Switching performance was calculated by counting the number of trials in the transition period following each switch. If the transition period had exactly three trials, this switch was removed from analysis for all comparisons except proportion of error switches in Fig 3.29. This was because these switches represented a mouse responding correctly in the first trial despite having no evidence of a block switch, simply due to making a mistake in following the rules of the old block, and therefore switching to the new block quicker than if the mouse was performing optimally. Including these switches would provide an inaccurate impression of switching speeds, so they were rejected.

In experiments not featuring transition states (muscimol and light-only controls), switching speeds were calculated by counting the number of trials featuring rewarded visual gratings that elapsed after a switch until the mouse responded correctly to three in a row. As the conventional probability of seeing a rewarded visual grating in a new visual block was 50%, and in a new odour

block was 35%, many more trials would likely elapse before the mouse had the opportunity to demonstrate knowledge of the switch in its responses to the visual gratings. This longer delay contributed to slower overall switching speeds, as without the train of rewarded gratings providing repeated reinforcement mice seemed to adapt their responses more slowly.

Stable behaviour was defined as any part of the block more than 10 trials after the end of the transition period. When analysing stable discrimination d' for silencing comparisons, only trials between this first stable trial and the end of the block were included. As the minimum block length was 30 non-transition trials, this meant each block provided at least 20 trials to this analysis.

3. Pharmacological silencing of ACC activity

After training in the switching task, mice were head-fixed while running on the wheel and infused bilaterally with 300nl muscimol (Sigma, 1µg/ µl) or saline at a rate of 0.25µl/min using a 1µl syringe (Hamilton) and syringe pump (World Precision Instruments SP100IZ). This was performed 30 minutes before the start of a switching session, and they were returned to their home cage during the wait. To allow full infusion of the drug, the tubing was left connected for 5 minutes before disconnecting from the cannulae. If a mouse was not able to trigger more than 100 trials at normal running parameters within the first 30 minutes of an experimental session, the session was discounted and the mouse was returned to their home cage.

4. Optogenetic silencing of ACC activity

Once mice had learned the full switching task, optogenetic silencing of ACC neurons was performed by connecting the optic fibre cannulae to a blue LED (470nm, Thorlabs), and delivering light while the mouse performed the task. Before implantation, each optic fibre was confirmed to have an effective power output of >1mW after cutting. Each dual-core cannula took input from 2 LEDs to give bilateral photoactivation of PV cells. Light was delivered either throughout the session (pulsed at 40Hz – Li et al., 2019), 0.5s before each visual stimulus continuing to the end of the stimulus ('peri-visual), or from the end of each visual stimulus until the beginning of the next visual stimulus ('inter-visual'). These three epochs were used to silence both ACC and PL on different days, creating 6 silencing conditions. These conditions were pseudorandomly chosen across consecutive days, with the order different between mice but the time between repeated conditions kept constant, and with control no-light sessions interspersed every third session. In the peri-stimulus and ITI epochs, light power was ramped down for the final 200ms of each pulse.

Dual ACC and PL silencing (Fig 3.25) was performed using light pulsed at 40Hz throughout the session, but with optic fibres connected to both sets of cannulae (a total of 4 LEDs). For one-trial un-silencing (Fig 3.27), the light was continuously pulsed throughout the session as above, but this was paused at the end of the last trial in the odour block and resumed at the start of the second trial of the visual block. For the laser-cue sessions (Fig 3.29), light was continuously pulsed as above only for the duration of the first trial of the visual block and was otherwise off for the entire session. The optic fibre was positioned around 20cm above the mouse's head, hanging vertically. These sessions were recorded after the initial 6 silencing sessions, as well as interspersed control sessions, had been recorded. They too were interspersed with control sessions to account for any changes in performance due to overtraining.

For ACC silencing during learning (Fig 3.31), the silencing group included all 8 optogenetic mice, and the non-silenced controls were the 10 coronal imaging mice. In the silencing group, light was pulsed at 40Hz for the duration of the session. Mice initially started with only odours, and once discrimination performance had surpassed 80% irrelevant gratings were introduced as in a regular odour block.

5. Two-photon calcium imaging

Imaging was performed using a custom-built resonant scanning two-photon microscope (Cosys) and a Chameleon Vision S laser (Coherent) at 930nm using a 16X, .8NA objective (Nikon). Images were acquired using a 12kHz resonant scanner (Cambridge Technology) and an FPGA module (PXIe-7965R FlexRIO, National Instruments). Two-photon calcium imaging of GCaMP7f-labelled neurons in the ACC was performed across 40 training sessions and 48 full task-switching sessions in these 10 mice. The microprism depth, injection coordinates, and cell morphology provided strong evidence that the imaging sites were located in layer 5. Multi-plane imaging was performed using a piezoelectric objective scanner (Physik Instrumente). Depending on the depth of GCaMP7f expression, each imaging volume consisted of either 6 or 8 imaging planes, 40µm apart, giving an effective imaging rate of 6.4 or 4.8Hz per volume respectively. 40µm was chosen as a step size to account for the larger soma size of layer V ACC neurons, in order to ensure the same neuron was not recorded on different steps.

The microscope had a working distance of 3mm. Light passing through the microprism accounted for 1.5mm of this distance, so the objective had to be closer to the face of the coverslip than in regular cranial window experiments not using a microprism. To account for this reduced space, I used head-plates custom made with a larger diameter, as well as designing 3D-printed

light-shields (MakerBot) that would block light from the screens reaching the objective without impeding the objective, distracting the mouse, or allowing the immersion media to leak out. This light-shield sat above the head-plate, secured on top of the head-plate screws, then was connected each session to a frame held loosely around the objective so that the objective could move in the z-axis without displacing the light-shield. Several light-shields were used depending on the position of the microprism relative to the head-plate.

Imaging timeline

Mice were trained first in the visual discrimination task, then had at least 3 training sessions in the visual-odour block switching task. Once mice had learned the switching task, at least 3 recordings of the mice performing the task were taken per mouse. Before each recording session the same imaging site was found by matching anatomical landmarks. A mouse that completed behavioural training would have at least 5 imaging sessions: 2 pre-learning sessions, 2 post-learning sessions, and at least 1 switching session. Following the first pre-learning session, the optogenetic calibration sessions used for Fig 4.25 were recorded. Here, screens were switched off and the laser was delivered at one of 6 laser powers for 1.5s. Running did not affect trial initiation, instead there was a 5s + 0.2s random jitter delay between each laser trial. Switching sessions were recorded with control sessions, peri-visual VIP activation, and inter-visual VIP activation sessions pseudo-randomly interleaved, with up to 6 total sessions recorded. If the site was still healthy at this point, due to the mouse progressing through training quicker than average, I looked for a new site with no shared cells with the previous site. From here I collected as many control switching sessions as possible before the overall health of the site deteriorated, never more than 2. Of the 10 mice trained, I was able to get second sites from 3, giving the 13 total sites included in the non-optogenetic mismatch analysis.

Anaesthetised z-stacks

After all *in-vivo* imaging data had been collected, a final high-quality image stack was acquired under anaesthesia. Subcutaneous injections of ketamine (100mg/kg) and xylazine (16mg/kg) were used to induce anaesthesia, with further injections of ketamine to maintain anaesthesia if necessary. Eye-cream (Maxitrol) was used to prevent drying, and body temperature was maintained using a heating pad. A separate z-stack was recorded with the laser set to an excitation wavelength of 930nm (for GCaMP), 830nm (for striatal-projecting cells expressing CTB-Alexa-647), and 1020nm (for ChrimsonR-tdtomato expression by VIP interneurons). Between the latter two z-stacks, the red filter was changed to selectively record far-red light from the CTB-expressing cells and near-red light for the tdtomato-expressing cells. Before each *in vivo* imaging session, a short recording (~100 volumes) was collected at each of these three wavelengths, with the red channel

collected as well as the green. In the main session recording, only the green channel was recorded. These red channel recordings, as well as later z-stacks, were used to identify cells that were striatal-projecting or VIP interneurons following segmentation.

6. Optogenetic activation of VIP interneurons

To perturb cells expressing ChrimsonR concurrently with 2-photon imaging, a 639nm laser (50mW, OBIS) was delivered via a Ø200µm, 0.39 NA optic fibre (Thorlabs) positioned around 3mm from the posterior edge of the microprism, at a 30° angle relative to the coverslip. The effective output power from the optic fibre, measured using a Power Meter (Thorlabs), was 5.3mW, with a blanking signal ensuring laser output only during turn-around times of the resonant scanner.

For optogenetic switching sessions, two laser epochs were used. In the peri-visual epoch, the laser began 0.1s before the visual stimulus and continued until the end of the visual stimulus. In the inter-visual epoch, the laser began at the offset of each visual stimulus and continued until the onset of the next visual stimulus. For either session type, only the maximum laser power 5.3mW was used to ensure a sufficient number of switches could be collected at a laser power shown to successfully perturb VIP interneurons.

7. Imaging data analysis

Pre-processing

Image stacks were corrected for motion, and regions of interest (ROIs) were selected for each active cell in each session using Suite2p (Pachitariu et al., 2016). Each site yielded between 129 and 925 cells, median = 499 cells. Raw fluorescence time series F(t) were obtained for each cell by averaging across pixels within each ROI. Baseline fluorescence F0(t) was computed by smoothing F(t) (causal moving average of 0.75s) and determining for each time point the minimum value in the preceding 60 s time window. The change in fluorescence relative to baseline, ΔF/F, was computed by taking the difference between F and F0, and dividing by F0.

Cell selection

Cell selection was performed on the segmented data following this pre-processing. For each plane within a recording, cells were selected based on their appearance, with coronally-recorded layer V neurons in the ACC having a particularly stereotypical pyramidal cell appearance. Following selection, the ΔF/F traces from each selected cell were aligned with the main behavioural triggers.

Red cell matching was also performed: using the short pre-session red channel recordings and final anaesthetised z-stacks, cells which appeared in both the green and red channel and that could not be explained by bleed-through from the green channel were marked, either as striatal-projecting or VIP interneurons depending on the red channel recording used.

Identifying responsive cells

For defining 'responsive' cells (Fig 4.06), each neuron's ΔF/F was aligned to every onset within a session of that task event. For stimuli (visual relevant, irrelevant, odours), only trials in which the mouse responded correctly were included. Licking was defined as a lick that was not preceded by any licking behaviour in the preceding 5 seconds. Reward was defined as the opening of the reward valve. Running was defined as any period in which the mouse's speed went from 0cm/s to above 5cm/s and sustained this speed for at least 3 seconds. Once activity had been aligned to each of these instances, a Wilcoxon signed-rank test comparing the neuron's averaged response 0-1.5s relative to the onset was compared with its averaged baseline -0.5 to 0s relative to the onset, with each baseline and response instance treated as paired. A responsive cell was defined as any cell that had significantly different activity in the response period compared to the baseline period, $p < 0.05$.

Mismatch cell identification

To analyse responses to the odour prediction mismatch trials, neuronal activity was aligned to the end of the preceding visual grating plus 2.0s, the average delay to the odour stimuli onset. Mismatch neurons were identified by comparing activity between three conditions in the window 0 to 1.5s aligned to this time: activity in 'expected odour' trials (i.e. after the first grating following a switch from an odour block to a visual block, provided the mouse did not already lick to the preceding grating), activity in the same time period following a stable unrewarded visual block trial up to 10 trials before the end of a visual block (when no odour should be expected) and activity during a stable odour block trial (when an odour is expected and received) following a correctly ignored visual grating, using a Wilcoxon rank-sum test with equal numbers of trials for each condition. If multiple trials were collected from each block for the stable visual block and stable odour block conditions, activity was averaged across trials from the same condition and same block.

'Expected odour' trials were defined as the first trial following a switch into a visual block, provided the mouse did not lick to the grating. 'Stable odour' trials were defined as rewarded odour trials within the last 15 trials of an odour block, in which the odour was preceded by an irrelevant grating that was correctly rejected. 'No odour' trials were defined as unrewarded visual

trials from the last 15 trials of a visual block, provided the mouse correctly rejected the visual grating. 'Unrewarded odour' trials (Fig 4.29) were selected using the same criteria as 'stable odour' trials, but using unrewarded odour trials instead. These conditions were designed to keep overt behaviour as similar as possible between comparisons: all epochs compared were preceded by a visual grating to which the mouse did not lick.

Mismatch neurons were defined as cells with significantly different activity in 'expected odour' trials when compared to each of the other conditions. Positive (class 1) and negative (class 4) mismatch neurons were those in which the response to the 'expected odour' was largest or smallest of the three conditions respectively. Two other combinations were observed, first with the odour condition significantly higher and no odour condition significantly lower compared to the prediction mismatch condition (99 cells), and second, the reverse of this (163 cells). To test whether activity in mismatch neurons could predict subsequent switching, average activity between 0-1.5s in odour prediction mismatch trials was compared between one-shot switches (in which the mouse responded correctly to the subsequent visual grating) and slower switches (in which the mouse continued to miss at least the next visual grating) using a Wilcoxon signed-rank test.

'New odour' mismatch trials (Fig 4.30-31) were taken from the first odour trial following a switch into an odour block, aligned to odour onset, and regardless of the identity of the odour stimulus. As this was not determined by the transition states, the stimulus could be rewarded or unrewarded. Activity 0-1.5s following this odour onset was compared to activity from the same period in 'stable odour' and 'no odour' trials, as with 'expected odour' mismatch. 432 neurons had significantly different activity in 'no odour' trials, compared to each of the other conditions. Of these, 285 neurons had activity that was more positive in this period than in either of the other two conditions.

Statistics

Unless specified specifically within the figure legend, significance thresholds used are: * $p < 0.05$, ** $p < 0.01$, *** $p < 0.001$. Bonferroni corrections for multiple comparisons were used when the same data were compared to more than one other dataset. Here these significance thresholds were divided by the number of multiple comparisons (never more than 2) to give the new significance thresholds. For tests with multiple comparisons: * $p < 0.025$, ** $p < 0.005$, *** $p < 0.0005$.

RESULTS

Results chapter 1:

The role of anterior cingulate cortex in task-switching behaviour

The attention-switching task used in this project features visual stimuli that transition between being motivationally-relevant and motivationally-irrelevant to the mouse. The paradigm offers a model of how circuit re-organisation can occur between attentional episodes in the multiple-demand system. Depending on the current sub-goal, certain inputs will be relevant or irrelevant, and attention must be allocated respectively. Processing in V1 is influenced by this relevance (Poort et al., 2015), suggesting a top-down influence of the multiple-demand system on sensory processing.

The ACC sends projections to V1 (Sesack et al., 1989) that can modulate local processing (Zhang et al., 2018). Though the ACC has a role in extra-dimensional set-shifts, the PL and IL have been shown to mediate attention-switching between different modalities (Marton et al., 2018; Ng et al., 2007), like in this task. ACC, conversely, is needed when the stimuli to be switched between are closely related, such as within the same modality (Ng et al., 2007). As the PL and IL do not project directly to V1, and the ACC is strongly interconnected with them both, it may be that the ACC is conveying top-down signals from PL and IL to V1. It may also be that the mPFC is not directly needed at all for this particular behaviour, and instead the top-down signals come from other sources such as the retrosplinial cortex (Makino & Tomiyama, 2015) or thalamus (Wimmer et al., 2015).

The first step of this study must therefore be to establish what, if any, role the ACC is playing in this task. To achieve this, I used different techniques to lesion the ACC for the duration of the task. Once I had established that mice were able to perform the task to a high level, I could examine how their performance suffered when ACC was inhibited. Photoinhibition became my preferred technique as the temporal precision allowed me to probe the effect of very short-term lesions for specific portions of the session or trial.

1. Mice can learn to perform an attentional-switching task

To elicit attention-switching behaviour, mice first had to learn the rules of the task. After several days of acclimatisation to head-fixation and sustaining running, food-restricted mice began training in the visual go/no-go paradigm (Fig 3.01). Here they were presented with one of two

drifting sinusoidal gratings, one rewarded and one unrewarded. Licking to the rewarded grating triggered a soya milk reward, while licking to the unrewarded grating triggered a 4 second time-out.

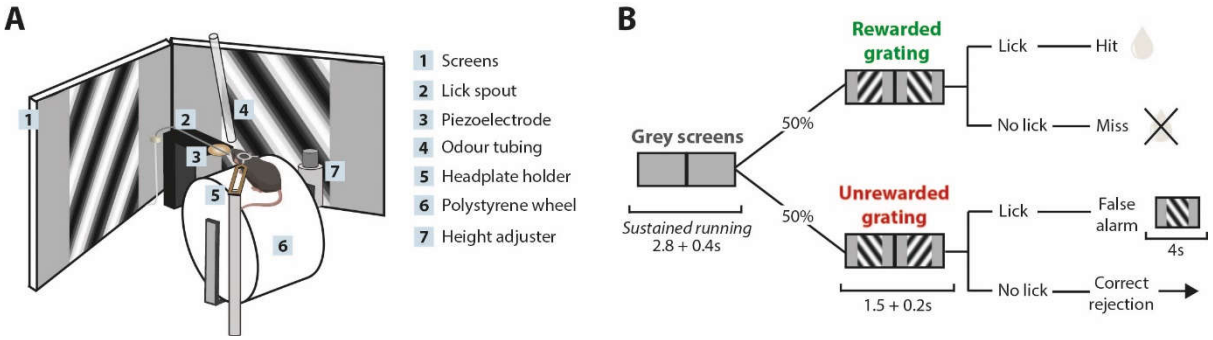

Figure 3.01. Visual discrimination task. A: Reconstruction of a mouse performing the behavioural task. Head-fixed mice are presented with visual or odour stimuli, to which they must either lick or withhold licks to demonstrate discrimination. B: Schematic of visual discrimination task. Square brackets show durations, added times are the means of random jitter added to the minimum duration taken from an exponential distribution. Mouse image taken from BioRender.

Mice typically learned to discriminate between the gratings accurately within 10 days of their first training session (Fig 3.02), with the fastest mice reaching post-learning status after 3 days. This was defined as sustained performance above a behavioural d' of 2.0 for 3 consecutive sessions (see Methods for calculation). The behavioural mice were not significantly quicker to reach this threshold than imaging mice (Wilcoxon rank sum test comparing mean number of days for each mouse to reach threshold p = 0.23).

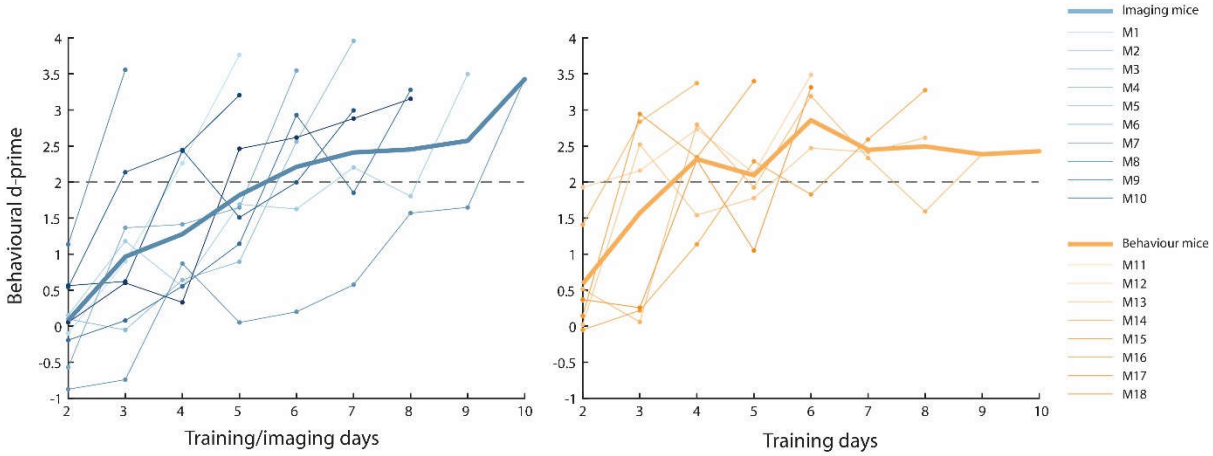

Figure 3.02 Visual discrimination learning. Summary of average discrimination performance across training for the mice that comprise the majority of this study. Left, GCaMP-expressing mice with imaging sessions performed at the beginning and end of learning timeline. Right, mice used exclusively to study behaviour. Thick lines represent mean d' across all mice for each day. Imaging mice N days to reach the threshold d' mean ± SD = 4.8 ± 1.99 days. Behavioural mice N days to reach the threshold d' = 3.57 ± 1.72 days.

Before learning, mice would indiscriminately slow their running and lick to either grating once it had been presented. Through trial-and-error over training, mice learned to discriminate the two visual stimuli and lick only in response to the rewarded grating (Fig 3.03 – from a representative

mouse). During unrewarded gratings the mice withheld licks and accelerated to quickly move on to the next trial.

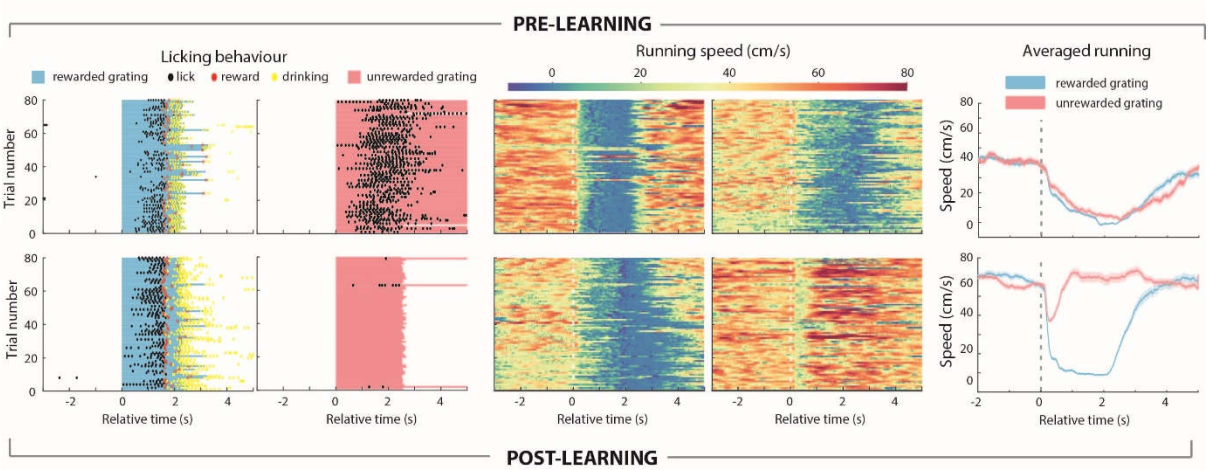

Figure 3.03. Behavioural changes over learning. First 80 trials of a pre-learning (top) and post-learning (bottom) session from the same representative mouse, with licking behaviour (left), running behaviour (middle), and averaged running (right) shown. In the licking behaviour raster plots (left), each dot represents a lick, with colour denoting the time of the lick relative to the reward valve opening. Licking and running behaviour is aligned to the onset of the visual grating on each trial.

After learning the visual discrimination task, mice were trained in the full task-switching paradigm (Fig 3.04). This used a block-wise structure, with each block employing 1 of 2 slightly different sets of rules. In a visual block, the mice performed visual discrimination with the same two gratings as before. In an odour block, mice were presented with one of two odour stimuli, one rewarded and one unrewarded. As with the visual stimuli they were required to either lick or withhold licks during these stimuli to trigger rewards. The key difference was that in the odour block, 70% of odour stimuli were preceded by one of the same visual gratings as in the visual block, but licking to either would not trigger a reward and they should both be ignored. Thus, a mouse performing correctly would alternate from attending to visual stimuli in the visual blocks to attending to odour stimuli, and ignoring the visual stimuli, in the odour blocks.

This change in strategy that occurred between blocks was not a straightforward extra-dimensional set-shift. An extra-dimensional set-shift did occur when the mouse transitioned from discriminating the visual stimuli to discriminating the odour stimuli, as it was applying the same rules to different stimuli. However, in the odour blocks the mice also had to remember not to apply the old rule to the now irrelevant visual stimuli. In this sense, a strategy change did occur as an old rule must be suppressed as part of the attention switch – so the shift is to some degree intra-dimensional. In this way the task modelled how attentional shifts between sub-goals would not just require the multiple-demand system to promote certain inputs to the level of attention, but to suppress others.

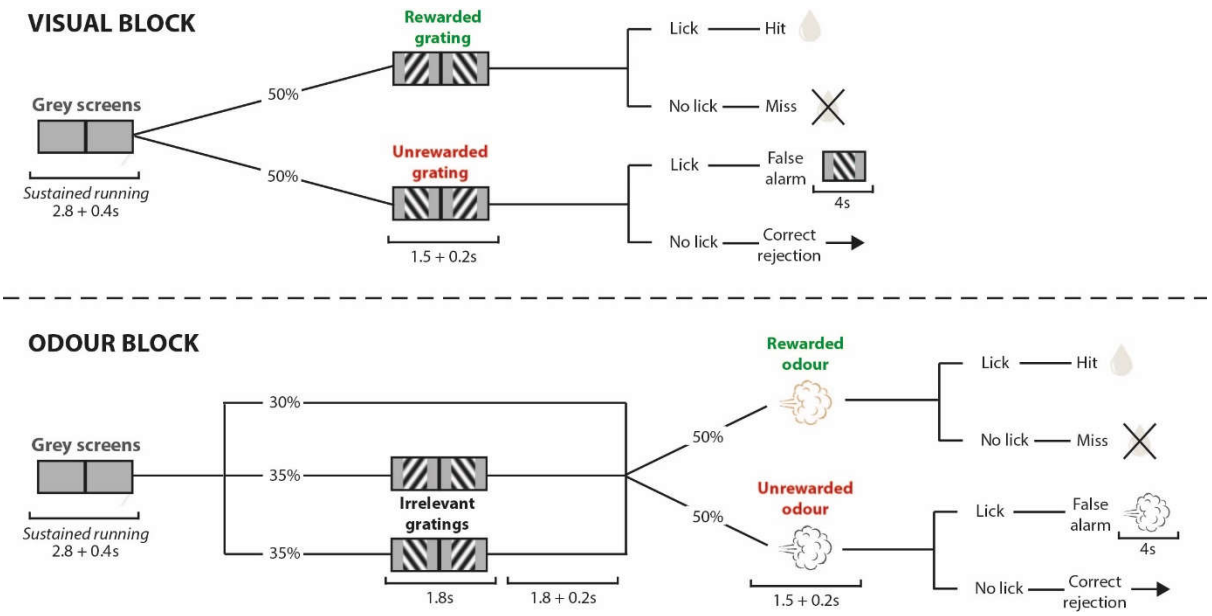

Figure 3.04. Full task-switching paradigm. Mice start each session in a visual block, and alternate between the two block types. Added times are the means of random jitter added to the minimum duration, taken from an exponential distribution.

The task structure allowed the comparison of the mouse's response to the same visual gratings when behaviourally relevant, in the visual block, and behaviourally irrelevant, in the odour block. Mice typically learned to discriminate between the odours in a single session and learned the full switching paradigm within 3 days (Fig 3.05).

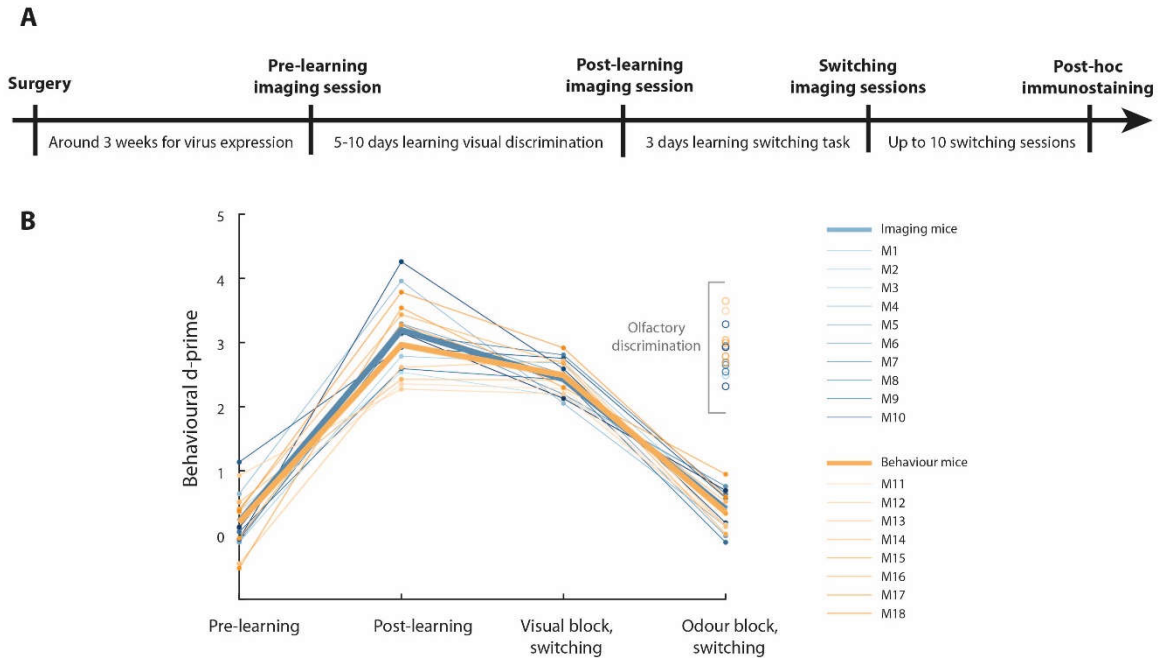

Figure 3.05. Full experimental timeline. A: Summary of each significant timepoint in an imaging experiment timeline, with all timepoints completed within 6 weeks of surgery. B: Visual discrimination performance of the main mice used in these experiments at each stage of training: pre-learning, post-learning, and in either block of a switching session once the full paradigm has been learned.

A typical switching session (Fig 3.06) began in a visual block, with block switches occurring once the mouse had demonstrated a good understanding of the current task rules over the previous 30 trials. This was defined as above 80% discrimination accuracy to the gratings in a visual block, and above 80% discrimination accuracy to the odour stimuli with reliable ignoring of the gratings (i.e., not licking in response to either grating) in an odour block. This stable performance was considered evidence that the mouse had fully switched their attention to the relevant stimulus modality of the block in question.

Worth noting is that while a visual grating did not always precede an odour stimulus in every odour block trial (see Fig 3.04, only 70% of trials), if a visual grating was seen in an odour block an odour stimulus would always follow it. Thus, a mouse could reliably predict that an odour stimulus would follow a grating if they believed they were in an odour block, but the random jitter added to this delay between the grating and odour meant that the mouse could not perfectly predict the time of the odour onset. However, the jitter in the delay between an irrelevant grating and odour was smaller than the jitter between the start of a new trial and the appearance of the first stimulus. Therefore, while the mouse could not perfectly predict when any event will occur during the task, the onset of an odour following an irrelevant grating was the most predictable stimulus onset in the task. This expectation of an odour following an irrelevant grating is reflected by the mouse's running during the irrelevant gratings (Fig 3.07).

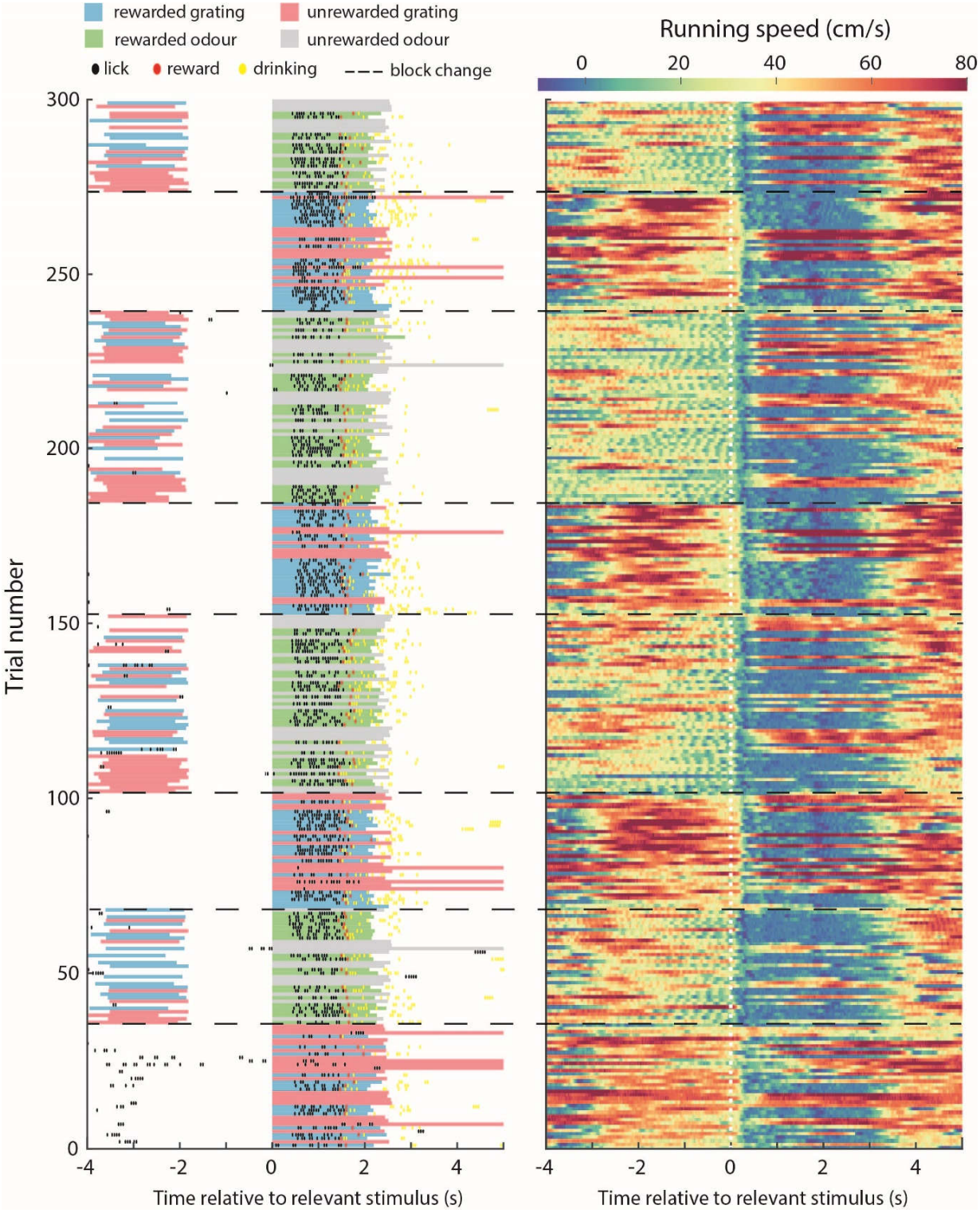

Figure 3.06. Behaviour in first 300 trials of an example switching session from a representative mouse, aligned to the relevant stimuli. Mice alternate between blocks of visual stimuli and blocks of odour stimuli often preceded by irrelevant visual stimuli. Mice learn to attend to and discriminate the relevant stimuli and ignore the irrelevant stimuli, reflected in their alternating choices to slow and lick, or to speed up and not lick.

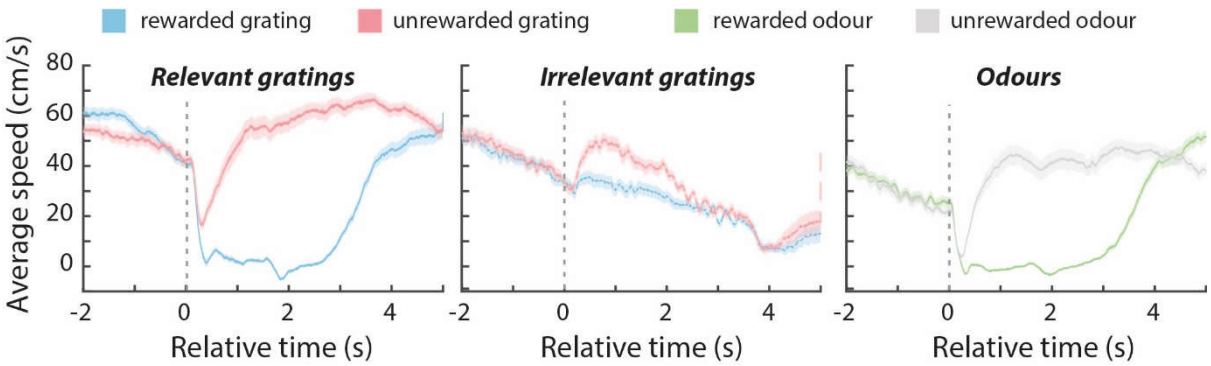

Figure 3.07. Averaged running to task stimuli. From example session in Fig 3.06. Mice slow down for rewarded relevant stimuli, but run through unrewarded relevant stimuli. Irrelevant stimuli are always followed by odour stimuli, so the mouse knows that further running is unnecessary.

Block transitions were not cued. Instead, mice needed to infer the block transitions by noticing changes in stimuli and in their reward associations. This evidence came from two aspects of the task: the disappearance and reappearance of the odour stimuli across the session, and the change in outcome when licking to the rewarded visual grating in either block. As a mouse transitioned from a visual block to an odour block, the sudden appearance of the odour stimuli provided a strong cue that a block change had occurred, with the ineffectiveness of licking to the now irrelevant rewarded grating providing further evidence. During a transition from an odour block to a visual block, the anticipated odour no longer arrived, and the mouse had to instead learn to lick to the rewarded visual grating to obtain a reward (Fig 3.08). As licking to the rewarded visual grating was what demonstrated whether the mouse had successfully transitioned between the two sets of rules, I imposed a 'transition' state upon entering a new block. This briefly ensured that all visual gratings the mouse encountered were rewarded. This meant that by measuring the trials taken to stop responding to the grating when entering an odour block, or to start responding to the grating when entering a visual block, the speed of transitioning between blocks could be quantified. The chances of receiving either odour did not change. Once mice had given the correct response to 3 visual gratings in a row the transition state ended, and the block resumed with the conventional 50% probabilities of seeing either visual grating.

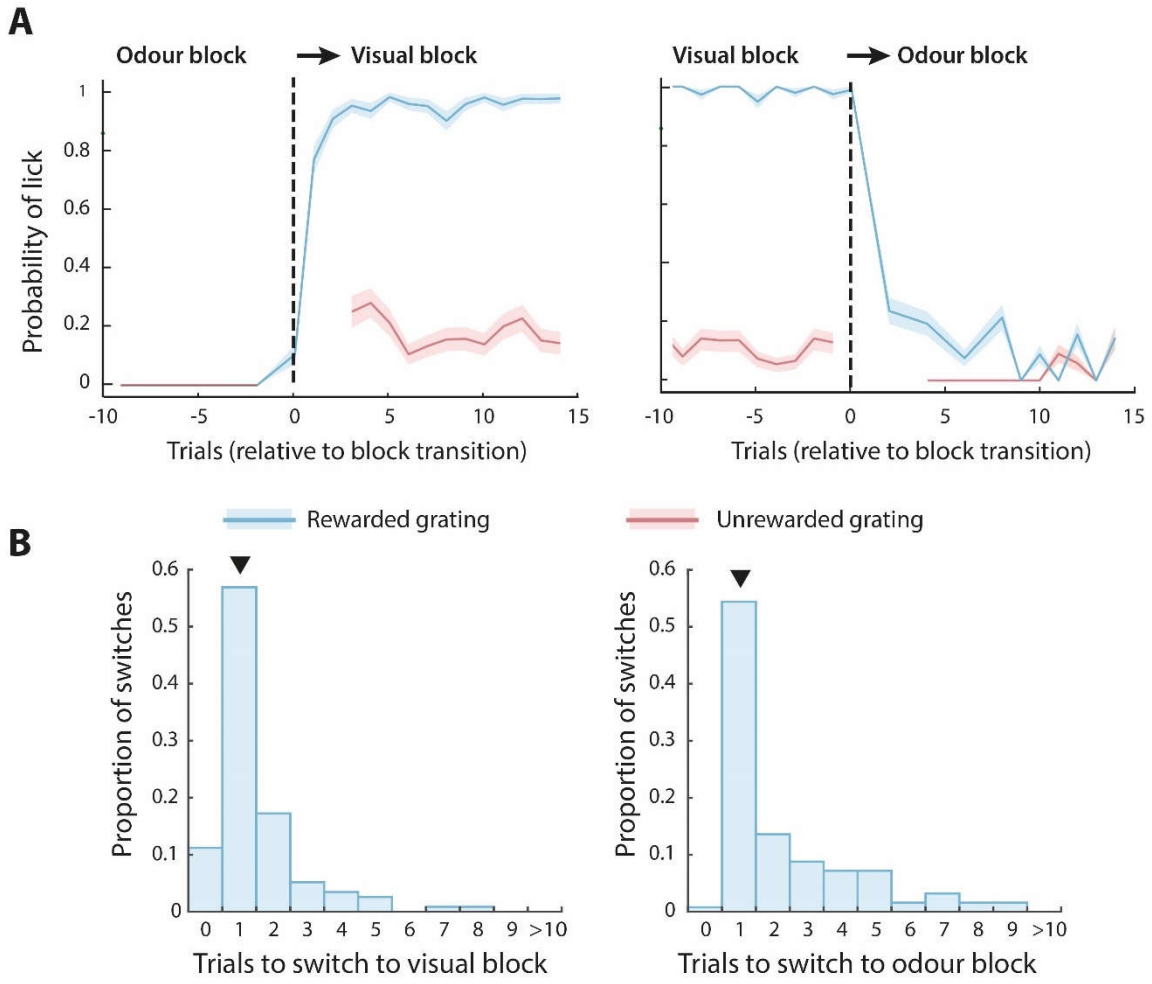

Figure 3.08. Licking behaviour across block transitions. A: Probability of licking across each trial relative to a block transition, averaged across 85 and 93 transitions respectively, 13 sessions, 10 mice. Transition states enforce rewarded gratings only for at least 3 trials post-switch: mice must respond correctly to 3 rewarded gratings in a row before the transition states end and it is possible for unrewarded gratings to appear. B: Histograms of number of trials required to switch in either direction. This is calculated from the number of trials that elapsed before mouse began to give correct responses required to end transition state (i.e., trial = 1 means that the mouse responded incorrectly to the very first trial of the new block, then responded correctly to the subsequent 3 trials and exited the transition state). N trials to switch to visual block mean ± SD = 4.83 ± 2.93, N trials to switch to odour block = 5.15 ± 1.88. Black triangles denote switches performed after a single error ('one-shot').

These transition states allowed the comparison of switching speeds across different block switches within a session, across sessions, and across mice. A switch performed after 1 trial demonstrated that the mouse changed behaviour on the second trial after a single incorrect response in the first trial of the new block, indicative of an optimal use of the evidence available to the mouse to learn. Mice performed these 'one-shot' (Achterberg et al., 2022) switches on over half of all switches in either direction (Fig 3.08B, black triangles indicate 'one-shot' switches). Mice were not significantly faster to switch in either direction (Wilcoxon rank sum test comparing trials to switch, from Fig 3.08B, $p = 0.14$).

2. Pharmacological silencing of ACC impairs task-switching

To interrogate what, if any, role the ACC plays in mice performing this attention-switching task, a first group of wildtype mice were implanted with bilateral cannulae (Fig 3.09) allowing the direct infusion of either the $GABA_A$ receptor agonist muscimol, to temporarily silence the ACC for the duration of the task, or saline, as a control infusion.

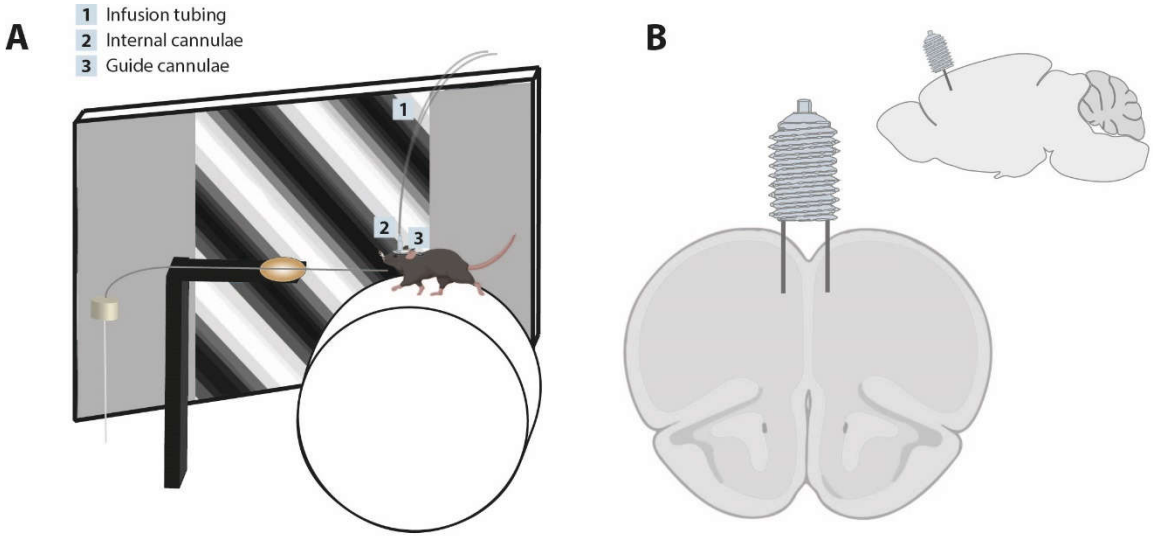

Figure 3.09. Muscimol silencing experiments. A: Reconstruction of infusion experiments. Infusions were performed while mice were head-fixed. B: Schematic of guide cannulae implantation in ACC. Mouse and coronal slice images taken from BioRender.

Attention-switching sessions were performed 30 minutes after the infusions ended and lasted for up to an hour. Only sessions in which the mouse was able to trigger at least 200 trials were included, as motivating mice to complete a full session was not reliable and seemed to be less likely following muscimol infusions. Surprisingly, muscimol infusions had no effect on basic discrimination performance (Fig 3.10), with mice still able to discriminate relevant gratings and odours and ignore irrelevant gratings across most sessions as well as control (N = 4 mice, 12 saline sessions vs 14 muscimol sessions, Wilcoxon rank sum test comparing relevant visual discrimination $p = 0.946$, irrelevant visual discrimination $p = 0.625$, odour discrimination $p = 0.313$).

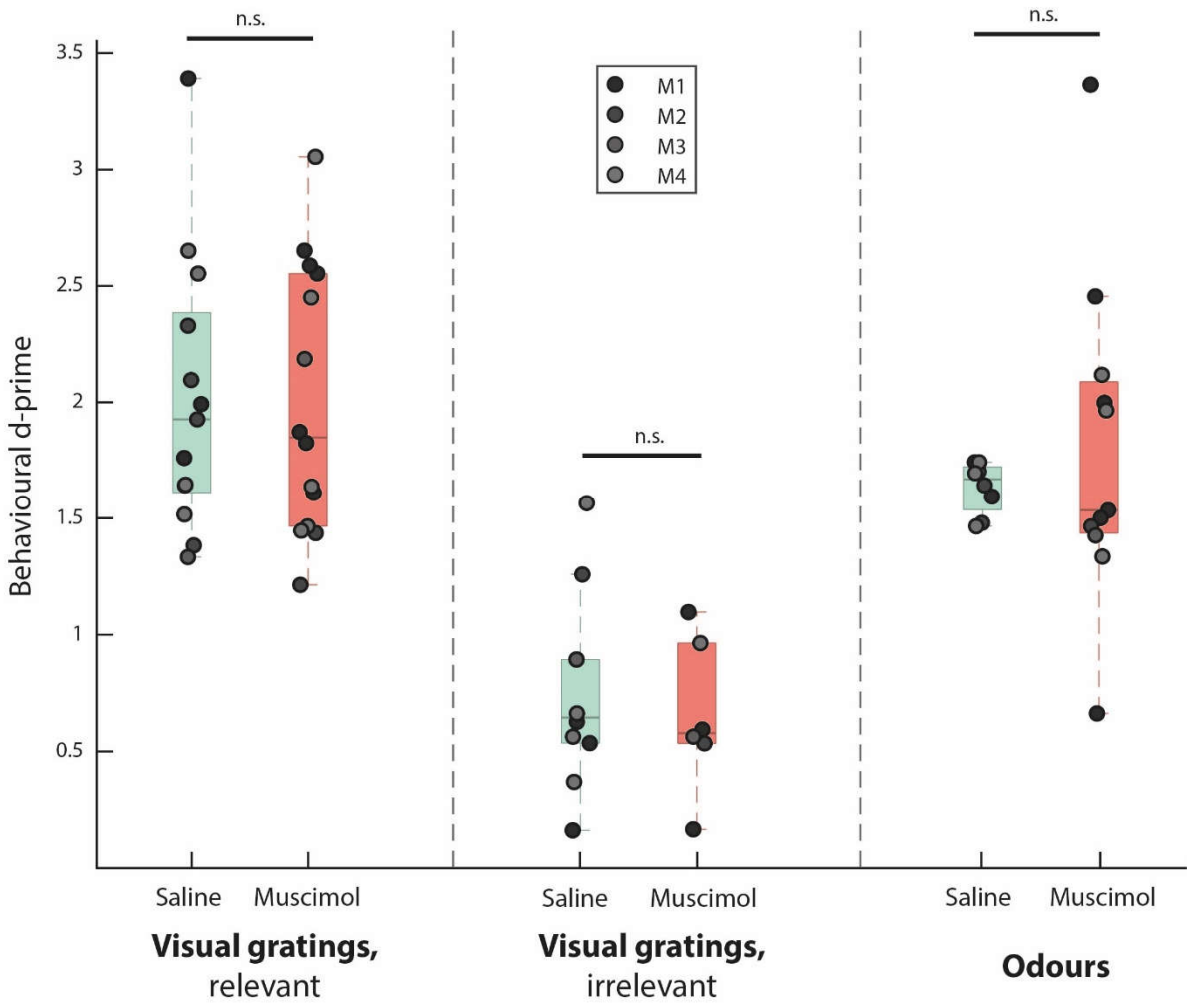

Figure 3.10. Effect of muscimol on basic discrimination performance. Discrimination of task stimuli during stable performance across all blocks in a session, following infusions of saline or muscimol into the ACC. Circles represent means across individual sessions. Shading indicates mouse. Boxes represent median +/- IQR, whiskers represent the most extreme values not considered outliers.

I next examined how quickly the mice were able to transition between blocks (Fig 3.11). Here the muscimol showed a clear effect: when switching from an odour block to a visual block, in which the mouse must transition from ignoring the visual gratings to attending to them, muscimol significantly increased the number of trials required (Wilcoxon rank sum test $p = 0.032$). When switching from a visual block to an odour block, in which the mouse must transition from attending to the visual gratings to ignoring them, muscimol significantly reduced the number of trials required (Wilcoxon rank sum test $p = 0.0012$).

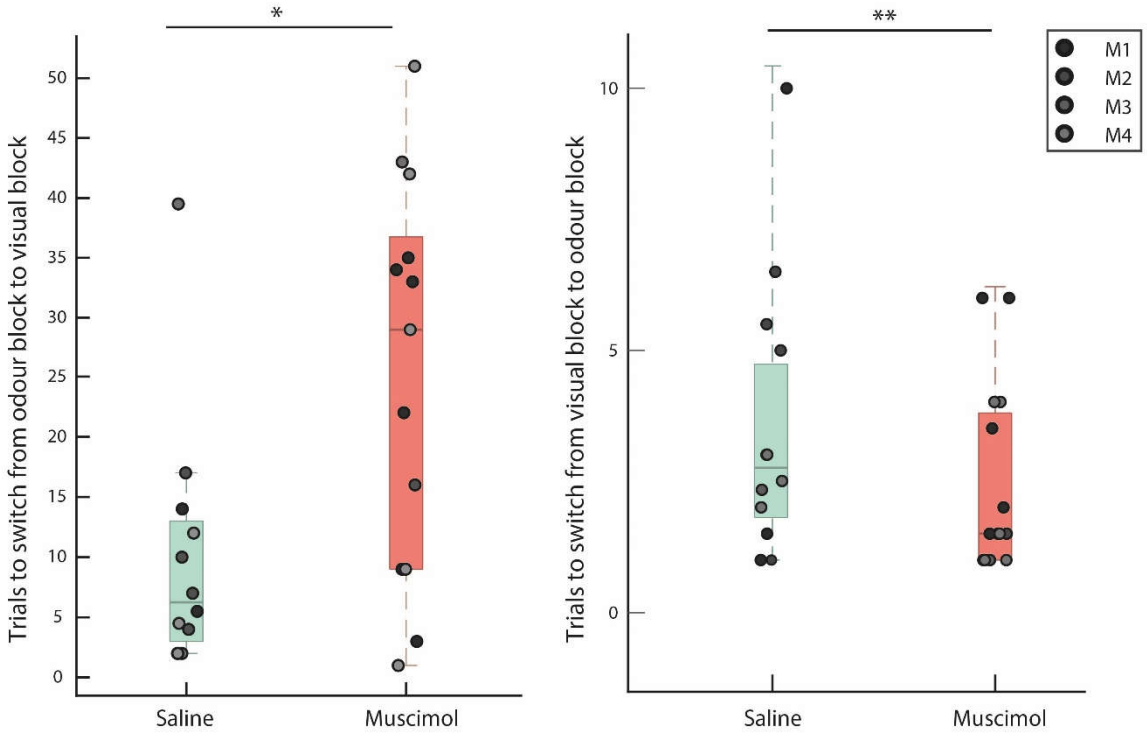

Figure 3.11. Effect of muscimol on block switching speeds. Left, number of trials taken for mouse to successfully lick to 3 consecutive rewarded gratings in a new visual block, averaged across all switches in a session. Right, number of trials taken for mouse to successfully ignore 3 consecutive rewarded gratings in a new odour block, averaged across all switches in a session. Circles represent means across individual sessions. Boxes represent median +/- IQR, whiskers represent the most extreme values not considered outliers.

A simple explanation for this effect could be that the mouse was experiencing a general deficit in their licking behaviour as a result of the muscimol infusion, biasing the mouse to a passive state of not licking that prohibited the switch to a visual block and facilitated the switch to an odour block. To test this, I examined licking behaviour by comparing the number of licks and reaction times to all rewarded stimuli in each condition (Fig 3.12). Comparisons showed a significant decrease in the number of licks per rewarded stimulus (saline N = 2196 trials, mean = 6.43 licks, muscimol N = 1194 trials, mean = 5.48 licks, two-sample t-test $p = 2.26^{-8}$), and a significant increase in reaction times to these rewarded stimuli (saline mean = 1s, muscimol mean p = 1.09s, two-sample t-test $p = 9.92 \times 10^{-12}$). These indicate that the muscimol infusions might indeed have inhibited licking behaviour, which may have contributed to the switching deficits observed.

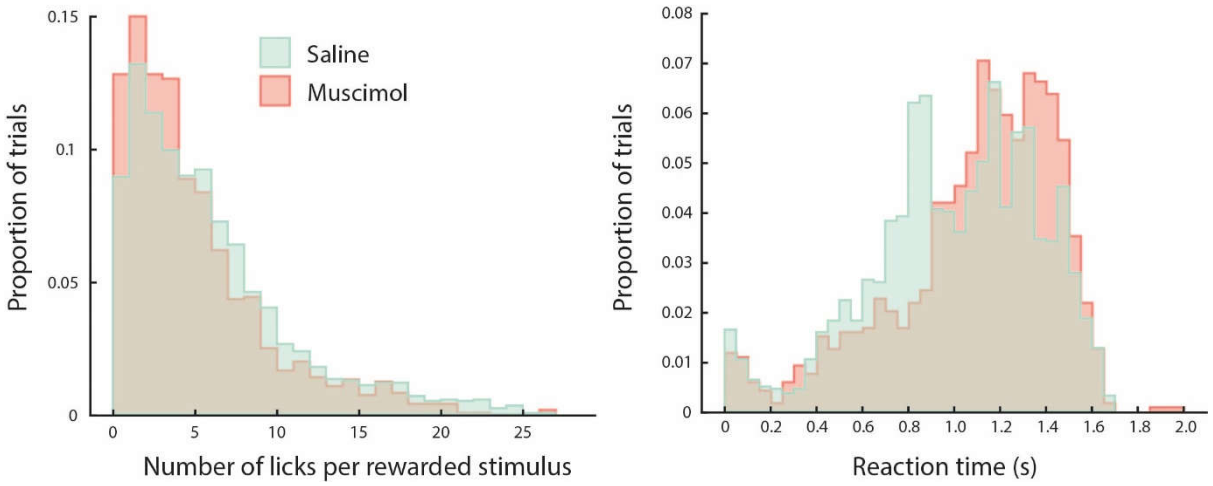

Figure 3.12. Effect of muscimol on licking behaviour. Left, number of licks per rewarded relevant stimulus, correct trials only (>0 licks). Right, reaction time for the same relevant stimuli. Each datapoint represents a single trial.

3. Optogenetic silencing of ACC impairs attention-switching

While the results from the muscimol infusions hinted at a role for the ACC in this attention-switching behaviour, the reduction in licking behaviour could imply off-target effects. Optogenetic silencing allowed me to clarify the effect both spatially and temporally. I repeated the experiment using bilateral optogenetic silencing of ACC (Fig 3.13), with light timings allowing control of when the ACC was silenced more precisely than the chronic silencing of muscimol infusions. To contrast with the ACC silencing, I also implanted optic fibre cannulae bilaterally into the PL.

The PL, along with the IL, could be considered homologous to the rvACC in primates (van Heukelum et al., 2020). In rodents, lesions to the PL increased errors immediately following a rule switch, while lesions to the ACC increased errors throughout the task by disrupting error-related feedback (Kosaki & Watanabe, 2012). During extra-dimensional set-shifting tasks, PL and IL mediate shifts when the sets of stimuli are dissimilar, such as from different modalities, while ACC mediates shifts when the stimuli overlap perceptually (Ng et al., 2007). The evidence would implicate the PL far more than the ACC in this switching behaviour, as the stimuli switched between are of different modalities. That muscimol infusions to the ACC significantly affected switching times while leaving stable task performance unscathed was unexpected, and seemed to more resemble these established roles for the PL and IL. PL was therefore selected as a proxy mPFC target with which to compare the effect of ACC silencing, to see whether PL silencing shared or even surpassed the impact of ACC silencing.

To achieve widespread silencing using optogenetics, I used mice derived from a cross between PV-Cre and FLEX-Channelrhodopsin2 lines, expressing the excitatory opsin Channelrhodopsin in

parvalbumin (PV)-positive interneurons. This interneuron-mediated method of photoinhibition has been shown to more effectively silence local populations of pyramidal cells than directly inhibiting the cells via expression of inhibitory opsins (Li et al., 2019).

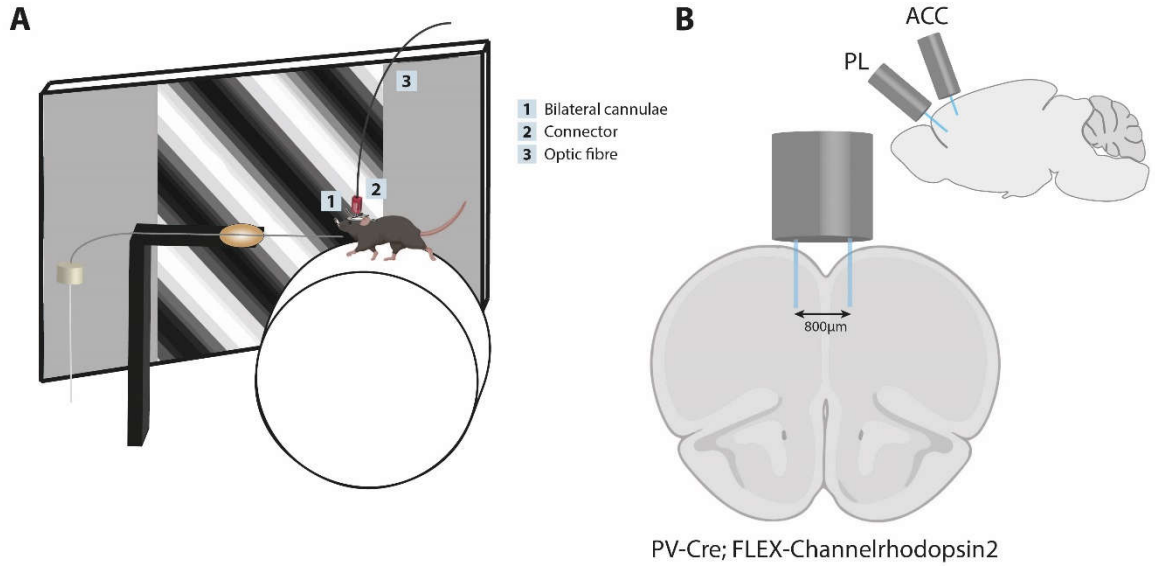

Figure 3.13. Optogenetic silencing experiments. A: Reconstruction of optogenetic experiments. B: Implantation of the cannulae in anterior cingulate and prelimbic cortices. Prelimbic implantation was angled to allow room for optic fibres to be connected to either. Mouse and coronal slice images taken from BioRender.

My first approach was to attempt to reproduce the chronic silencing of the muscimol, but with a more controlled area of inhibition. To achieve this, I used 470nm light pulsed at 40Hz with a 50% duty cycle over the duration of a session, delivered to either the ACC or PL. This protocol has been shown to elicit constant activation of the PV cells and thus inactivation of the surrounding pyramidal cells more effectively than a constant photostimulus (Li et al., 2019). I found that this continuous silencing had no effect on basic discrimination in either the ACC or PL cortex, compared to sessions with no optogenetic light (Fig 3.14 – N = 8 mice, 3-4 sessions per mouse per condition, Wilcoxon signed-rank test comparing control and continuous ACC silencing: relevant visual $p = 0.843$, irrelevant visual $p = 0.640$, odours $p = 0.742$, comparing control and continuous PL silencing: relevant visual $p = 0.546$, irrelevant visual $p = 0.460$, odours $p = 0.460$, comparing continuous ACC and continuous PL silencing: relevant visual $p = 0.546$, irrelevant visual $p = 0.742$, odours $p = 0.148$).

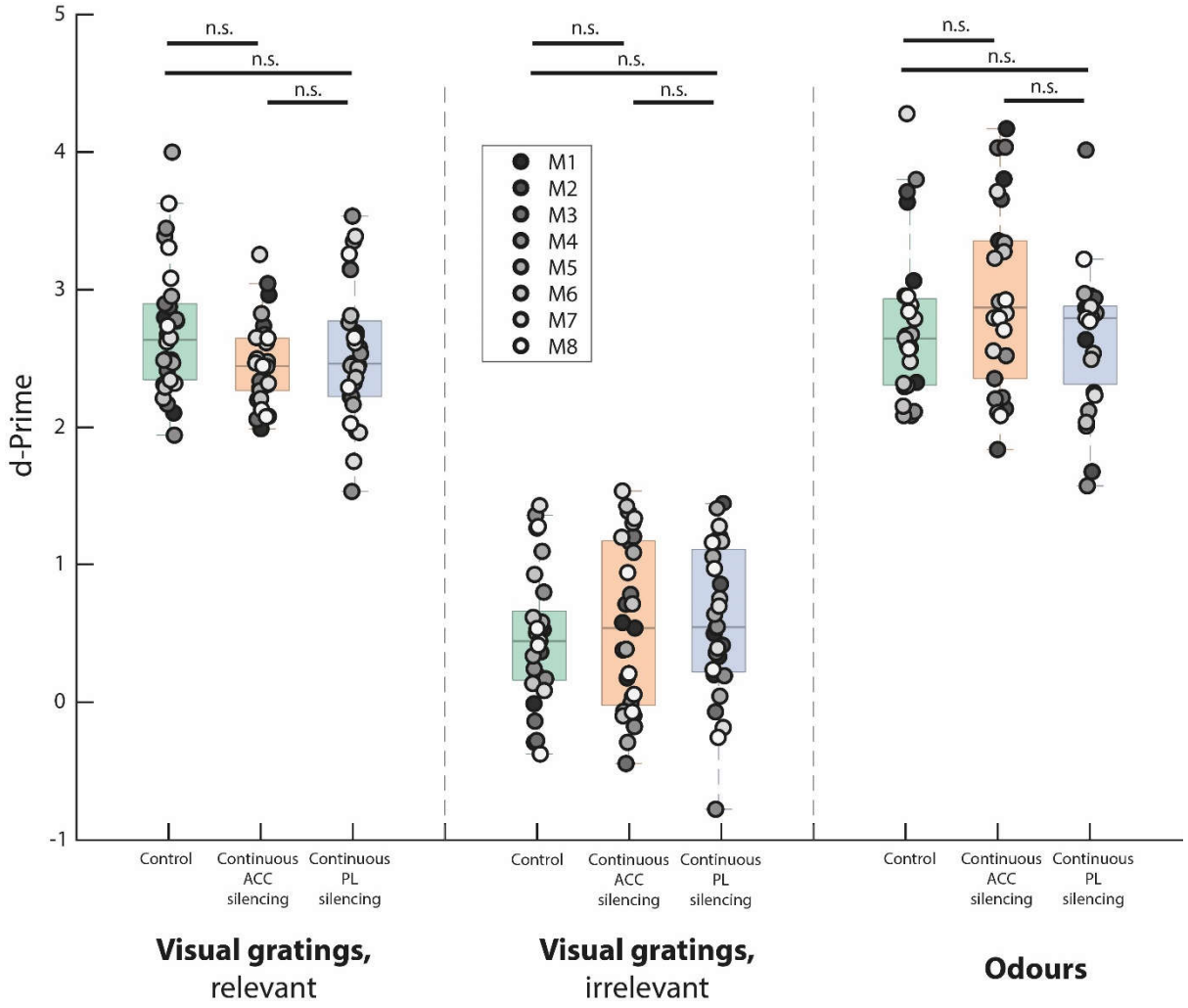

Figure 3.14. Effect of PFC silencing on basic discrimination performance. Discrimination of task stimuli during stable performance across all blocks in a session, during either control sessions or while 40Hz pulsed blue light is delivered to the ACC or PL cortex. Circles represent means across individual sessions. Boxes represent median +/- IQR, whiskers represent the most extreme values not considered outliers.

With basic discrimination intact, I next examined whether block-switching speeds were affected as with the muscimol infusions. A clear effect of ACC silencing emerged when looking at the number of trials taken to switch from an odour block to a visual block, in which the mouse must start licking to the previously irrelevant gratings (Fig 3.15). During ACC silencing, mice took significantly longer to begin responding to the gratings following the switch. This effect was not seen during PL silencing, or when mice switched in the opposite direction to transition from responding to visual gratings to ignoring them (N = 8 mice, 3-4 sessions per mouse, Wilcoxon signed-rank test of number of trials taken to switch comparing control and continuous ACC silencing: odour to visual block $p = 6.2 \times 10^{-4}$, visual to odour block $p = 0.064$, comparing control and continuous PL silencing: odour to visual block $p = 0.782$, visual to odour block $p = 0.775$, comparing continuous ACC and continuous PL silencing odour to visual block $p = 0.024$, visual to odour block $p = 0.033$).

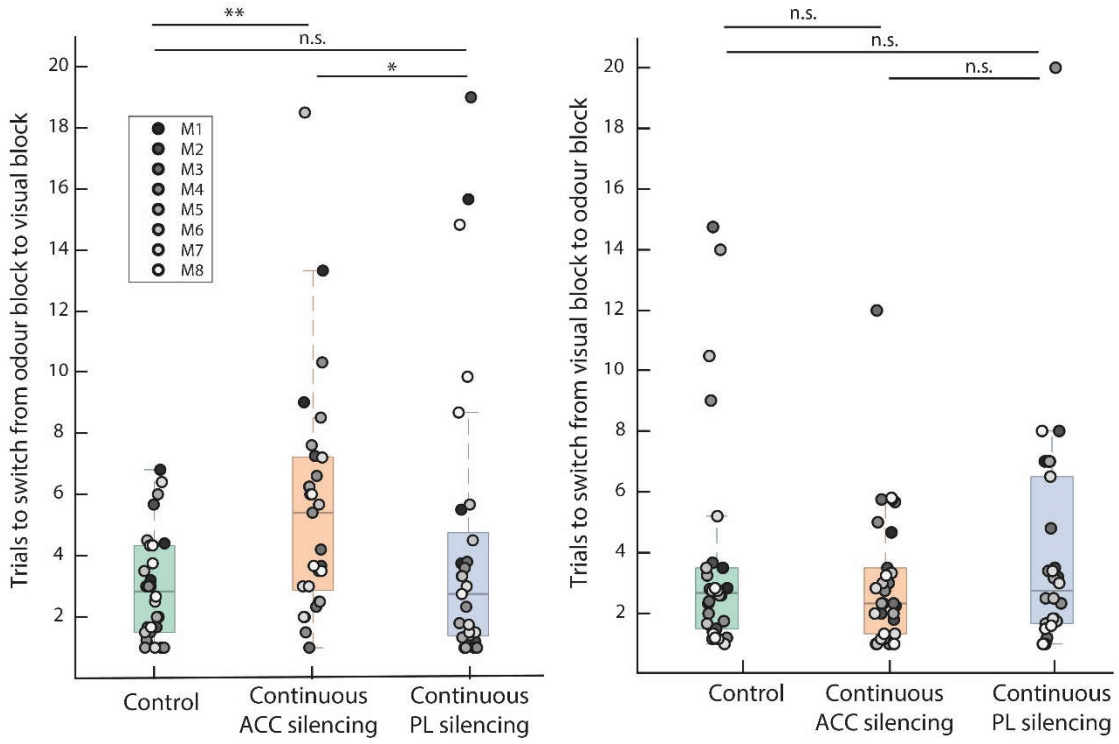

Figure 3.15. Effect of PFC silencing on block switching speeds. Left, number of trials taken for mouse to successfully lick to 3 consecutive rewarded gratings in a new visual block. Right, number of trials taken for mouse to successfully ignore 3 consecutive rewarded gratings in a new odour block. Circles represent means across individual sessions. Boxes represent median +/- IQR, whiskers represent the most extreme values not considered outliers. Significance thresholds following Bonferroni correction for multiple comparisons: * $p < 0.025$, ** $p < 0.005$, *** $p < 0.0005$.

This deficit seen with ACC silencing was not seen on every switch into a visual block. Instead, it manifested as an overall reduction in the number of fast switches performed in a 'one-shot' manner and an increase in slower switches, with either a few or many errors before eventual switching (Fig 3.16 – Wilcoxon rank sum test comparing trials taken to switch across all control and continuous ACC silencing session switches, switching into a visual block $p = 4.8 \times 10^{-5}$, switching into an odour block $p = 0.52$).

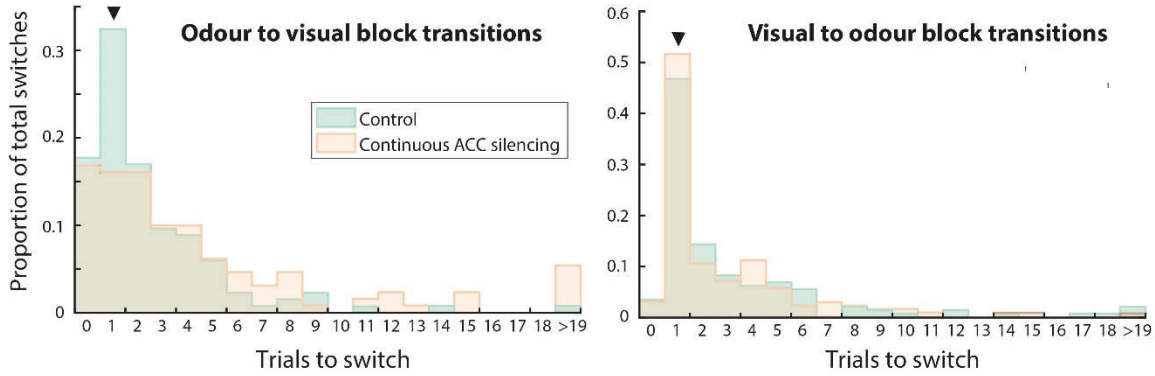

Figure 3.16. Appearance of ACC silencing effect. Left, number of trials to switch to a new visual block. Right, number of trials to switch to a new odour block. Black triangles denote switches performed after a single error. Each datapoint represents an individual switch. N trials to switch into a visual block mean ± SD control = 5.97 ± 3.04, continuous ACC silencing = 8.5 ± 6.05. N trials to switch into an odour block control = 6.41 ± 4.81, continuous ACC silencing = 5.86 ± 3.01.

Mice were generally able to switch eventually, albeit with highly variable delays. This suggests that either the silencing did not sufficiently silence enough of ACC to fully prevent switching, or that the ACC is not crucial for the entire ability to switch attention from ignoring to attending to a visual target. The ACC may instead be necessary specifically to switch attention quickly and with minimal evidence that the switch had occurred. In this task, the first clear evidence that the switch into a visual block has occurred does not come from the first visual grating of the new block - this could well still be an irrelevant grating. Instead, the evidence comes from the absence of the odour that would be reliably expected to follow this grating. Thus - if a mouse is performing optimally in the switching task - it would use the first instance of this odour absence to drive its attention back to the visual stimuli and would lick on the next grating, the second grating of the visual block. I refer to switches that follow this pattern as 'perfect' switches (Fig 3.17). Comparing probabilities of perfect switches when switching from an odour block to a visual block clearly demonstrated this impairment in perfect switching ability when ACC is silenced (Fig 3.18, N = 8 mice, mean across 3-4 sessions per mouse, Fisher's exact test comparing control and continuous ACC silencing $p = 0.0011$, comparing control and continuous PL silencing $p = 0.653$, comparing continuous ACC and continuous PL silencing $p = 0.0037$), which is not seen when switching in the other direction (Fisher's exact test comparing control and continuous ACC silencing $p = 0.852$, comparing control and continuous PL silencing $p = 0.723$, comparing continuous ACC and continuous PL silencing $p = 0.857$).

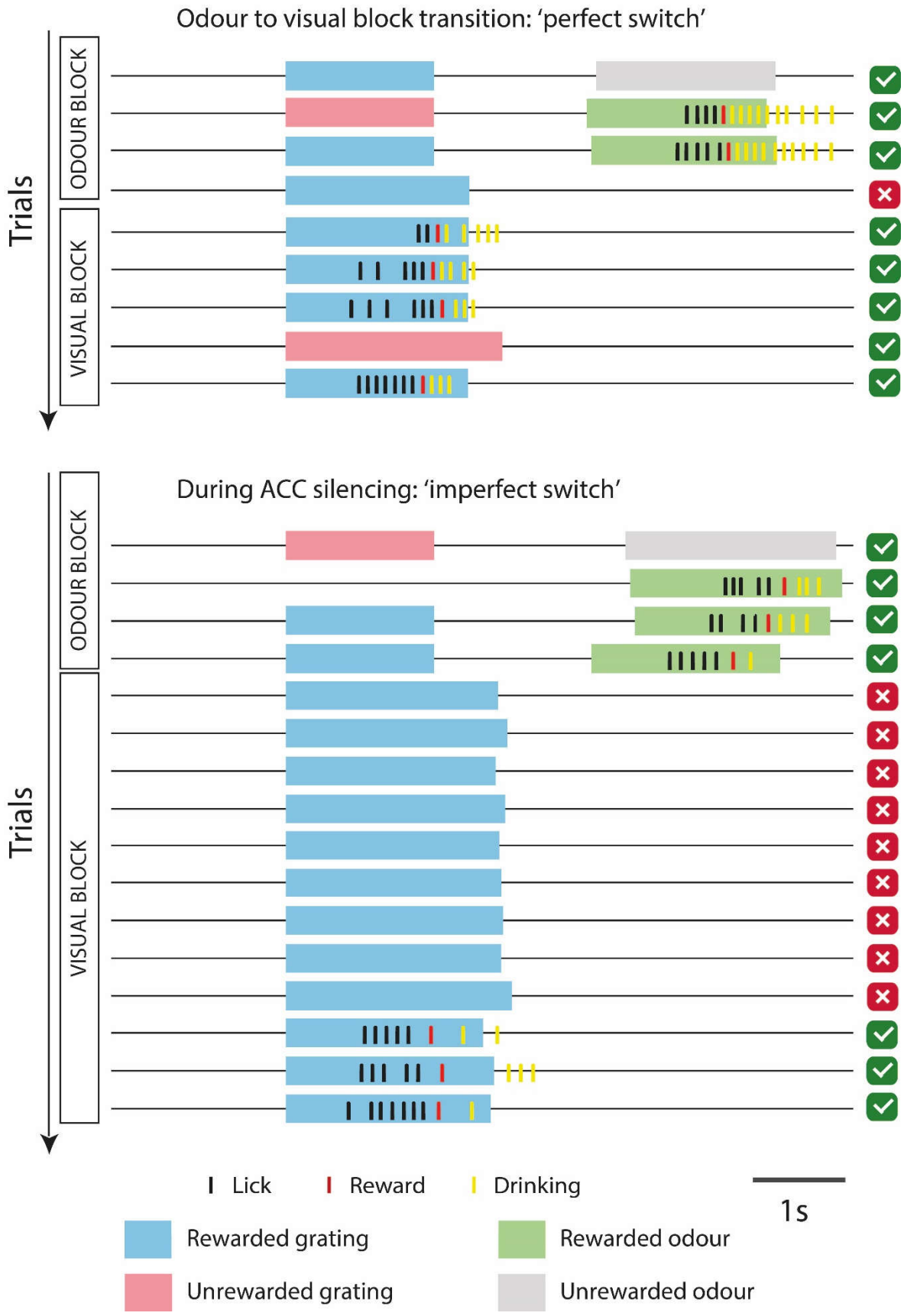

Figure 3.17. Schematic of perfect/imperfect switches. Top, lick raster showing a switch from an odour block to a visual block during a control session, in which the mouse was able to respond to the rewarded visual grating after a single miss trial. Bottom, lick raster showing a switch from an odour block to a visual block during a continuous ACC silencing session, in which the mouse missed 9 trials before responding to the rewarded visual grating.

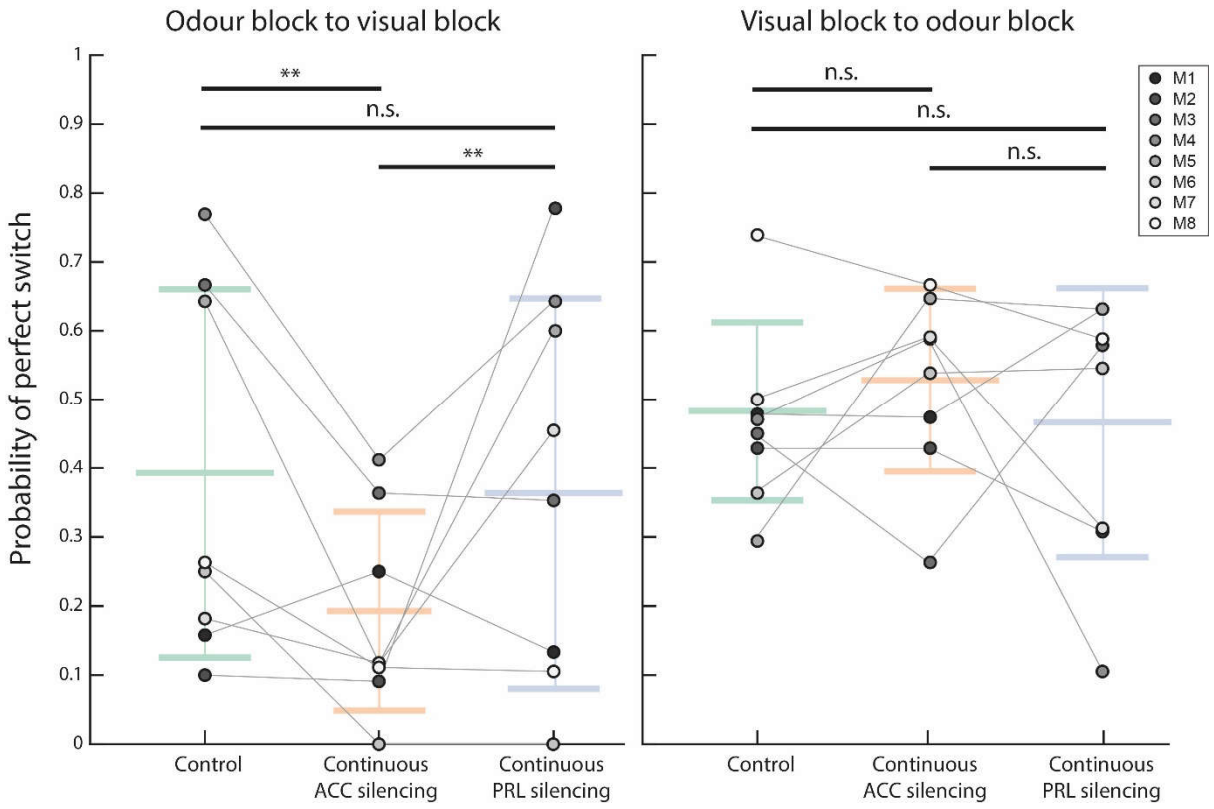

Figure 3.18. Effect of PFC silencing on perfect switching. Left, probability of a perfect switch from an odour block to a visual block. Right, probability of a perfect switch from a visual block to an odour block. Circles represent mean probability across all switches and sessions for each mouse. Lines represents means across all mice +/- SD. Significance thresholds following Bonferroni correction for multiple comparisons: * $p < 0.025$, ** $p < 0.005$, *** $p < 0.0005$.

Finally, I wanted to ensure that this effect of silencing ACC could not be attributed to the distracting properties of the blue light itself, without any optogenetic effects. While the absence of any effect during PL silencing suggests this is unlikely, data from earlier attempts at optogenetically silencing the ACC provided direct evidence that the light alone could not produce the effect. Recordings from 3 PV-Cre mice not expressing ChR2, and 3 PV-Cre;FLEX-ChR2 mice, showed a significant effect of optogenetic light on the number of trials taken to switch from an odour block to a visual block only when the mouse was expressing ChR2 (Fig 3.19 – PV-Cre mice N = 3 mice, 6 sessions per condition, Wilcoxon rank sum test comparing optogenetic light sessions with no light sessions $p = 0.857$, PV-Cre;FLEX-ChR2 mice N = 3 mice, 9 no light vs 4 optogenetic light sessions, Wilcoxon rank sum test comparing no light and optogenetic light sessions $p = 0.0028$, comparing optogenetic light PV-Cre sessions and optogenetic light PV-Cre;FLEX-ChR2 sessions $p = 0.0095$).

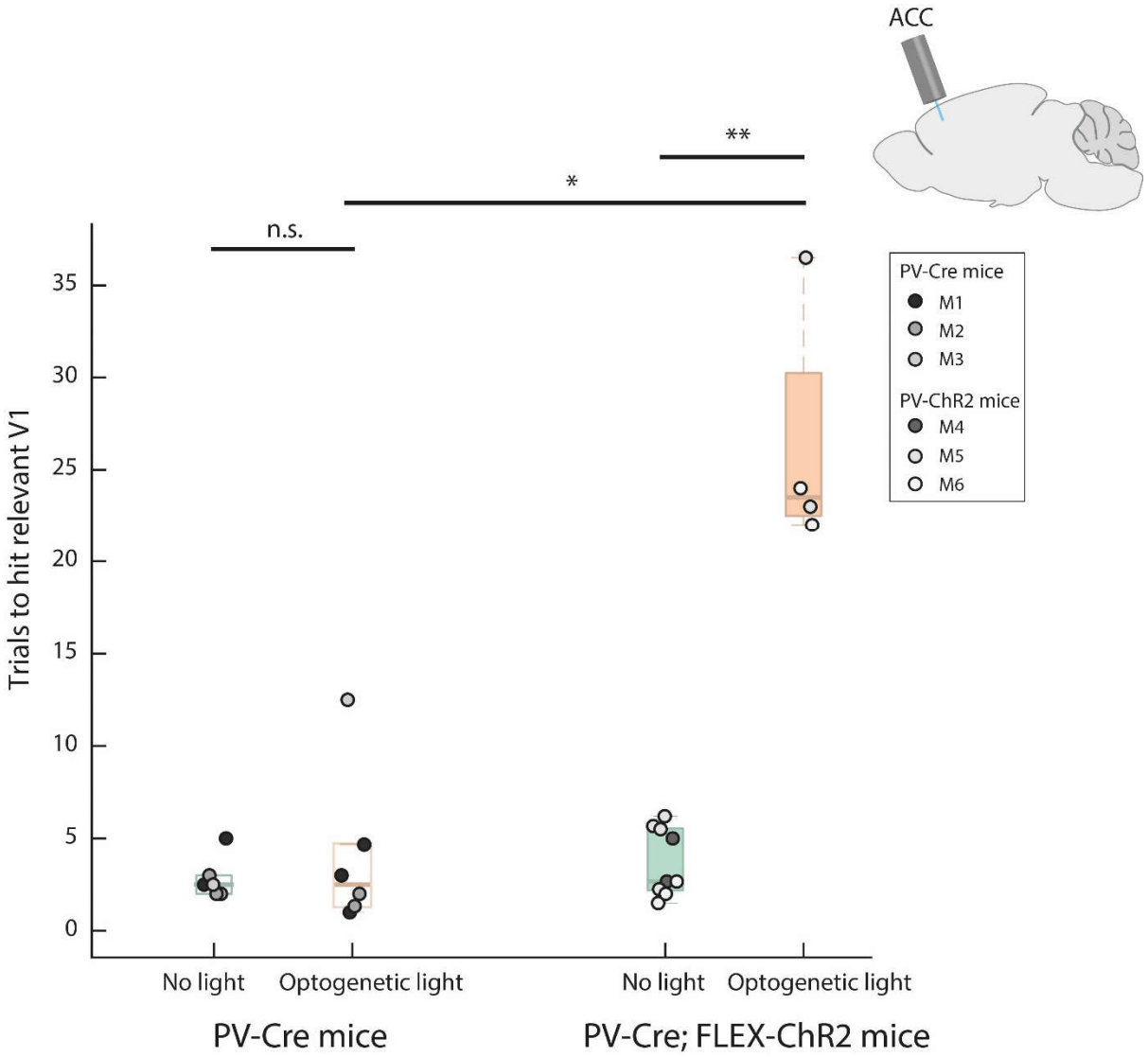

Figure 3.19. Light alone is not sufficient to impair switching. Bottom, number of trials taken for mouse to successfully lick to 3 consecutive rewarded gratings in a new visual block, averaged across all switches in a session. Circles represent means across individual sessions. Boxes represent median +/- IQR, whiskers represent the most extreme values not considered outliers. Significance thresholds following Bonferroni correction for multiple comparisons: * $p < 0.025$, ** $p < 0.005$, *** $p < 0.0005$. Top-right, schematic of optic cannulae implantation for these mice.

4. ACC is required throughout the trial for attention-switching

Having established that silencing the ACC for the entire duration of the switching session impaired switching in one direction but not the other, I investigated whether this ACC requirement could be isolated to a specific epoch within the trial. Specifically, I wanted to probe whether the ACC is needed during the interval between visual stimuli, when the mouse should notice the absence of the expected odour and prepare its response for the upcoming visual stimulus, or during the visual stimuli, when the licking response itself is required. If silencing around but not during the gratings could fully reproduce the effect, it would indicate that the ACC is involved in detecting the absent odour and preparing the response to the upcoming stimulus,

but not in delivering the response itself. This would conform to the theorised role for the ACC in encoding outcome predictions to update internal models. Conversely, if silencing during but not around the gratings could fully reproduce the effect, it would suggest that the ACC is not involved in recognising the absent odour, and instead is directly involved in producing the licking behaviour required to respond to the grating. This could conform to the adaptation and persistence model, with the ACC involved in response selection when multiple responses are possible. The decision to lick to the visual gratings, when not licking was the *status quo*, could mirror the decision to leave in foraging experiments, with the ACC promoting a shift away from the default strategy.

I introduced two separate optogenetic silencing epochs to explore these possibilities (Fig 3.20). Light appeared at the same relative time on every trial in a session to prevent the light providing any kind of cue for the mouse to determine which block it was in. Sessions involving these epochs were interleaved between continuous silencing and control sessions, with no condition repeated on consecutive days.

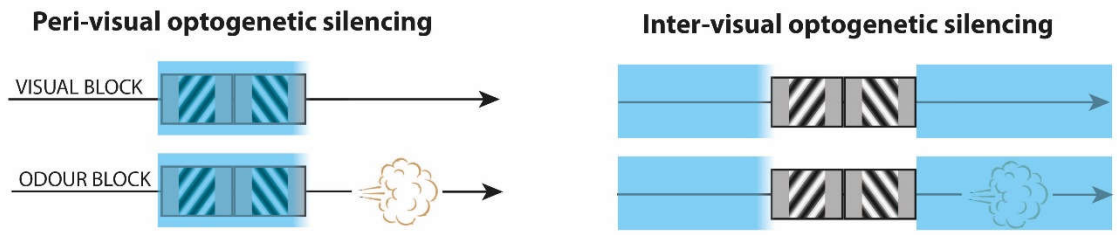

Figure 3.20. Optogenetic silencing epochs. Left, peri-visual optogenetic silencing. Optogenetic light activates 100ms before the onset of the visual stimulus and continues to the offset of the grating. Right, inter-visual optogenetic silencing. Optogenetic light activates at the offset of the visual stimulus and continues until the onset of the next stimulus. For the final 200ms of each light epoch, light power ramped down linearly to prevent any rebound activity in target neurons caused by a sudden offset.

In contrast to these expectations, either silencing epoch was sufficient to significantly impair switching from an odour block to a visual block (Fig 3.21 - N = 8 mice, 3-4 sessions per condition, Wilcoxon signed-rank test comparing trials taken to switch from an odour block to a visual block between control sessions and inter-visual ACC silencing $p = 0.021$, control sessions and peri-visual ACC silencing $p = 0.0087$, inter-visual and peri-visual ACC silencing $p = 0.39$). Switching in the other direction was unaffected (Wilcoxon signed-rank test comparing trials taken to switch from a visual block to an odour block between control sessions and inter-visual ACC silencing $p = 0.19$, between control sessions and peri-visual ACC silencing $p = 0.24$, and between inter-visual ACC silencing and peri-visual ACC silencing $p = 0.88$).

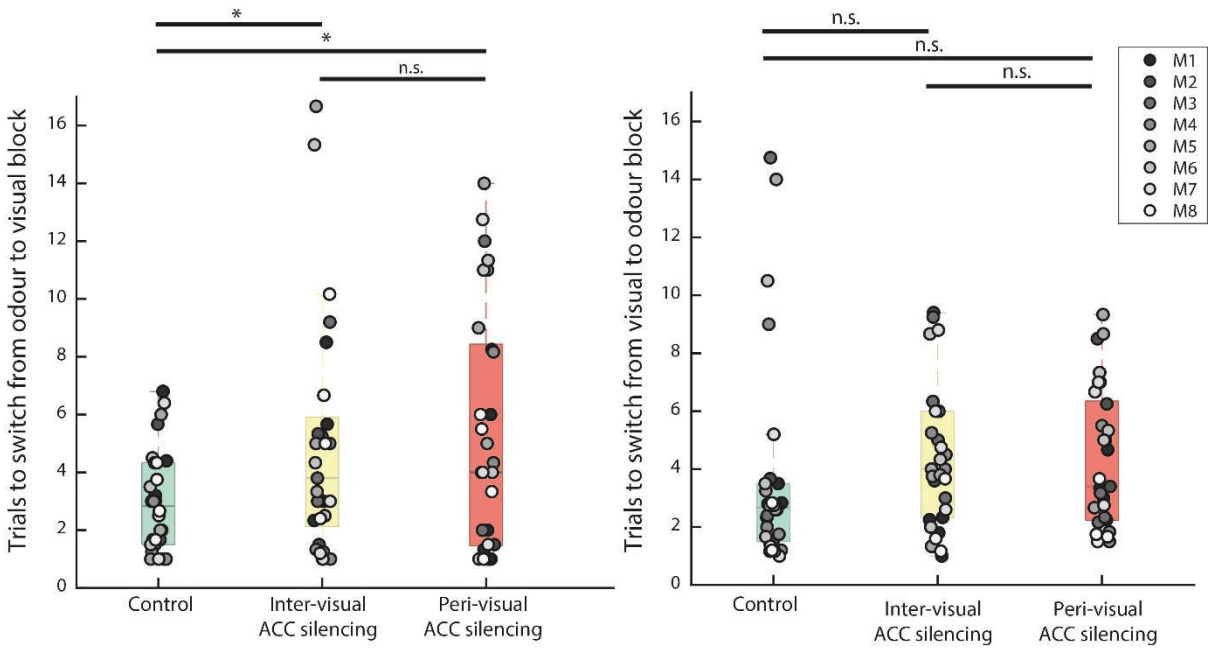

Figure 3.21. Effect of ACC silencing over discrete epochs of trial. Left, number of trials taken for mouse to successfully lick to 3 consecutive rewarded gratings in a new visual block, averaged across all switches in a session. Right, number of trials taken for mouse to successfully ignore 3 consecutive rewarded gratings in a new odour block, averaged across all switches in a session. Circles represent means across individual sessions. Boxes represent median +/- IQR, whiskers represent the most extreme values not considered outliers. Significance thresholds following Bonferroni correction for multiple comparisons: * $p < 0.025$, ** $p < 0.005$, *** $p < 0.0005$.

These results cannot be reconciled with either of the earlier stated theories of ACC involvement exclusively; it appears that ACC signalling both during and between visual stimuli is required for optimal switching. The importance of the ACC to task switching clearly goes beyond a brief contribution during or after the presentation of the grating.

5. The effect of ACC silencing on attention-switching decays over time

An observation made immediately after collecting these recordings was that optogenetic silencing performed later in a mouse's experimental timeline seemed to induce less obvious deficits to the mouse's ability to switch from an odour block to a visual block, compared to their performance in earlier sessions. To examine this, I plotted trials taken to switch into a visual block across the first 3 switches of each session, and across the first 3 sessions recorded from each mouse for each condition (Fig 3.22 – N = 8 mice, up to 8 datapoints per switch per session, after removing switches performed without any errors – see methods).

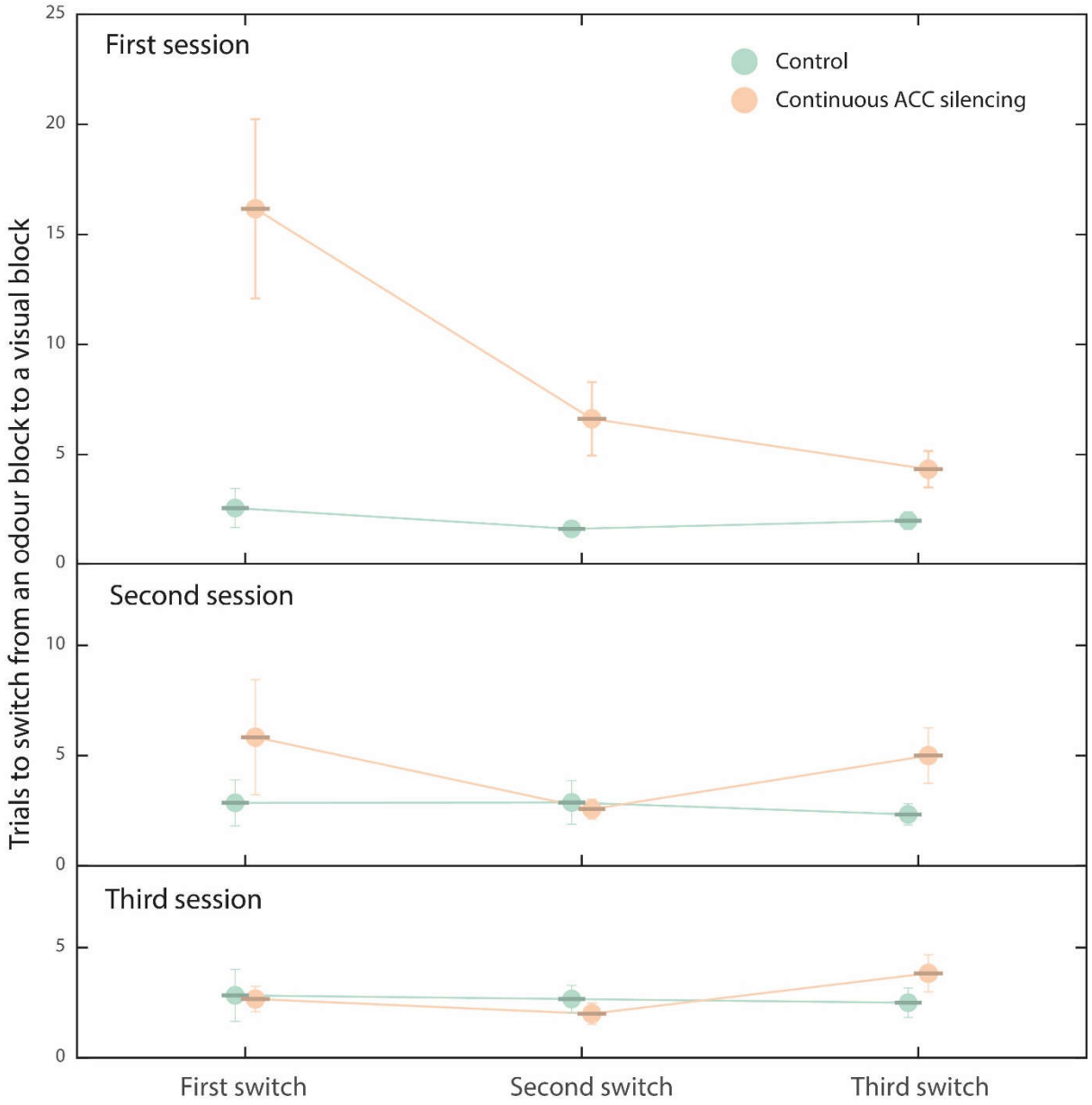

Figure 3.22. Effect of continuous ACC silencing decays over time. Number of trials taken for mouse to successfully lick to 3 consecutive rewarded gratings in a new visual block, for the first 3 switches in the first 3 sessions from each mouse. Lines represent means for all mice +/- SEM, with switches in which the mouse responded to the very first trial removed.

This phenomenon was even more pronounced in inter-visual and peri-visual ACC silencing epochs (Fig 3.23).

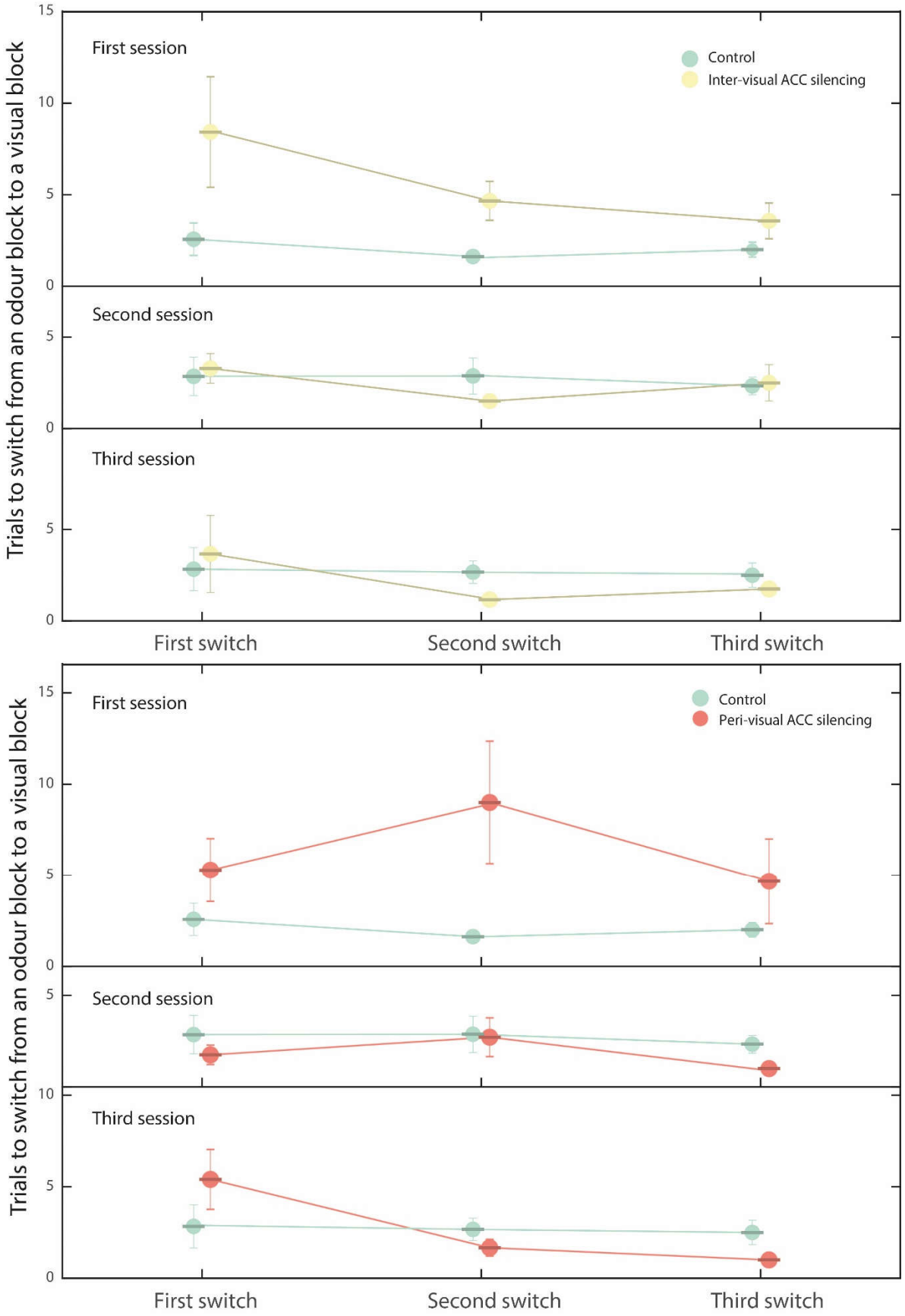

Figure 3.23. Effect of epochal ACC silencing decays over time. Number of trials taken for mouse to successfully lick to 3 consecutive rewarded gratings in a new visual block, for the first 3 switches in the first 3 sessions from each mouse. Lines represent means for all mice +/- SEM, with switches in which the mouse responded to the very first trial removed. Top, inter-visual ACC silencing. Bottom, peri-visual ACC silencing.

The decay of this effect was surprising and did not seem to depend on the order in which each silencing condition was performed. Silencing conditions were pseudorandomly selected so that each mouse performed each of the 7 silencing conditions (continuous ACC/PL, peri-visual ACC/PL, inter-visual ACC/PL, and control sessions) in different orders. This meant that each type of session had at least 8 days between repetitions, with each repetition equally separated in time. It seemed that the mouse was able to compensate for the deficit caused by ACC silencing over time, perhaps via new behavioural strategies that engaged unaffected brain regions. A further observation was that the impairment in the probability of a perfect switch from an odour block to a visual block across the first 3 switches of a session persisted for longer, across the first two sessions (Fig 3.24, N = 8 mice, Fisher's exact test comparing probability of perfect switch for day 1: comparing control and continuous ACC silencing $p = 7.42 \times 10^{-4}$, control and continuous PL silencing $p = 0.51$, continuous ACC silencing and continuous PL silencing $p = 0.0052$, for day 2: comparing control and continuous ACC silencing $p = 0.0323$, control and continuous PL silencing $p = 0.12$, continuous ACC silencing and continuous PL silencing $p = 0.1272$, for day 3: comparing control and continuous ACC silencing $p = 0.29$, control and continuous PL silencing $p = 0.97$, continuous ACC silencing and continuous PL silencing $p = 0.25$).

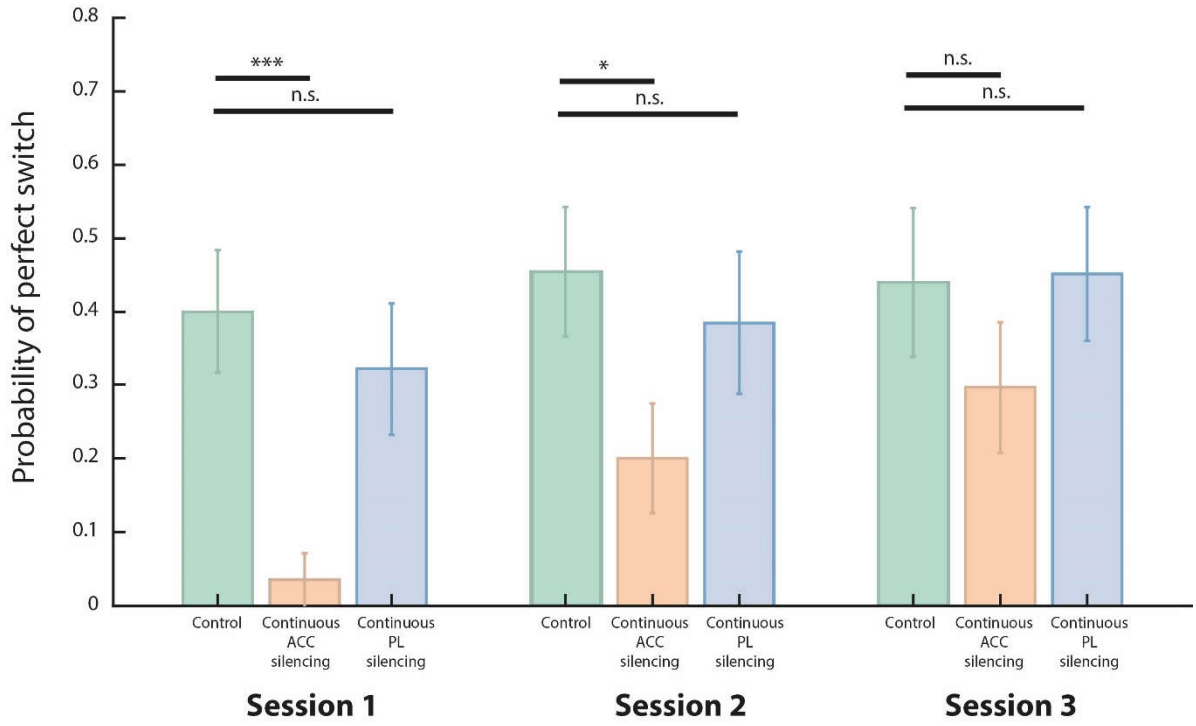

Figure 3.24. Probability of perfect switch across repeat sessions. Probability of a perfect switch in the first three switches of each of the first 3 sessions. Bars represent means, error bars represent SEM.

These results suggest that while this deficit in trials taken to switch caused by continuous ACC silencing receded reasonably quickly, the overall deficit to the mouse's ability to switch optimally (within a single trial) was slower to recover. Clearly these two phenomena are heavily interconnected: a mouse with fewer perfect switches will therefore take a greater number of trials to switch. After collecting a complete set of repetitions of these silencing conditions, the effect had receded to the extent that even simultaneous and continuous ACC and PL silencing was unable to reproduce it (Fig 3.25 – Wilcoxon signed-rank test comparing trials to switch from an odour block to a visual block $p = 0.47$, comparing trials to switch from a visual block to an odour block $p = 0.57$).

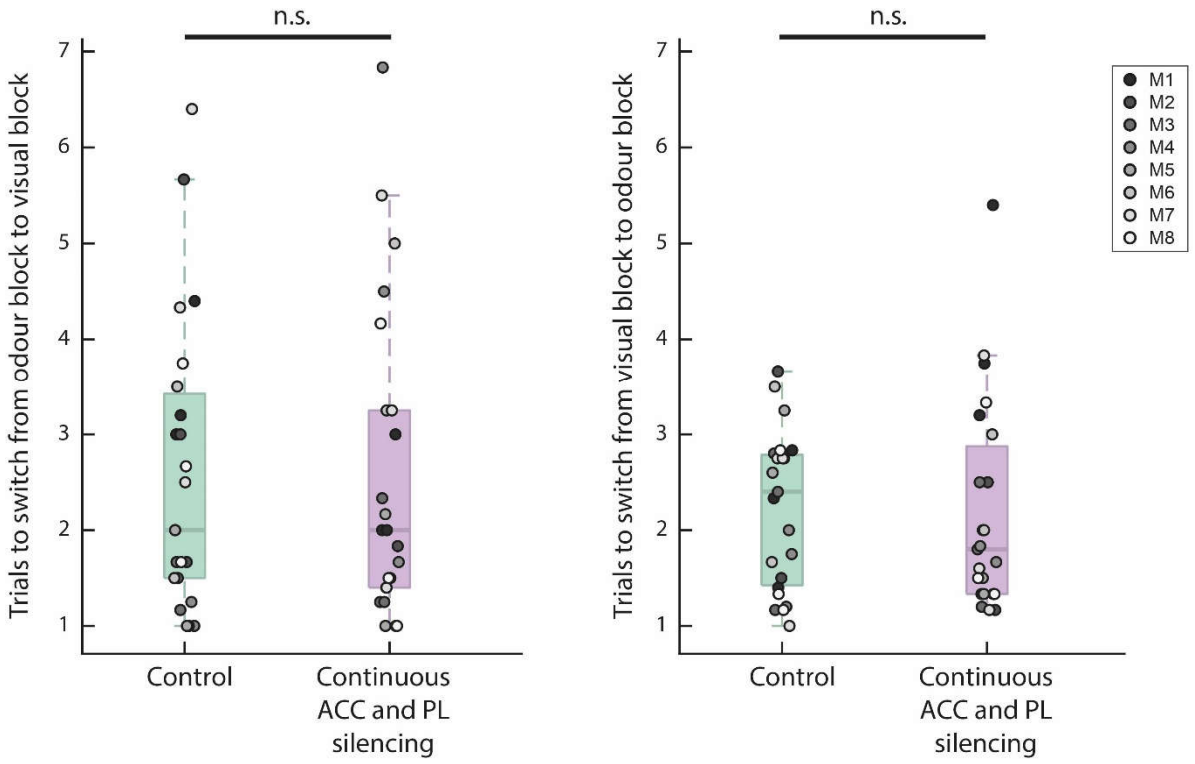

Figure 3.25. Simultaneous continuous silencing of ACC and PL. Recorded after 3 sessions of each of the 7 initial silencing conditions had been collected. Left, number of trials taken for mouse to successfully lick to 3 consecutive rewarded gratings in a new visual block. Right, number of trials taken for mouse to successfully ignore 3 consecutive rewarded gratings in a new odour block. Circles represent means across individual sessions. Boxes represent median +/- IQR.

6. ACC silencing is ineffective after the first trial of the visual block

These earlier results demonstrated that continuous ACC silencing slowed switching - at least in initial sessions - from an odour block to a visual block. The effect seemed to be relatively more pronounced and robust when examining specifically whether the switch was 'one-shot' - performed at the first informed opportunity. This suggested that the ACC may be critically involved in this first trial, immediately after switching, in which the mouse must be observant of the first absence of the expected odour to drive a change in behaviour. To examine this, I altered the optogenetic light epoch so that the ACC was continuously silenced, with 40Hz pulses as

before, except for this first trial following a switch from an odour block to a visual block (Fig 3.26). Unfortunately, these experiments were performed after the aforementioned delay of the effect, so the impact on silencing must be caveated by the knowledge that at this point of experimenting even continuous silencing of the ACC and PL was unable to reproduce the switching impairment seen in the earlier silencing sessions.

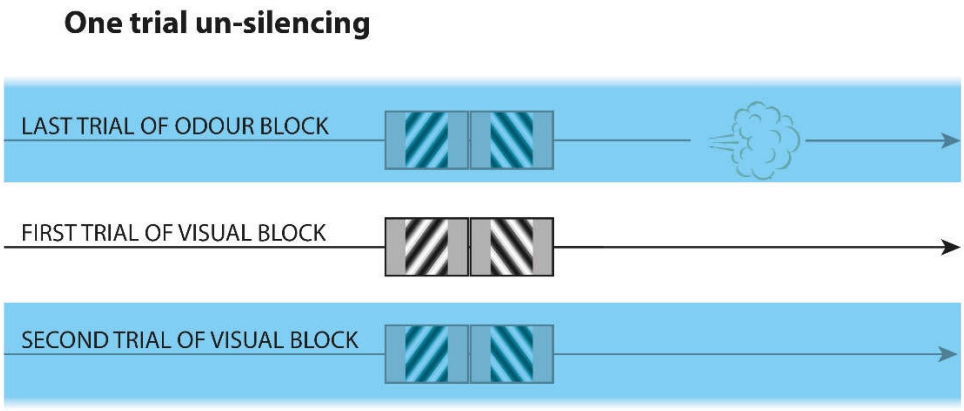

Figure 3.26. Schematic of one trial un-silencing epoch. Light offset is at the beginning of the first trial of a visual block and remains off until the start of the next trial. Light is otherwise pulsed for the entire session.

When silencing but for this first trial, the deficit in switching seen during the full ACC silencing epoch was unsurprisingly not reproduced, as the effect had receded by this point. Strikingly however, un-silencing the ACC for this single trial in fact produced a marked improvement in performance over control (Fig 3.27 – 8 mice, 2-3 sessions per mouse, A: Wilcoxon signed-rank test comparing trials to switch from odour block to visual block: control and continuous ACC silencing $p = 2.74 \times 10^{-4}$, control and one trial un-silencing $p = 0.0084$, continuous ACC silencing and one trial un-silencing $p = 0.0016$, B: Fisher's exact test comparing probability of perfect switch: control and continuous ACC silencing $p = 2.54 \times 10^{-4}$, control and one trial un-silencing $p = 2.03 \times 10^{-4}$, continuous ACC silencing and one trial un-silencing $p = 5.16 \times 10^{-12}$).

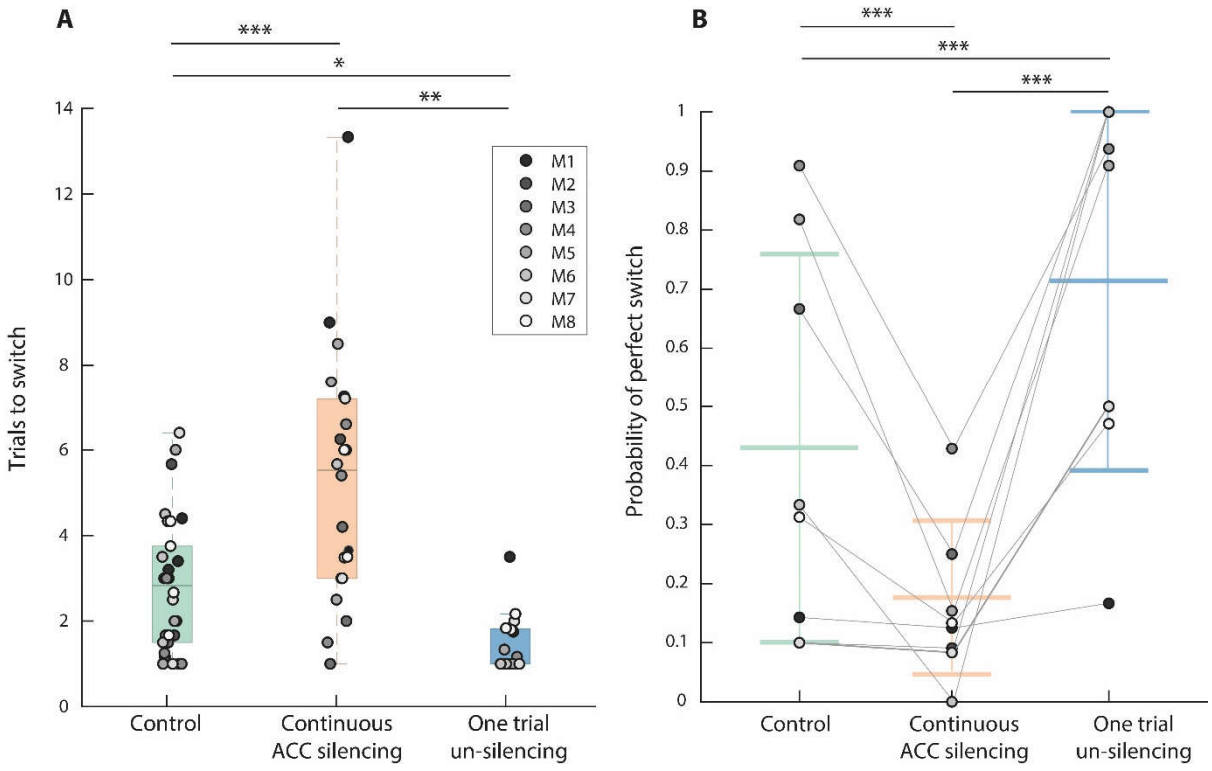

Figure 3.27. One trial un-silencing improves switching. A: Number of trials taken for mouse to successfully lick to 3 consecutive rewarded gratings in a new visual block. Circles represent means across individual sessions. Boxes represent median +/- IQR, whiskers represent the most extreme values not considered outliers. B: Probability of perfect switch when switching from an odour block to a visual block. Circles represent mean probability across all switches. Lines represent mean +/- SD. Significance thresholds following Bonferroni correction for multiple comparisons: * $p < 0.025$, ** $p < 0.005$, *** $p < 0.0005$.

This improvement in switching was an unexpected result. It could not be attributed solely to the mouse's overall improvement over the course of repeated sessions, as it remained significantly quicker when compared to control sessions only taken after these recordings. One simple explanation was that mice were using the sudden disappearance of the blue light, which was otherwise on for every trial except this first trial of the new visual block, as a cue to draw their attention to the fact that the block had changed. To address this, I attempted the reverse of this epoch, with the light only turning on for this first trial of the new visual block (Fig 3.28). In this experiment, the optic fibre was disconnected from the cannulae and instead hung several centimetres above the mouse's eyeline, providing a distracting cue at least as noticeable as the optogenetic light would be when connected to the cannulae, but with no optogenetic effects.

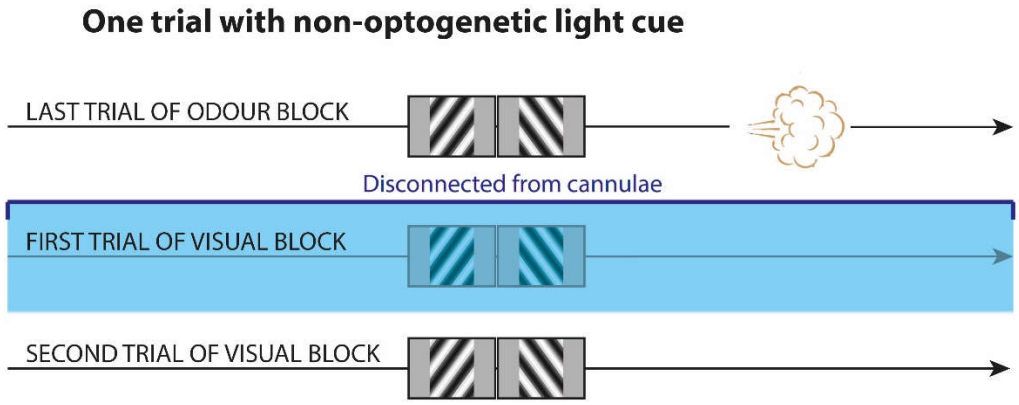

Fig 3.28 Schematic of light cue epoch. Optic fibre provides distracting light only in the first trial of each visual block.

This light cue epoch did not produce the same increase in probability of perfect switches seen in the one trial un-silencing epoch. Instead, I saw the probability of the mouse performing a perfect switch stay at control levels, and the probability that the mouse would lick pre-emptively, during the trial in which the light came on, rise significantly (Fig 3.29 – N = 8 mice, 2-3 sessions per mouse, Fisher's exact test of probability of perfect switch: comparing control and light cue p = 0.13, Fisher's exact test of probability of error switch: comparing control and continuous ACC silencing p = 0.83, control and one trial un-silencing p = 0.069, control and light cue p = 8.15 x 10^{-4}).

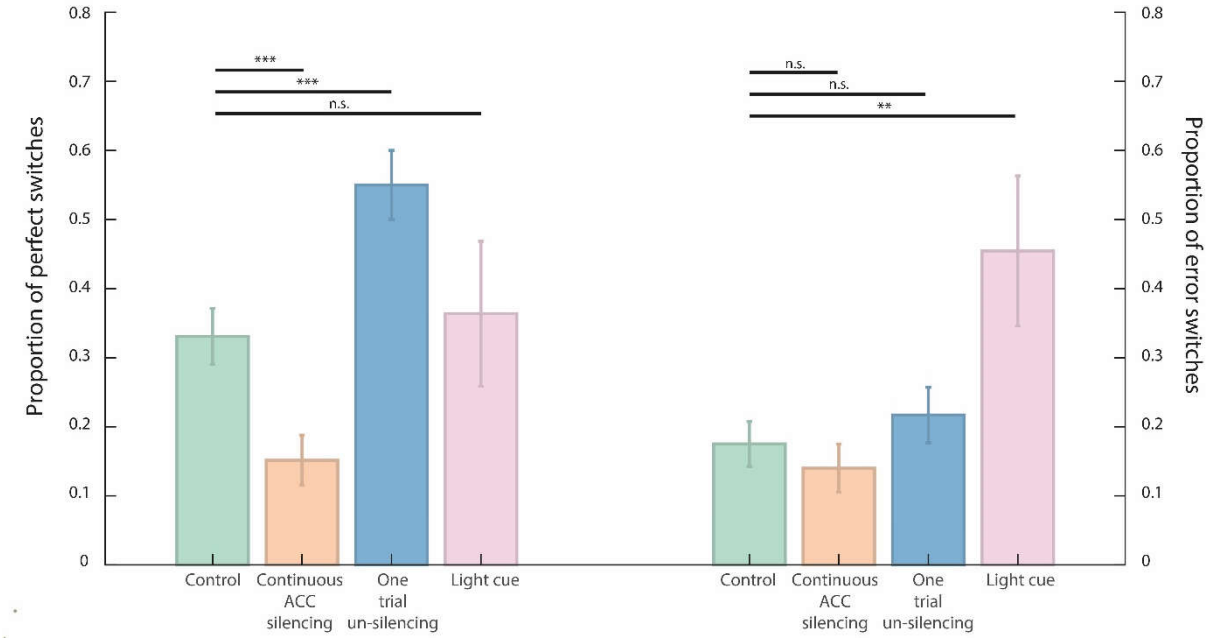

Figure 3.29. Probability of perfect and error switches across single trial epochs. Left, probability of perfect switch when switching from an odour block to a visual block. Right, probability of error switch (lick to first visual trial) when switching from a visual block to an odour block. Bars represent means, error-bars represent SEM. Significance thresholds following Bonferroni correction for multiple comparisons: * $p < 0.025$, ** $p < 0.005$, *** $p < 0.0005$.

This increase in probability of 'error' switches (Fig 3.30) suggested that the mice were reacting reflexively to the sudden appearance of the blue light by licking, without any coherent expectation that they were in a visual block. Upon receiving this unexpected reward, they could

then switch their attention back to the visual gratings. This means if the one trial un-silencing result was purely a reaction to the cue (the disappearance of the light) we would expect similar results: instead, we saw a reaction on the next trial after the light has resumed. It is still possible that the disappearance of the light was directing the mouse to attend to the visual stimuli, if not providing as immediate a cue as the light cue condition.

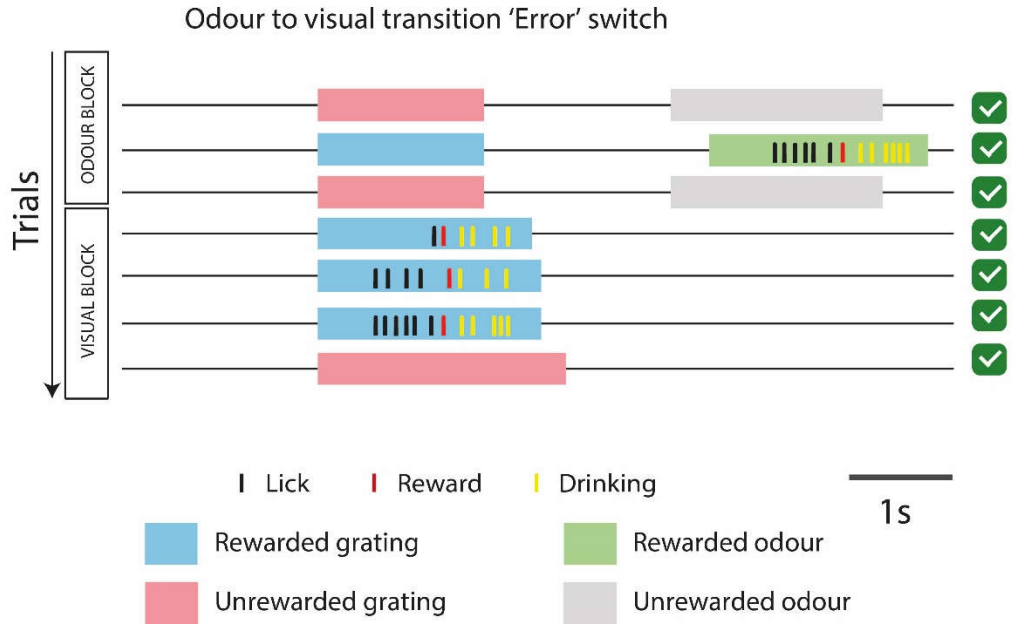

Figure 3.30. Schematic of an error switch. Lick raster extracted from a switch from an odour to a visual block during a control session, in which the mouse licked to the very first rewarded grating despite receiving no clear evidence from the task that the block change has occurred.

Nonetheless, these results demonstrate that the ACC was not essential after this first trial of the new visual block for the mouse to switch. This underlined the importance of ACC function specifically in this first trial for triggering an immediate switch in the next. What is unclear is how relevant these observed improvements in switching during un-silencing, and the overall attenuation of the silencing effects over time, are to this established role of ACC.

Discussion chapter 1:

The role of anterior cingulate cortex in task-switching behaviour

In this chapter, I demonstrated that the mice were able to first learn the visual discrimination task, then the full attention-switching task, to a high enough level of performance to examine the effects of lesions. Initial attempts at silencing the ACC using muscimol infusions revealed an asymmetric effect, with switching from an odour block to a visual block impaired but switching from a visual block to an odour block enhanced following muscimol infusions. Repeating these experiments using continuous optogenetic inhibition instead reproduced the impairment when switching into a visual block, but not the enhancement when switching into an odour block. Silencing the PL had no effect on this switching behaviour.

By limiting the epoch of photoinhibition, I showed that silencing the ACC either only during or only around the visual stimuli were both sufficient to impair this switching into a visual block. These impairments receded over subsequent sessions, and after the third session could not be reproduced even by simultaneous ACC and PL silencing. Un-silencing the ACC during the first visual trial only did not reproduce the impairments, and instead led to significantly quicker switching in a visual block. This may have been due to the distracting properties of the light, as drawing attention to this first trial without any optogenetic perturbations was also sufficient to drive licking to the visual gratings.

1. Mice can learn to perform an attention-switching task

Go/no-go task-switching

A key feature of this behavioural task which distinguishes it from many other switching tasks also featuring multiple modalities of sensory stimuli is its asymmetry: the disappearance and reappearance of odour stimuli in respective blocks. When contrasting relevant and irrelevant visual stimuli this structure is an advantage, the odours providing an unambiguous dominant stimulus modality to which the mouse can switch its attention towards and therefore away from the visual stimuli. However, when examining transitions between the different blocks, the asymmetry produces an identifiable cue that provides the mouse with all the information that should be necessary to determine the current context after a single trial of the new block. If a

mouse is fully engaged in the task, and has a comprehensive understanding of its structure, then theoretically switch should never involve more than a single mistake following the switch.

The data, however, show that this is not the case. In well-trained mice we see that this 'perfect' switching accounts for around half of transitions in either direction (Fig 3.08A), which is particularly striking in the switches into an odour block, when the appearance of the odour stimulus should be impossible for the mouse to ignore. Symmetric task-switching paradigms usually require the mouse to repeatedly sample the environment to gather evidence and eventually discern the current context. Instead, this task allows us to model a common real-world situation, in which the information required for us to modify our behaviour correctly is immediately available, but whether through a lapse in concentration, attending to the wrong targets, or an inability to develop the new strategy quickly enough, we fail to adapt our behavioural optimally and proceed to make unnecessary errors.

The other relatively unusual feature of this task structure is in the switch from an odour block to a visual block. The asymmetry allows the mouse to experience "positive" surprise when the odour appears in the first trial of a new odour block - when something happens that was not expected. But in the other direction the mouse experiences "negative" surprise when the odour fails to arrive - that is, when something is expected to happen but does not. Both require monitoring of the external environment to create a consistent internal structure of expectations. The effect of ACC silencing is to impair switching only when the disappearance of the odour is the cue.

The human ACC is responsive to prediction-errors regardless of whether the outcome was more positive or negative than expected (Oliveira et al., 2007). In the PRO model the ACC does not encode positive or negative outcomes, instead encoding this positive and negative surprise (Alexander & Brown, 2011). The mouse experienced both during block transitions, but only during negative surprise did the ACC seem to be crucial. I would argue this is because experiencing negative surprise requires closer monitoring, as a subtraction from this internal structure is less immediately apparent than an addition. Studies of effort-based decision-making in rodents may also support this: ACC lesions bias rodents to prefer a lower-reward, lower-effort choice (Kashay et al., 2022; Rudebeck et al., 2006). It may be that prediction-error signalling is disrupted by ACC silencing, but only when the mouse is transitioning from a low-effort response – not licking – to a higher-effort response – licking.

Many behavioural tasks, such as bandits (Atilgan et al., 2022; Siniscalchi et al., 2016), vary probabilities of certain stimuli or outcomes. These require the mice to repeatedly sample both options available to establish which has the greater change of a favourable outcome in the current

context. As either probability is rarely 1, the mouse will still experience a reasonable rate of failures to the correct choice, so should learn not to radically alter its behaviour in response to a single error. This contrasts with our task, in which the probability of one of the stimulus modalities being relevant is always 1, and a single error in predicting this is enough to inform the mouse that it should change behaviour. An interesting future direction would be to vary the probability of the odour, so that the mouse's certainty that the odour should arrive, and thus surprise when it does not, could be probed. This would require a more complex internal model of actions and predictions, with the outcomes of each action being monitored for prediction errors every trial in order to constantly update this model.

Transfer of learning during training

A key tool for cognition is the transfer of learning - using concepts and principles developed from solving certain problems to facilitate solving new problems despite an unfamiliarity with the novel situation. We see that mice learning this task take up to 10 days to learn the visual task, but when subsequently learning the odour task reach post-learning status within 3 days, often within a single session. The rules for the relevant stimuli are the same across the two tasks - to lick to one of the stimuli and withhold licks to the other – so it follows that the mice may well be using this learned knowledge of the task structure to expediate the forming of new associations between the novel odour stimuli and the correct responses.

Studies in humans have shown that training in an olfactory memory task allows participants to learn a subsequent visual memory task more quickly, but learning the visual task first has no effect on their ability to learn the olfactory task (Olofsson et al., 2020). The authors argued that olfaction plays a special role in facilitating the transfer of learning to other sensory structures that does not occur in the opposite direction. However, the relative importance of vision and olfaction to a mouse's normal behaviour are the inverse of those seen in humans, who typically rely on visual information far more than olfactory information in most scenarios, so it may still be possible that this is happening in our task. The information transferred is relatively abstract: that in a given pair of stimuli one is rewarded, and one is not. Learning the rule initially should expedite subsequent associations, regardless of the modality.

The prefrontal cortex, and its connectivity with the hippocampus, have been implicated in transfer of learning, with differences in these connections correlating with person-to-person variability in ability to transfer learning (Gerraty et al., 2014). To investigate ACC involvement I silenced the ACC for the duration of the PV-Cre;ChR2 mice's initial odour learning sessions, and compared the trials taken for them to learn to discriminate odours (defined as over 80% discrimination in a 30 trial moving window) and ignore irrelevant gratings (15 consecutive gratings

without a lick) with mice used for my imaging experiments, which were not perturbed (Fig 3.31 – N = 8 mice from control group, VIP-Cre mice, and 8 mice with continuous ACC silencing, PV-Cre;ChR2, 1 session per mouse, Wilcoxon rank sum test comparing trials to discriminate odours p = 0.34, comparing trials to ignore irrelevant gratings p = 0.11). I saw no overall difference in time taken to discriminate odours or ignore irrelevant gratings. This suggests that if transfer of learning is occurring, the ACC is not solely responsible for it. This is not completely unexpected: while the mPFC signals rule information in set-shifting tasks, lesions to the mPFC do not prevent rule learning (Birrell & Brown, 2000; Bissonette et al., 2008) – instead this relies on projections from the hippocampus (Navawongse & Eichenbaum, 2013). However, these studies refer to initial rule learning - it is still possible that this secondary transfer of learning may use different mechanisms.

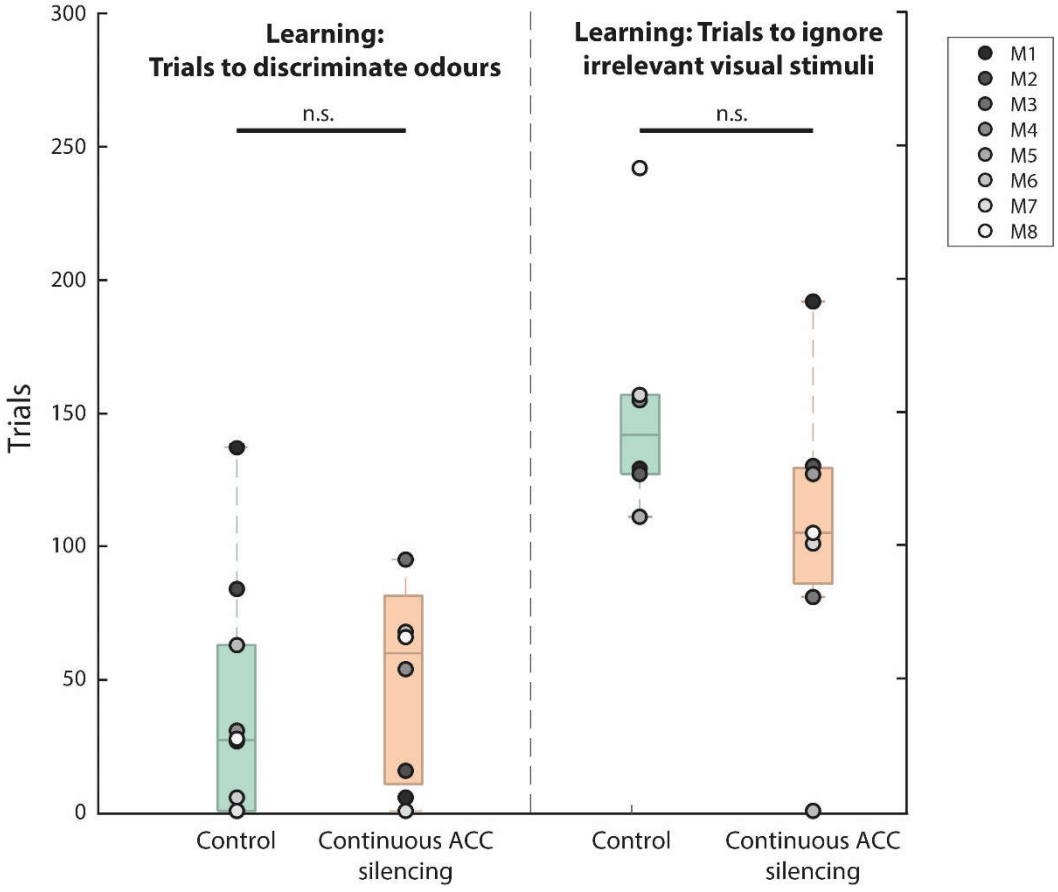

Figure 3.31. ACC silencing does not impair learning of the odour task. Left, trials taken to discriminate odour stimuli in first odour session. Right, trials taken to ignore irrelevant visual gratings in first switching session, relative to their introduction. Circles represent individual sessions. Boxes represent median +/- IQR, whiskers represent the most extreme values not considered outliers.

The lack of an effect here suggests either ACC is not involved, or that this faster learning of odour discrimination compared to visual discrimination is not a result of transfer of learning - maybe instead just a feature of the mouse's superior ability to perceive odours, as Broca observed. Certainly, within the modality itself the difference in sensory features is much less subtle; visual

stimuli are simply reflected images of each other, while the unrewarded odour stimulus features a unique chemical (p-Cymene) not featured anywhere else in the task and with a distinct odour profile even easily perceived by humans, so likely unmistakeable for mice. To properly test ACC involvement, I would need to reverse the order of the task learning so that some mice learn visual discrimination second to see if this is accelerated, or to instead use pairs of modalities on a more even footing within the mouse's sensory hierarchy, such as odours with whisker stimulation or visual with auditory stimuli.

2. Pharmacological silencing of ACC impairs task-switching

These muscimol experiments were the first I performed for this project. As a result, I believe they suffered from my inexperience in training mice, with only 4 of the 8 mice trained reaching the level of competence with the switching paradigm required to record successful sessions. Key to this is motivating the mice correctly: partly through the food restriction that keeps them motivated to seek the soya milk reward, but also through removing impediments to their best performance, like ensuring they are comfortable to run on the wheel and are not stressed during the head-fixing procedure. I believe the improvements seen in mouse behaviour and training times across all other mice included in this study are almost entirely due to aggregated small improvements in my own skills relative to the initial standard seen during these experiments.

In tandem with these the method of muscimol infusion could be imprecise, with the volume of infusion affected by how well the cannulae tubing was prepared. Tubing upstream of the saline or muscimol had to be filled with mineral oil to ensure the pressure applied by the syringe pump was even and constant. I could not risk the oil getting into the infusion, so ensured that more muscimol or saline than was needed was front-filled into the tubing, with the dose controlled by the speed and duration of the pressure applied by the syringe pump. The issue with this approach was that positive pressure needed to be applied before even attaching the tubing, so that air did not get between the muscimol and the cannulae, which meant as soon as the tubing was attached muscimol would begin to slowly infuse. Thus, the infusions were almost certainly larger than intended, and depended on how quickly the infusion could be performed and the tubing detached.

I believe these large infusions explain the main differences between muscimol infusions and continuous optogenetic silencing seen in these two experiments. These infusions were almost certainly silencing a larger region of the ACC, already implicated in motivation (Bliss-Moreau et al., 2021) and may well have affected the premotor region directly superior to the ACC. These off-

target effects may well explain why I saw a bidirectional switching deficit, a reduction in licking speed and repetitions, and an overall difficulty in motivating infused mice to complete the task, and were a key driving factor in choosing a new silencing technique for further experiments.

With this said, I believe the main finding from these set of experiments that survives scrutiny is the lack of an impairment in visual discrimination with the ACC silenced (Fig 3.10). That the mice continue to discriminate the relevant gratings well, and to not discriminate the irrelevant gratings, even with a large area of ACC silenced I believe provides the strongest evidence of this study that the ACC was not involved in maintaining attention switches in this task. If ACC had any involvement in keeping attention, once switched, on the visual gratings, or keeping attention away from the irrelevant gratings, we would surely have seen a decrease in stable visual discrimination during the visual blocks and an increase in stable visual discrimination during the odour blocks, which was my initial expectation when beginning these experiments.

This is an interesting result – previous studies have shown that ACC lesions lead to a consistent increase in errors throughout continuous performance (Hvoslef-Eide et al., 2018) and intra-dimensional set-shifting (Kosaki & Watanabe, 2012) tasks. This was attributed to a disruption of error-feedback signalling, so that animals would fail to correct their strategies following mistakes. This could be due to the differences in the difficulty of the task, or the aptitude of the animals. In the continuous performance task, mice's discrimination rarely rose above d' = 1 (Hvoslef-Eide et al., 2018). Their hit rate was less than 50%, whereas in this task it could be expected to be close to 100% for either of the relevant rewarded stimuli, while the false alarm rates were roughly equivalent. It could be that the incidence of errors in this task was just too rare for error-signalling in the ACC to have a meaningful impact on task performance.

3. Optogenetic silencing of ACC impairs task-switching

Prelimbic cortex

The muscimol silencing experiments seemed to eliminate ACC as a possible mediator of sustained attention during stable visual discrimination of the relevant or irrelevant gratings. Another likely candidate for this in PFC was the PL cortex, directly anterior to the ACC. Lesions to this area cause deficits to sustained attention in a working memory task (Kahn et al., 2012) and a failure to ignore redundant visual cues (Sharpe & Killcross, 2014). In the aforementioned set-shifting task, lesions to the PL but not ACC increased errors following a block change (Kosaki & Watanabe et al., 2012). Unlike ACC, PL stimulation could also reliably activate V1 neurons (Nguyen et al., 2015). The PL cortex is a well-defined constituent of the mouse mPFC with a body of

evidence implicating it in task-switching behaviour, so seemed a reliable candidate for a role in this behaviour to which the ACC silencing effects could be contrasted.

It was a surprise, therefore, to find no effect of PL silencing across any of the metrics examined, with seemingly no role either in allowing the mouse to switch attention when transitioning between blocks or in sustaining attention and discrimination once the switch had been achieved. Most striking was how, once the effect of ACC silencing had receded, even silencing both simultaneously was insufficient to impair switching (Fig 3.25).

Any attempt to explain this lack of an effect must start with the possibility that the PL was not silenced properly, or an insufficiently large area was silenced. No concurrent recordings were performed to confirm a reduction in activity in the targeted areas. However, the reliable effect seen in initial ACC silencing sessions across mice, similar to those seen in muscimol silencing experiments and unreproducible with light alone, was evidence at least that some sort of lesion does seem to be occurring. PL is a relatively small structure, particularly when compared to ACC, and the confirmed output powers from the optic fibre cannulae should have been sufficient for effective silencing.

The other potential explanation is the PL was not engaged by this task to a sufficient extent that its removal would significantly impair the mouse's overall task performance. This seems unlikely, given the substantial evidence positioning PL as a main source of the PFC's contribution to task-switching (Rich & Shapiro, 2009, Oualian & Gisquet-Verrier, 2010, Marton et al., 2018). It is possible that the 'transition states' version of the task used here - designed to maximise switches and minimise block lengths - is too easy to fully engage the PFC, whose activity correlates with task difficulty (Rossi et al., 2012). The aforementioned asymmetry of the task would make switching easier for a trained mouse than a symmetrical version with odours in both blocks, and the visual discrimination task was the easiest version possible. The difficulty of the discrimination tasks could be increased by using gratings with an orientation closer to vertical (and therefore more similar) or odour pairs with less distinct profiles. This might increase the engagement of the PL, and ACC, as the task would require greater cognitive control.

Light pulsing frequency

The continuous silencing conditions were achieved using light pulsed at 40Hz. Cortical oscillations in the gamma frequency band (30-80Hz) are associated with enhanced sensory responses (Cardin et al., 2009) and sustained attention (Gregoriou et al., 2014), and can be induced by synchronous activation of PV interneurons. Optogenetic activation of PV cells in the PFC at 30-40Hz enhanced performance in an attentional task, while inhibition of the PV cells impaired

performance (Zhang et al., n.d.)(Kim et al., 2016). While no improvement in performance is seen with the 40Hz activation of PV cells during the continuous silencing conditions, this may explain the lack of a deterioration – but would require concurrent PL recordings to confirm. In future experiments light would ideally be pulsed with a sinusoidal wave, rather than a square wave, to prevent the light entraining synchrony within the PV network with its sharp onsets and offsets.

Rodent homology

The PL comprises the superior portion of the area of rodent mPFC whose homology with primates remains a subject of debate. According to van Heukelum and colleagues' (2020) repartitioning of the rodent mPFC, the PL cortex most closely conforms to the primate rvACC, sitting at the most rostral point of the cingulate. Finding no effect here might support this attribution: the primate rvACC shows greater involvement in tasks with an emotional affective component, compared to the dACC to which this rodent ACC should conform (Bush et al., 2000). The rvACC also showed a greater role in error signalling (Braver et al., 2001; Menon et al., 2001), potentially due to the emotionally-negative implications of detecting errors. Human patients with rvACC lesions would slow less after errors and move more quickly onto the next trial (Carter et al., 2000). Finding that the PL is not required for behavioural changes following switching errors might suggest that the mice were not processing these errors in this way, perhaps showing a reduced awareness or emotional reaction.

ACC silencing impairs switching

Unlike with muscimol infusions, optogenetic inhibition of the ACC impairs the mice's ability to switch from an odour block into a visual block but has no effect in the other direction. Nonetheless, the explanation given for the bidirectional muscimol effect could still hold for these recordings: if silencing the ACC is causing a reduction in overall licking behaviour, both in speed and frequency, this may explain how the mouse can easily stop licking in the new odour block but struggled to start licking again in the new visual block. To assess this, I looked at licking behaviour during correct relevant rewarded trials between the two conditions (Fig 3.32), as with the muscimol experiments. The number of licks per stimulus (control sessions N = 6907 trials, mean = 4.51 licks, continuous ACC silencing sessions N = 5932 trials, mean = 4.42 licks, two-sample t-test p = 0.07) did not significantly change, while the reaction times (control sessions mean = 1.07s, continuous ACC silencing sessions mean = 0.98s, two-sample t-test p = 4.21×10^{-28}) were significantly faster during ACC silencing, in contrast to the effect of muscimol silencing.

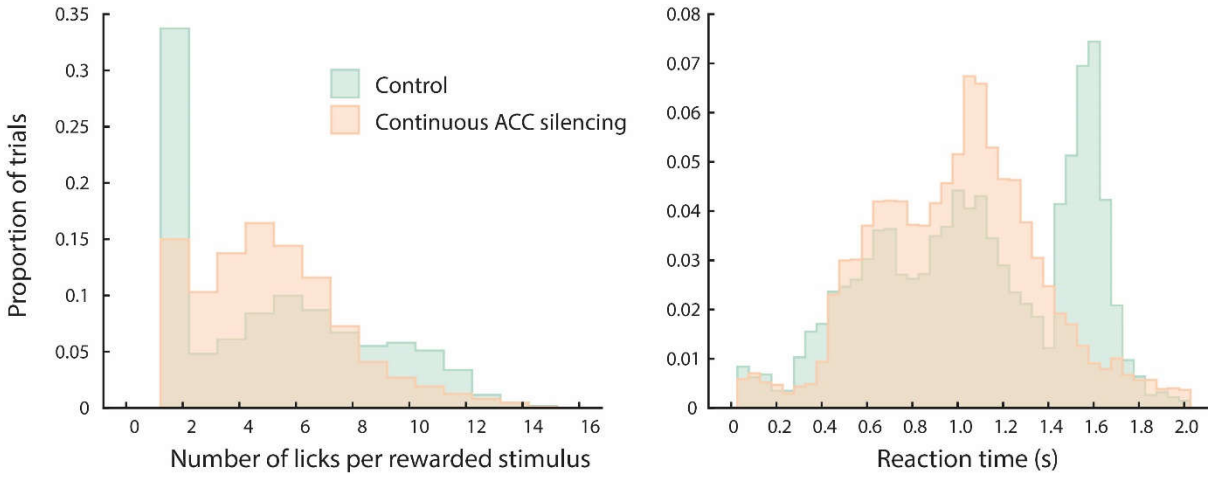

Figure 3.32. Effect of continuous ACC silencing on licking behaviour. Left, number of licks per rewarded relevant stimulus, correct trials only (>0 licks). Right, reaction time for the same relevant stimuli. Each datapoint represents a single trial.

These results provide confirmation that the mouse was not experiencing a simple deficit in its ability to lick to the task stimuli, seeming if anything to lick more readily once a rewarded stimulus was presented. If the cause of this effect is rooted in licking behaviour, it seems more likely to be restricted just to making the decision to lick around the block transitions.

Another possible interpretation is that the bidirectional muscimol effect is genuine, and the unidirectional optogenetic effect simply reflects an inability to silence as large a region of ACC as with the infusions. If the ACC has a specific role in promoting attentional shifts towards and away from visual stimuli, silencing fewer of the projections to V1 might attenuate this. Silencing a larger volume of tissue - for example by using a tapered optic fibre with a larger diameter, ideally paired with bouton recordings in V1 of ACC projections - could help confirm this possibility.

4. ACC is required throughout the trial for attention-switching

Each silencing epoch used was designed to challenge a specific theory of ACC function. If the inter-visual epoch, but not the peri-visual epoch, could impair switching into the visual block, it would support a prediction-error view. The ACC might signal a prediction error once the expected odour does not arrive, with this triggering an attentional shift back to the visual stimuli. If the reverse was true, it would support an adaption and persistence view of the ACC encoding different possible actions and driving an adaption away from the current response strategy.

The fact that both were able to disrupt switching suggests, to me, that the ACC may well be serving both functions. Its role in signalling prediction violations specifically to update internal models is well-established (O'Reilly et al., 2013), as is its role in triggering behavioural adaptations following a change in the feedback information (Camille et al., 2011; Tervo et al., 2014). These may

well be different interpretations of the same function, with the ACC encoding the change in the environment (the absence of the expected odour) and consequently driving the behavioural adaptation to respond to the next visual grating. Whichever is the exact role of the ACC in this behaviour, it is clearly not a brief involvement.

5. The effect of ACC silencing on attention-switching decays over time

The disappearance of the impairment to switching over repeated performances of the silencing conditions was unexpected, as it was not seen in earlier optogenetic experiments or in the muscimol infusions. The main cause is likely over-training in the behavioural task, and there are key differences in these final experiments which I believe all contribute to this diminishment.

The sheer number of silencing conditions, with two target structures and three epochs, as well as control sessions, meant that mice were extremely proficient in the task by the time of the final recordings, with at least 3 training switching sessions and 14 experimental switching sessions completed already. The task itself was relatively straightforward, with distinct task rules and features. A mouse with intimate knowledge of the task could predict block switches without having to perceive the absence of odour: for example, if the mouse remembers the last two stimuli it received it should know that: if one of them was an odour, it is likely in an odour block, and if both are visual gratings, it is likely in a visual block. Alternatively, as block length was not jittered, but instead relied on the mouse performing above a certain threshold for 30 trials, a mouse with reliably good discrimination performance could predict when a block change should occur. Mice's ability to predict block changes from the number of trials elapsed has been shown in other switching tasks (Atilgan et al., 2022).

In addition to this, 2 of the 3 silencing epochs involved silencing sections of PFC for long durations. As well as in continuous silencing, inter-visual silencing could last for as long as it took a mouse to trigger the next trial. This meant that in more than half of the sessions, the mouse was performing the task with a section of PFC silenced for more than half of the duration. PFC is made up of a number of interconnected sub-compartments with diverse, overlapping functions (Le Merre et al., 2021). It follows that chronic silencing of a small region of cortex during a cognitive task would engage non-silenced regions to compensate, perhaps shifting the responsibility for detecting block switches to other parts of the ACC similar to what might be seen following frontal brain damage.

This is only speculation, as the structure of PFC makes recording simultaneously from its many regions difficult. Repeating these experiments with an implanted multi-electrode array in the other

regions of the PFC may help clarify whether it is indeed compensatory plasticity in other regions of PFC, or whether the mouse is developing strategies that engage entirely disparate regions of the brain without a reliance on PFC at all. One change that could have been made during the experiments to alleviate the effects of overtraining would be to drop the PL silencing epochs, as it became quickly apparent the PL silencing was having no effect.

6. ACC silencing is ineffective after the first trial of the visual block

One trial un-silencing

The results of the one trial un-silencing experiments allow two claims to be made, both with different caveats and further research needed. The first is that one trial un-silencing is not sufficient to reproduce the switching deficit seen with continuous ACC silencing. This is clearly true from the data, but these recordings were performed after the previously shown silencing sessions had all been collected, with the mice having performed at least 21 experimental switching sessions each. Due to the decay of the effect we can expect that by this point the deficit caused by silencing the ACC would have all but disappeared, so we would have no reason to expect any different from an identical paradigm but for one trial un-silenced.

The second claim that could be made is that, far beyond failing to reproduce the impairment, the one trial un-silencing actually enhances switching. This goes beyond the decay of the switching deficit, with mice switching faster than in control sessions recorded afterwards. The sudden removal of silencing may cause transient hyperexcitability of the ACC, or post-inhibitory facilitation (Dodla et al., 2006). This hyperexcitability would then coincide with the prediction-mismatch event, enhancing ACC signalling during this critical trial and increasing the probability of a correct response to the next grating. The light-cue condition demonstrates that this phenomenon cannot be simply explained by reflexive licking to an unexpected event, as mice would respond a trial earlier.

Non-optogenetic light cue

To investigate whether this effect is genuine, the logical next step would be to activate ACC neurons during this prediction-mismatch trial to see if it enhances perfect switching as with un-silencing. The light-cue condition demonstrates the obstacle: mice are clearly sensitive to the sudden appearance of a light, so activating exclusively on this crucial first visual trial will inevitably draw attention to it. A blue masking light (such as in O'Connor et al., 2013) could help reduce the distracting effect of the optogenetic light.

This was the reason for selecting this light-cue condition, which otherwise might seem an illogical choice for comparing to one trial un-silencing. The better comparison would have been to reproduce the one trial un-silencing epoch exactly but with the optic fibre disconnected, to reproduce all the distracting effects but no optogenetic effects. The light-cue condition was to test the viability of a potential future experiment activating the ACC just on this trial, and demonstrated that any optogenetic effect would likely be overwhelmed by the attention-grabbing effect of the light itself.

Silencing the ACC revealed a critical role in facilitating attention switches. Specifically, the ACC is required for switches based on expectation violations caused by the omission of an expected odour. Optimal switching requires ACC function throughout this prediction-mismatch trial, but not after the switch has been achieved. Mice can compensate for this deficit, but only after a large number of repeated sessions. This evidence heavily implicates the ACC in the prediction-mismatch trial; I next investigated how ACC neurons might encode this experience of expectation violation.

Results chapter 2:

Prediction-mismatch signalling in the anterior cingulate cortex

Inactivating during the attention-switching behaviour revealed a specific role for the ACC in quickly driving attention back to the visual stimuli following a switch from an odour block to a visual block. The effect was asymmetrical, as ACC silencing had no effect on switching speeds when the mouse had to ignore the visual stimuli. The task structure allowed mice to use the disappearance and reappearance of the odour to determine the block more quickly than trial-and-error responding to the visual stimuli would allow. When switching in the affected direction, the mouse was required to notice the absence of an expected odour in order to register the block switch after a single trial.

To notice this absence, the mouse would need to have established a prediction that the odour would appear. The primate dACC is required for associating actions with their outcomes (Rudebeck et al., 2008), particularly if the outcomes involve rewards (Hadland et al., 2003). The identity of the outcome, not the action, was important for this signalling (Weiss et al., 2018). Here the odour is associated with two actions, lick or withhold licks, and two outcomes, reward or no reward. A non-specific prediction of the odour would therefore not be a direct 1:1 representation of reward, instead representing a 50% chance of one outcome requiring one action to receive a reward.

If this is the role of the rodent ACC in this task, there must be some difference in the signalling when the prediction of the odour is not realised. Primate dACC activity was highest when an outcome was not predicted (Carter et al., 2000), but only if this surprise was meaningful to understanding later trials (O'Reilly et al., 2013). To investigate this, I used 2-photon calcium imaging to record from neurons in the mouse ACC while they performed the attention-switching task.

The first step was to establish that neurons could be imaged with a sufficient clarity to match across days. This was important not only for seeing how the networks changed across repeated sessions of the same behaviour, but also as the mouse's behaviour changes throughout learning. Once this had been established, I analysed the recordings initially just to see to what extent the ACC was encoding task features. After this, I focused entirely on the behaviour mostly impaired by ACC silencing. Looking at the first trial of the new visual block, I compared activity in this period

when the odour should be expected to arrive. Using retrograde tracing I could investigate whether the identified cells had a specific projection target. Finally, using the benefit of having clear, matchable sites I investigated how these signals in the ACC changed over days, and were affected by optogenetic interneuron perturbations.

1. ACC neurons encode task features

ACC is a deep cortical structure, so cannot be accessed directly from the surface of the brain using conventional cranial windows. The problem to solve was how to provide optical access to ACC with the requisite clarity for matching sites across days without causing excess damage to the tissue above. Pilot excavation surgeries (Dombeck et al., 2010) proved too invasive, so I opted to adapt a technique (Low et al., 2014) using microprisms with a reflective hypotenuse to orthogonally reflect imaging light to access the ACC from the contralateral hemisphere (Fig 4.01). While these sagittal implantation surgeries were capable of yielding sites with many clearly visible cells, the overall quality was not sufficient to reliably match across days. Adapting the surgery to a coronal implantation - in which the microprism is implanted in the same hemisphere, posterior to the ACC - yielded consistently matchable sites (Fig 4.02), without causing any noticeable deficits in mouse behaviour.

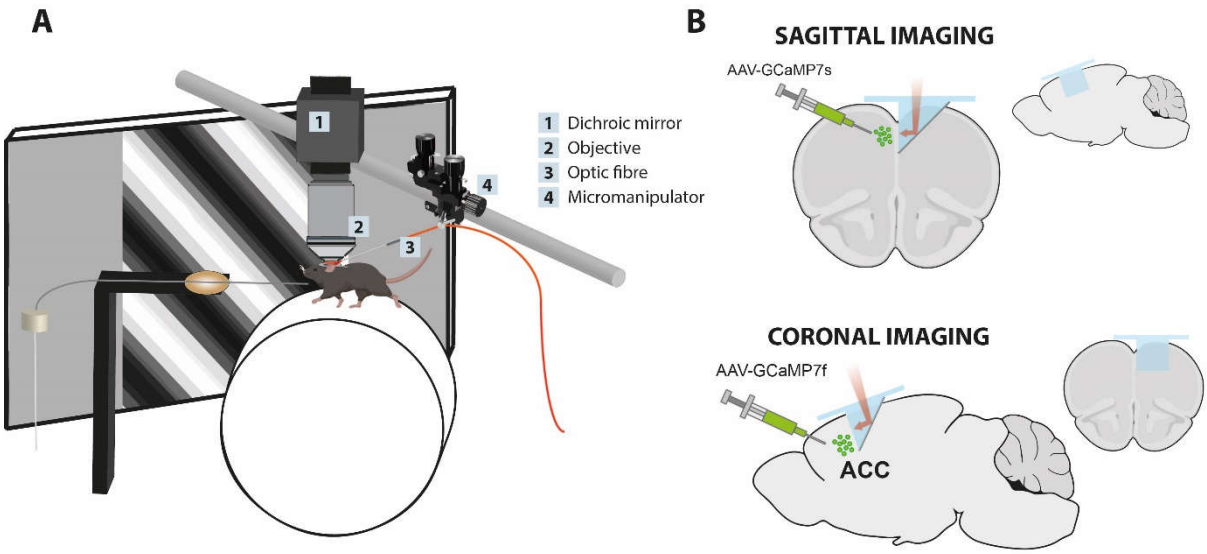

Figure 4.01. *In vivo* 2-photon calcium imaging. A: Reconstruction of mouse performing behavioural task with concurrent 2-photon calcium imaging and optogenetic perturbation. Not pictured is a custom-made lightshield used to prevent light from the screens reaching the objective. B: Schematic of sagittal and coronal imaging microprism implantations. Microprisms were affixed to skull via attached coverslip, using dental cement. GCaMP injections were performed during surgery prior to prism implantation. Mouse and coronal slice images taken from BioRender.

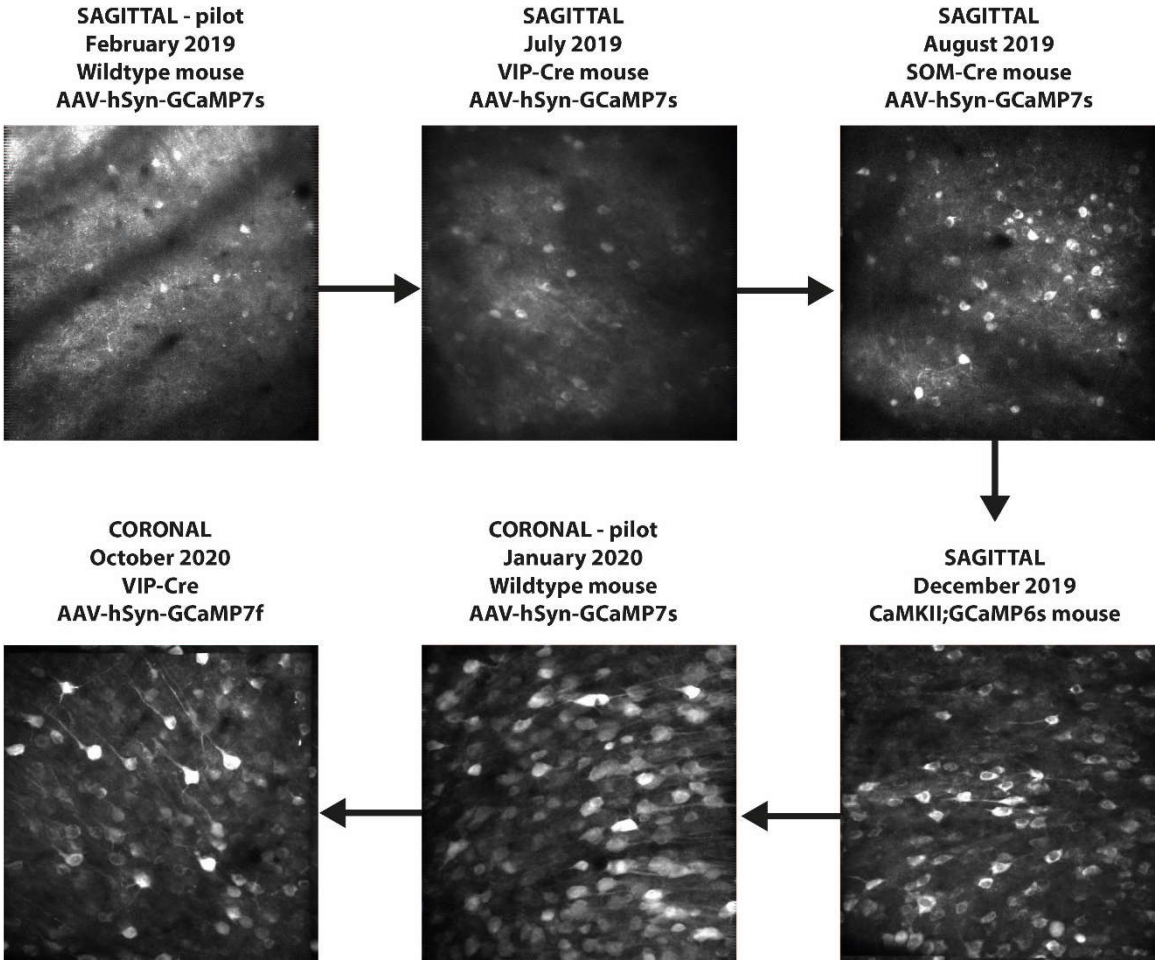

Figure 4.02. Development of microprism implantation surgeries. Representative sites from successful surgeries over the course of the project. Coronal surgeries had a greater chance of yielding sites acceptable for chronic 2-photon imaging.

The objective when developing the surgical approach was not to maximise the number of cells visible, but to reliably produce sites with a signal-to-noise ratio that allowed non-cell landmarks, such as smaller blood vessels, to be easily resolved. Unlike the cells, the landmarks would not change appearance over time so could be used as references when re-aligning over subsequent days. 2-photon imaging and pupil recordings were collected while the mouse performed the same behavioural task as in the previous chapter. The microscope objective was rapidly repositioned along the z axis using a piezoelectric actuator motor to collect multiple 2-D imaging planes. This allowed for the collection of volumes comprised of 6 or 8 planes separated by 40µm steps in z (Fig 4.03), giving a greater yield of cells per recording but with a reduced effective sampling rate of 6.4 or 4.8Hz per volume.

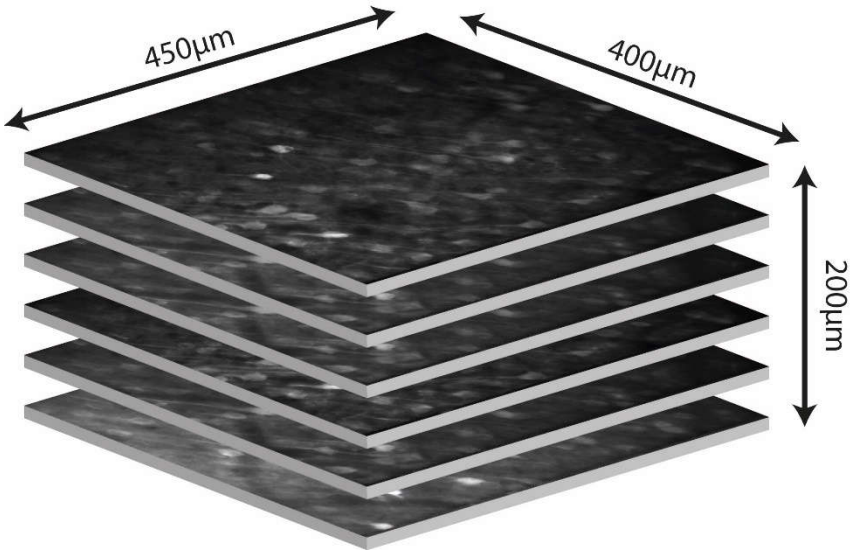

Figure 4.03. Imaging volume. Example imaging volume recorded across 6 planes, each separated by 40µm steps, with a volume collected every 156ms.

Simultaneous imaging of neuron activity in the ACC with behaviour and pupil recordings showed cells that reliably respond to the task stimuli (Fig 4.04). The virus used a synapsin promotor which allowed expression of GCaMP7f by excitatory and inhibitory neurons, but prevented expression by glial cells (Chen et al., 2013).

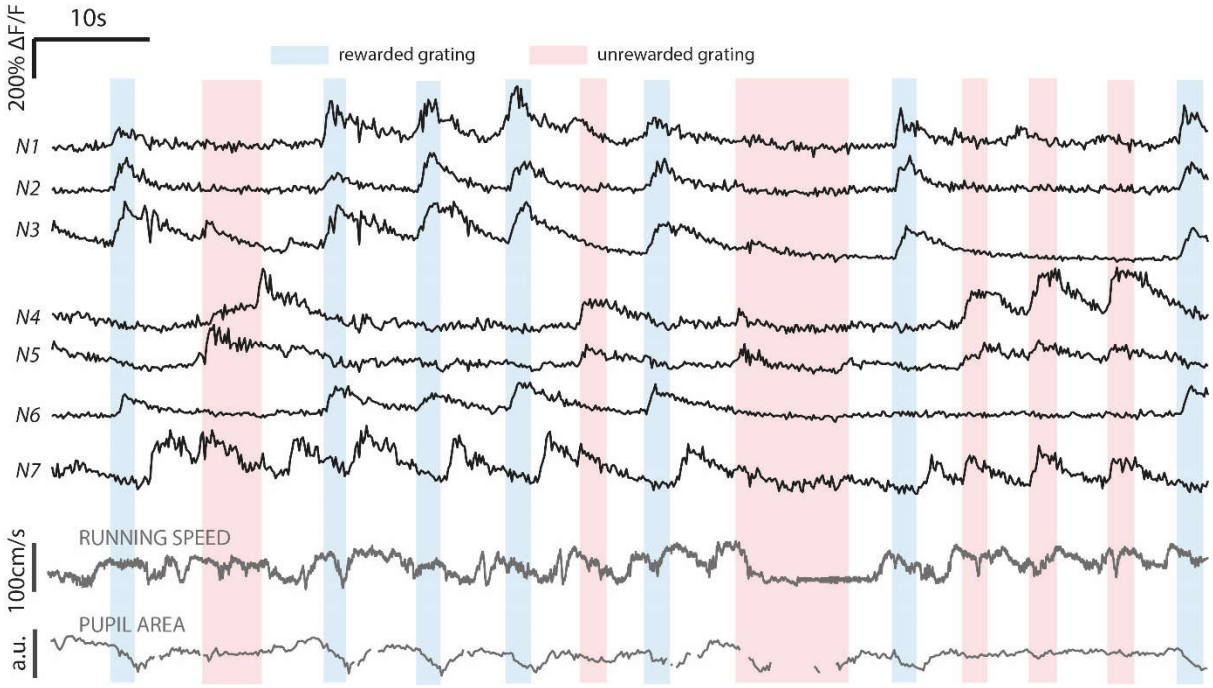

Figure 4.04. Example ΔF/F traces from an imaging session. ΔF/F traces from 7 example neurons in an imaging session, with concurrent visual gratings (shading) overlaid and recorded running and pupil area aligned. Missing values from pupil area trace are from blinking and grooming behaviour, during which pupils were not visible.

By aligning each cell's ΔF/F trace to the onset of each task event, subtracting their pre-event baseline, then averaging across all trials of this type, I extracted peri-stimulus time histograms (PSTHs) that demonstrated the cells' average responsiveness to each type of task event (Fig 4.05).

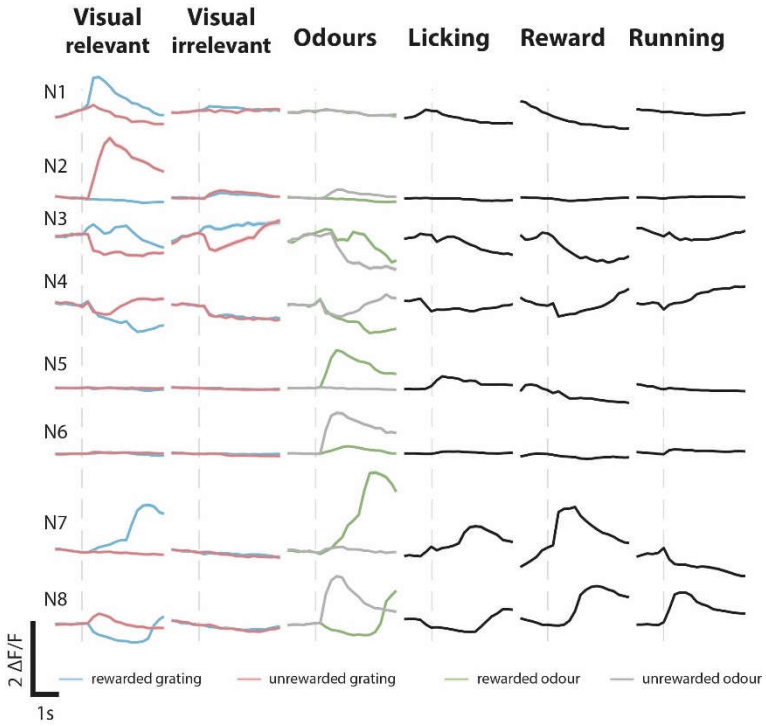

Figure 4.05. Example neuron PSTHs. Activity of 8 example neurons aligned to the main task events and averaged across all trials. Neurons can be positively or negatively responsive to visual stimuli, odour stimuli, licking, reward, and running. Many of these conditions overlap, as rewarded relevant stimuli are associated with licking and reward, and unrewarded relevant stimuli are associated with running. Some neurons are selective for specific stimuli, and others for specific behavioural responses by the mouse. Lines represent mean activity over all trials of that condition, shading represents SEM.

As a structure involved in monitoring the outcomes of actions during goal-directed behaviour, the ACC has a role in integrating diverse sensory inputs including taste, smell, texture, and vision (Rolls, 2015). It is therefore unsurprising that ACC neurons show a diverse range of responsiveness to the different events of this task (Fig 4.06), necessary for internally representing the task (Rigotti, 2010). Neurons recorded from coronal microprism implants, mostly found in layer V of the ACC, showed greater overall responsiveness than neurons recorded from sagittal implants, mostly found in layer II/III, consistent with the greater excitability seen in layer V ACC neurons (Medalla et al., 2022). The remainder of this chapter includes only imaging sessions from these coronal microprism implants, as only these had the requisite clarity to be matched across days.

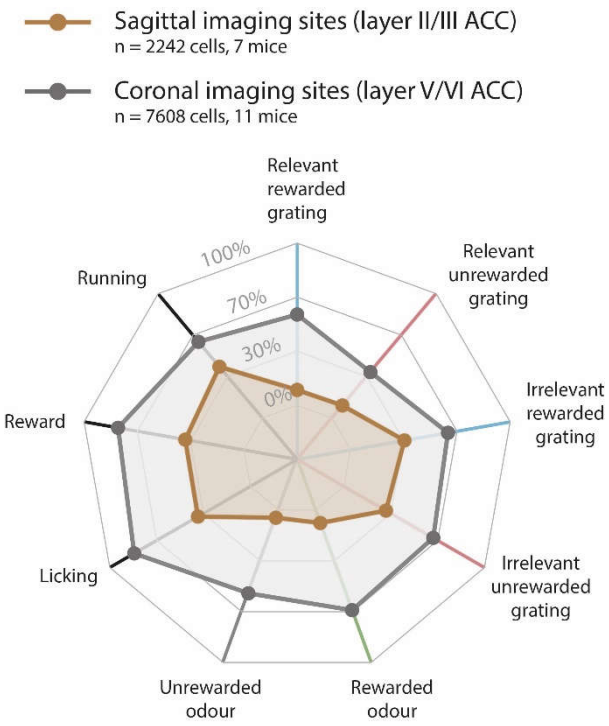

Figure 4.06. Responsiveness of ACC neurons. Percentages of recorded neurons positively or negatively responsive to each of the 9 major task events. Inner area shows neurons from sagittal recordings, most likely from layer II/III of ACC. Outer area shows neurons from coronal recordings, most likely from layer V.

2. Cells in the ACC respond to prediction-mismatch

Unsurprisingly, ACC neurons showed a diverse responsiveness to features of the task. However, from the silencing experiments we know that the ACC is not essential for stable task performance - instead it is required to switch attention when transitioning into a visual block. As each block transition requires the mouse to have been in the current block long enough to develop consistent expectations about the upcoming stimuli, the challenge was to maximise the number of block transitions within a session while keeping block lengths long enough for stable performance to be achieved. To achieve this, I automated block switches so that as soon as mice had sustained performance over a certain threshold for 30 trials, the block would switch, allowing for up to 14 block transitions within a single session (Fig 4.07 – N = 10 mice, 6-14 transitions, median = 13 transitions, median block length ±IQR visual block = 33±1, odour block = 35± 8).

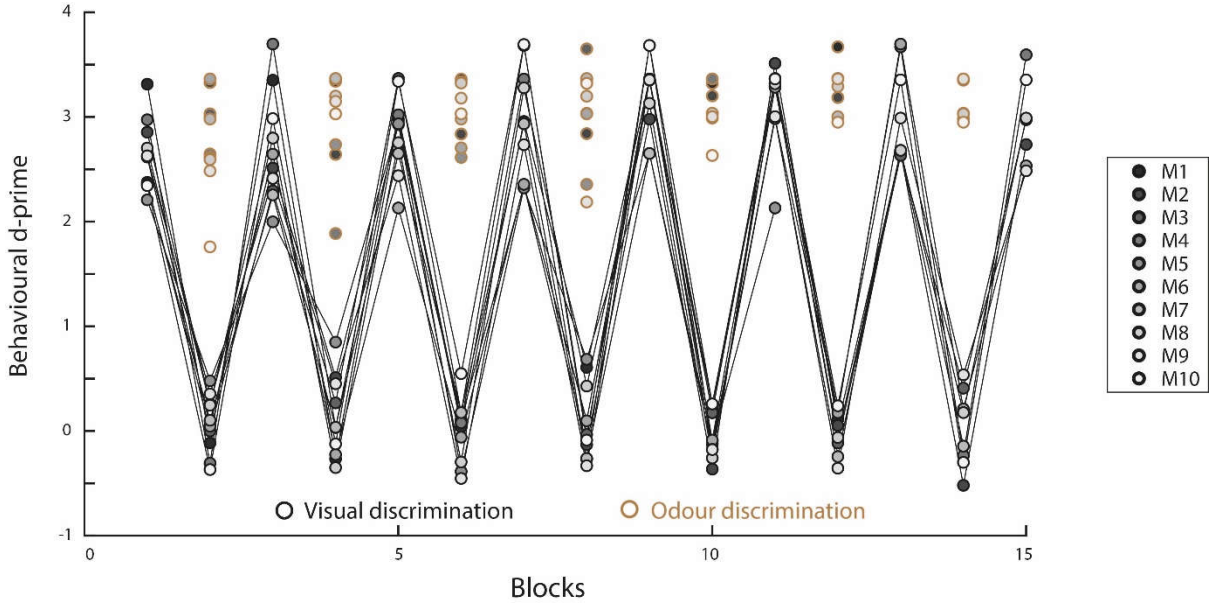

Figure 4.07. Discrimination performance across blocks. Stable discrimination performance across blocks of the switching sessions used for upcoming analysis. Black circles represent visual d', gold circles represent odour d'. Mice performed up to 14 switches within a session, while maintaining accurate discrimination within stable periods of each block.

Maximising the number of switches in a session allowed activity at block switches to be investigated, with enough repetitions to average neural responses across block transitions. The silencing data tell us that this first trial of the new visual block is crucial - when the mouse is expecting an odour that does not arrive, which I called 'prediction-mismatch'. To isolate cells that were active specifically in this instance, I aligned activity to the same timepoint across visual and odour blocks relative to the offset of the visual gratings - the time at which the odour would be expected to arrive. For odour block trials this was simply a case of aligning to the odour stimulus; for visual trials I took the average delay between irrelevant visual grating offset and odour stimulus onset across odour trials to estimate the expected onset of the odour. I then compared activity aligned to this moment during the first visual trial of a new block ('expected odour') with the same time window during stable odour block trials, when an odour is expected and arrives ('stable odour'), and with this window during stable visual block trials, when an odour is neither expected nor arrives ('no odour') (Fig 4.08A). Significant differences in the first comparison indicated a cell which fired differently based on whether an odour did or did not arrive, while significant differences in the second comparison indicated a cell which fired differently based on whether an odour was or was not expected. Therefore, a cell which satisfies both comparisons must be sensitive to both expectation of the odour and the odour's arrival. I named the cells that met both these comparisons 'mismatch' neurons (Fig 4.08B).

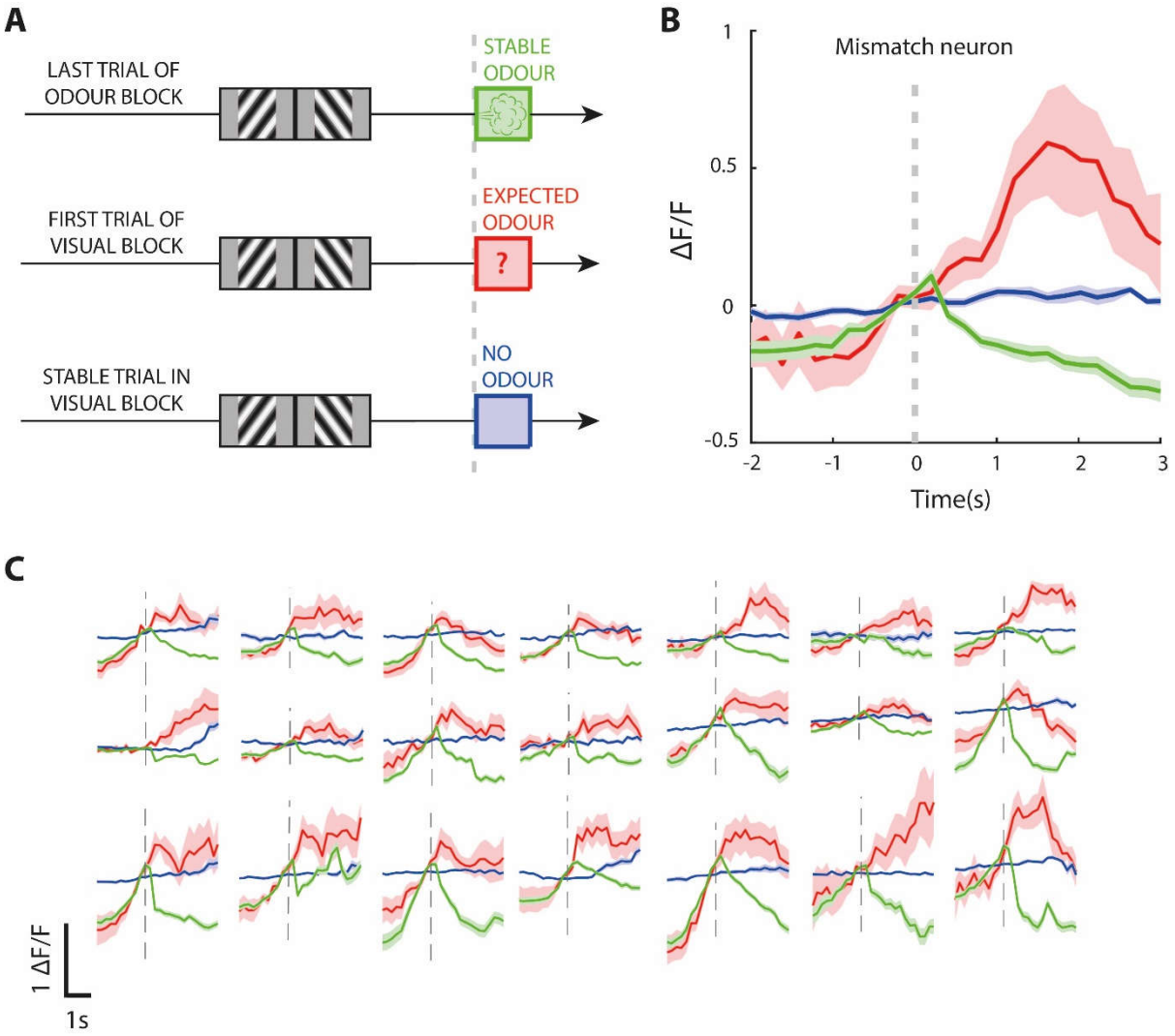

Figure 4.08. Mismatch neuron characterisation. A: Schematic of trials from which activity is compared to isolate mismatch cells. Dotted line denotes timepoint to which activity was aligned before comparisons. B: Example positive mismatch cell. Activity during 'expected odour' and 'stable odour' trials follow similar time-course before odour onset, but when odour arrives cell's activity is inhibited, whilst when odour fails to arrive cells becomes active and remains active for several seconds. In 'no odour' trials cell is entirely silent. Dotted line denotes timepoint to which activity was aligned. C: 18 example positive mismatch neurons across all 13 recordings. These mismatch cells have a distinct activity pattern, differing mainly in the duration for which the cell remains active during the 'expected odour' trial.

Mismatch neurons comprised 9% of all the recorded neurons (Fig 4.09). I compared this to recordings from V1 performed by a colleague (Dylan Myers-Joseph) for a separate ongoing project. From sessions with the same transition states and maximised switch numbers, fewer than 1% of V1 cells met the same criteria (Fig 4.10), indicating that these mismatch neurons were not widespread across the cortex.

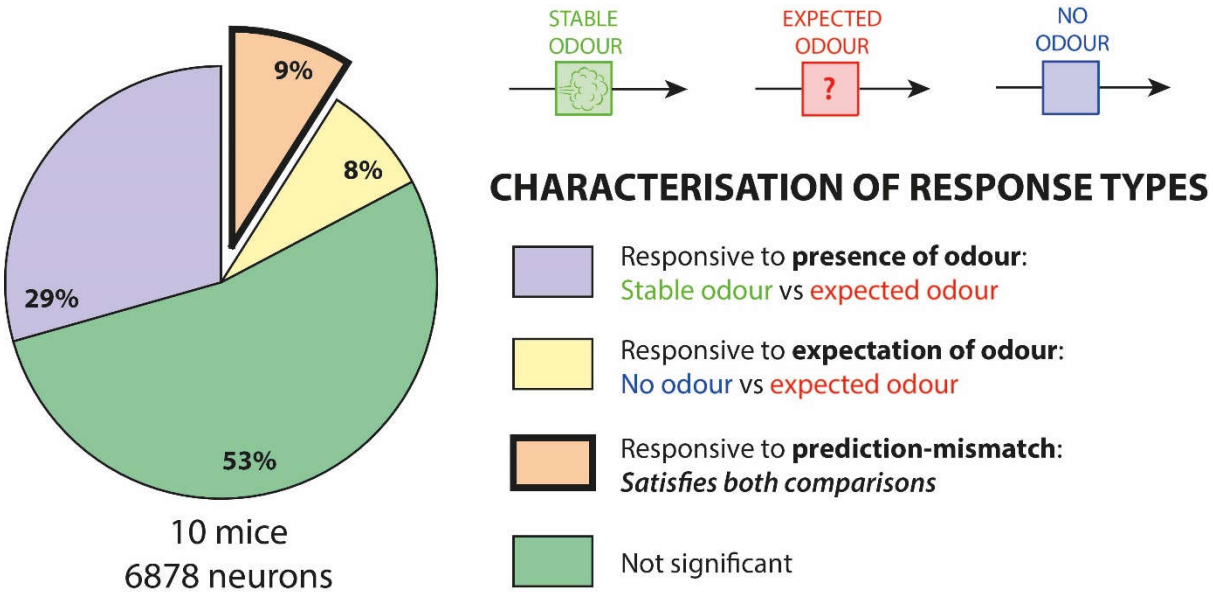

Figure 4.09. Proportion of mismatch cells in ACC. Pie showing proportion of neurons recorded from all sites (N = 10 mice, 13 sessions) that meet one or both of the statistical comparisons used to identify mismatch cells.

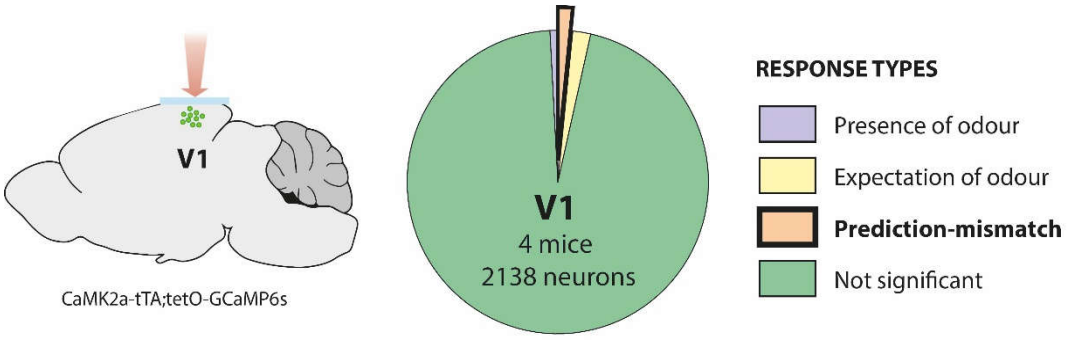

Figure 4.10. Mismatch cells in visual cortex. Left, schematic of 2-photon calcium imaging of V1 neurons. Right, pie showing proportion of neurons recorded (N = 4 mice) that meet the same statistical comparisons.

The example neurons given in Fig 4.08 are what I termed 'positive mismatch' neurons – cells with a more positive response in the 'expected odour' condition than in the other two conditions. These only represent 1 of the 4 possible arrangements of responses (Figure 4.11). The significance tests used to identity this sub-population of mismatch cells within the ACC did not specify the direction of the difference in responses between the three mismatch conditions. To clarify, I separated the mismatch cells depending on the order of the 3 responses from most positive to most negative, with 4 possible conformations. Of these 4 "classes", the two I consider most informative are class 1 'positive mismatch' neurons and class 4 'negative mismatch' neurons, as they are the two classes whose activity does not scale monotonically with running speed. Many neurons in the ACC have activity correlated with locomotion (Sachuriga et al., 2021, 17.6% of neurons). If we compare mean class 2 and 3 cell activity with the averaged running speeds in each condition, their activity could be at least partially explained by a straightforward correlation with running: negatively for class 2, and positively for class 3.

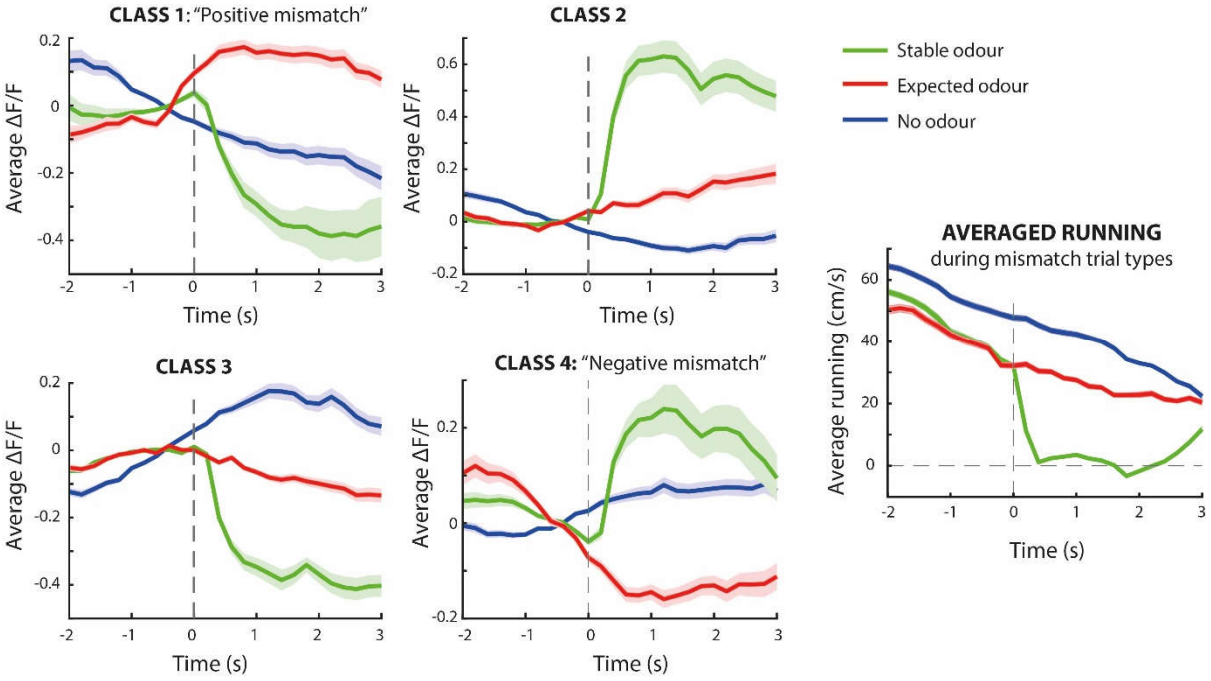

Figure 4.11. Mismatch cell classes. Left, mean response PSTHs for class 1 (N = 167 neurons), class 2 (N = 103 neurons), class 3 (N = 174 neurons), and class 4 (N = 154 neurons). Right, mean running across all trials used for each condition.

This correlation with motor behaviour is a possible confound. While these class 1 and class 4 neurons cannot be directly explained by the different patterns of running and licking in each condition, there may well be an interaction. Some support comes from the contrasting responses of these cells in the 'expected odour' and 'no odour' condition, despite the running and licking behaviour being particularly similar between the two: a slow deceleration from a fast running speed, and no licking.

From the example neurons in Fig 4.08, we can see that this 'expected odour' response can either return to baseline fairly quickly or sustain for several seconds. The average response across positive and negative mismatch neurons (Fig 4.12) shows that 'expected odour' responses remain significantly different from 'stable odour' responses from the point of prediction-mismatch until the start of the next visual grating, many seconds later (Wilcoxon signed-rank test comparing average mismatch neuron activity in 'expected odour' and 'stable odour' trials aligned to mismatch: positive mismatch cells $p = 1.69 \times 10^{-28}$, negative mismatch cells $p = 1.61 \times 10^{-28}$, aligned to next visual stimulus: positive mismatch cells $p = 5.45 \times 10^{-15}$, negative mismatch cells $p = 6.57 \times 10^{-17}$). This fits findings from the silencing experiments using inter-visual and peri-visual ACC silencing epochs. Both could impair switching from an odour block to a visual block (Fig. 3.21). If these mismatch cells are responsible for driving this switching, their time-course shows that either silencing epoch could disrupt their signalling.

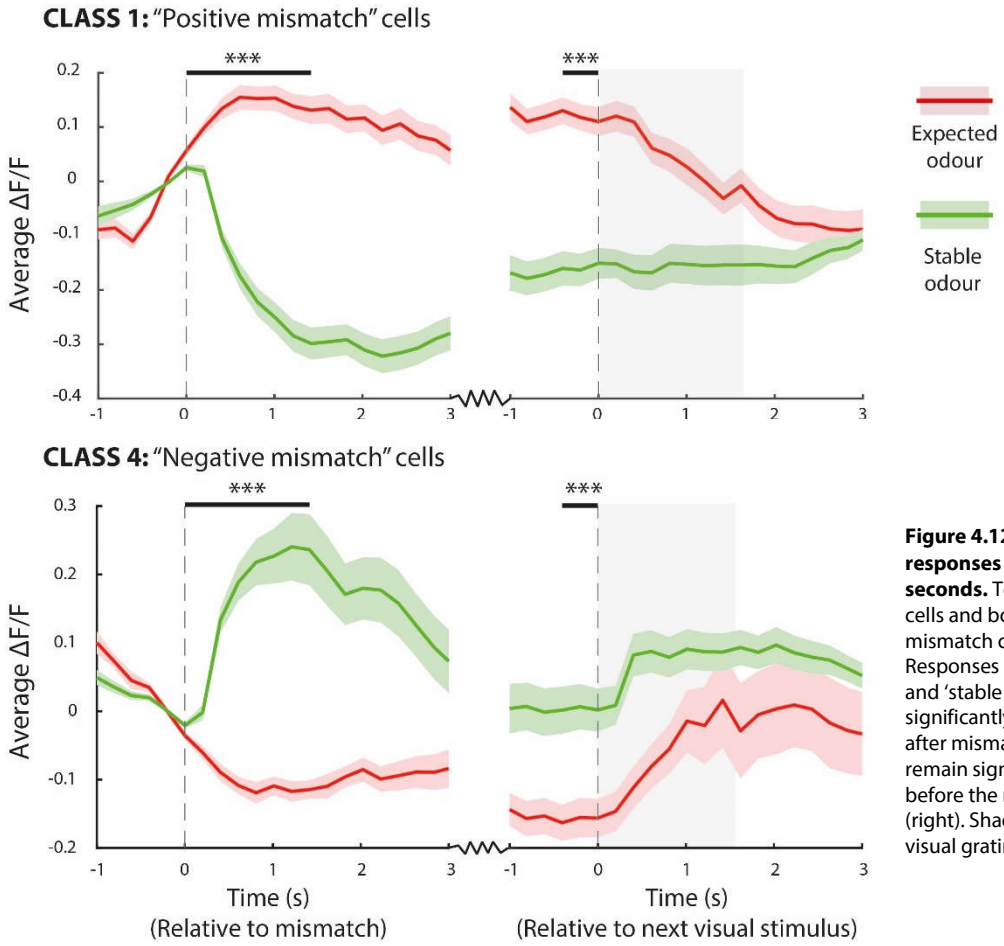

Figure 4.12. Mismatch responses sustain for several seconds. Top, positive mismatch cells and bottom, negative mismatch cells, averaged PSTHs. Responses in 'expected odour' and 'stable odour' conditions are significantly different 0 to 1.5s after mismatch event (left) and remain significant -0.5 to 0s before the next visual stimulus (right). Shaded area represents visual grating presentation.

The other observation from the silencing experiments was that the ACC seemed to be required for the switch from an odour to a visual block only during first trial of the new visual block. I aligned the activity of the mismatch cells to this same 'expected odour' timepoint - relative to the visual grating offset - of the first 4 trials of new visual blocks (Fig 4.13). The prediction-mismatch response is indeed restricted only to this first trial, as the 'expected odour' response is only significantly above baseline on trial 1 (Wilcoxon signed-rank test comparing mean 'expected odour' baseline (-0.5 to 0s) with response amplitude (0 to 1.5s) for all positive mismatch neurons, trial 1 $p = 2.98 \times 10^{-15}$).

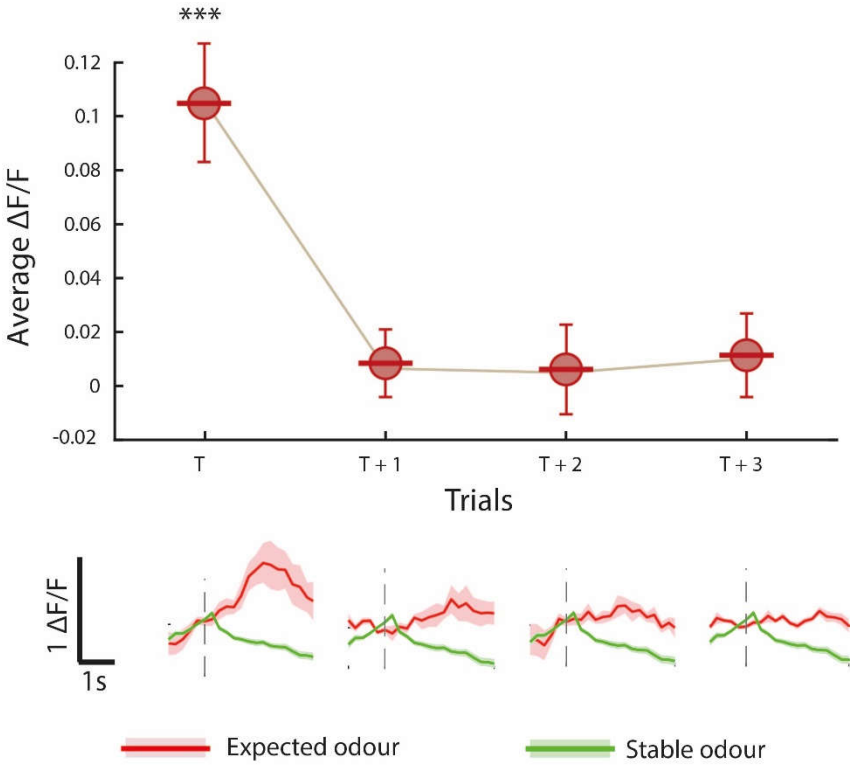

Figure 4.13. Mismatch responses are seen only in the first visual trial. Top, average 'expected odour' response seen in first, second, third, and fourth trial following switch into visual block across positive mismatch cells, aligned to 2s following visual grating offset. Bottom, example PSTHs from a mismatch cell aligned to these same trial timepoints. 'Stable odour' response is presented as a reference.

These mismatch cells follow the logic of switching from an odour block to a visual block, responsive specifically when an odour is expected but does not arrive. The time-course of these responses follows what we know of the timing of ACC involvement in switching from the silencing data. However, we still lack any direct evidence that these neurons are causally involved in provoking the mouse to switch attention to the visual stimuli when entering the new visual block.

To examine this, I compared 'expected odour' responses in these first visual trials preceding perfect switches, when the mouse would lick on the very next trial, to those preceding imperfect switches, when the mouse failed to lick on at least one more trial before responding (Fig 4.14A). The actual behaviour in either trial type was the same: the mouse ignored the grating and waited for the expected odour. However, silencing the ACC during this trial caused a significant decrease in the chance of a perfect switch and an increase in the chance of an imperfect switch. This implies that activity in the ACC is crucial for allowing the mouse to switch behaviour after only one missed trial.

Positive mismatch neurons showed significantly larger 'expected odour' response amplitudes in trials that preceded perfect switches than in trials that preceded imperfect switches (Fig 4.14B - Wilcoxon signed-rank test comparing 'expected odour' responses of positive mismatch cells preceding perfect and imperfect switches, aligned to the expected odour onset $p = 0.0003$, aligned to next visual stimulus $p = 0.019$), suggesting that this activity was indeed related to the mouse's successful switching in the next trial.

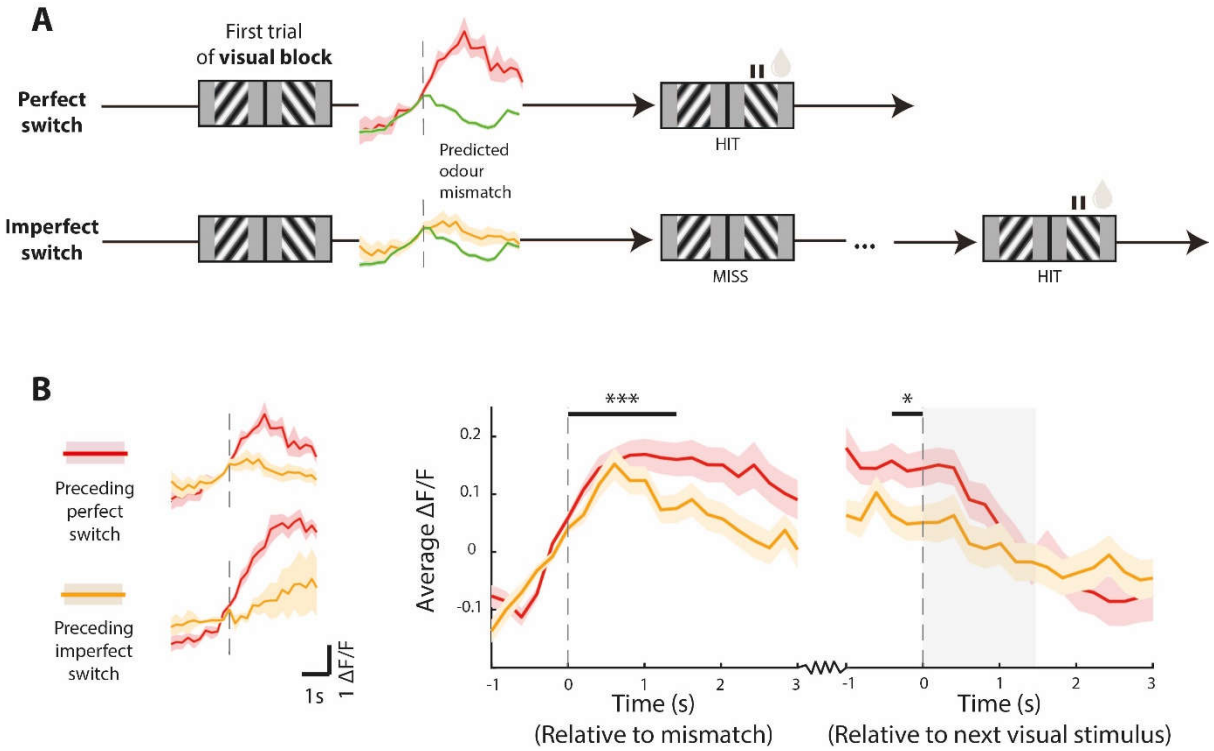

Figure 4.14. Positive mismatch responses predict switching. A: Schematic of perfect and imperfect switches, showing the point in switching timeline to which mismatch responses are aligned. B: Left, example PSTHs of 2 positive mismatch cells' 'expected odour' responses preceding perfect and imperfect switches. Right, average PSTHs across positive mismatch cells (N = 146 cells), with average response amplitudes in 'expected odour' trials that precede perfect and imperfect switches compared at 0 to 1.5s relative to mismatch and -0.5 to 0s relative to the next visual grating. Grey shading indicates visual stimulus appearance.

This difference in activity could not be explained simply by differences in locomotion. Comparing mean running speeds during perfect and imperfect switches revealed no significant differences when aligned to either the mismatch trial or the next visual grating (Fig 4.15 – Wilcoxon signed-rank test comparing running speeds during perfect and imperfect switches, aligned to the expected odour onset p = 0.101, aligned to the next visual stimulus p = 0.413).

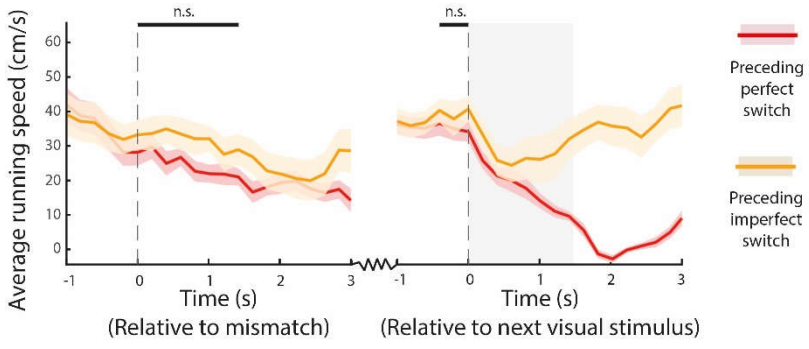

Figure 4.15. Running speeds are the same preceding perfect and imperfect switches. Averaged running speeds preceding perfect and imperfect switches aligned to (left) the expected odour onset and (right) the onset of the next visual grating. Averaged running speeds from 0-1.5s relative to expected odour onset and from -0.5 to 0s relative to visual grating onset used for comparisons. Grey shading indicates visual stimulus appearance.

Expanding this analysis to all mismatch cell classes, both class 1 and class 4 mismatch neurons showed significantly more positive responses in 'expected odour' trials that preceded perfect switches than in those that preceded imperfect switches (Fig 4.16 – Wilcoxon signed-rank test comparing class 1 cells p = 0.0003, class 2 cells p = 0.082, class 3 cells p = 0.061, class 4 cells p =

0.0039, all mismatch cells p = 0.031). Class 2 and 3 'expected odour' responses did not differ significantly before perfect and imperfect switches. This supported an interpretation of their role as being reflective of the motor differences between the three conditions – as there were no motor differences between these two 'expected odour' trial types - rather than signalling prediction-mismatch to cause changes in behaviour.

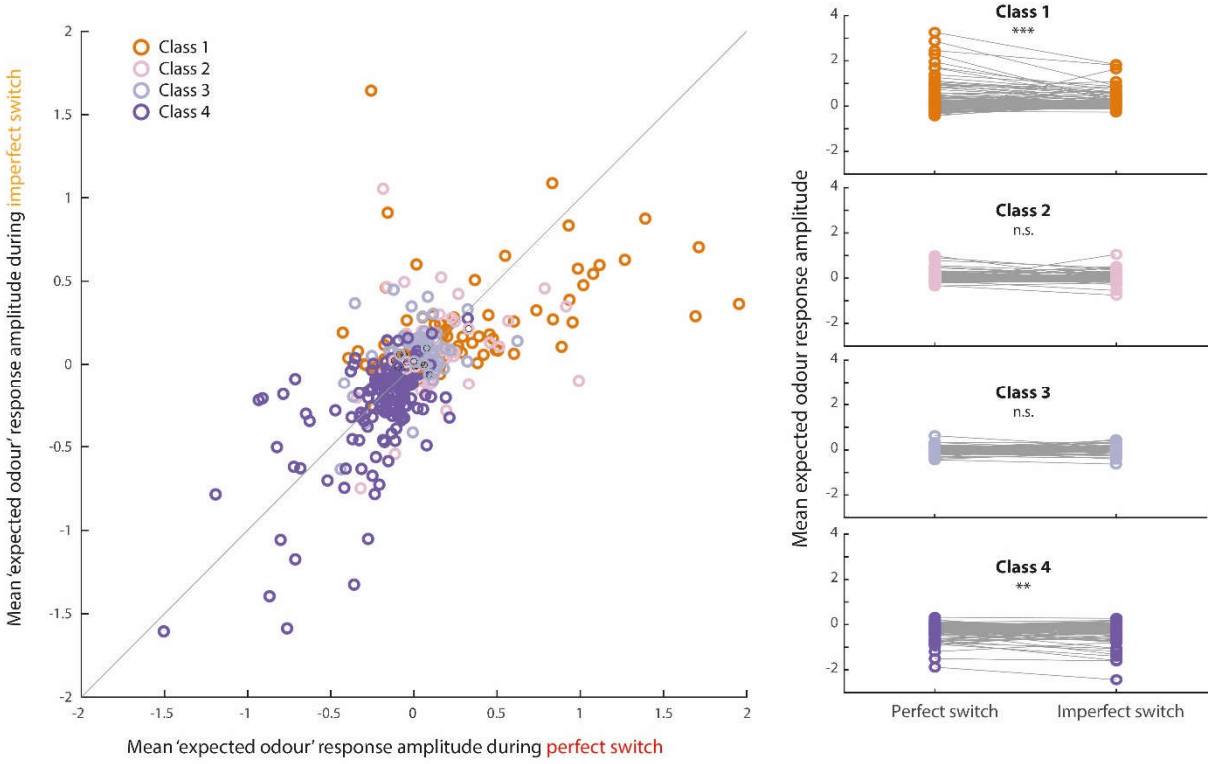

Figure 4.16. Mismatch responses preceding perfect/imperfect switches across classes. Left, scatter of 'expected odour' responses of mismatch cells, averaged 0 to 1.5s relative to mismatch, preceding perfect and imperfect switches. Colours denote mismatch class. Right, same data separated by mismatch class. Only class 1 and class 4 'expected odour' response are significantly different before perfect and imperfect switches.

3. Striatal projecting cells are underrepresented in this prediction-mismatch population

These results demonstrated a sub-population of neurons in ACC whose activity well-suited the previously characterised role of the ACC in this task-switching behaviour. The next question to ask was: where were these prediction-mismatch signals propagated to? One likely candidate was the striatum, a major projection target of PFC in top-down control (Zhang et al., 2016) with a well-characterised role in expected reward (Fiorillo et al., 2008) and prediction-error signalling (Lak et al., 2018). Before these experiments, I injected the retrograde tracer CTB-Alexa-647 in the dorsomedial striatum, which receives direct glutamatergic inputs from ACC (McGeorge & Faull, 1989), so that ACC cells projecting to this area would fluoresce in the far-red channel (Fig 4.17A). Of the 8 mice that exhibited striatal-projecting cell labelling clear enough to confidently distinguish

cells expressing Alexa-647 and cells expressing only GCaMP, I found a significantly lower proportion of mismatch cells in the striatal-projecting population than in the non-striatal projecting population (Fig 4.17B – Chi-squared test of proportion comparing proportions of mismatch cells between striatal-projecting and non-striatal-projecting populations p = 0.0015).

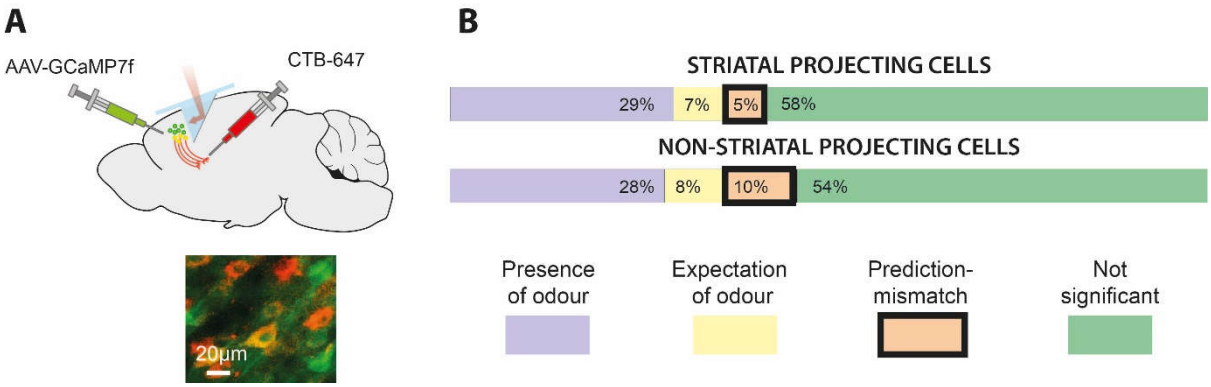

Figure 4.17. Proportion of mismatch cells projecting to striatum. A: Top, schematic of surgery, bottom, example site with cells expressing GCaMP7f in green, Alexa-647 in red, and co-expressing both in yellow. B: Proportions of cells responsive to prediction-mismatch among striatal-projecting (N = 421 cells) and non-striatal-projecting (N = 4888 cells) neurons.

It seemed that striatal-projecting cells were significantly underrepresented amongst this mismatch cell sub-population. This suggested that if there was a common projection target of this population, the dorsomedial striatum was not it. I examined whether this difference was reflected by a larger difference in responsiveness across the striatal-projecting and non-striatal-projecting populations, but found their patterns of responses almost indistinguishable (Figure 4.18).

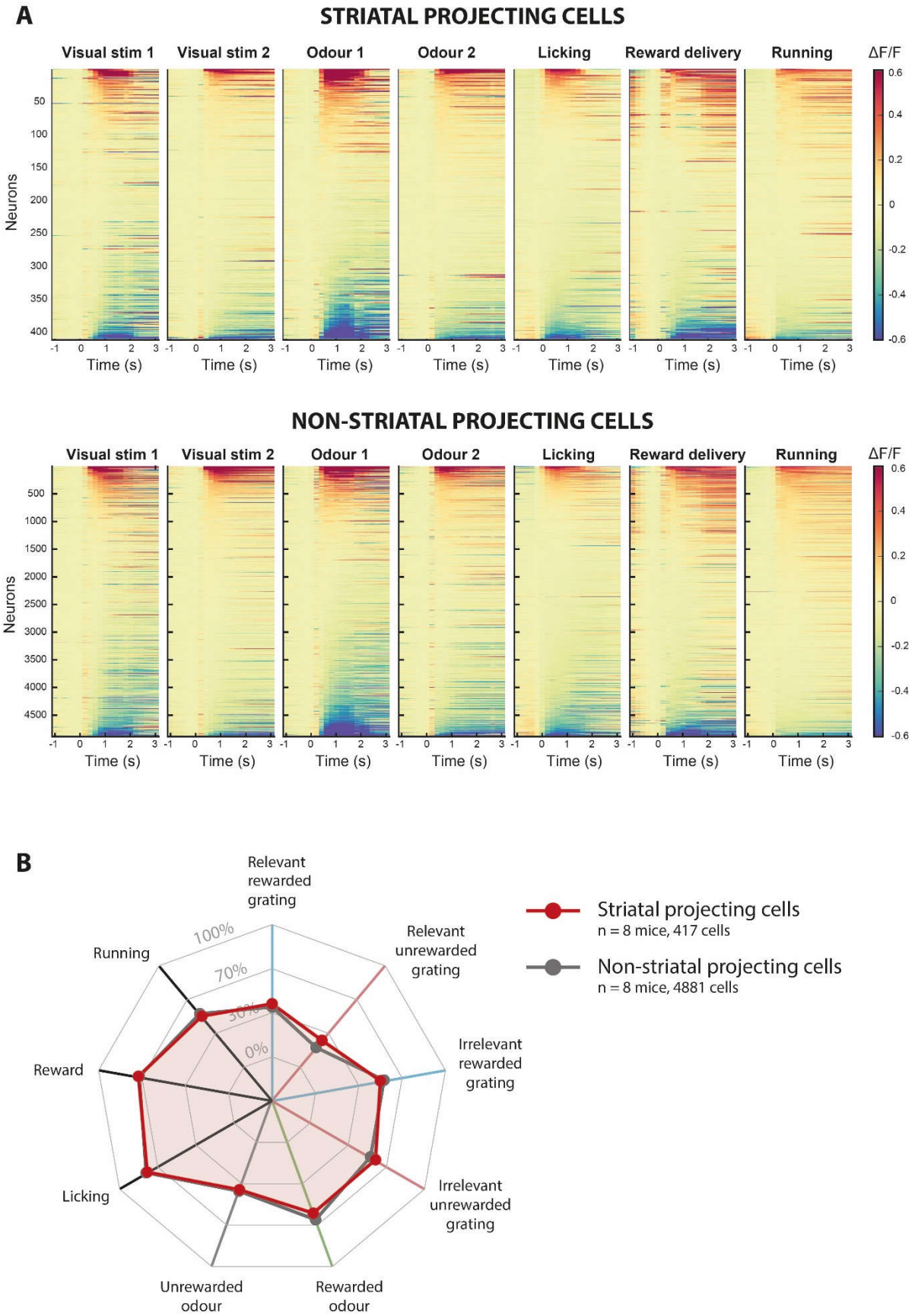

Figure 4.18. Basic responsiveness of striatal/non-striatal-projecting cells. A: PSTH arrays of all striatal (N = 421) and non-striatal (N = 4888) projecting neurons' mean responses to the main task events, recorded across 8 mice. Each array is sorted independently from the most positively-responding neuron to most negatively-responding neuron. B: Spider plot of percentages of responsive neurons in each sub-population to the main task events.

4. Prediction-mismatch populations reconfigure across days

My characterisation of mismatch neurons revealed a sub-population in ACC that fired specifically during prediction-mismatch. A key advantage of the coronal microprism implants was the improved site clarity, which allowed matching of sites across days. This allowed me to investigate how these sub-populations changed over repeated switching sessions. Chronic 2-photon calcium imaging of visual cortex neurons revealed ensembles which only lasted for individual sessions, and other ensembles which remained stable for weeks (Pérez-Ortega et al., 2021). The first challenge was to establish whether my cells could be reliably matched; image segmentation required cells to be active during consecutive sessions, and the aforementioned study indicated that across any two imaging sessions less than half of visual cortex neurons remained active. Of the mice with sites from which more than one switching imaging session was recorded, just under half of the cells could be matched to at least one other day (Fig 4.19 – N = 7 mice, 10 sites).

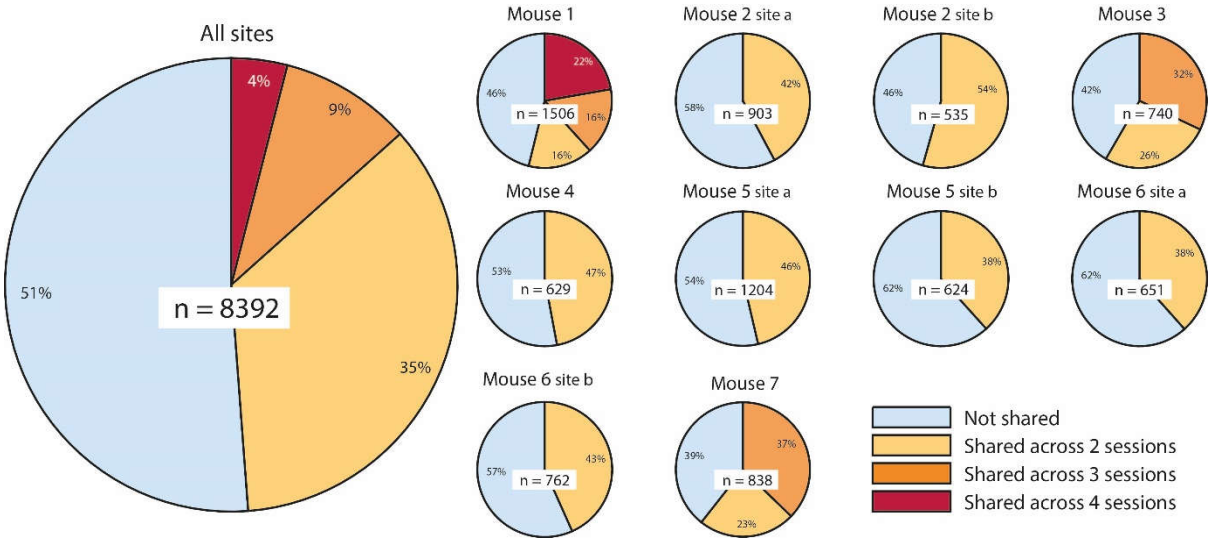

Figure 4.19. Cell matching across repeated sessions. Proportions of matched cells from each site with more than one switching session. 4112 cells were shared across at least 2 sessions.

To characterise the stability of ACC neuron responses over repeated sessions, I first looked at simple selectivity to the task stimuli (Fig 4.20). This is defined as the degree to which a neuron fires preferentially to one stimulus, in a stimulus pair, over the other, divided by its overall responsiveness to both. Selectivity approaching 1 indicated a preference for the rewarded stimulus, while selectivity approaching -1 indicated a preference for the unrewarded stimulus. Selectivity to the relevant visual stimuli and odour stimuli remained stable over days, while selectivity to the irrelevant gratings in the first switching session did not correlate well with selectivity in the second. Looking at relevant visual stimuli specifically, I saw a very small

proportion of neurons which changed their selectivity from significantly positive to significantly negative.

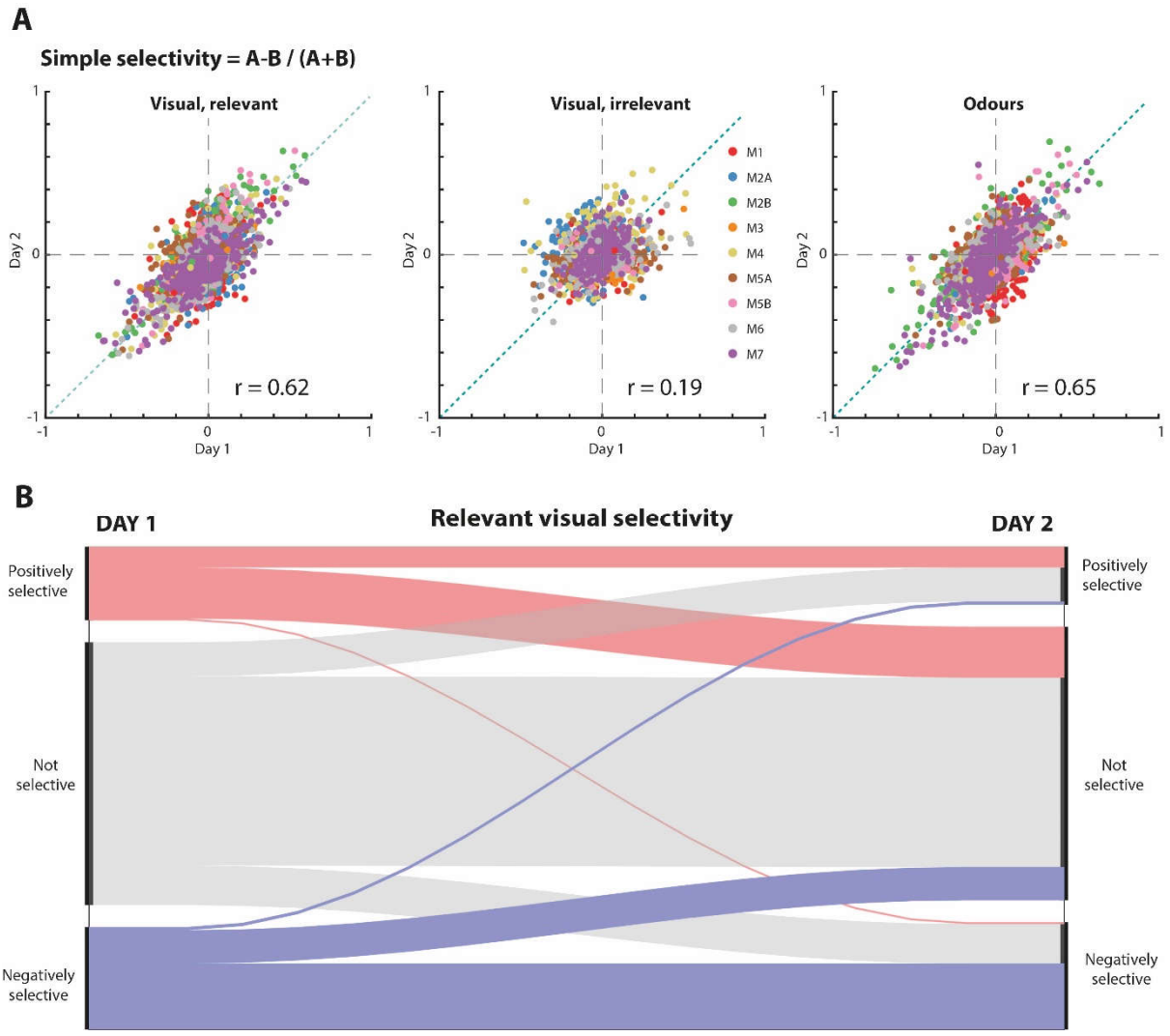

Figure 4.20. Stability of simple selectivity. A: Simple selectivity of neuronal responses to relevant visual stimuli (left), irrelevant visual stimuli (middle), and odours (right) during the first and second switching session. Matched cells only N = 3133. Colours denote site to which cell belongs. Correlation coefficients for selectivity to each stimulus pair between day 1 and day 2 are given as r. B: Change in proportion of the matched cells which were positively or negatively selective for relevant visual stimuli from day 1 to day 2.

It seemed that neuronal selectivity to task stimuli remained reasonably stable across days, but only when those stimuli were relevant. The correlation between selectivity to the pairs of stimuli on day 1 and day 2 was significantly higher for relevant visual stimuli and odours than for irrelevant visual stimuli (relevant visual vs irrelevant visual $p < 0.001$, odours vs irrelevant visual $p < 0.001$, using an online significant correlation difference calculator by Soper, 2022). This is not too surprising: behaviourally relevant stimuli were associated with differing motor responses (licking and slowing down vs not licking and running) whereas the irrelevant gratings elicited similar motor responses, so we might expect cells that are modulated by motor behaviour to exhibit relevant stimulus selectivity across days.

The responses of positive and negative mismatch cells were not clearly influenced by motor behaviour. The number of mismatch cells identified from a session had a close relationship to the number of switches within that session - the more 'expected odour' trials available for comparison, the more likely the statistical test was to identify significantly responsive neurons Because the number of switches across different sessions was not equal, I needed to limit the number of switches across repeated sessions from the same site to their lowest number to force them to be equal. This meant fewer switches on average, thus a lower proportion of mismatch cells. With the number of switches kept even, the proportion of mismatch cells in the population did not change drastically across repeated sessions (Fig 4.21A). The identities of the mismatch cells within the population, however, did change, with many neurons in each mismatch category changing membership between the two sessions (Fig 4.21B).

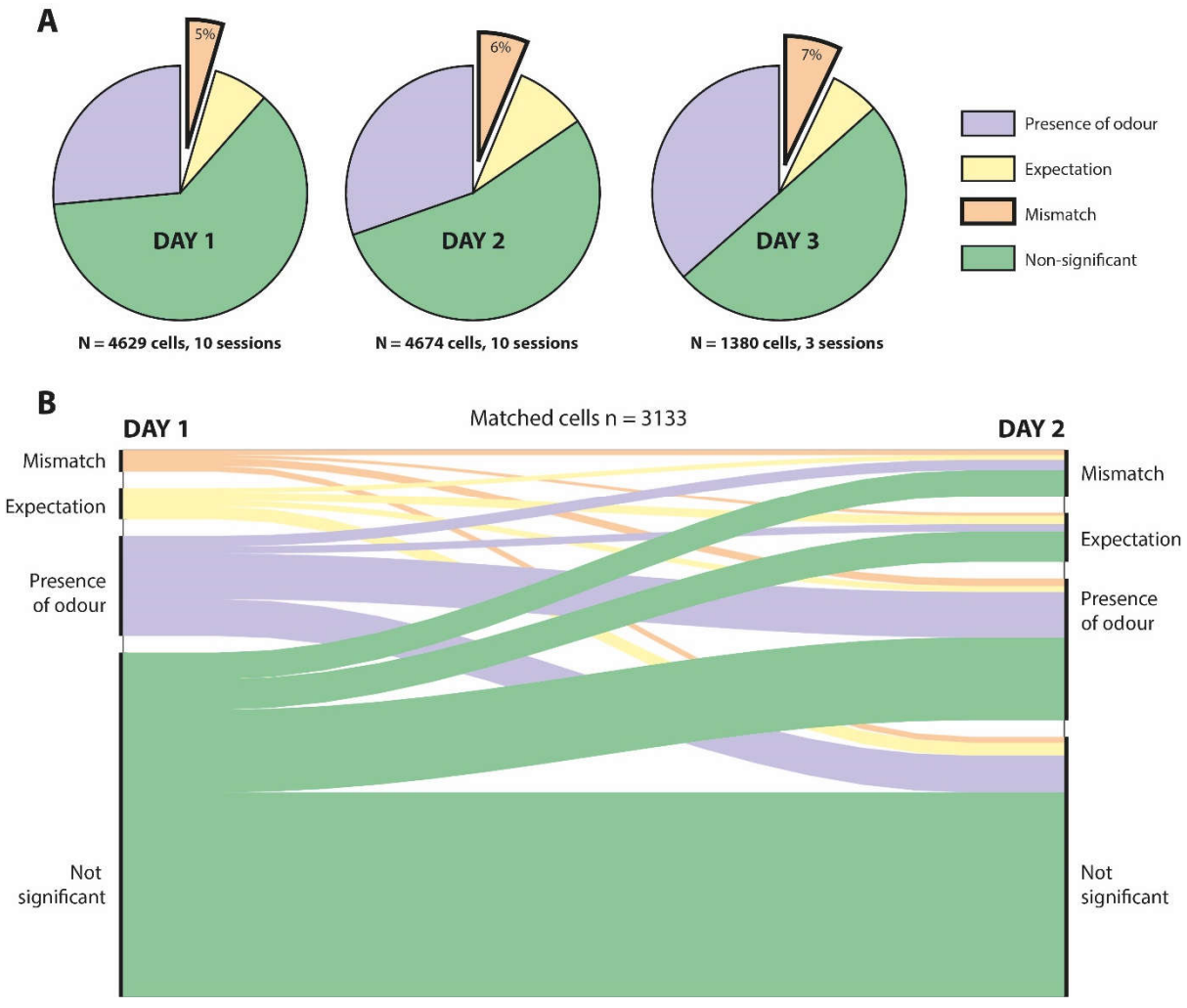

Figure 4.21. Proportion of mismatch cells across repeat sessions. A: Pies showing the proportion of mismatch cells across all sites with more than 1 switching session, matched and unmatched cells. Day 1 N = 231 mismatch cells, day 2 N = 280 mismatch cells, day 3 N = 97 mismatch cells. Mean number of switches from odour block to visual block = 4.8. B: Change in proportion of cells in each mismatch category from first session to second session. Matched cells only N = 3133.

It seemed that the identities of cells responsive to prediction-mismatch largely reconfigured over days, but the proportion of mismatch cells within the population remained fairly stable. Identification of mismatch neurons depended on comparing activity in 'expected odour' trials with activity in 'no odour' and 'stable odour' trials, so I investigated which of these is driving this reconfiguration (Fig 4.22).

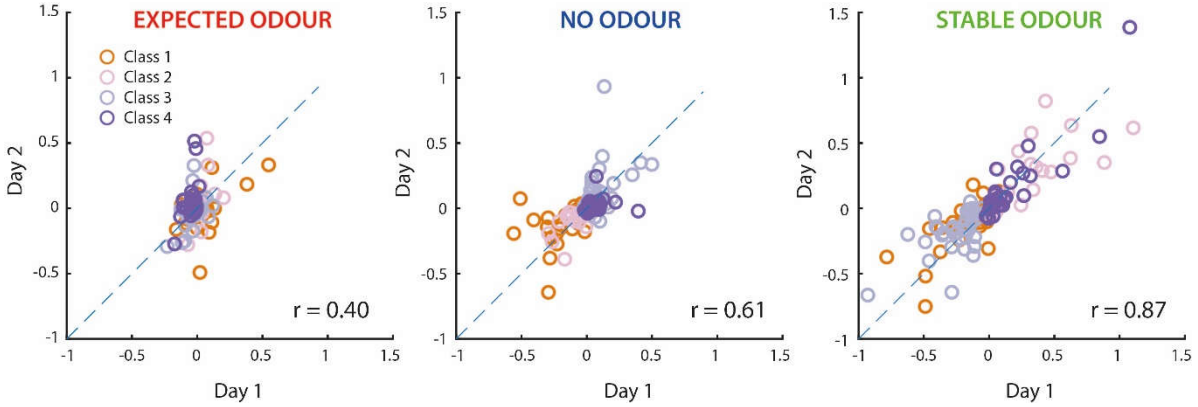

Figure 4.22. Stability of mismatch responses. Mean amplitude of matched mismatch cells identified on day 1 (N = 141 cells), showing responses to 'expected odour' (left), 'no odour' (middle), and 'stable odour' (right) averaged over 0 to 1.5s, on switching session 1 and 2. Colours denote mismatch class (class 1 N = 37, class 2 N = 25, class 3 N = 43, class 4 N = 36). Correlation coefficients for each response type across all mismatch classes between day 1 and day 2 are given as r.

Responses in 'expected odour' trials across all the mismatch classes were significantly less correlated between the two imaging days than 'no odour' responses and 'stable odour' responses ('expected odour' vs 'no odour' $p = 0.019$, ''expected odour' vs 'stable odour' $p < 0.001$, using an online significant correlation difference calculator by Soper, 2022). It seemed that the reconfiguration of mismatch cells within the population was largely down to changes in their responses during these prediction-mismatch trials, while their responses during 'stable odour' trials remained stable between the two imaging days.

5. VIP interneuron activation disrupts prediction-mismatch signalling

Thus far these recorded cells have been treated as if they were a unitary network. However, cortical ensembles have a distinct inhibitory pattern across multiple classes of cells (Fig 4.23) essential for context-dependent behaviour (Kuchibhotla et al., 2017). Vasoactive intestinal protein (VIP) interneurons mediate disinhibitory control by suppressing primarily somatostatin (SOM) interneurons, reducing their inhibition of excitatory pyramidal neurons and PV interneurons (Pi et al., 2013). This VIP-mediated disinhibition is critical for signalling mismatches between visual flow and motor behaviour in the visual cortex (Attinger et al., 2017), and for the spatial specificity of top-down modulation of visual processing by ACC (Zhang et al., 2014). VIP interneurons receive a larger proportion of cortical input than the other subtypes (Wall et al., 2016), so are well-positioned

for integrating these top-down connections. They then influence PV and SOM interneurons, whose firing can bookend the decision to stay in a foraging task (Kvitsiani et al., 2013). They therefore seemed well-placed to mediate the integration of top-down predictions and bottom-up sensory inputs required for prediction-mismatch signalling.

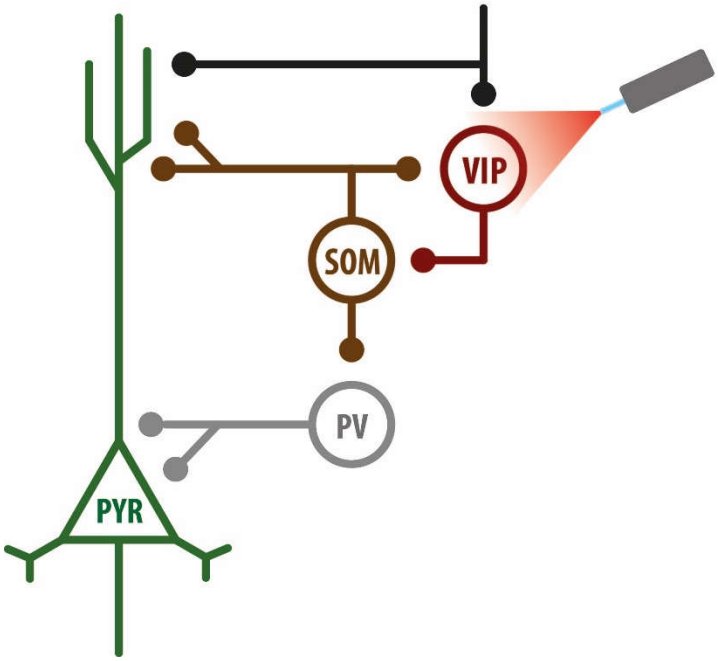

Figure 4.23. Schematic of cortical interneuron motif. Optogenetic activation of VIP interneurons causes inhibition of SOM interneurons, which in turn reduces their inhibition of pyramidal (PYR) cell dendrites and PV interneurons.

\

The all-optical approach of these experiments allowed the involvement of VIP cells in this mismatch signalling to be probed, via their selective optogenetic excitation within the imaged ensembles during behaviour. Prior to these experiments I injected the excitatory opsin FLEX-ChrimsonR-tdTomato into the ACC, alongside GCaMP7f (Fig 4.24). As these were VIP-Cre mice, this limited Chrimson expression only to VIP-positive interneurons.

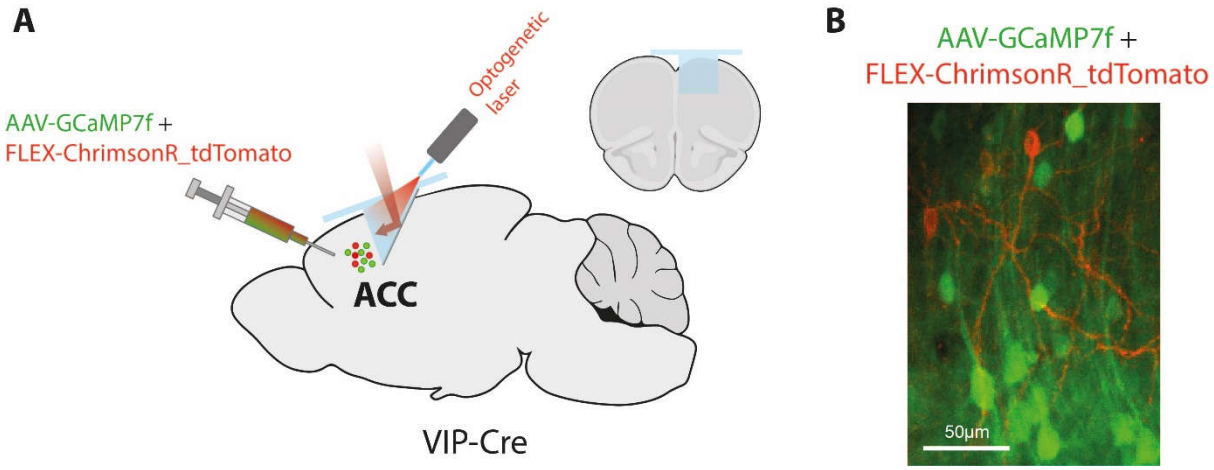

Figure 4.24. Optogenetic VIP interneuron activation experiments. A: Schematic of opsin injection during surgery and optogenetic laser positioning during recordings. B: Example site showing cells expressing GCaMP7f in green and VIP cells expressing ChrimsonR-tdTomato in red.

To assess whether Chrimson had expressed correctly in the ACC, on the first day of imaging I recorded 200 optogenetic-only trials. Here, mice sat in the dark while the optogenetic laser - positioned parallel to the hypotenuse of the microprism - delivered light at a range of powers (Fig 4.25) with a minimum of 5s between each laser trial. Only mice from which successful attention-switching sessions featuring the optogenetic laser were later recorded are included here (N = 8 mice). Averaging responses over all cells in each optogenetic-only session showed a graded activation in response to the ascending laser powers, which was also reflected in individual VIP cell firing (where VIP cells could be identified). This seemed to confirm that VIP cells were indeed expressing the opsin, with each laser power recruiting more VIP cells to disinhibit the surrounding neurons.

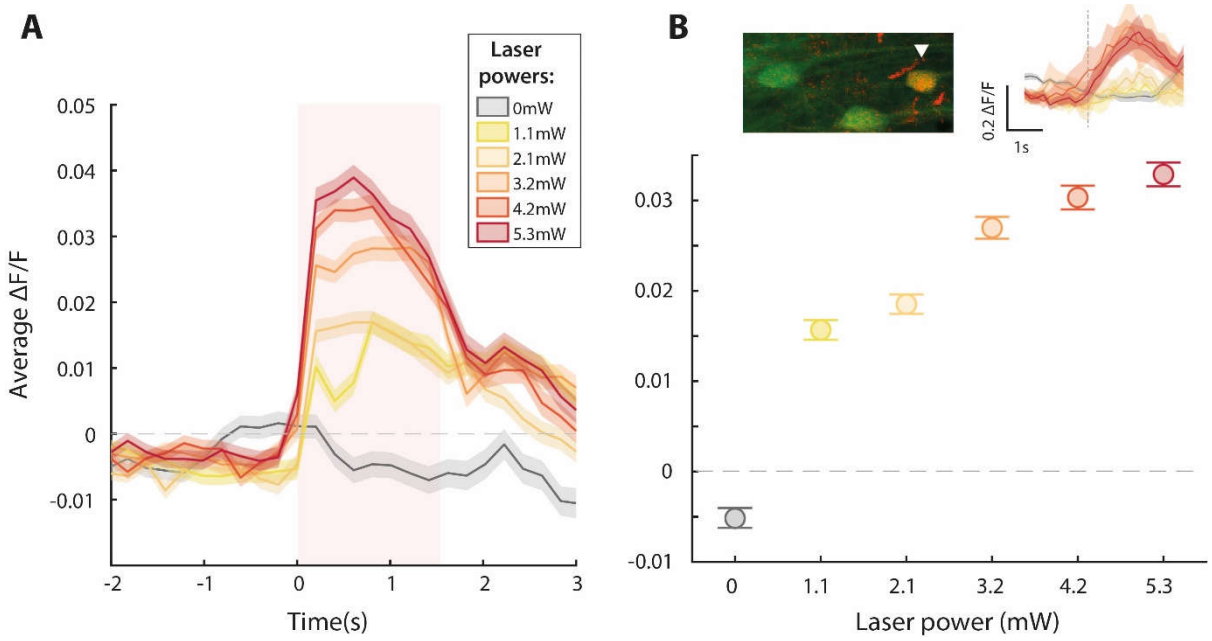

Figure 4.25. Optogenetic calibration. A: Average PSTHs across all cells recorded from mice with later optogenetic recordings (N = 2467 neurons, 8 mice). Colours denote optogenetic laser power. B: Top, example site (left) and PSTH (right) of putative VIP interneuron co-expressing Chrimson and GCaMP. Bottom, average responses from data in A averaged from 0 to 1.5s relative to laser onset. Colours denote optogenetic laser power.

To probe the contributions of VIP cells to the mismatch circuitry, I re-used the epochs from the previous chapter's silencing experiments to create three optogenetic conditions: no laser control sessions, peri-visual VIP activation sessions, and inter-visual VIP activation sessions (Fig 4.26A). Of the 10 mice used, it was possible to record a session of each condition in 8. The decision to vary laser timings across, rather than within, sessions was made to ensure enough switches for mismatch identification within a session without allowing the laser onset to become a cue by having it occur only on specific trials/blocks.

Silencing the ACC bilaterally via PV cells impaired switching, so it was possible that unilaterally perturbing the ACC via VIP cell activations might also affect behaviour. VIP activation during either

epoch did not affect discrimination of the task stimuli (Fig 4.26B – Wilcoxon signed-rank test comparing relevant visual stimuli discrimination: control vs inter-visual $p = 0.25$, control vs peri-visual $p = 0.94$, inter-visual vs peri-visual $p = 0.25$, comparing irrelevant visual stimuli discrimination: control vs inter-visual $p = 0.64$, control vs peri-visual $p = 0.10$, inter-visual vs peri-visual $p = 0.46$, comparing odour discrimination: control vs inter-visual $p = 0.74$, control vs peri-visual $p = 0.38$, inter-visual vs peri-visual $p = 0.84$), nor did it impair switching across blocks in either direction (Fig 4.26C – Wilcoxon signed-rank test comparing trials taken to switch into a visual block: control vs inter-visual $p = 0.46$, control vs peri-visual $p = 0.05$, inter-visual vs peri-visual $p = 0.10$, comparing trials taken to switch into an odour block: control vs inter-visual $p = 0.66$, control vs peri-visual $p = 0.14$, inter-visual vs peri-visual $p = 0.28$).

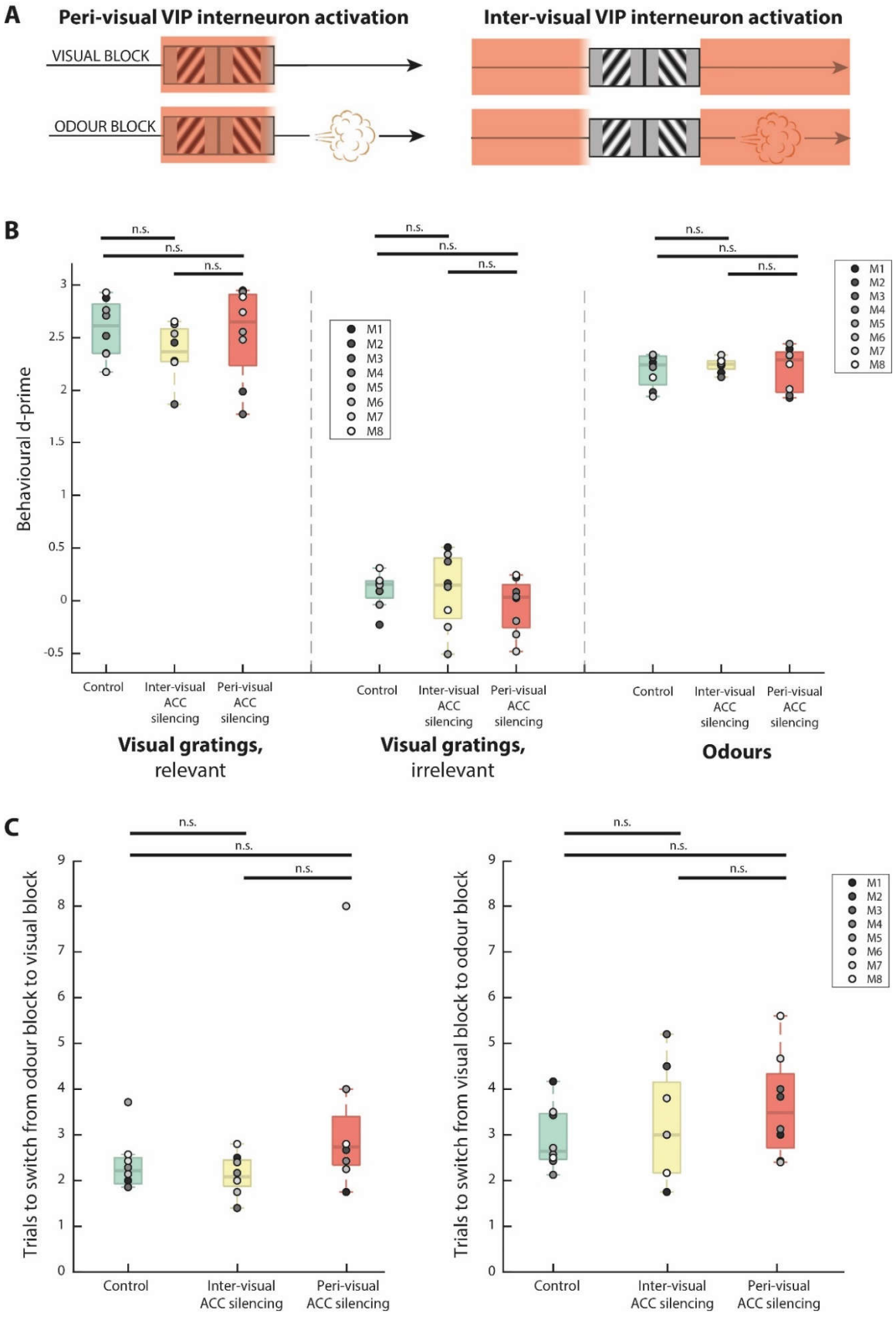

Figure 4.26. Optogenetic VIP activation has no effect on behaviour. A: Schematic of VIP activation epochs. B: Discrimination of task stimuli during stable performance across all blocks in a session, during control sessions, inter-visual VIP activation, and peri-visual VIP activation epochs. C: Left, number of trials taken for mouse to successfully lick to 3 consecutive rewarded gratings in a new visual block. Right, number of trials taken for mouse to successfully ignore 3 consecutive rewarded gratings in a new odour block. Circles represent means across individual sessions (N = 8 mice, 1 session per condition). Boxes represent median +/- IQR.

Unilateral VIP activation did not affect behaviour, but did it disrupt mismatch signalling in the local network? I separately identified mismatch cells from the population of cells recorded during each VIP activation condition, again limiting the number of switches to match the session from that mouse with the fewest switches. This revealed that 5% cells could be identified as mismatch during control sessions, compared to 1% during inter-visual VIP activation sessions and 2% in peri-visual VIP activation sessions (Fig 4.27A). Amongst the cells that were identified, the class 1 mismatch cells in control sessions showed similar signalling to those seen before. Meanwhile, cells identified as class 1 during sessions with VIP activation seemed to show a reduced amplitude of mismatch signalling (Fig 4.27B).

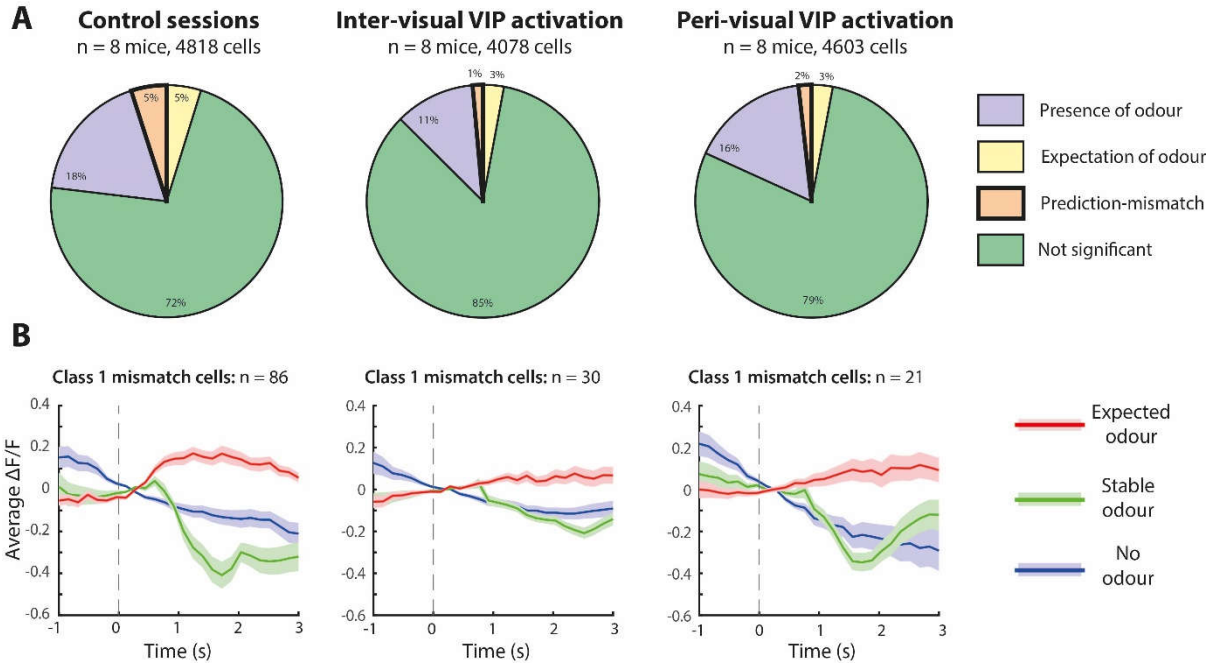

Figure 4.27. Mismatch cells across VIP activation epochs. A: Pies with proportion of mismatch cells identified in each of the 3 VIP activation conditions. Number of switches from an odour to visual block were limited to be equal across all 3 recordings from each site, mean N switches = 4.2. B: Mean PSTHs of class 1 mismatch cells identified during each VIP activation condition.

To quantify this, I compared responses to the three mismatch trial types across the 3 VIP activation conditions (Fig 4.28). Responses to the 'expected odour' were significantly smaller when VIP cells were activated during the inter-visual epoch, compared to control and peri-visual VIP activation sessions. There were no significant differences between the responses to either of the other two mismatch trial types across the 3 VIP activation conditions (Wilcoxon rank-sum test comparing class 1 cell responses in 'expected odour' trials: control vs inter-visual $p = 0.0044$, control vs peri-visual $p = 0.55$, inter-visual vs peri-visual $p = 0.0013$, comparing responses in 'stable odour' trials: control vs inter-visual $p = 0.37$, control vs peri-visual $p = 0.50$, inter-visual vs peri-visual $p = 0.98$, comparing responses in 'no odour' trials: control vs inter-visual $p = 0.66$, control vs peri-visual $p = 0.14$, inter-visual vs peri-visual $p = 0.28$).

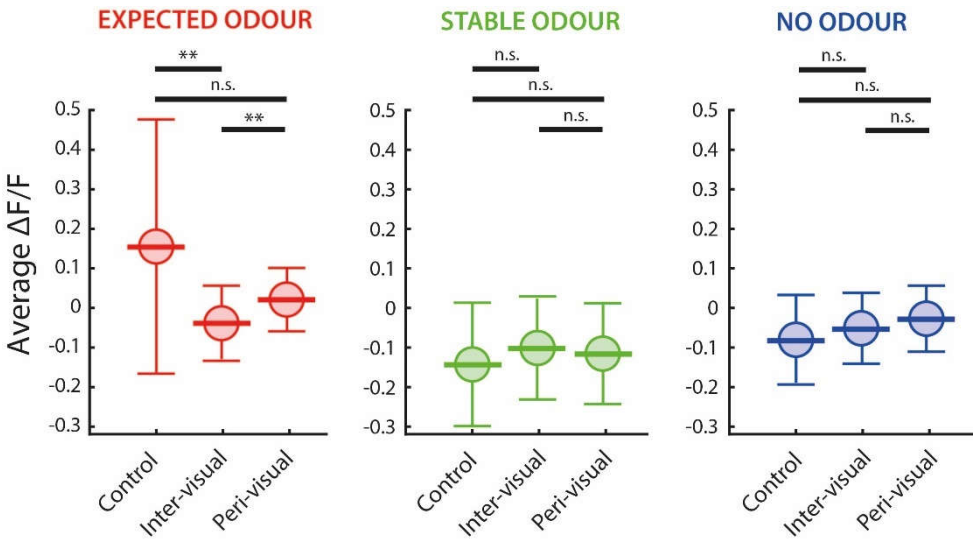

Figure 4.28. Mismatch response amplitudes across VIP activation conditions. Mean response amplitudes from class 1 mismatch cells, as plotted in 4.26B, averaged from 0 to 1.5s relative to mismatch. Left, responses to 'expected odour' across the 3 VIP activation conditions. Middle, responses to 'stable odour'. Right, responses to 'no odour'. Central lines represent mean, error bars represent SEM. Significance thresholds following Bonferroni correction for multiple comparisons: * $p < 0.025$, ** $p < 0.005$, *** $p < 0.0005$.

Selective excitation of VIP cells in the ACC appeared to disrupt mismatch signalling, without any effect on behaviour. This manifested in a reduction in the proportion of mismatch cells during either optogenetic perturbation, beyond what would reasonably be expected over repeated recording sessions as seen in the previous sub-chapter. Additionally, a significant reduction in 'expected odour' response amplitudes was seen when the VIP activation epoch coincided with the expected arrival of the odour - during inter-visual VIP activation sessions.

Discussion chapter 2:

Prediction-mismatch signalling in the anterior cingulate cortex

In the first results chapter, I identified a specific role for the mouse ACC in driving attention back towards visual stimuli following the absence of an expected odour. *In vivo* 2-photon calcium imaging revealed a sub-population of neurons in the ACC that responded maximally in the first trial of a new visual block, during the time in which the mouse would expect to experience an odour stimulus, but it did not arrive. When the mouse had no expectation of the odour, these neurons did not fire. When the expected odour did arrive, these neurons' firing was inhibited. These prediction-mismatch responses sustained for several sessions, but responses on subsequent trials did not significantly differ from baseline. Comparing subsequent behaviour showed that these prediction-mismatch responses were significantly higher when mice proceeded to switch attention in the very next trial.

Retrograde labelling revealed that these cells were not well-represented amongst the striatal-projecting neurons in the ACC. Matching the cells over days showed that only a small proportion of these cells could be classified as mismatch across repeated behavioural sessions. Despite this, a similar proportion of the overall population could be independently classified as mismatch in each session. Optogenetic activation of VIP interneurons reduced this proportion of cells that could be classified as mismatch. Activation during the relative period of the trial in which the odour would arrive significantly reduced the amplitude of the identified cells' prediction-mismatch responses. Here I will attempt to contextualise these findings amongst the wider literature.

1. ACC neurons encode task features

Diversity of responses

The first observation when analysing the calcium transients of the imaged ACC neurons was that a large proportion were responsive to all of the different task stimuli and actions. The ACC integrates information from many different sensory modalities (Rolls, 2015), and this diversity in responsiveness is fundamental for prefrontal regions to adapt their tuning during complex cognitive tasks (Rigotti et al., 2013). This fluid coding across attentional episodes has been seen in rodents (Lapish et al., 2008; Durstewitz et al., 2010), with activity in the PFC re-configuring to represent the current task.

It is therefore unsurprising that the ACC would respond to these task events, as they represent what is currently motivationally relevant to the mouse. What is surprising is the relatively high percentage of cells responsive to both of the irrelevant visual gratings (Fig 4.06, around 65%), greater than the proportion responsive to either relevant unrewarded stimulus. This would suggest greater ACC overall engagement when attention towards a modality is suppressed, compared to when the mouse attends to the stimulus and chooses not to respond.

To test this, responses to either irrelevant visual grating could be compared to see whether cells in the ACC are selective or if these responses indeed reflect a non-specific suppression of attention towards them. Selectivity would suggest the irrelevant stimuli are actually being encoded by the ACC, which would contrast with prefrontal studies showing stimuli features are no longer encoded when they become task-irrelevant (Rao et al., 1997). Worth noting is that in the first results chapter, ACC silencing did not significantly impact the mouse's ability to ignore the visual stimuli early or late in an odour block. If the ACC is involved in suppressing attention towards these stimuli, it is not essential for the process.

Layer II/III vs layer V/VI responses

Overall responsiveness of layer II/III neurons to all task events was reduced relative to layer V/VI neurons. This was most pronounced in responses to odour stimuli and relevant rewarded visual stimuli, as well as reward and licking. Inputs from premotor cortex are predominantly seen in these deeper layers (Calderazzo et al., 2021), which may explain this greater responsiveness to the task events that involve licking. It should be noted that these cells are from different cohorts - used early and late in the project timeline respectively - so may well be subject to systemic errors that could influence these findings.

All data after this first section were collected from cells recorded using these coronal microprism implants. They were categorised as layer V/VI cells, rather than layer II/III, based on the larger size of the cells (~40µm), despite the fact that GCaMP had been injected into both layers II/III and layers V/VI during the surgery. We can see in Fig 2.02 that expression of GCaMP seemed higher in these deeper layers, but also that expression may have spread superior to the ACC into secondary motor areas. I attempted to ensure the recorded areas were layer V of the ACC by ensuring recording sites were selected that were closer to the front, lateral corner of the microprism – ensuring the site was deeper than the secondary motor area and more lateral than the superficial layers. Matching these recorded cells to post-hoc slices, with immunostaining to categorise the major cell sub-classes, will allow the exact location of the recorded sites to be confirmed.

2. Cells in the ACC respond to prediction-mismatch

Prediction-mismatch signalling

These analyses revealed a sub-population of cells which appeared to signal prediction-mismatch in a manner predictive of subsequent behaviour. Unlike cells signalling a mismatch in visuomotor coupling (Attinger et al., 2017), these odour prediction-mismatch cells were not seen in visual cortex. The positive ("class 1") and negative ("class 4") mismatch cells followed a distinct pattern, with a similar trajectory in 'expected odour' and 'stable odour' trials until the odour was received, whereupon activity in these trials returned to baseline.

Their distinct time-course - a prolonged activation following prediction-mismatch that continued until the next visual grating but was limited just to the 'expected odour' period of the first visual trial - complemented findings from the silencing experiments. Inter-visual and peri-visual ACC silencing were both sufficient to impair switching, and either would coincide with these cells' periods of sustained activity. Silencing after the first trial of the visual block did not impair switching, and we see from Fig 4.13 that by this trial the average responses of the cells were no longer significantly different from baseline. It seems that if a single sub-population could be held responsible for the observed role of ACC in this task-switching, these positive and negative mismatch cells would be strong candidates.

Prediction-mismatch signalling predicts behaviour

The strongest evidence for a link between the silencing results and these imaged cells comes from the significantly more positive activity in the positive and negative mismatch cells in trials preceding a perfect switch. The average running speeds remained constant between trials preceding perfect and imperfect switches (Fig 4.15), so were unlikely to be the cause of this difference. Finding a link between these signals and subsequent behaviour aligns with human research, which shows that the dACC responds to surprising stimuli only when they are informative for updating an internal model (O'Reilly et al., 2013). As the absence of the odour here is always informative, the response amplitudes of these cells instead seemed to reflect whether the internal model has been successfully updated.

What causes this difference in activity? Effort-based decision making relies on circuitry between the ACC and the nucleus accumbens (NAc, Hauber & Sommer, 2009) or ventral tegmental area (VTA, Elston et al., 2019), while switching between strategies relies on inputs to the ACC from the locus coeruleus (LC, Tervo et al., 2014). These regions are associated with motivation and arousal, so could be facilitating prediction-mismatch signalling in the ACC when the mouse is particularly engaged with the task. Noradrenergic signalling from the LC seems a particularly likely candidate,

as LC neurons signal action outcomes and prediction-errors in a manner predictive of subsequent behaviour changes (Aston-Jones & Cohen, 2005; Sales et al., 2019). Serotonergic signalling with the dorsal raphe nucleus is another candidate, with depletion of serotonin in the PFC associated with cognitive inflexibility (Clarke et al., 2004). Alternatively, the difference could originate in the ACC, with changes in the stochastic firing of these neurons determining whether the prediction-mismatch signal is sufficient to trigger a behavioural change on the next trial or not. Further experiments would need to employ multiple projection-specific optogenetic perturbations to test these possibilities, ideally with concurrent recordings from these regions.

Mismatch classification

Neurons were classified as mismatch cells if their baseline-corrected responses during the first trial of the visual block differed significantly from their responses during an expected rewarded odour and when an odour was not expected, later in the visual block. Each response was defined as the average response on each trial 0-1.5s relative to when the odour actually arrived or would have been most predicted to arrive. This meant that the 'expected odour' condition could at most have one value for every switch from an odour block to a visual block, with switches removed in which mice licked to the preceding grating (an 'error' switch). From Fig 4.07 we can see that the most switches any of the mice performed was 14, so this meant a maximum of 7 samples for this condition. To prevent unequal sample sizes in the statistical tests, for each 'expected odour' sample one sample for the other two conditions was taken from the corresponding visual or odour block. If multiple trials in the block fit the criteria, the response was averaged across them to give a more representative sample.

The limited sample size for 'expected odour' trials is a limitation of this study, but one that cannot be easily corrected. In order to provoke prediction-error signalling, a prediction must first be reliably created. This requires the mice to be stably performing the task before a switch can occur. I found that requiring above 80% performance over 30 trials was the minimum threshold that could reliably separate a mouse performing well from a mouse not discriminating properly, but instead benefitting from a chain of rewarded stimuli. I think it would be very difficult with the current task to increase the number of switches further. Perhaps by removing the unrewarded stimuli, and therefore any discrimination requirement, the task could be simplified into mice choosing to respond only to the modality of the stimulus, not its identity. This would allow a greater number of switches, giving a greater number of 'expected odour' trials, and so allowing for better estimations of the underlying population distributions of each neuron's responses in these trials.

The small sample sizes may have caused an underestimation of the proportion of mismatch cells, but it seemed that it may have also been overestimated. Classifying all cells that have significantly

different responses across the three conditions as mismatch cells has yielded the "class 2" and "class 3" neurons which do not seem to fit the pattern of the other classes, but represent 38% of the identified "mismatch" neurons in Fig 4.09. While the pattern of their responses can be most easily explained by a straightforward correlation with running, this explanation seems insufficient. One option would be to regress each neuron's activity on the mouse's locomotor activity, then remove neurons from subsequent analysis whose activity can be particularly well predicted by this motor behaviour. Alternatively, repeating this analysis with a task in which running is not required to trigger trials could remove this possible confound.

While the comparison criteria used to isolate mismatch cells seemed appropriate from the structure of the task, it seems likely that the coarse nature of the comparisons has included cells that do not show the expected characteristics of mismatch cells and the likely exclusion of cells that do. Further refinement of the method used to identify these cells is needed for future experiments.

Decay of mismatch responses

When comparing responses of positive mismatch cells during the same epoch of the first 4 trials of a new visual block (Fig 4.13), only responses in this first mismatch trial were significantly larger than their pre-mismatch baseline. However, we can see from their average responses in Fig 4.12 and the example mismatch cell in Fig 4.13 that even a baseline mismatch response would likely be significantly different from the response to a 'stable odour', which caused the cells to be inhibited. Following responses in these epochs across trials, as the expectation of an odour fully disappears over the course of the visual block, then re-appears following the switch into an odour block until it becomes the response we see in 'stable odour' trials, could inform how this change in prediction signalling occurs. I would interpret that the response in the T + 1 trial (second trial of the visual block) reflects the ACC no longer encoding a prediction, so the cells were not responsive. In the 'stable odour' trials, these cells were about to signal a prediction, but were inhibited when the prediction was met. During the 'expected odour' period of the first visual trial, the lack of an odour meant the cells were not inhibited, so they continued to respond maximally to signal the prediction. Thus the ACC integrates predictions and sensory inputs, with the predictions driving the initial response and the sensory input inhibiting this response.

3. Striatal projecting cells are underrepresented in this prediction-mismatch population

Reward prediction-errors

The striatum is a major projection target of the ACC, associated with top-down control (Zhang et al., 2016). Reward prediction-error (RPE) signals have been seen in both the primate dACC and striatum (Parker et al., 2016; Wittmann et al., 2016), with a time-course that suggested these signals were propagated from the ACC to the striatum (Oemisch et al., 2019). This corticostriatal circuit from ACC to dorsomedial striatum has also been implicated in reward-driven learning for spatial memory (Pooters et al., 2017) and operant conditioning (McKee et al., 2010). Once prediction-error signalling neurons had been identified in the ACC, it seemed likely that the striatum could be their projection target.

However, a lower proportion of the cells which expressed both GCaMP7f, injected in the ACC, and the retrograde tracer CTB-Alexa-647, injected in the dorsomedial striatum, were identified as mismatch cells than in the rest of the population. If these prediction-errors did follow this projection pathway, we could expect the mismatch cells to make up a larger proportion of this striatal pathway. This does not conclusively discount the striatum as the key output target for these prediction errors: the striatum is a large structure, and evidence from humans implicates more ventral areas in reward expectation (Daniel & Pollmann, 2014). Repeat experiments with retrograde labelling would be needed to discount the striatum fully.

Furthermore, there are factors which challenge the interpretation of these signals as RPEs. RPEs in dopaminergic midbrain neurons are typically enhanced when a reward is larger than expected, and reduced when the reward is smaller than expected (Schultz, 2016). If the prediction-mismatch signal we saw here represents the failure of the reward associated with an odour to arrive, the pattern of increased activity following reward omission did not match these midbrain RPEs. Furthermore, the omitted odour itself was only predictive of a reward 50% of the time. If these positive mismatch neurons were just responding to the omission of a predicted reward, they should have also showed significantly increased activity when the unrewarded odour was delivered, as it too represents reward omission. However, comparing these conditions showed that 'expected odour' responses were also significantly larger than unrewarded odour responses in positive mismatch cells (Fig 4.29 – Wilcoxon signed-rank test comparing responses to 'expected odour' and unrewarded odour averaged 0 to 1.5s after mismatch event $p = 1.69 \times 10^{-28}$, averaged -0.5 to 0s from the next visual grating $p = 5.45 \times 10^{-15}$). It seemed the cells only responded positively when the outcome was genuinely unexpected: an omission of the odour, rather than the appearance of either of the two anticipated odours.

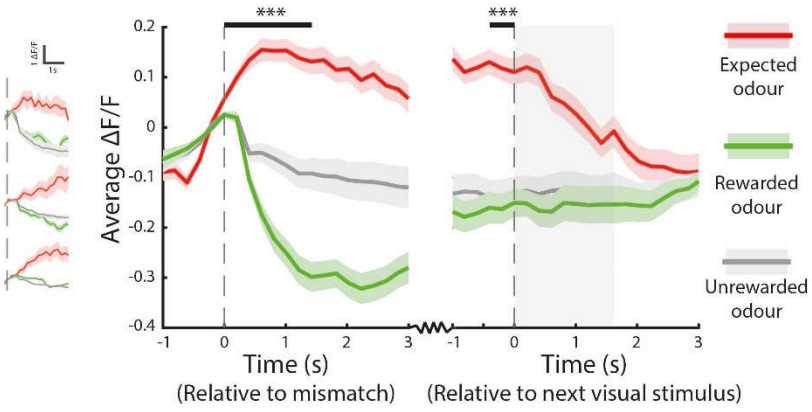

Figure 4.29. Mismatch responses are not simple RPEs. Left, PSTHs from 3 example positive mismatch cells. Right, averaged PSTHs across all positive mismatch cells aligned to mismatch event (middle) and next visual grating (right). Significance bars reflect comparison between 'expected odour' and unrewarded odour responses. Significance thresholds following Bonferroni correction for multiple comparisons: * $p < 0.025$, ** $p < 0.005$, *** $p < 0.0005$.

This difference suggests that the prediction-error signals seen here are not simply straightforward failures to predict a reward. This does not discount them being RPEs, as all relevant task stimuli in this task are directly informative about a reward, whether through a positive or negative association. This is how the task models attentional episodes, with different stimuli being associated with reward in each block to make them motivationally relevant to the mouse. If the ACC contributes prediction-error signalling to this process, we would expect it not to be a generic signaller of surprise but instead signal violations of motivationally-relevant predictions. We see this in the humans, with dACC activity increasing only when the surprising position of the stimulus provides information for upcoming trials (O'Reilly et al., 2013).

To test how tied these prediction errors are to reward, future experiments could vary associations to reward. Removing unrewarded stimuli, as mentioned in the previous section, would make each odour 100% predictive of reward and the associated prediction error a clear RPE. At the other end of the spectrum, training mice in an oddball paradigm in which the mouse is passively experiencing repeated odours without any chance of reward or reason to engage would entirely disassociate the odour from any motivational relevance. Observing prediction errors in the former and not the latter would suggest that these prediction errors are signalled by the ACC only if they are meaningful to obtaining rewards, while observing them in both would suggest the ACC is signalling generic prediction errors without the predictions requiring motivational relevance. In a recent study, electrophysiology revealed prediction-mismatch signals in the mPFC, including the ACC, when anaesthetised rats heard a sequence of auditory tones with one tone missing or the wrong pitch for the sequence (Casado-Román et al., 2020). These signals were larger and longer lasting than those seen in the auditory cortex. In their paradigm there was no motivational relevance to perceiving the prediction-mismatch, suggesting that the relationship between prediction-error signalling in the ACC and reward predictions may not be straightforward.

Positive surprise

The PRO model attempts to reconcile results associating the ACC with reward predictions and with errors and conflict by suggesting that the ACC's primary function is in calculating surprise (Alexander & Brown, 2011). Here, rather than signalling positive or negative RPEs depending on whether the received reward was larger or smaller than expected, the ACC signals positive or negative surprise. Negative surprise is what we see in these 'expected odour' trials, when the animal is expecting an outcome that does not occur. Positive surprise is the opposite, when an outcome occurs that was not expected.

This task features each on respective block switches. When switching from a visual block to an odour block, an unexpected odour will follow the now irrelevant visual grating in the first trial. If the ACC is indeed this surprise calculator, it should respond differently to this initial unexpected odour compared to the 'stable odour' later in the odour block. Comparing responses in this 'new odour' mismatch condition with the 'stable odour' and 'no odour' comparison conditions as before revealed 6% of the ACC neurons that had significantly different activity in these 'new odour' trials (Fig 4.30A). Looking at the positive 'new odour' mismatch neurons revealed a similar pattern to the 'expected odour' mismatch neurons, with activity significantly higher for a sustained period when the odour arrives and is unexpected, compared to when either odour arrives and is expected (Fig 4.30B).

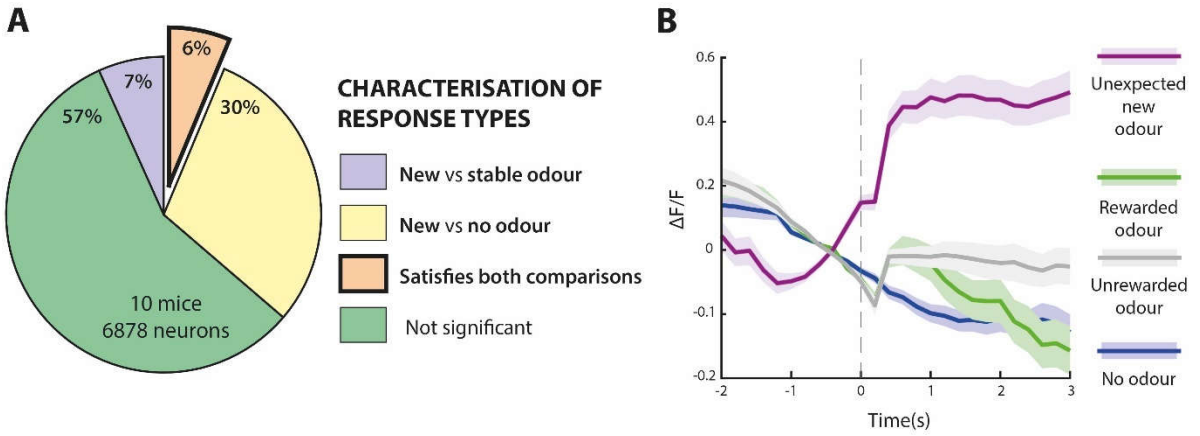

Figure 4.30. New odour mismatch cells in ACC. A: Pie showing proportion of neurons recorded from all sites that meet one or both of the statistical comparisons used to identify these 'new odour' mismatch cells. B: Mean response PSTH for class 1 (N = 285 neurons) 'new odour' mismatch neurons. Shading represents SEM.

It appeared a smaller proportion of ACC neurons were responsive to this positive surprise. This may be again due to the asymmetry of the task. When switching from an odour block to a visual block, the first evidence of a switch comes from the absence of the expected odour, as the mouse will typically not lick to the preceding grating and will therefore not realise it is now rewarded. However, in the other direction the mouse expects the visual gratings to be relevant. Therefore, on

this first odour trial it will typically lick to the first irrelevant grating, but fail to trigger a reward. This means that by the time the new odour arrives, the mouse has already accrued some evidence of the block switch from the failure to gain a reward during this first grating. This might explain the lower proportion of cells signalling this positive surprise, as the surprise itself is less informative to the mouse than the corresponding negative surprise in the other direction. I investigated to what degree these positive-surprise-responsive neurons overlapped with the negative-surprise-responsive neurons (Fig 4.31).

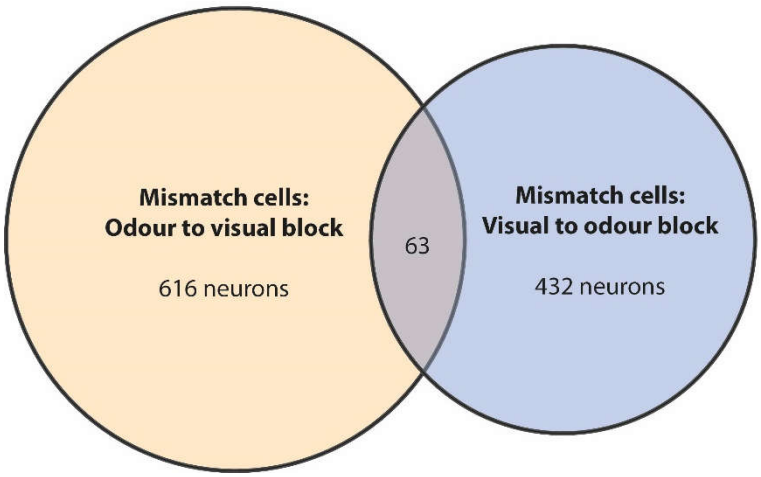

Figure 4.31. Positive and negative-surprise-responsive neurons are from largely different sub-populations. Venn diagram showing overlap between negative-surprise mismatch neurons (left) and positive-surprise mismatch neurons (right).

This showed that only 63 of the 1048 identified cells were responsive to both forms of surprise. The silencing results show that the ACC signalling this positive surprise is not essential for switching, as no effect of ACC silencing is seen when switching into an odour block. This could be due to the critical evidence of the switch coming more from the earlier visual grating in this process, or because the appearance of an odour stimulus is a salient enough cue to engage more areas of the brain and not solely require the ACC signalling prediction errors. These results do support a role for the ACC in signalling both positive and negative surprise.

Co-expression

One caveat of the striatal-projection findings was that the co-expression of GCaMP7f and CTB-647 was very low. Most identified striatal-projecting cells failed to also express GCaMP, meaning that the reported striatal population only represented a small fraction of the available striatal-projecting cells. Additional experiments that can record from a larger proportion of these cells, potentially via the use of a retro-labeller that competes less with GCaMP or deeper GCaMP injections, could better identify the roles of these striatal projecting cells in this task.

4. Prediction-mismatch populations reconfigure across days

Stability of task stimulus selectivity

I started by examining changes in simple selectivity to the task stimuli over days in an attempt to establish how stable the network was in responding to the more tangible task events. Matched neurons were stable in their selectivity for the relevant stimuli, but less stable when the visual stimuli were irrelevant. That cells encoding behaviourally-relevant stimuli were stable over days aligns with previous research from the PFC (Bari et al., 2019). Whether or not this is because these cells were modulated by licking and running - which would make them appear as selective for these stimuli - it appeared that these circuits were more stable than those involved in prediction-error signalling. Neurons seemed less selective overall for the irrelevant gratings, which may reflect the ACC preferentially encoding task-relevant information as is seen in the primate PFC (Rao et al., 1997), but may also reflect the lack of differences in licking and running behaviour between the two irrelevant stimuli.

Stability of mismatch responses

Across the cells matched between the first and second switching sessions, only 7.7% of the mismatch cells on day 1 remained mismatch cells on day 2. When comparing how well the responses of these day 1 mismatch cells correlated with their responses on day 2 during the same trial conditions (Fig 4.22), responses to the 'expected odour' were significantly less correlated than responses to 'no odour' and to 'expected odour' across all mismatch classes. This indicated that it was primarily changes in their response during the prediction-mismatch trial that caused so many of these cells to no longer be classified as mismatch on day 2.

The high correlation of responses to the 'stable odour' may correspond with the stability of selectivity to relevant stimuli seen across the population. These 'stable odour' trials are associated with a specific motor profile: the mouse slowing and licking to the rewarded odour. This may reflect specific inputs to the ACC conveying motor information that are not re-organised over time, so cells responsive to changes in locomotion or licking remain stable over these repeated sessions. This would not explain the higher correlation in 'no odour' trials, relative to 'expected odour', as this epoch is not associated with any specific motor behaviours except for steady running above the speed threshold to trigger the next trial.

Stability of mismatch circuits

When classifying mismatch cells across repeated attention-switching sessions, the proportion of mismatch cells within the population remained relatively stable (Fig 4.21A) while the actual identities of the mismatch cells changed substantially (Fig 4.21B). Similar drift has been seen in the

parietal cortex (Driscoll et al., 2017) and hippocampus (Ziv et al., 2013) during spatial tasks, with individual cells changing their firing properties but the overall network representations of spatial features remaining stable. Each day a subset of neurons could be found that corresponded to position, but the population had entirely reconfigured their activity from the previous day. This can even occur within a session: population activity in the ACC and PL of rats trained to switch strategies multiple times within a session changed between stable firing states as the rules changed. When the same rule was enforced a second time in the same session, the neurons entered a new firing state distinct from what was seen in the first instance of the rule (Malagon-Vina et al., 2018).

It might seem that this encoding drift would hinder long-term associations between different brain regions, such as with regions involved in memory. However, having a wide variety of possible circuit combinations that can encode a specific behaviour would protect these representations from redundancy, such as the failure of an individual neuron to fire. If the representations are high-dimensional, able to be encoded by different combinations of neurons, then they will be more resistant to one component of the network failing (Rule et al., 2019). Here we have seen cells whose responsiveness to different task stimuli and to different kinds of surprise overlap. The ACC would need high-dimensional representations of the task to still robustly encode task-relevant predictions despite the redundancy of individual units.

What drives this circuit re-organisation over time? The drift itself may reflect noise within the circuit, but may also be due to network changes caused by new instances of learning. Rule and colleagues (2019) suggest that the brain may adapt to these changes in order to maintain representations by using predictive coding. If the network drifts too far, it will no longer coherently represent the task. Therefore, projection targets of the network will learn to predict their expected input, and when the network re-configures to the extent that the input has changed, send a prediction-error signal that drives plasticity in the source network to regain a consistent representation of the task.

This process seems a valuable mechanism for sustaining attentional episodes. A network that robustly encodes the inputs, rules, and actions of a specific sub-goal over days would be limited in the number of different sub-goals it could represent with the same number of neurons. However, a network that can re-organise fluidly to represent the same task in a number of different ways over different days would have the capacity to represent a much larger number of possible tasks. I plan to further analyse how these ACC neurons represent the task and signal prediction errors over time. Of particular interest is how the network re-configures over learning, and between repeated blocks within an attention-switching session. It may be that the prediction-error circuits are re-

organising even between blocks in the same session, like strategy encoding in the rat ACC (Malagon-Vina et al., 2018), and by comparing all prediction-mismatch trials across a session I only identify the small subset of neurons that are consistently responsive across all these different network combinations.

5. VIP interneuron activation disrupts prediction-mismatch signalling

Light artefacts

Other recordings from colleagues in my laboratory have shown that the optogenetic light power used in these experiments is sufficient to trigger artefactual responses from neurons in the visual cortex. ACC does not receive direct projections from the retina, so may be less susceptible to this effect, but the possibility cannot be discounted. During earlier rounds of interneuron optogenetic experiments, I performed similar calibration sessions with a mouse expressing the same opsin (Chrimson) in SOM interneurons and a mouse expressing an inhibitory opsin (ArchT) in the same VIP interneurons (Fig 4.32). In both cases the same maximum laser power (5.3mW) elicited overall inhibition across the recorded population. This shows that the opsins were dominating the response; I am planning the further experiment using the same laser powers in VIP-Cre mice expressing no opsin that would be necessary to genuinely discount the possibility of an artefact in these experiments.

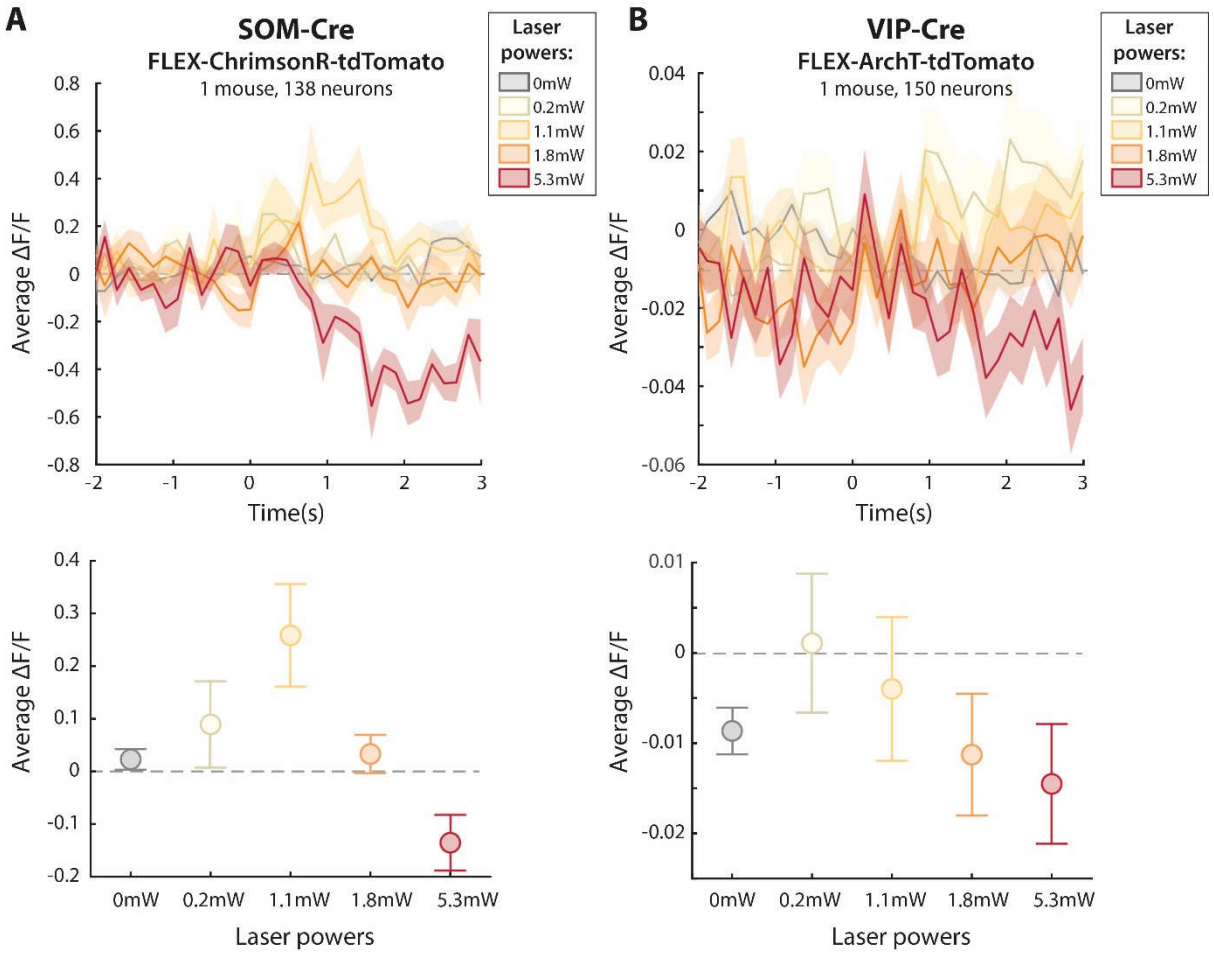

Figure 4.32. Alternate optogenetic calibrations. A: Top, average PSTHs across all cells recorded from a SOM-Cre mouse injected with FLEX-ChrimsonR-tdTomato. Bottom, responses averaged from 0 to 1.5s relative to laser onset. B: As in A, across all cells recorded from a VIP-Cre mouse injected with FLEX-ArchT-tdTomato. Colours denote optogenetic laser power.

VIP interneurons in prediction-mismatch signalling

Finding that VIP activation didn't affect behaviour was fairly expected. The volume of tissue perturbed was likely limited by the injection volume, as well by the distance between the fibres and the opsin-expressing cells. As the internal space of the microprism accounted for half of the working distance of the objective, it had to be positioned closer to the surface of the cranial window. This lack of remaining space meant that the optic fibre had to be positioned further from the cranial window's surface, and the maximum laser power was used to compensate. Furthermore, unlike in the silencing experiments this perturbation affected only one hemisphere, allowing the unaffected hemisphere to compensate for any deficits. While the calibration sessions indicate significant local perturbations of circuits, the small, unilateral area of effect was likely insufficient to disrupt mismatch signals throughout the ACC. The lack of a behavioural effect at least provided some reassurance that the red light was not significantly distracting the mouse.

The impact of VIP activation on prediction-mismatch signalling gives some insight into how these circuits may arise. A computational model showed how an interconnected network with different

interneuron subtypes can give rise to both negative and positive prediction-error neurons (Hertäg & Clopath, 2022), with the interneurons required to establish an excitatory/inhibitory (E/I) balance. If this balance relies on inputs relaying sensory information and their related predictions – for example, by PV or SOM cells receiving the sensory inputs and VIP cells receiving the predictions – then the E/I balance will be broken when one input outweighs the other, with the direction determining the type of prediction-error neuron. For negative prediction-error networks like these, the E/I balance is preserved when the sensory input is equal to or larger than the prediction, but temporarily broken when it is smaller than predicted. A similar mechanism of selective inhibition using PV and SOM cells, and disinhibition using VIP cells, to create centre-surround inhibition for processing has been seen in ACC projections to V1 (Zhang et al., 2014).

This might explain why I saw a reduction in the proportion of mismatch cells when VIP cells were activated in either epoch, even though the peri-visual epoch did not coincide with the activity used for the mismatch comparisons. If a delicate E/I balance is required for prediction-error signalling, disruption at any time may cause an impact. VIP activation may imbalance the signalling in favour of sensory or predictive input, to such an extent that when the true sensory input is reduced in the 'expected odour' trial (as the odour does not arrive), the difference does not meaningfully alter the balance. Along the same line, activation of PV cells during the silencing experiments in chapter 1 may have the reverse effect, unbalancing the network in favour of inhibition to disrupt mismatch signalling. The larger area of effect, both in terms of number of cells activated and hemispheres affected, might explain why bilateral PV activation disrupted behaviour but unilateral VIP activation did not.

Inter-visual vs peri-visual VIP activation

The two activation epochs could be differentiated by their effects on positive mismatch cell signalling. Responses in the 'expected odour', but not 'stable' or 'no odour' trials, were significantly reduced only when VIP cells were concurrently activated in the inter-visual epoch. This seemed slightly counterintuitive: VIP activation should disinhibit the surrounding network and increase excitability. Instead, the results suggested that VIP involvement in mismatch signalling is not straightforward – perhaps the prediction-mismatch signals that arose in this trial relied on a precise balance of interneuron inputs, or a temporally-precise VIP activation that was prohibited by the constant photostimulation. Explaining these results would require further analysis of activity during control sessions.

VIP experimental design

A key issue with interpreting these optogenetic results is that we lack a clear idea of what these interneurons are normally doing during this behaviour. After all imaging sessions had been completed, the brains were fixed by trans-cardiac perfusion of 4% paraformaldehyde. Slices were taken parallel to the imaging plane, and immunostained for the 3 major interneuron sub-classes, to allow post-hoc categorisation of these imaged neurons, like in earlier research (Khan et al., 2018). However, this data was not available before starting the experiments, so the activation epochs were selected to mirror those from the silencing experiments, rather than with any specific pre-hoc hypothesis of VIP interneuron contributions to prediction-error signalling in mind.

Once this post-hoc categorisation is complete, further experiments can be designed based on the identified contributions of the interneuron sub-classes to this behaviour. My assumption would have been that the inhibition seen on 'stable odour' trials once the odour arrives is due to local inhibition by PV or SOM interneurons, and so activating VIP interneurons during this period would prevent this inhibition and give responses like those seen when the odour does not arrive. This would mean that a well-timed VIP activation could simulate the prediction-mismatch response seen in these cells even on trials without an expectation violation. However, we see from these optogenetic experiments this does not seem to be the case: activating VIP cells instead inhibits the 'expected odour' response while leaving the 'stable odour' response unchanged. Once the normal activity of VIP interneurons has been characterised in this behaviour, new perturbations could be tried with timings attuned to the interneurons' activity during this prediction-mismatch signalling.

DISCUSSION

Discussion chapter 3:

The anterior cingulate cortex in flexible behaviour

In this final chapter I will summarise the key findings of this project. I will identify the key issues that remain with connecting the findings from the first results chapter, behavioural changes during ACC silencing, to the findings from the second chapter, prediction-mismatch signalling in ACC neurons. I will explore other possibilities from previous studies into the function of ACC in primates and rodents, and possible experiments to test these. Finally, I will attempt to position this study within the wider literature of flexible behaviour and cognition.

1. Prediction-error signalling in the ACC

This project took a two-step approach to identifying the contribution of ACC in the flexible behaviour required for the attention-switching task: first, identifying what role ACC plays by observing the behavioural changes caused by lesions, and second, examining activity in the ACC at these times during normal behaviour. Through lesions, I found a specific role for ACC in facilitating attention switches towards the visual stimuli following the absence of an expected odour stimulus. This was not limited to a specific period of the trial, and the deficit receded over many repeated sessions. Through calcium imaging, I identified a sub-population of ACC neurons that were specifically responsive when this same odour stimulus was expected but did not arrive, in a manner predictive of the mouse switching attention in subsequent trials. The cells did not share the striatum as a projection target, changed their prediction-mismatch responsiveness over days, and could be disrupted via VIP interneuron perturbation.

The trial types and epochs chosen for activity comparisons across ACC neurons in order to isolate these mismatch neurons were selected on the basis of the results from these lesion experiments. The implicit assumption is that these mismatch neurons were driving the role of the ACC seen in the lesion experiments, signalling a prediction-mismatch in the first visual trial to drive an attention switch in the next. The strongest evidence comes from the structure of the task, with odour prediction-mismatches seeming the earliest and clearest evidence of an odour to visual block switch, and from the significant differences in this prediction-mismatch response preceding perfect and imperfect switches. However, this project still lacks a direct causative link between the behavioural and imaging findings.

The next step to prove that these cells are responsible for the behaviour would be to selectively activate or inhibit them during behaviour, while leaving the rest of the circuit unaffected. Other members of this lab are currently using single-cell optogenetics to selectively target specific cells in the field of view, activating and inactivating depending on the opsin expressed through the population. If inactivating the mismatch cells specifically could reproduce the behavioural deficit, this would be the strongest evidence of a causal link between the prediction-mismatch signalling and the attention-switching behaviour. However, other experiments in this project have identified a few obstacles to performing this inactivation. First, the light-cue epoch (Fig 3.28) demonstrated that any light that appears only for the crucial prediction-mismatch trial can influence behaviour, without any optogenetic effects. Second, the failure of the VIP activation experiments to disrupt behaviour suggest that unilateral perturbations over the area of tissue imaged is insufficient to disrupt ACC activity as effectively as bilateral inactivation using PV cells, despite severely disrupting the mismatch cells' signalling. Inactivating just the mismatch cells within the field of view may not be widespread enough to affect behaviour. Third, identifying these cells in order to direct the optogenetic light would require same-session identification of mismatch cells. We have seen that this takes the comparison of activity over several switches, and the same cells are unlikely to remain mismatch cells over days. This means that these cells would need to be identified and silenced in the same session, which would be very difficult – the method for identification would need to be refined, so that mismatch cells can be identified after a single switch.

2. The role of the rodent ACC

Prediction-error signalling seems the explanation for the observed role of ACC in this behaviour that fits best, and seems well-represented amongst the recorded neurons. However, this is only one of the many functions of the ACC seen in primates that seems well-preserved in rodent studies. Papez associated ACC damage with a "loss of spontaneity" (Papez, 1937), while cingulotomy patients showed specific deficits in their vigour and self-initiated behaviour (Cohen et al., 2001). This translated well to rodents: ACC lesions caused a bias towards low-effort, low-reward options during decision-making (Rudebeck et al., 2006; Kashay et al., 2022). Similarly, the behavioural deficit seen during lesions in this task could be interpreted as an issue of motivation. Remaining observant for the absence of an expected stimulus, and then transitioning from not licking to licking in response to the visual gratings, would rely on the mouse being in a relatively high state of task engagement. If ACC lesions are causing a general reduction in motivation or arousal, this could also explain the asymmetrical effects on switching – the switch from a visual

block to an odour block involved the introduction of a clear and motivationally-salient odour stimulus (as the rewarded odour was the smell of the reward), so could still be accomplished despite a reduction in engagement.

The behavioural deficits that resulted from ACC lesions were only seen when silencing continued throughout the session, whether throughout the trial or just in the peri/inter-visual epochs. The failure of the one trial un-silencing epoch (Fig 3.26) to reproduce the deficit would have undermined this motivational hypothesis (as the only trial un-silenced in the prediction-mismatch trial, and motivation should be otherwise inhibited), but the fact that these experiments were performed after the inhibiting effect of any ACC silencing had receded undermines any conclusions from this epoch. These experiments would need to be repeated on different mice that had not been overtrained to test this theory. An overall deficit in task engagement may yet explain the silencing results.

This alternate explanation seems unsatisfying in terms of explaining the specific role of the ACC in the behaviour. Early lesion studies identified this general role in sustained motivation (Cohen et al., 2001), but recordings from primates and rodents suggested a more specialised role that might be itself influenced by motivational signals from other areas. Increased dACC activity during incongruent Stroop task trials (Pardo et al., 1990) was alternately interpreted as the dACC signalling the different possible responses, from a behavioural adaption and persistence perspective, or the need to calculate and allocate cognitive control for the task, as in the EVC model. Both of these could explain the behavioural deficits observed here: a failure to signal the alternate strategy for the visual stimuli (licking) or a failure to allocate control for switching attention following the switch into a visual block. However, I have not identified these signals in my analysis to date, and they do not explain the specific deficit to optimal switching into a visual block quite as well as prediction-error signalling.

It seems likely that motivation and arousal would be contributory factors to all these identified ACC functions. Future experiments could clarify this by employing projection-specific optogenetics using retrograde viruses or bouton silencing. The locus coeruleus (LC) and ventral tegmental area (VTA) are projection targets of the ACC implicated in these behaviours. The LC is implicated in arousal, and signals task engagement and behavioural adaption (Aston-Jones & Cohen, 2005; Sales et al., 2019), whose connections to the ACC mediate strategy switches in rats (Tervo et al., 2014). The VTA is a dopaminergic midbrain structure implicated in supporting reward-motivated behaviour via prediction-mismatch signalling (Arsenault et al., 2014).

If silencing connections between the LC and ACC can reproduce the switching deficit, this would suggest the ACC's role is dependent on task-engagement and noradrenergic signalling. Alternatively, if silencing connections between the ACC and VTA can reproduce this effect, it would suggest this motivational influence comes via dopaminergic signalling. Motivation is clearly fundamental for the mice in this task: their behaviour relies on food-restriction and offered rewards. Further experiments probing these projection targets and varying mice's task engagement would help understanding this relationship between the ACC's role in the task and motivation.

3. Conclusion

Determining what these results tell us about the wider role of the ACC in flexible behaviour is contingent on confirming the link between the silencing and imaging data via the suggested future experiments. However, if we assume that the ACC is essential for this prediction-mismatch signalling, which seems the most likely interpretation of the silencing data, then this project has some value to our understanding of the ACC's role in cognition, at least in mice. It has shown a specific role for the ACC, but not the PL, in signalling prediction-mismatches that are essential for specific changes in strategy. Prediction-mismatch signals have been seen in the rodent ACC before (Casado-Román et al., 2020), but to my knowledge these are the first that can predict subsequent changes in behaviour. This mirrors findings in primates, in which the dACC signals surprise only when it is informative for updating internal models of the task (O'Reilly et al., 2013). If the ACC was responding indiscriminately to prediction errors with no involvement in downstream behavioural changes, as seen in the mPFC by Casado-Román et al. (2020) and in V1 by Attinger et al. (2017), we would not expect to see this difference in activity preceding perfect and imperfect switches.

The failure of PL silencing to reproduce the effect suggests that this behaviourally-critical prediction-error signalling is exclusive to the ACC, at least amongst the mPFC. Comparisons of connectivity and function support a homology for the rodent ACC with the primate dACC, and the rodent PL and IL with the primate rvACC (van Heukelum et al., 2020). While both areas are associated with error signalling (di Pellegrino et al., 2017), similar reward-related prediction-error signalling has been attributed to the dACC (Ito et al., 2003). Prediction errors seen in the rvACC tended to occur in social tasks, when the action-outcomes to be monitored are happening to another person (Diaconescu et al., 2017). The discrepancy in prediction-error signalling supports a perspective of the rvACC tracking predictions during social interactions, while the dACC tracks predictions of one's own behaviour (Lockwood & Wittmann, 2018). This may even fit the overall compartmentalising of the ACC into cognitive dorsal and affective rostro-ventral sub-divisions

(Bush et al., 2000), with cognitive tasks typically involving the self while emotional tasks typically invoke other people. Determining whether the PL signals prediction-errors in mice would require a different task with a social component.

Regardless, what this result indicates is that the prediction-mismatch signalling required to switch from an odour block to a visual block in this task is localised to the ACC, and seemingly not other parts of the rodent mPFC or beyond. Advancing through a series of attentional episodes would require a new set of predictions in each episode, as the relevant inputs, objectives, and potential actions change. Identifying a region of the multiple-demand system that is specifically involved in signalling behaviourally-relevant prediction violations suggests that this system, like the many lower-order regions of the brain, has functional specialisations that yield a form of modularity. Rather than specialising in specific modalities of stimulus or actions, the components of the multiple-demand system may specialise in different constituents of attentional episodes: for example, with the dACC signalling expectation violations based on predictive coding from the relevant sensory region, then signalling to another region in the system to promote re-evaluation of response selection to achieve the current sub-goal.

However, this should be qualified with the caveats inherent in comparing this behaviour to complex cognition in humans. This behavioural paradigm is not an ideal model for episodic cognition, as the tasks in each block does not advance sequentially to some overall goal. Instead, mice alternate between two block types with similar stimuli, possible actions, and outcomes. The odour is the only meaningfully unpredictable stimulus, and these predictions are based upon at least 30 consecutive previous instances of odour presentation. Finding these prediction-mismatch signals in the ACC during different tasks requiring a wider variety of predictions, with different modalities and responses, would be necessary to position the rodent ACC as a crucial structure for prediction-error signalling across cognitive tasks. Even then, proving that the ACC is specifically involved in flexibly signalling prediction errors throughout attentional episodes organised hierarchically towards a larger goal may be difficult in mice, or even non-human primates.

The advantage of using mice comes with the available tools to probe circuit dynamics. The interneuron-specific insights that this project has so far yielded are reasonably small. That activating VIP interneurons disrupts prediction-mismatch signalling supports a model of prediction-error circuits relying on interneuron heterogeneity (Hertäg & Clopath, 2022). However, without more specific activation timings, knowledge of the underlying interneuron-specific contributions, or perturbations of the other sub-classes it is difficult to understand the exact role of these interneurons in the prediction-mismatch signalling. Short-term analysis to identify the

recorded neuron subtypes, and long-term experiments to perturb the other sub-classes, are required to really make use of this advantage of the choice of model organism.

It could be argued that this project has also not made best use of the choice of task. The attention-switching task used is perfectly suited to comparing how visual stimuli are processed when they are task-relevant and task-irrelevant. Before starting the project, my hypothesis was that the ACC would play a direct role in this attentional modulation of processing. ACC lesions caused deficits to focused and sustained attention in humans (Cohen et al., 1999), and to intra-dimensional set-shifts in mice (Bissonette et al., 2008). However, whether because the stimuli to be switched between were too different (Ng et al., 2007), or due to the asymmetry of the task, ACC silencing did not affect the mice's ability to sustain attention either towards or away from the visual stimuli. Instead, ACC silencing impaired their ability to change their behaviour following an experience of negative prediction-mismatch.

This was an unplanned use of the behavioural paradigm, but potentially one that it was well-suited for. The ACC seemed necessary for optimal switching following a negative surprise, but not when switching in the other direction following a positive surprise – an element that would have been missed by a symmetrical task. The block-wise structure was necessary for establishing over repeated trials the expectation of the odour: that it would appear in the odour blocks and would not appear in the visual blocks. The visual stimuli themselves then became necessary for predicting the odour in time, so that the moment of prediction-mismatch could be reliably estimated. The relative novelty of finding these prediction-mismatch signals in the ACC that predict future behavioural changes may be a result of the choice of task: able to elicit reliable negative surprise while making that surprise meaningful for adapting behaviour.

The original hypothesis that the ACC is involved in the attentional modulation of visual processing cannot be rejected, however. ACC neurons signal sustained attention in rats towards a range of modalities (Wu et al., 2017), and we have seen here that ACC neurons show consistent selectivity for the visual stimuli when they are behaviourally-relevant. The failure to see a behavioural effect of ACC silencing during stable periods of the task might instead reflect the relative easiness of the task and over-training of the mice, to the extent that the enhancement of visual selectivity seen during attention (Poort et al., 2015) is not necessary for the mouse to discriminate the gratings in the visual block, so they show no behavioural deficits in discrimination. Increasing the difficulty by making stimuli harder to distinguish would likely reveal a role for ACC in sustaining attention.

Instead, this project has demonstrated a specific role for the ACC not in sustaining attention but in triggering attentional shifts in response to prediction-mismatches. These mismatch circuits re-organise between experimental days, but the ACC retains a proportion of cells dedicated to signalling this mismatch during each session. This re-organisation demonstrates a mechanism by which these prediction-mismatch circuits could flexibly transition between attentional episodes, depending on the predictions that are relevant to that sub-goal. Similar task-switching experiments have demonstrated ACC circuit re-organisation between repeat blocks of the same task during a session (Malagon-Vina et al., 2018), so this re-assembly may be occurring even between individual instances of prediction-mismatch. Matching cells between the recorded imaging days across stages of task learning will allow further analysis to examine how the circuits are initially assembled and how they reconfigure over different extents of time.

Prediction-error signalling is just one of the many cognitive functions of the ACC that has been identified in last few decades. This project helps demonstrate how this function is preserved from humans and other primates to mice, contrary to Broca's predictions. Our understanding of the importance of this section of the cingulate cortex has progressed to a point at which it is unrecognisable from his structure "low in the intellectual hierarchy" (Broca, 1878), instead filling a variety of select but crucial roles in complex cognition. Even in mice, and even when predicting their "bestial" sense of olfaction, the ACC remains an important component for cognition.

Acknowledgements

I have been lucky enough to receive fantastic support from everyone at the CDN, and this project wouldn't have been possible without them, so outcome-dependent they should all receive credit/blame. The first person to thank is my supervisor, Adil, without whom I would never have started this project in the first place. His enthusiasm, patience, and seemingly endless reserves of knowledge about every field has been invaluable and I likely would not have finished the project without him either – as thanks I promise to this time definitely finish Strunk & White.

I'd also like to thank all the members of the Khan lab, past and present: Dylan, Matt, Fran, Filipe, Rob, Francesca, Marian, and Jade. Dylan has been a great friend and a patient presence since the very beginning, and Matt's pathological optimism and cheerfulness has helped through many tough moments. Fran's support prevented the first few years from getting too intense, and the time Filipe has spent patiently listening to me vent has been enormously appreciated. Rob and Francesca contributed substantially to this project during their time in the lab, and were both fantastic to work with. Marian's knowledge and expertise, as well as her calmness and patience, has had such a demonstrable effect on the quality of our research that I only wish she had arrived earlier to stop me making so many mistakes.

I'd like to thank my other supervisor, Matt Grubb, for always being available to help me figure out the bigger picture of the project, and for his invaluable advice and time while I have been writing up. My thesis committee, Juan Burrone and Jasper Poort, have also provided incredibly helpful feedback throughout the project.

Finally, I'd like to thank my partner Hannah for supporting me throughout the project, particularly during my intense periods of living in the lab during lockdowns and the rapid declines in both my sanity and personal hygiene during the writing up. She has been a reliable source of warmth and understanding, despite reminding me how easy she found each stage of her PhD by comparison. As I know she will have skipped to only reading this section, I put it last – thank you for everything, and whatever comes next, I look forward to doing with you.

And thank you very much for reading – I hope it wasn't as painful to read as it was to write.

REFERENCES

References

Aarts, E., & Roelofs, A. (2011). Attentional Control in Anterior Cingulate Cortex Based on Probabilistic Cueing. *Journal of Cognitive Neuroscience,* 23(3), 716–727. https://doi.org/10.1162/jocn.2010.21435

Abe, N., Greene, J. D., & Kiehl, K. A. (2018). Reduced engagement of the anterior cingulate cortex in the dishonest decision-making of incarcerated psychopaths. *Social Cognitive and Affective Neuroscience*, *13*(8), 797–807. https://doi.org/10.1093/scan/nsy050

Abler, B., Hofer, C., & Viviani, R. (2008). Habitual emotion regulation strategies and baseline brain perfusion. *NeuroReport*, *19*(1), 21–24. https://doi.org/10.1097/WNR.0b013e3282f3adeb

Achterberg, J., Kadohisa, M., Watanabe, K., Kusunoki, M., Buckley, M. J., & Duncan, J. (2022). A One-Shot Shift from Explore to Exploit in Monkey Prefrontal Cortex. *The Journal of Neuroscience*, *42*(2), 276–287. https://doi.org/10.1523/JNEUROSCI.1338-21.2021

Akam, T., Rodrigues-Vaz, I., Marcelo, I., Zhang, X., Pereira, M., Oliveira, R. F., Dayan, P., & Costa, R. M. (2021). The Anterior Cingulate Cortex Predicts Future States to Mediate Model-Based Action Selection. *Neuron*, *109*(1), 149-163.e7. https://doi.org/10.1016/j.neuron.2020.10.013

Alexander, W. H., & Brown, J. W. (2011). Medial prefrontal cortex as an action-outcome predictor. *Nature Neuroscience*, *14*(10), 1338–1344. https://doi.org/10.1038/nn.2921

Alexander, W. H., & Brown, J. W. (2019). The Role of the Anterior Cingulate Cortex in Prediction Error and Signaling Surprise. *Topics in Cognitive Science*, *11*(1), 119–135. https://doi.org/10.1111/tops.12307

Allam, A. K., Larkin, M. B., Katlowitz, K. A., Shofty, B., & Viswanathan, A. (2022). Case report: MR-guided laser induced thermal therapy for palliative cingulotomy. *Frontiers in Pain Research*, *3*, 1028424. https://doi.org/10.3389/fpain.2022.1028424

Amiez, C., Joseph, J.-P., & Procyk, E. (2005). Anterior cingulate error-related activity is modulated by predicted reward. *European Journal of Neuroscience*, *21*(12), 3447–3452. https://doi.org/10.1111/j.1460-9568.2005.04170.x

Amiez, C., & Petrides, M. (2014). Neuroimaging evidence of the anatomo-functional organization of the human cingulate motor areas. *Cerebral Cortex (New York, N.Y. : 1991)*, *24*(3), 563–578. https://doi.org/10.1093/cercor/bhs329

Arsenault, J. T., Rima, S., Stemmann, H., & Vanduffel, W. (2014). Role of the Primate Ventral Tegmental Area in Reinforcement and Motivation. *Current Biology*, *24*(12), 1347–1353. https://doi.org/10.1016/j.cub.2014.04.044

Aston-Jones, G., & Cohen, J. D. (2005). An Integrative Theory of Locus Coeruleus-Norepinephrine Function: Adaptive Gain and Optimal Performance. *Annual Review of Neuroscience*, *28*(1), 403–450. https://doi.org/10.1146/annurev.neuro.28.061604.135709

Atiani, S., David, S. V., Elgueda, D., Locastro, M., Radtke-Schuller, S., Shamma, S. A., & Fritz, J. B. (2014). Emergent selectivity for task-relevant stimuli in higher-order auditory cortex. *Neuron*, *82*(2), 486–499. https://doi.org/10.1016/j.neuron.2014.02.029

Atilgan, H., Murphy, C. E., Wang, H., Ortega, H. K., Pinto, L., & Kwan, A. C. (2022). *Change point estimation by the mouse medial frontal cortex during probabilistic reward learning* [Preprint]. Neuroscience. https://doi.org/10.1101/2022.05.26.493245

Attinger, A., Wang, B., & Keller, G. B. (2017). Visuomotor Coupling Shapes the Functional Development of Mouse Visual Cortex. *Cell*, *169*(7), 1291-1302.e14. https://doi.org/10.1016/j.cell.2017.05.023

Badre, D., & D'Esposito, M. (2009). Is the rostro-caudal axis of the frontal lobe hierarchical? *Nature Reviews Neuroscience*, *10*(9), 659–669. https://doi.org/10.1038/nrn2667

Barch, D. M., Braver, T. S., Sabb, F. W., & Noll, D. C. (2000). Anterior Cingulate and the Monitoring of Response Conflict: Evidence from an fMRI Study of Overt Verb Generation. *Journal of Cognitive Neuroscience*, *12*(2), 298–309. https://doi.org/10.1162/089892900562110

Beauregard, M., Lévesque, J., & Bourgouin, P. (2001). Neural Correlates of Conscious Self-Regulation of Emotion. *The Journal of Neuroscience*, *21*(18), RC165–RC165. https://doi.org/10.1523/JNEUROSCI.21-18-j0001.2001

Birrell, J. M., & Brown, V. J. (2000). Medial Frontal Cortex Mediates Perceptual Attentional Set Shifting in the Rat. *The Journal of Neuroscience*, *20*(11), 4320–4324. https://doi.org/10.1523/JNEUROSCI.20-11-04320.2000

Bisiach, E., & Luzzatti, C. (1978). Unilateral Neglect of Representational Space. *Cortex*, *14*(1), 129–133. https://doi.org/10.1016/S0010-9452(78)80016-1

Bissonette, G. B., Martins, G. J., Franz, T. M., Harper, E. S., Schoenbaum, G., & Powell, E. M. (2008). Double Dissociation of the Effects of Medial and Orbital Prefrontal Cortical Lesions on Attentional and Affective Shifts in Mice. *Journal of Neuroscience*, *28*(44), 11124–11130. https://doi.org/10.1523/JNEUROSCI.2820-08.2008

Bissonette, G. B., Powell, E. M., & Roesch, M. R. (2013). Neural structures underlying set-shifting: Roles of medial prefrontal cortex and anterior cingulate cortex. *Behavioural Brain Research*, *250*, 91–101. https://doi.org/10.1016/j.bbr.2013.04.037

Bliss-Moreau, E., Santistevan, A. C., Bennett, J., Moadab, G., & Amaral, D. G. (2021). Anterior Cingulate Cortex Ablation Disrupts Affective Vigor and Vigilance. *The Journal of Neuroscience*, *41*(38), 8075–8087. https://doi.org/10.1523/JNEUROSCI.0673-21.2021

Boeree, C. G. (2008). General psychology. *Jogjakarta: Prismasophie*.

Boettiger, C. A. (2005). Frontal Networks for Learning and Executing Arbitrary Stimulus-Response Associations. *Journal of Neuroscience*, *25*(10), 2723–2732. https://doi.org/10.1523/JNEUROSCI.3697-04.2005

Boorman, E. D., Rushworth, M. F., & Behrens, T. E. (2013). Ventromedial Prefrontal and Anterior Cingulate Cortex Adopt Choice and Default Reference Frames during Sequential Multi-Alternative Choice. *Journal of Neuroscience*, *33*(6), 2242–2253. https://doi.org/10.1523/JNEUROSCI.3022-12.2013

Botvinick, M. M., Braver, T. S., Barch, D. M., Carter, C. S., & Cohen, J. D. (2001). Conflict monitoring and cognitive control. *Psychological Review*, *108*(3), 624–652. https://doi.org/10.1037/0033-295x.108.3.624

Braver, T. S. (2001). Anterior Cingulate Cortex and Response Conflict: Effects of Frequency, Inhibition and Errors. *Cerebral Cortex*, *11*(9), 825–836. https://doi.org/10.1093/cercor/11.9.825

Broca, P. (n.d.). *Anatomie comparée des circonvolutions cérébrales: Le grand lobe limbique et la scissure limbique dans la série des mammifères*.

Broca, P. (1861). Remarks on the seat of the faculty of articulated language, following an observation of aphemia (loss of speech). *Bulletin de La Société Anatomique*, *6*, 330–357.

Brown, J. W. (2009). Multiple cognitive control effects of error likelihood and conflict. *Psychological Research Psychologische Forschung*, *73*(6), 744–750. https://doi.org/10.1007/s00426-008-0198-7

Brown, J. W., & Braver, T. S. (2005). Learned Predictions of Error Likelihood in the Anterior Cingulate Cortex. *Science*, *307*(5712), 1118–1121. https://doi.org/10.1126/science.1105783

Brown, V. J., & Bowman, E. M. (2002). Rodent models of prefrontal cortical function. *Trends in Neurosciences*, *25*(7), 340–343. https://doi.org/10.1016/S0166-2236(02)02164-1

Bryden, D. W., Johnson, E. E., Tobia, S. C., Kashtelyan, V., & Roesch, M. R. (2011). Attention for Learning Signals in Anterior Cingulate Cortex. *Journal of Neuroscience*, *31*(50), 18266–18274. https://doi.org/10.1523/JNEUROSCI.4715-11.2011

Buckley, M. J., Mansouri, F. A., Hoda, H., Mahboubi, M., Browning, P. G. F., Kwok, S. C., Phillips, A., & Tanaka, K. (2009). Dissociable Components of Rule-Guided Behavior Depend on Distinct Medial and Prefrontal Regions. *Science*, *325*(5936), 52–58. https://doi.org/10.1126/science.1172377

Bunge, S. A., Hazeltine, E., Scanlon, M. D., Rosen, A. C., & Gabrieli, J. D. E. (2002). Dissociable Contributions of Prefrontal and Parietal Cortices to Response Selection. *NeuroImage*, *17*(3), 1562–1571. https://doi.org/10.1006/nimg.2002.1252

Burton, H., Abend, N. S., MacLeod, A. M., Sinclair, R. J., Snyder, A. Z., & Raichle, M. E. (1999). Tactile attention tasks enhance activation in somatosensory regions of parietal cortex: A positron emission tomography study. *Cerebral Cortex (New York, N.Y. : 1991)*, *9*(7), 662–674. https://doi.org/10.1093/cercor/9.7.662

Bush, G., Luu, P., & Posner, M. I. (2000). Cognitive and emotional influences in anterior cingulate cortex. *Trends in Cognitive Sciences*, *4*(6), 215–222. https://doi.org/10.1016/S1364-6613(00)01483-2

Bush, G., Whalen, P. J., Rosen, B. R., Jenike, M. A., McInerney, S. C., & Rauch, S. L. (1998). The counting stroop: An interference task specialized for functional neuroimaging—Validation study with functional MRI. *Human Brain Mapping*, *6*(4), 270–282. https://doi.org/10.1002/(SICI)1097-0193(1998)6:4<270::AID-HBM6>3.0.CO;2-0

Calderazzo, S. M., Busch, S. E., Moore, T. L., Rosene, D. L., & Medalla, M. (2021). Distribution and overlap of entorhinal, premotor, and amygdalar connections in the monkey anterior cingulate cortex. *Journal of Comparative Neurology*, *529*(4), 885–904. https://doi.org/10.1002/cne.24986

Camille, N., Tsuchida, A., & Fellows, L. K. (2011). Double Dissociation of Stimulus-Value and Action-Value Learning in Humans with Orbitofrontal or Anterior Cingulate Cortex Damage. *Journal of Neuroscience*, *31*(42), 15048–15052. https://doi.org/10.1523/JNEUROSCI.3164-11.2011

Cardin, J. A., Carlén, M., Meletis, K., Knoblich, U., Zhang, F., Deisseroth, K., Tsai, L.-H., & Moore, C. I. (2009). Driving fast-spiking cells induces gamma rhythm and controls sensory responses. *Nature*, *459*(7247), 663–667. https://doi.org/10.1038/nature08002

Carter, C. S., Macdonald, A. M., Botvinick, M., Ross, L. L., Stenger, V. A., Noll, D., & Cohen, J. D. (2000). Parsing executive processes: Strategic vs. evaluative functions of the anterior cingulate cortex. *Proceedings of the National Academy of Sciences*, *97*(4), 1944–1948. https://doi.org/10.1073/pnas.97.4.1944

Carter, C. S., Mintun, M., Nichols, T., & Cohen, J. D. (1997). Anterior Cingulate Gyrus Dysfunction and Selective Attention Deficits in Schizophrenia: [15O]H2O PET Study During Single-Trial Stroop Task Performance. *American Journal of Psychiatry*, *154*(12), 1670–1675. https://doi.org/10.1176/ajp.154.12.1670

Casado-Román, L., Carbajal, G. V., Pérez-González, D., & Malmierca, M. S. (2020). Prediction error signaling explains neuronal mismatch responses in the medial prefrontal cortex. *PLOS Biology*, *18*(12), e3001019. https://doi.org/10.1371/journal.pbio.3001019

Chen, T.-W., Wardill, T. J., Sun, Y., Pulver, S. R., Renninger, S. L., Baohan, A., Schreiter, E. R., Kerr, R. A., Orger, M. B., Jayaraman, V., Looger, L. L., Svoboda, K., & Kim, D. S. (2013). Ultrasensitive fluorescent proteins for imaging neuronal activity. *Nature*, *499*(7458), 295–300. https://doi.org/10.1038/nature12354

Clarke, H. F., Dalley, J. W., Crofts, H. S., Robbins, T. W., & Roberts, A. C. (2004). Cognitive Inflexibility After Prefrontal Serotonin Depletion. *Science*, *304*(5672), 878–880. https://doi.org/10.1126/science.1094987

Cohen, R. A. (2014). *The Neuropsychology of Attention*. Springer US. https://doi.org/10.1007/978-0-387-72639-7

Cohen, R. A., Kaplan, R. F., Zuffante, P., Moser, D. J., Jenkins, M. A., Salloway, S., & Wilkinson, H. (1999). Alteration of Intention and Self-Initiated Action Associated With Bilateral Anterior Cingulotomy. *J Neuropsychiatry Clin Neurosci*, 10.

Cohen, R. A., Paul, R., Zawacki, T. M., Moser, D. J., Sweet, L., & Wilkinson, H. (2001). Emotional and personality changes following cingulotomy. *Emotion*, *1*, 38–50. https://doi.org/10.1037/1528-3542.1.1.38

Crittenden, B. M., & Duncan, J. (2014). Task Difficulty Manipulation Reveals Multiple Demand Activity but no Frontal Lobe Hierarchy. *Cerebral Cortex*, *24*(2), 532–540. https://doi.org/10.1093/cercor/bhs333

Curtis, C. E., Cole, M. W., Rao, V. Y., & D'Esposito, M. (2005). Canceling Planned Action: An fMRI Study of Countermanding Saccades. *Cerebral Cortex*, *15*(9), 1281–1289. https://doi.org/10.1093/cercor/bhi011

Dan, Y., Atick, J. J., & Reid, R. C. (1996). Efficient Coding of Natural Scenes in the Lateral Geniculate Nucleus: Experimental Test of a Computational Theory. *The Journal of Neuroscience*, *16*(10), 3351–3362. https://doi.org/10.1523/JNEUROSCI.16-10-03351.1996

Daniel, R., & Pollmann, S. (2014). A universal role of the ventral striatum in reward-based learning: Evidence from human studies. *Neurobiology of Learning and Memory*, *114*, 90–100. https://doi.org/10.1016/j.nlm.2014.05.002

Deecke, L., Scheid, P., & Kornhuber, HansH. (1969). Distribution of readiness potential, pre-motion positivity, and motor potential of the human cerebral cortex preceding voluntary finger movements. *Experimental Brain Research*, *7*(2). https://doi.org/10.1007/BF00235441

Delatour, B., & Gisquet-Verrier, P. (2000). Functional role of rat prelimbic-infralimbic cortices in spatial memory: Evidence for their involvement in attention and behavioural flexibility. *Behavioural Brain Research*, *109*(1), 113–128. https://doi.org/10.1016/S0166-4328(99)00168-0

Devinsky, O., Morrell, M. J., & Vogt, B. A. (1995). Contributions of anterior cingulate cortex to behaviour. *Brain*, *118*(1), 279–306. https://doi.org/10.1093/brain/118.1.279

di Pellegrino, G., Ciaramelli, E., & Làdavas, E. (2007). The Regulation of Cognitive Control following Rostral Anterior Cingulate Cortex Lesion in Humans. *Journal of Cognitive Neuroscience*, *19*(2), 275–286. https://doi.org/10.1162/jocn.2007.19.2.275

Diaconescu, A. O., Mathys, C., Weber, L. A. E., Kasper, L., Mauer, J., & Stephan, K. E. (2017). Hierarchical prediction errors in midbrain and septum during social learning. *Social Cognitive and Affective Neuroscience*, *12*(4), 618–634. https://doi.org/10.1093/scan/nsw171

Dodla, R., Svirskis, G., & Rinzel, J. (2006). Well-Timed, Brief Inhibition Can Promote Spiking: Postinhibitory Facilitation. *Journal of Neurophysiology*, *95*(4), 2664–2677. https://doi.org/10.1152/jn.00752.2005

Dombeck, D. A., Harvey, C. D., Tian, L., Looger, L. L., & Tank, D. W. (2010). Functional imaging of hippocampal place cells at cellular resolution during virtual navigation. *Nature Neuroscience*, *13*(11), 1433–1440. https://doi.org/10.1038/nn.2648

Driscoll, L. N., Pettit, N. L., Minderer, M., Chettih, S. N., & Harvey, C. D. (2017). Dynamic Reorganization of Neuronal Activity Patterns in Parietal Cortex. *Cell*, *170*(5), 986-999.e16. https://doi.org/10.1016/j.cell.2017.07.021

Duncan, J. (2001). An adaptive coding model of neural function in prefrontal cortex. *Nature Reviews Neuroscience*, *2*(11), 820–829. https://doi.org/10.1038/35097575

Duncan, J. (2010a). The multiple-demand (MD) system of the primate brain: Mental programs for intelligent behaviour. *Trends in Cognitive Sciences*, *14*(4), 172–179. https://doi.org/10.1016/j.tics.2010.01.004

Duncan, J. (2010b). How Intelligence Happens. *Yale University Press,* 1–244.

Duncan, J. (2013). The Structure of Cognition: Attentional Episodes in Mind and Brain. *Neuron*, *80*(1), 35–50. https://doi.org/10.1016/j.neuron.2013.09.015

Durstewitz, D., Vittoz, N. M., Floresco, S. B., & Seamans, J. K. (2010). Abrupt Transitions between Prefrontal Neural Ensemble States Accompany Behavioral Transitions during Rule Learning. *Neuron*, *66*(3), 438–448. https://doi.org/10.1016/j.neuron.2010.03.029

Durston, S. (2003). Parametric manipulation of conflict and response competition using rapid mixed-trial event-related fMRI. *NeuroImage*, *20*(4), 2135–2141. https://doi.org/10.1016/j.neuroimage.2003.08.004

Durston, S., Thomas, K. M., Worden, M. S., Yang, Y., & Casey, B. J. (2002). The Effect of Preceding Context on Inhibition: An Event-Related fMRI Study. *NeuroImage*, *16*(2), 449–453. https://doi.org/10.1006/nimg.2002.1074

Ebitz, R. B., & Hayden, B. Y. (2016). Dorsal anterior cingulate: A Rorschach test for cognitive neuroscience. *Nature Neuroscience*, *19*(10), 1278–1279. https://doi.org/10.1038/nn.4387

Elston, T. W., Croy, E., & Bilkey, D. K. (2019). Communication between the Anterior Cingulate Cortex and Ventral Tegmental Area during a Cost-Benefit Reversal Task. *Cell Reports*, *26*(9), 2353-2361.e3. https://doi.org/10.1016/j.celrep.2019.01.113

Euston, D. R., & McNaughton, B. L. (2006). Apparent Encoding of Sequential Context in Rat Medial Prefrontal Cortex Is Accounted for by Behavioral Variability. *Journal of Neuroscience*, *26*(51), 13143–13155. https://doi.org/10.1523/JNEUROSCI.3803-06.2006

Fiorillo, C. D., Newsome, W. T., & Schultz, W. (2008). The temporal precision of reward prediction in dopamine neurons. *NATURE NEUROSCIENCE*, *11*(8), 8.

Fisher, R. A. (1921). On the Probable Error of a Coefficient of Correlation Deduced from a Small Sample. *Metron*, 1, 3-32.

Freedman, D. J., Riesenhuber, M., Poggio, T., & Miller, E. K. (2001). Categorical representation of visual stimuli in the primate prefrontal cortex. *Science*, *291*(5502), 312–316. https://doi.org/10.1126/science.291.5502.312

Freidin, E., & Kacelnik, A. (2011). Rational Choice, Context Dependence, and the Value of Information in European Starlings (Sturnus vulgaris). *Science*, *334*(6058), 1000–1002. https://doi.org/10.1126/science.1209626

Friston, K. (2010). The free-energy principle: A unified brain theory? *Nature Reviews Neuroscience*, *11*(2), 127–138. https://doi.org/10.1038/nrn2787

Frith, C. D., Friston, K., Liddle, P. F., & Frackowiak, R. S. J. (1991). Willed action and the prefrontal cortex in man: A study with PET. *Proceedings of the Royal Society of London. Series B: Biological Sciences*, *244*(1311), 241–246. https://doi.org/10.1098/rspb.1991.0077

Gehring, W. J., Goss, B., Coles, M. G. H., Meyer, D. E., & Donchin, E. (2018). The Error-Related Negativity. *Perspectives on Psychological Science*, *13*(2), 200–204. https://doi.org/10.1177/1745691617715310

Gerraty, X. R. T., Davidow, J. Y., Wimmer, X. G. E., Kahn, I., & Shohamy, D. (n.d.). *Transfer of Learning Relates to Intrinsic Connectivity between Hippocampus, Ventromedial Prefrontal Cortex, and Large-Scale Networks*. 7.

Gregoriou, G. G., Rossi, A. F., Ungerleider, L. G., & Desimone, R. (2014). Lesions of prefrontal cortex reduce attentional modulation of neuronal responses and synchrony in V4. *Nature Neuroscience*, *17*(7), 1003–1011. https://doi.org/10.1038/nn.3742

Hadland, K. A., Rushworth, M. F. S., Gaffan, D., & Passingham, R. E. (2003). The Anterior Cingulate and Reward-Guided Selection of Actions. *Journal of Neurophysiology*, *89*(2), 1161–1164. https://doi.org/10.1152/jn.00634.2002

Hauber, W., & Sommer, S. (2009). Prefrontostriatal circuitry regulates effort-related decision making. *Cerebral Cortex (New York, N.Y. : 1991)*, *19*(10), 2240–2247. https://doi.org/10.1093/cercor/bhn241

Hayden, B. Y., Pearson, J. M., & Platt, M. L. (2011). Neuronal basis of sequential foraging decisions in a patchy environment. *Nature Neuroscience*, *14*(7), 933–939. https://doi.org/10.1038/nn.2856

Hertäg, L., & Clopath, C. (2022). Prediction-error neurons in circuits with multiple neuron types: Formation, refinement, and functional implications. *Proceedings of the National Academy of Sciences*, *119*(13), e2115699119. https://doi.org/10.1073/pnas.2115699119

Hillman, K. L., & Bilkey, D. K. (2012). Neural encoding of competitive effort in the anterior cingulate cortex. *Nature Neuroscience*, *15*(9), 1290–1297. https://doi.org/10.1038/nn.3187

Hohwy, J., Roepstorff, A., & Friston, K. (2008). Predictive coding explains binocular rivalry: An epistemological review. *Cognition*, *108*(3), 687–701. https://doi.org/10.1016/j.cognition.2008.05.010

Holroyd, C. B. (2013). Theories of anterior cingulate cortex function: Opportunity cost. Behavioral and Brain Sciences, 36(6), 693–694. Cambridge Core. https://doi.org/10.1017/S0140525X13001052

Holroyd, C. B., & Yeung, N. (2012). Motivation of extended behaviors by anterior cingulate cortex. *Trends in Cognitive Sciences*, *16*(2), 122–128. https://doi.org/10.1016/j.tics.2011.12.008

Hu, Y., van Wingerden, M., Sellitto, M., Schäble, S., & Kalenscher, T. (2021). Anterior Cingulate Cortex Lesions Abolish Budget Effects on Effort-Based Decision-Making in Rat Consumers. *The Journal of Neuroscience*, *41*(20), 4448–4460. https://doi.org/10.1523/JNEUROSCI.2541-20.2021

Hvoslef-Eide, M., Nilsson, S. R. O., Hailwood, J. M., Robbins, T. W., Saksida, L. M., Mar, A. C., & Bussey, T. J. (2018). Effects of anterior cingulate cortex lesions on a continuous performance task for mice. *Brain and Neuroscience Advances*, *2*, 239821281877296. https://doi.org/10.1177/2398212818772962

Hyman, J. M., Holroyd, C. B., & Seamans, J. K. (2017). A Novel Neural Prediction Error Found in Anterior Cingulate Cortex Ensembles. *Neuron*, *95*(2), 447-456.e3. https://doi.org/10.1016/j.neuron.2017.06.021

Ito, S., Stuphorn, V., Brown, J. W., & Schall, J. D. (2003). Performance monitoring by the anterior cingulate cortex during saccade countermanding. *Science (New York, N.Y.)*, *302*(5642), 120–122. https://doi.org/10.1126/science.1087847

Jahn, A., Nee, D. E., Alexander, W. H., & Brown, J. W. (2014). Distinct regions of anterior cingulate cortex signal prediction and outcome evaluation. *NeuroImage*, *95*, 80–89. https://doi.org/10.1016/j.neuroimage.2014.03.050

Janer, K. W., & Pardo, J. V. (1991). Deficits in Selective Attention Following Bilateral Anterior Cingulotomy. *Journal of Cognitive Neuroscience*, *3*(3), 231–241. https://doi.org/10.1162/jocn.1991.3.3.231

JANSEN, J. J., ANDERSEN, P., & KAADA, B. R. (1955). Subcortical mechanisms in the searching or attention response elicited by prefrontal cortical stimulation in unanesthetized cats. *The Yale Journal of Biology and Medicine*, *28*(3–4), 331–341.

Jehee, J. F. M., Rothkopf, C., Beck, J. M., & Ballard, D. H. (2006). Learning receptive fields using predictive feedback. *Journal of Physiology-Paris*, *100*(1–3), 125–132. https://doi.org/10.1016/j.jphysparis.2006.09.011

Jessup, R. K., Busemeyer, J. R., & Brown, J. W. (2010). Error Effects in Anterior Cingulate Cortex Reverse when Error Likelihood Is High. *Journal of Neuroscience*, *30*(9), 3467–3472. https://doi.org/10.1523/JNEUROSCI.4130-09.2010

Jhang, J., Lee, H., Kang, M. S., Lee, H.-S., Park, H., & Han, J.-H. (2018). Anterior cingulate cortex and its input to the basolateral amygdala control innate fear response. *Nature Communications*, *9*(1), 2744. https://doi.org/10.1038/s41467-018-05090-y

Jimeno, A. L., & Paniagua, J. L. (1969). [The gyrus cinguli and aggressivity]. *Actas luso-espanolas de neurologia y psiquiatria*, *28*(4), 289–298.

Kahn, J. B., Ward, R. D., Kahn, L. W., Rudy, N. M., Kandel, E. R., Balsam, P. D., & Simpson, E. H. (2012). Medial prefrontal lesions in mice impair sustained attention but spare maintenance of information in working memory. *Learning & Memory*, *19*(11), 513–517. https://doi.org/10.1101/lm.026302.112

Kane, G. A., James, M. H., Shenhav, A., Daw, N. D., Cohen, J. D., & Aston-Jones, G. (2022). Rat Anterior Cingulate Cortex Continuously Signals Decision Variables in a Patch Foraging Task. *The Journal of Neuroscience*, *42*(29), 5730–5744. https://doi.org/10.1523/JNEUROSCI.1940-21.2022

Karlsson, M. P., Tervo, D. G. R., & Karpova, A. Y. (2012). Network Resets in Medial Prefrontal Cortex Mark the Onset of Behavioral Uncertainty. *Science*, *338*(6103), 135–139. https://doi.org/10.1126/science.1226518

Kashay, A. Q., Cheung, J. Y., Vaknalli, R. N., Delaney, M. J., Navarro, M. B., Neuwirth, M. E., & Wilke, S. A. (2022). *Neural activity in the anterior cingulate cortex is required for effort-based decision making* [Preprint]. Neuroscience. https://doi.org/10.1101/2022.03.22.485350

Kennerley, S. W., Behrens, T. E. J., & Wallis, J. D. (2011). Double dissociation of value computations in orbitofrontal and anterior cingulate neurons. *Nature Neuroscience*, *14*(12), 1581–1589. https://doi.org/10.1038/nn.2961

Kennerley, S. W., Dahmubed, A. F., Lara, A. H., & Wallis, J. D. (2009). Neurons in the Frontal Lobe Encode the Value of Multiple Decision Variables. *Journal of Cognitive Neuroscience*, *21*(6), 1162–1178. https://doi.org/10.1162/jocn.2009.21100

Kennerley, S. W., Walton, M. E., Behrens, T. E. J., Buckley, M. J., & Rushworth, M. F. S. (2006). Optimal decision making and the anterior cingulate cortex. *Nature Neuroscience*, *9*(7), 940–947. https://doi.org/10.1038/nn1724

Kepecs, A., & Fishell, G. (2014). Interneuron cell types are fit to function. *Nature*, *505*(7483), 318–326. https://doi.org/10.1038/nature12983

Khan, A. G., Poort, J., Chadwick, A., Blot, A., Sahani, M., Mrsic-Flogel, T. D., & Hofer, S. B. (2018). Distinct learning-induced changes in stimulus selectivity and interactions of {GABAergic} interneuron classes in visual cortex. *Nature Neuroscience*, *21*(6), 851–859. https://doi.org/10.1038/s41593-018-0143-z

Kim, C., Johnson, N. F., Cilles, S. E., & Gold, B. T. (2011). Common and Distinct Mechanisms of Cognitive Flexibility in Prefrontal Cortex. *Journal of Neuroscience*, *31*(13), 4771–4779. https://doi.org/10.1523/JNEUROSCI.5923-10.2011

Kim, D., Jeong, H., Lee, J., Ghim, J.-W., Her, E. S., Lee, S.-H., & Jung, M. W. (2016). Distinct Roles of Parvalbumin- and Somatostatin-Expressing Interneurons in Working Memory. *Neuron*, *92*(4), 902–915. https://doi.org/10.1016/j.neuron.2016.09.023

Kok, P., Failing, M. F., & de Lange, F. P. (2014). Prior expectations evoke stimulus templates in the primary visual cortex. *Journal of Cognitive Neuroscience*, *26*(7), 1546–1554. https://doi.org/10.1162/jocn_a_00562

Kolling, N., Behrens, T. E. J., Mars, R. B., & Rushworth, M. F. S. (2012). Neural Mechanisms of Foraging. *Science*, *336*(6077), 95–98. https://doi.org/10.1126/science.1216930

Kolling, N., Wittmann, M. K., Behrens, T. E. J., Boorman, E. D., Mars, R. B., & Rushworth, M. F. S. (2016). Value, search, persistence and model updating in anterior cingulate cortex. *Nature Neuroscience*, *19*(10), 1280–1285. https://doi.org/10.1038/nn.4382

Kosaki, Y., & Watanabe, S. (2012). Dissociable roles of the medial prefrontal cortex, the anterior cingulate cortex, and the hippocampus in behavioural flexibility revealed by serial reversal of three-choice discrimination in rats. *Behavioural Brain Research*, *227*(1), 81–90. https://doi.org/10.1016/j.bbr.2011.10.039

Kuchibhotla, K. V., Gill, J. V., Lindsay, G. W., Papadoyannis, E. S., Field, R. E., Sten, T. A. H., Miller, K. D., & Froemke, R. C. (2017). Parallel processing by cortical inhibition enables context-dependent behavior. *Nature Neuroscience*, *20*(1), 62–71. https://doi.org/10.1038/nn.4436

Kvitsiani, D., Ranade, S., Hangya, B., Taniguchi, H., Huang, J. Z., & Kepecs, & A. (2013). *Distinct behavioural and network correlates of two interneuron types in prefrontal cortex*. https://doi.org/10.1038/nature12176

Lak, A., Okun, M., Moss, M., Gurnani, H., Wells, M. J., Reddy, C. B., Harris, K. D., & Carandini, M. (2018). *Dopaminergic and frontal signals for decisions guided by sensory evidence and reward value*. https://doi.org/10.1101/411413

Lapish, C. C., Durstewitz, D., Chandler, L. J., & Seamans, J. K. (2008). Successful choice behavior is associated with distinct and coherent network states in anterior cingulate cortex. *Proceedings of the National Academy of Sciences*, *105*(33), 11963–11968. https://doi.org/10.1073/pnas.0804045105

Laubach, M., Amarante, L. M., Swanson, K., & White, S. R. (2018). What, If Anything, Is Rodent Prefrontal Cortex? *Eneuro*, *5*(5), ENEURO.0315-18.2018. https://doi.org/10.1523/ENEURO.0315-18.2018

Le Merre, P., Ährlund-Richter, S., & Carlén, M. (2021). The mouse prefrontal cortex: Unity in diversity. *Neuron*, *109*(12), 1925–1944. https://doi.org/10.1016/j.neuron.2021.03.035

Lee, J.-Y., You, T., Lee, C.-H., Im, G. H., Seo, H., Woo, C.-W., & Kim, S.-G. (2022). Role of anterior cingulate cortex inputs to periaqueductal gray for pain avoidance. *Current Biology*, *32*(13), 2834-2847.e5. https://doi.org/10.1016/j.cub.2022.04.090

Lee, T. S., & Mumford, D. (2003). Hierarchical Bayesian inference in the visual cortex. *Journal of the Optical Society of America A*, *20*(7), 1434–1448. https://doi.org/10.1364/JOSAA.20.001434

Li, F., Li, M., Cao, W., Xu, Y., Luo, Y., Zhong, X., Zhang, J., Dai, R., Zhou, X.-F., Li, Z., & Li, C. (2012). Anterior cingulate cortical lesion attenuates food foraging in rats. *Brain Research Bulletin*, *88*(6), 602–608. https://doi.org/10.1016/j.brainresbull.2012.05.015

Li, N., Chen, S., Guo, Z. V., Chen, H., Huo, Y., Inagaki, H. K., Chen, G., Davis, C., Hansel, D., Guo, C., & Svoboda, K. (2019). Spatiotemporal constraints on optogenetic inactivation in cortical circuits. *ELife*, *8*, e48622. https://doi.org/10.7554/eLife.48622

Lockwood, P. L., & Wittmann, M. K. (2018). Ventral anterior cingulate cortex and social decision-making. *Neuroscience & Biobehavioral Reviews*, *92*, 187–191. https://doi.org/10.1016/j.neubiorev.2018.05.030

Long, C. J., Pueschel, K., & Hunter, S. E. (1978). Assessment of the effects of cinglulate gyrus lesions by neuropsychological techniques. *Journal of Neurosurgery*, *49*(2), 264–271. https://doi.org/10.3171/jns.1978.49.2.0264

Low, R. J., Gu, Y., & Tank, D. W. (2014). Cellular resolution optical access to brain regions in fissures: Imaging medial prefrontal cortex and grid cells in entorhinal cortex. *Proceedings of the National Academy of Sciences*, *111*(52), 18739–18744. https://doi.org/10.1073/pnas.1421753111

Magno, E. (2006). The Anterior Cingulate and Error Avoidance. *Journal of Neuroscience*, *26*(18), 4769–4773. https://doi.org/10.1523/JNEUROSCI.0369-06.2006

Magno, E., Simões-Franklin, C., Robertson, I. H., & Garavan, H. (2009). The Role of the Dorsal Anterior Cingulate in Evaluating Behavior for Achieving Gains and Avoiding Losses. *Journal of Cognitive Neuroscience*, *21*(12), 2328–2342. https://doi.org/10.1162/jocn.2008.21169

Makino, H., & Komiyama, T. (2015). Learning enhances the relative impact of top-down processing in the visual cortex. *Nature Neuroscience*, *18*(8), 1116–1122. https://doi.org/10.1038/nn.4061

Malagon-Vina, H., Ciocchi, S., Passecker, J., Dorffner, G., & Klausberger, T. (2018). Fluid network dynamics in the prefrontal cortex during multiple strategy switching. *Nature Communications*, *9*(1), 1–13. https://doi.org/10.1038/s41467-017-02764-x

Marton, T., Seifikar, H., Luongo, F. J., Lee, A. T., & Sohal, V. S. (2018). Roles of prefrontal cortex and mediodorsal thalamus in task engagement and behavioral flexibility. *The Journal of Neuroscience*, 1728–17. https://doi.org/10.1523/JNEUROSCI.1728-17.2018

Mashhoori, A., Hashemnia, S., McNaughton, B. L., Euston, D. R., & Gruber, A. J. (2018). Rat anterior cingulate cortex recalls features of remote reward locations after disfavoured reinforcements. *ELife*, *7*, e29793. https://doi.org/10.7554/eLife.29793

Matsumoto, M., Matsumoto, K., Abe, H., & Tanaka, K. (2007). Medial prefrontal cell activity signaling prediction errors of action values. *Nature Neuroscience*, *10*(5), 647–656. https://doi.org/10.1038/nn1890

McGeorge, A. J., & Faull, R. L. M. (1989). The organization of the projection from the cerebral cortex to the striatum in the rat. *Neuroscience*, *29*(3), 503–537. https://doi.org/10.1016/0306-4522(89)90128-0

McGuire, J. T., & Botvinick, M. M. (2010). Prefrontal cortex, cognitive control, and the registration of decision costs. *Proceedings of the National Academy of Sciences*, *107*(17), 7922–7926. https://doi.org/10.1073/pnas.0910662107

McKee, B. L., Kelley, A. E., Moser, H. R., & Andrzejewski, M. E. (2010). Operant learning requires NMDA-receptor activation in the anterior cingulate cortex and dorsomedial striatum, but not in the orbitofrontal cortex. *Behavioral Neuroscience*, *124*(4), 500–509. https://doi.org/10.1037/a0020270

Medalla, M., Chang, W., Ibañez, S., Guillamon-Vivancos, T., Nittmann, M., Kapitonava, A., Busch, S. E., Moore, T. L., Rosene, D. L., & Luebke, J. I. (2022). Layer-specific pyramidal neuron properties underlie diverse anterior cingulate cortical motor and limbic networks. *Cerebral Cortex*, *32*(10), 2170–2196. https://doi.org/10.1093/cercor/bhab347

Menon, V., Adleman, N. E., White, C. D., Glover, G. H., & Reiss, A. L. (2001). Error-related brain activation during a Go/NoGo response inhibition task. *Human Brain Mapping*, *12*(3), 131–143. https://doi.org/10.1002/1097-0193(200103)12:3<131::AID-HBM1010>3.0.CO;2-C

Miltner, W. H., Braun, C. H., & Coles, M. G. (1997). Event-related brain potentials following incorrect feedback in a time-estimation task: Evidence for a 'generic' neural system for error detection. *Journal of Cognitive Neuroscience*, *9*(6), 788–798. https://doi.org/10.1162/jocn.1997.9.6.788

Mohanty, A., Engels, A. S., Herrington, J. D., Heller, W., Ringo Ho, M.-H., Banich, M. T., Webb, A. G., Warren, S. L., & Miller, G. A. (2007). Differential engagement of anterior cingulate cortex subdivisions for cognitive and emotional function. *Psychophysiology*, 44(3), 343–351. https://doi.org/10.1111/j.1469-8986.2007.00515.x

Morris, R. W., Dezfouli, A., Griffiths, K. R., Le Pelley, M. E., & Balleine, B. W. (2022). The Neural Bases of Action-Outcome Learning in Humans. *The Journal of Neuroscience*, *42*(17), 3636–3647. https://doi.org/10.1523/JNEUROSCI.1079-21.2022

Muckli, L., Kohler, A., Kriegeskorte, N., & Singer, W. (2005). Primary Visual Cortex Activity along the Apparent-Motion Trace Reflects Illusory Perception. *PLoS Biology*, *3*(8), e265. https://doi.org/10.1371/journal.pbio.0030265

Nakamura, K., Roesch, M. R., & Olson, C. R. (2005). Neuronal Activity in Macaque SEF and ACC During Performance of Tasks Involving Conflict. *Journal of Neurophysiology*, *93*(2), 884–908. https://doi.org/10.1152/jn.00305.2004

Navawongse, R., & Eichenbaum, H. (2013). Distinct Pathways for Rule-Based Retrieval and Spatial Mapping of Memory Representations in Hippocampal Neurons. *Journal of Neuroscience*, *33*(3), 1002–1013. https://doi.org/10.1523/JNEUROSCI.3891-12.2013

Ng, C.-W., Noblejas, M. I., Rodefer, J. S., Smith, C. B., & Poremba, A. (2007). Double Dissociation of Attentional Resources: Prefrontal Versus Cingulate Cortices. *Journal of Neuroscience*, *27*(45), 12123–12131. https://doi.org/10.1523/JNEUROSCI.2745-07.2007

Nguyen, H. N., Huppé-Gourgues, F., & Vaucher, E. (2015). Activation of the mouse primary visual cortex by medial prefrontal subregion stimulation is not mediated by cholinergic basalo-cortical projections. *Frontiers in Systems Neuroscience*, *9*(FEB). https://doi.org/10.3389/fnsys.2015.00001

O'Connor, D. H., Hires, S. A., Guo, Z. V., Li, N., Yu, J., Sun, Q.-Q., Huber, D., & Svoboda, K. (2013). Neural coding during active somatosensation revealed using illusory touch. *Nature Neuroscience*, *16*(7), 958–965. https://doi.org/10.1038/nn.3419

Oemisch, M., Westendorff, S., Azimi, M., Hassani, S. A., Ardid, S., Tiesinga, P., & Womelsdorf, T. (2019). Feature-specific prediction errors and surprise across macaque fronto-striatal circuits. *Nature Communications*, *10*(1), 176. https://doi.org/10.1038/s41467-018-08184-9

Oliveira, F. T. P., McDonald, J. J., & Goodman, D. (2007). Performance monitoring in the anterior cingulate is not all error related: Expectancy deviation and the representation of action-outcome associations. *Journal of Cognitive Neuroscience*, *19*(12), 1994–2004. https://doi.org/10.1162/jocn.2007.19.12.1994

Olofsson, J. K., Ekström, I., Lindström, J., Syrjänen, E., Stigsdotter-Neely, A., Nyberg, L., Jonsson, S., & Larsson, M. (2020). Smell-Based Memory Training: Evidence of Olfactory Learning and Transfer to the Visual Domain. *Chemical Senses*, *45*(7), 593–600. https://doi.org/10.1093/chemse/bjaa049

O'Reilly, J. X., Schüffelgen, U., Cuell, S. F., Behrens, T. E. J., Mars, R. B., & Rushworth, M. F. S. (2013). Dissociable effects of surprise and model update in parietal and anterior cingulate cortex. *Proceedings of the National Academy of Sciences*, *110*(38). https://doi.org/10.1073/pnas.1305373110

Oualian, C., & Gisquet-Verrier, P. (2010). The differential involvement of the prelimbic and infralimbic cortices in response conflict affects behavioral flexibility in rats trained in a new automated strategy-switching task. *Learning & Memory*, *17*(12), 654–668. https://doi.org/10.1101/lm.1858010

Pachitariu, M., Stringer, C., Dipoppa, M., Schröder, S., Rossi, L. F., Dalgleish, H., Carandini, M., & Harris, K. D. (2016). *Suite2p: Beyond 10,000 neurons with standard two-photon microscopy* [Preprint]. Neuroscience. https://doi.org/10.1101/061507

Palmer, E. D., Rosen, H. J., Ojemann, J. G., Buckner, R. L., Kelley, W. M., & Petersen, S. E. (2001). An Event-Related fMRI Study of Overt and Covert Word Stem Completion. *NeuroImage*, *14*(1), 182–193. https://doi.org/10.1006/nimg.2001.0779

Paneri, S., & Gregoriou, G. G. (2017). Top-Down Control of Visual Attention by the Prefrontal Cortex. Functional Specialization and Long-Range Interactions. *Frontiers in Neuroscience*, *11*, 545. https://doi.org/10.3389/fnins.2017.00545

Papez, J. W. (1937). A PROPOSED MECHANISM OF EMOTION. *Archives of Neurology And Psychiatry*, *38*(4), 725. https://doi.org/10.1001/archneurpsyc.1937.02260220069003

Pardo, J. V., Pardo, P. J., Janer, K. W., & Raichle, M. E. (1990). The anterior cingulate cortex mediates processing selection in the Stroop attentional conflict paradigm. *Proceedings of the National Academy of Sciences of the United States of America*, *87*(1), 256–259. https://doi.org/10.1073/pnas.87.1.256

Parker, N. F., Cameron, C. M., Taliaferro, J. P., Lee, J., Choi, J. Y., Davidson, T. J., Daw, N. D., & Witten, I. B. (2016). Reward and choice encoding in terminals of midbrain dopamine neurons depends on striatal target. *Nature Neuroscience*, *19*(6), 845–854. https://doi.org/10.1038/nn.4287

Parvizi, J., Rangarajan, V., Shirer, W. R., Desai, N., & Greicius, M. D. (2013). The Will to Persevere Induced by Electrical Stimulation of the Human Cingulate Gyrus. *Neuron*, *80*(6), 1359–1367. https://doi.org/10.1016/j.neuron.2013.10.057

Pérez-Ortega J, Alejandre-García T, Yuste R. (2021) Long-term stability of cortical ensembles. *Elife*. 2021 Jul 30;10:e64449. doi: 10.7554/eLife.64449. PMID: 34328414; PMCID: PMC8376248.

Peterson, B. S., Kane, M. J., Alexander, G. M., Lacadie, C., Skudlarski, P., Leung, H.-C., May, J., & Gore, J. C. (2002). An event-related functional MRI study comparing interference effects in the Simon and Stroop tasks. *Cognitive Brain Research*, *13*(3), 427–440. https://doi.org/10.1016/S0926-6410(02)00054-X

Pi, H.-J., Hangya, B., Kvitsiani, D., Sanders, J. I., Huang, Z. J., & Kepecs, A. (2013). Cortical interneurons that specialize in disinhibitory control. *Nature*, *503*(7477), 521–524. https://doi.org/10.1038/nature12676

Poort, J., Khan, A. G., Pachitariu, M., Nemri, A., Orsolic, I., Krupic, J., Bauza, M., Sahani, M., Keller, G. B., Mrsic-Flogel, T. D., & Hofer, S. B. (2015). Learning Enhances Sensory and Multiple Non-sensory Representations in Primary Visual Cortex. *Neuron*, *86*(6), 1478–1490. https://doi.org/10.1016/j.neuron.2015.05.037

Poort, J., Wilmes, K. A., Blot, A., Chadwick, A., Sahani, M., Clopath, C., Mrsic-Flogel, T. D., Hofer, S. B., & Khan, A. G. (2022). Learning and attention increase visual response selectivity through distinct mechanisms. *Neuron*, 110(4), 686-697.e6. https://doi.org/10.1016/j.neuron.2021.11.016

Pooters, T., Laeremans, A., Gantois, I., Vermaercke, B., Arckens, L., & D'Hooge, R. (2017). Comparison of the spatial-cognitive functions of dorsomedial striatum and anterior cingulate cortex in mice. *PLOS ONE*, *12*(5), e0176295. https://doi.org/10.1371/journal.pone.0176295

Porter, B. S., Hillman, K. L., & Bilkey, D. K. (2019). Anterior cingulate cortex encoding of effortful behavior. *Journal of Neurophysiology*, *121*(2), 701–714. https://doi.org/10.1152/jn.00654.2018

Posner, M. I., & DiGirolamo, G. J. (1998). Executive attention: Conflict, target detection, and cognitive control. *The Attentive Brain.*, 401–423.

Pouratian, N. (2016). Anterior Cingulotomy for the Treatment ofChronic Intractable Pain: A Systematic Review. *Pain Physician*, *8;19*(8;11), 537–550. https://doi.org/10.36076/ppj/2016.19.537

Preuss, T. M. (1995). Do Rats Have Prefrontal Cortex? The Rose-Woolsey-Akert Program Reconsidered. *Journal of Cognitive Neuroscience*, *7*(1), 1–24. https://doi.org/10.1162/jocn.1995.7.1.1

Price, D. D. (2000). Psychological and Neural Mechanisms of the Affective Dimension of Pain. *Science*, *288*(5472), 1769–1772. https://doi.org/10.1126/science.288.5472.1769

Rao, R. P. N., & Ballard, D. H. (1999). Predictive coding in the visual cortex: A functional interpretation of some extra-classical receptive-field effects. *Nature Neuroscience*, *2*(1), 79–87. https://doi.org/10.1038/4580

Rao, S. C., Rainer, G., & Miller, E. K. (1997). Integration of what and where in the primate prefrontal cortex. *Science*, *276*(5313), 821–824. https://doi.org/10.1126/science.276.5313.821

Rigotti, M. (2010). Internal representation of task rules by recurrent dynamics: The importance of the diversity of neural responses. *Frontiers in Computational Neuroscience*, *4*. https://doi.org/10.3389/fncom.2010.00024

Rigotti, M., Barak, O., Warden, M. R., Wang, X.-J., Daw, N. D., Miller, E. K., & Fusi, S. (2013). The importance of mixed selectivity in complex cognitive tasks. *Nature*, *497*(7451), 585–590. https://doi.org/10.1038/nature12160

Rimpler, A. (2020). On the search for continuous depletion in a task switch paradigm. Thesis, Cognitive Neuropsychology, Tilburg University.

Rolls, E. T. (2015). Neural Integration of Taste, Smell, Oral Texture, and Visual Modalities. In R. L. Doty (Ed.), *Handbook of Olfaction and Gustation* (pp. 1027–1048). John Wiley & Sons, Inc. https://doi.org/10.1002/9781118971758.ch46

Roxo, M. R., Franceschini, P. R., Zubaran, C., Kleber, F. D., & Sander, J. W. (2011). The Limbic System Conception and Its Historical Evolution. *The Scientific World JOURNAL*, *11*, 2427–2440. https://doi.org/10.1100/2011/157150

Roy, J. E., Riesenhuber, M., Poggio, T., & Miller, E. K. (2010). Prefrontal Cortex Activity during Flexible Categorization. *Journal of Neuroscience*, *30*(25), 8519–8528. https://doi.org/10.1523/JNEUROSCI.4837-09.2010

Rubin, J., Ulanovsky, N., Nelken, I., & Tishby, N. (2016). The Representation of Prediction Error in Auditory Cortex. *PLOS Computational Biology*, *12*(8), e1005058. https://doi.org/10.1371/journal.pcbi.1005058

Rudebeck, P. H., Behrens, T. E., Kennerley, S. W., Baxter, M. G., Buckley, M. J., Walton, M. E., & Rushworth, M. F. S. (2008). Frontal Cortex Subregions Play Distinct Roles in Choices between Actions and Stimuli. *Journal of Neuroscience*, *28*(51), 13775–13785. https://doi.org/10.1523/JNEUROSCI.3541-08.2008

Rudebeck, P. H., Walton, M. E., Smyth, A. N., Bannerman, D. M., & Rushworth, M. F. S. (2006). Separate neural pathways process different decision costs. *Nature Neuroscience*, *9*(9), 1161–1168. https://doi.org/10.1038/nn1756

Rule, M. E., O'Leary, T., & Harvey, C. D. (2019). Causes and consequences of representational drift. *Current Opinion in Neurobiology*, *58*, 141–147. https://doi.org/10.1016/j.conb.2019.08.005

Sachuriga, Nishimaru, H., Takamura, Y., Matsumoto, J., Ferreira Pereira de Araújo, M., Ono, T., & Nishijo, H. (2021). Neuronal Representation of Locomotion During Motivated Behavior in the Mouse Anterior Cingulate Cortex. *Frontiers in Systems Neuroscience*, *15*, 655110. https://doi.org/10.3389/fnsys.2021.655110

Sales, A. C., Friston, K. J., Jones, M. W., Pickering, A. E., & Moran, R. J. (2019). Locus Coeruleus tracking of prediction errors optimises cognitive flexibility: An Active Inference model. *PLOS Computational Biology*, *15*(1), e1006267. https://doi.org/10.1371/journal.pcbi.1006267

Schouten, J. F., & Bekker, J. A. (1967). Reaction time and accuracy. *Acta Psychologica*, *27*, 143–153. https://doi.org/10.1016/0001-6918(67)90054-6

Schultz, W. (2016). Dopamine reward prediction error coding. *Dialogues in Clinical Neuroscience*, *18*(1), 23–32. https://doi.org/10.31887/DCNS.2016.18.1/wschultz

Sesack, S. R., Deutch, A. Y., Roth, R. H., & Bunney, B. S. (1989). Topographical organization of the efferent projections of the medial prefrontal cortex in the rat: An anterograde tract-tracing study with Phaseolus vulgaris leucoagglutinin. *Journal of Comparative Neurology*, *290*(2), 213–242. https://doi.org/10.1002/cne.902900205

Severino, F. P. U., Lawal, O., Sakers, K., Wang, S., Kim, N., Friedman, A., Johnson, S., Sriworarat, C., Hughes, R., Soderling, S., Kim, I. H., Yin, H., & Eroglu, C. (2021). *Training-Induced Circuit-Specific Excitatory Synaptogenesis is Required for Effort Control* [Preprint]. Neuroscience. https://doi.org/10.1101/2021.04.20.440613

Sharpe, M. J., & Killcross, S. (2014). The Prelimbic Cortex Contributes to the Down-Regulation of Attention Toward Redundant Cues. *Cerebral Cortex*, *24*(4), 1066–1074. https://doi.org/10.1093/cercor/bhs393

Shenhav, A., Cohen, J. D., & Botvinick, M. M. (2016). Dorsal anterior cingulate cortex and the value of control. *Nature Neuroscience*, *19*(10), 1286–1291. https://doi.org/10.1038/nn.4384

Shenhav, A., Straccia, M. A., Cohen, J. D., & Botvinick, M. M. (2014). Anterior cingulate engagement in a foraging context reflects choice difficulty, not foraging value. *Nature Neuroscience*, *17*(9), 1249–1254. https://doi.org/10.1038/nn.3771

Sheth, S. A., Mian, M. K., Patel, S. R., Asaad, W. F., Williams, Z. M., Dougherty, D. D., Bush, G., & Eskandar, E. N. (2012). Human dorsal anterior cingulate cortex neurons mediate ongoing behavioural adaptation. *Nature*, *488*(7410), 218–221. https://doi.org/10.1038/nature11239

Shidara, M., & Richmond, B. J. (2002). Anterior Cingulate: Single Neuronal Signals Related to Degree of Reward Expectancy. *Science*, *296*(5573), 1709–1711. https://doi.org/10.1126/science.1069504

Shin, L. M., Whalen, P. J., Pitman, R. K., Bush, G., Macklin, M. L., Lasko, N. B., Orr, S. P., McInerney, S. C., & Rauch, S. L. (2001). An fMRI study of anterior cingulate function in posttraumatic stress disorder. *Biological Psychiatry*, *50*(12), 932–942. https://doi.org/10.1016/S0006-3223(01)01215-X

Siniscalchi, M. J., Phoumthipphavong, V., Ali, F., Lozano, M., & Kwan, A. C. (2016). Fast and slow transitions in frontal ensemble activity during flexible sensorimotor behavior. *Nature Neuroscience*, *19*(9), 1234–1242. https://doi.org/10.1038/nn.4342

Soper, D.S. (2022). Significance of the Difference between Two Correlations Calculator [Software]. Available from https://www.danielsoper.com/statcalc

Srinivasan, M. V., Laughlin, S. B., & Dubs, A. (1982). Predictive coding: A fresh view of inhibition in the retina. *Proceedings of the Royal Society of London. Series B, Biological Sciences*, *216*(1205), 427–459. https://doi.org/10.1098/rspb.1982.0085

Stevens, F. L. (2011). Anterior Cingulate Cortex: Unique Role in Cognition and Emotion. J Neuropsychiatry Clin Neurosci, 6.

Taylor, S. F. (2006). Medial Frontal Cortex Activity and Loss-Related Responses to Errors. *Journal of Neuroscience*, *26*(15), 4063–4070. https://doi.org/10.1523/JNEUROSCI.4709-05.2006

Tervo, D. G. R., Kuleshova, E., Manakov, M., Proskurin, M., Karlsson, M., Lustig, A., Behnam, R., & Karpova, A. Y. (2021). The anterior cingulate cortex directs exploration of alternative strategies. *Neuron*, *109*(11), 1876-1887.e6. https://doi.org/10.1016/j.neuron.2021.03.028

Tervo, D. G. R., Proskurin, M., Manakov, M., Kabra, M., Vollmer, A., Branson, K., & Karpova, A. Y. (2014). Behavioral Variability through Stochastic Choice and Its Gating by Anterior Cingulate Cortex. *Cell*, *159*(1), 21–32. https://doi.org/10.1016/j.cell.2014.08.037

Tölle, T. R., Kaufmann, T., Siessmeier, T., Lautenbacher, S., Berthele, A., Munz, F., Zieglgänsberger, W., Willoch, F., Schwaiger, M., Conrad, B., & Bartenstein, P. (1999). Region-specific encoding of sensory and affective components of pain in the human brain: A positron emission tomography correlation analysis. *Annals of Neurology*, *45*(1), 40–47. https://doi.org/10.1002/1531-8249(199901)45:1<40::aid-art8>3.0.co;2-l

Tow, P. M., & Whitty, C. W. (1953). Personality changes after operations on the cingulate gyrus in man. *Journal of Neurology, Neurosurgery, and Psychiatry*, *16*(3), 186–193. https://doi.org/10.1136/jnnp.16.3.186

Vertechi, P., Lottem, E., Sarra, D., Godinho, B., Treves, I., Quendera, T., Lohuis, M. N. O., & Mainen, Z. F. (2020). Inference-Based Decisions in a Hidden State Foraging Task: Differential Contributions of Prefrontal Cortical Areas. *Neuron*. https://doi.org/10.1016/j.neuron.2020.01.017

Vogt, B. A. (2005). Pain and emotion interactions in subregions of the cingulate gyrus. *Nature Reviews Neuroscience*, *6*(7), 533–544. https://doi.org/10.1038/nrn1704

Vogt, B. A., Finch, D. M., & Olson, C. R. (1992). Functional heterogeneity in cingulate cortex: The anterior executive and posterior evaluative regions. *Cerebral Cortex (New York, N.Y. : 1991)*, *2*(6), 435–443. https://doi.org/10.1093/cercor/2.6.435-a

Vogt, B. A., Hof, P. R., Zilles, K., Vogt, L. J., Herold, C., & Palomero-Gallagher, N. (2013). Cingulate area 32 homologies in mouse, rat, macaque and human: Cytoarchitecture and receptor architecture: Anterior Cingulate Area 32 Homologies. *Journal of Comparative Neurology*, *521*(18), 4189–4204. https://doi.org/10.1002/cne.23409

Wall, N. R., De La Parra, M., Sorokin, J. M., Taniguchi, H., Huang, Z. J., & Callaway, E. M. (2016). Brain-Wide Maps of Synaptic Input to Cortical Interneurons. *The Journal of Neuroscience*, *36*(14), 4000–4009. https://doi.org/10.1523/JNEUROSCI.3967-15.2016

Watson, R. T., Heilman, K. M., Cauthen, J. C., & King, F. A. (1973). Neglect after cingulectomy. *Neurology*, *23*, 1003–1007. https://doi.org/10.1212/WNL.23.9.1003

Weiss, A. R., Gillies, M. J., Philiastides, M. G., Apps, M. A., Whittington, M. A., FitzGerald, J. J., Boccard, S. G., Aziz, T. Z., & Green, A. L. (2018). Dorsal Anterior Cingulate Cortices Differentially Lateralize Prediction Errors and Outcome Valence in a Decision-Making Task. *Frontiers in Human Neuroscience*, *12*, 203. https://doi.org/10.3389/fnhum.2018.00203

Weissman, D. H., Giesbrecht, B., Song, A. W., Mangun, G. R., & Woldorff, M. G. (2003). Conflict monitoring in the human anterior cingulate cortex during selective attention to global and local object features. *NeuroImage*, *19*(4), 1361–1368. https://doi.org/10.1016/S1053-8119(03)00167-8

Westbrook, A., & Braver, T. S. (2015). Cognitive effort: A neuroeconomic approach. *Cognitive, Affective, & Behavioral Neuroscience*, *15*(2), 395–415. https://doi.org/10.3758/s13415-015-0334-y

Whalen, P. J., Bush, G., McNally, R. J., Wilhelm, S., McInerney, S. C., Jenike, M. A., & Rauch, S. L. (1998). The emotional counting stroop paradigm: A functional magnetic resonance imaging probe of the anterior cingulate affective division. *Biological Psychiatry*, *44*(12), 1219–1228. https://doi.org/10.1016/S0006-3223(98)00251-0

WHITTY, C. W. M., DUFFIELD, J. E., TOV', P. M., & CAIRNS, H. (1952). Anterior cingulectomy in the treatment of mental disease. *Lancet (London, England)*, *1*(6706), 475–481. https://doi.org/10.1016/s0140-6736(52)90051-2

Wilson, D. H., & Chang, A. E. (1974). Bilateral anterior cingulectomy for the relief of intractable pain. Report of 23 patients. *Confinia Neurologica*, *36*(1), 61–68. https://doi.org/10.1159/000102783

Wimmer, R. D., Schmitt, L. I., Davidson, T. J., Nakajima, M., Deisseroth, K., & Halassa, M. M. (2015). Thalamic control of sensory selection in divided attention. *Nature*, *526*(7575), 705–709. https://doi.org/10.1038/nature15398

Wittmann, M. K., Kolling, N., Akaishi, R., Chau, B. K. H., Brown, J. W., Nelissen, N., & Rushworth, M. F. S. (2016). Predictive decision making driven by multiple time-linked reward representations in the anterior cingulate cortex. *Nature Communications*, *7*(1), 12327. https://doi.org/10.1038/ncomms12327

Wu, D., Deng, H., Xiao, X., Zuo, Y., Sun, J., & Wang, Z. (2017). Persistent Neuronal Activity in Anterior Cingulate Cortex Correlates with Sustained Attention in Rats Regardless of Sensory Modality. *Scientific Reports*, *7*(1), 43101. https://doi.org/10.1038/srep43101

Zelano, C., Mohanty, A., & Gottfried, J. A. (2011). Olfactory Predictive Codes and Stimulus Templates in Piriform Cortex. *Neuron*, *72*(1), 178–187. https://doi.org/10.1016/j.neuron.2011.08.010

Zhang, S., Xu, M., Kamigaki, T., Do, J. P. H., Chang, W.-C., Jenvay, S., Miyamichi, K., Luo, L., & Dan, Y. (n.d.). *Long-range and local circuits for top-down modulation of visual cortex processing*. 7.

Ziv, Y., Burns, L. D., Cocker, E. D., Hamel, E. O., Ghosh, K. K., Kitch, L. J., Gamal, A. E., & Schnitzer, M. J. (2013). Long-term dynamics of CA1 hippocampal place codes. *Nature Neuroscience*, *16*(3), 264–266. https://doi.org/10.1038/nn.3329